Formic acid aided catalytic lignin conversion in ethanol and water media

Mikel Oregi Bengoetxea

Dissertation for the degree of philosophiae doctor (PhD)

at the University of Bergen

2016

Dissertation date: 21/12/2016

Year: 2016

Title: Formic acid aided catalytic lignin conversion in ethanol and water media

Author: Mikel Oregui Bengoechea

Print: AIT Bjerch AS / University of Bergen

Preface

This thesis, submitted for the degree of Philosophiae Doctor at the University of Bergen, consists of two parts. The first includes an introduction, an experimental section, a summary of the main results of the papers presented in the second part, and an overall discussion and conclusion. The second part consists of six research papers.

The main part of the work has been carried out at the Department of Chemistry of the University of Bergen in the period 2012-2016, including a 5 months guest research stay at the Department of Chemical and Environmental Engineering of the University of the Basque Country. Part of the work was also carried out in collaboration with the Arrhenius Laboratory of the Stockholm University.

The project was partially funded by the Research Council of Norway (grant no. 190965/S60) in collaboration with additional partners - Statoil ASA, Borregaard Industries Ltd., Allskog BA, Cambi AS, Xynergo AS, Hafslund ASA and Weyland AS- through the LignoRef project ("Lignocellulosics as a basis for second generation biofuels and the future biorefinery").

The aim of the work conducted was to develop stable and active catalyst for the conversion of lignin in a formic acid/solvent media. Several catalytic formulations have been investigated using both water and ethanol as a solvent. The research was also oriented to the understanding of the catalytic LtL reaction system more in detail. The fundamental knowledge acquired and the considerable catalyst screening effort represent a considerable improvement of the scientific basis for the future development of more specific LtL catalysts.

Acknowledgements

First and foremost I would like to thank Tanja Barth for giving me the opportunity to carry out this PhD and for the personal and professional support provided during all my time at the University of Bergen. She has given me the freedom I needed to build my professional competences within the project. I would also like to thank my department colleagues Solmaz Ghoreishi and Camilla Løhre and the master students who helped me with the lab work, Agnethe Hertzber, Sveinung F. Simonsen, Audun Kronstad and Mari H. Vogt.

I would further like to thank the staff at the University of Bergen (UiB) for their administrative and professional support: Bjarte Holmelid and Johan E. Carlson for the scientific support and assistance, Knut Børve for his patience and personal support, Inge-Johanne Fjellanger for her assistance with the elemental analysis, Egil Nodland and Bjørn Grung for the discussions on experimental design and chemometrics, Mali H. Rosnes for helping me with the N_2-adsorption analysis, Svein A. Mjøs for his assistance on gas-chromatography analysis, Erwan Le Roux for the technical support, and Reidun A. Myklebust, Steinar Vatne, Martin A., Hansen and Lisbet Sørensen for their technical assistance. I hope I have not missed anyone.

My sincerest gratitude further goes to the staff of the Chemical and Environmental Engineering from the University of the Basque Country (UPV-EHU) without whom I doubt I would have been able to finish this work. I would like to particularly thank Pedro L. Arias and Iñaki Gandarias for helping me through this long and tedious journey. Working with Nemanja Miletíc has also been a real pleasure. Thanks to Aihnoa, Iker Obragon, Iker Garcia and Sara for helping me during my stay at the UPV-EHU. I would also like to thank the members of the Arrhenius Laboratory of the Stockholm University for their productive collaboration, particularly Wenming Hao and Niklas Hedin.

Last but not least, a special thanks to Matina Karakitsiu, Ida Portice, Coralie Quadri and James Gasson for making Bergen less rainy and the UiB a bit more colorful. Thanks to Elvira Jalon and Markus Baumman for contributing to a nicer working environment.

No me gustaría olvidar a todos aquellos amigos que han hecho que estos cuatro años en Bergen sean difíciles de olvidar. Gracias a Mónica, Lolo, Antonio, Belén, Dinka, Momo, Mireia, Diana, Leire, Luzzo, Camilla, Guille, Georgina, Tamara, Ona, Alba, Maite, Nicholas, Katerina y el largo etcétera de personas que han llenado de alegría mi estancia en Noruega. Un especial agradecimiento a mis compañeros de Olav Kyrres Gate por los buenos momentos y mejores fiestas que hemos compartido, Humberto, Marquitos, Piero, David y el siempre presente Nico. Gracias también a los Berlinenes y esas escapaditas necesarias, Juan, Imna, Sergio y Azzurra.

Y como no un especial agradecimiento a los de la Kuadrilla, por esas Navidades, ese veranito Erasmus, los pintxo-potes, las visitas a Noruega, y sobre todo por no dejarme acabar la tesis a tiempo. Un abrazo especial para Ion Ander, Hodei, Jon, Gabirel, Unai, Eder, Ioseba, Torti, Winston, Javi, Iker, Otxoa y los de un año menos. También, como no, a los Inasmetos y a todos los demás que por espacio no he podido incluir.

Esta tesis querría dedicársela a mis padres. Me han acompañado desde el principio de mi viaje y han sido el mejor apoyo posible en los momentos más difíciles. También a mi hermano Iñigo por su apoyo, comprensión y por dejarme ocupar su casa. Besarkada handi bat, familia!

Abstract

The viability of future lignocellulosic bio-refineries is highly dependent on the efficient conversion of the lignin component. A promising and relatively new lignin conversion methodology is the Lignin-to-Liquid (LtL) process, which involves the conversion of the lignin biopolymer in a reducing formic acid/solvent media. However, in order to make this process economically competitive, some important process parameters need to be improved: (i) shorter reaction times, (ii) lower reaction temperatures and (iii) the reduction of low-value side streams i.e., gas and solid phases.

One possibility to address these challenges is the use of heterogeneous catalysts in the process. The main focus of this work was therefore the systematical evaluation of different catalysts for the LtL process. Additionally, the valorization of the low-value solid phase into magnetic activated carbons (MACs) was investigated. MACs were produced by KOH chemical activation of the LtL solids (hydrochars) and were further evaluated as CO_2 sorbents and catalytic supports.

The activity of different noble metal catalysts such as Rh/Al_2O_3, Pd/Al_2O_3, Ru/Al_2O_3 and Ru/C was studied using both ethanol and water as solvents. Traditional NiMo catalysts supported on Al_2O_3, ZrO_2 and MACs, on the other hand, were analyzed only in ethanol media. The results suggest that the activity of the catalyst is highly dependent on the type of metallic system; the effect of the support in the activity of the catalyst is limited, although it is a key factor when evaluating its stability upon recycling. Noble metal based catalysts increased the oil yield and reduced the solid yield for all the reaction conditions and solvent systems studied. NiMo, catalysts, on the other hand, were only active in ethanol media and at high temperatures (i.e. 320 °C or above). The oil yield at low temperatures (i.e. 300 °C) could be, however, increased by supporting the NiMo species over renewable MACs.

The catalyst screening approach carried out in this work revealed the complexity of the LtL system: several chemical reactions such as aliphatic ether bond cleavage, HDO and alkylation reactions involving the depolymerized lignin monomers and formic acid decomposition occur simultaneously. The formic acid aided aliphatic ether bond cleavage was the most relevant reaction for the production of bio-oil. It was found that formic acid induces a lignin degradation mechanism different from the one induced by other hydrogen sources such as H_2 or isopropanol. The exact reaction mechanism is not fully understood but is believe to happen through a formylation-elimination-hydrogenolysis/hydrolysis mechanism. HDO and alkylation reactions contribute to a lesser extent to the production of bio-oil by stabilizing the lignin monomers and hindering their re-polymerization. Furthermore, alkylation reactions could also be favored by selecting a suitable solvent.

List of publications

Paper A Oregui Bengoechea, M.; Hertzberg, A.; Miletić, N.; Arias, P. L.; Barth, T., Simultaneous catalytic de-polymerization and hydrodeoxygenation of lignin in water/formic acid media with Rh/Al_2O_3, Ru/Al_2O_3 and Pd/Al_2O_3 as bifunctional catalysts. *Journal of Analytical and Applied Pyrolysis* **2015,** *113*, 713-722[I].

Paper B Oregui Bengoechea, M.; Miletíc, N.; Vogt, M. H.; Arias, P.L.; Barth, T., Analysis of the effect of temperature and reaction time on yields, compositions and oil quality in catalytic and non-catalytic lignin solvolysis with formic acid using experimental design. *Biomass & Bioenergy* **2016**, submitted.[II]

Paper C Hao, W.; Björnerbäck, F.; Trushkina, Y.; Oregui Bengoechea, M.; Salazar-Alvarez, G.; Barth, T.; Hedin, N., High-performance magnetic activated carbon from renewable resources. Part I: using solid waste from lignin conversion processes. Ready for submission.

Paper D Oregui Bengoechea, M.; Miletíc, N.; Hao, W.; Björnerbäck, F.; Rosnes M. H.; Hedin, N.; Arias, P.L.; Barth, T., High-performance magnetic activated carbon from renewable resources. Part II: Evaluation as NiMo catalyst supports. Ready for submission.

Paper E Oregui Bengoechea, M.**;** Miletíc, N.; Simonsen, S.F.; Kronstad A.; Gandarias, I.; Arias, P.L.; Barth, T., Thermocatalytic conversion of lignin in ethanol/formic acid media with $NiMo/Al_2O_3$ and $NiMo/ZrO_2$ catalysts. Ready for submission.

Paper F Oregui Bengoechea, M.; Gandarias, I.; Arias, P.L.; Barth, T., Unraveling the role of formic acid and the type of solvent in the catalytic conversion of lignin: a holistic approach. *ChemSusChem* **2016**, submitted.[III]

[I] Reprints were made with permission from © 2015 Elsevier B.V.
[II] Reprints were made with permission from © 2016 Elsevier Ltd.
[III] Reprints were made with permission from © 2016 Wiley-VCH GmbH & Co. KGaA, Weinheim

Abbreviations

AFEX	Ammonia fiber explosion
BET	Brunauer-Emmett-Teller model
BCD	Based catalyzed de-polymerization
BJH	Barret-Joyner-Halenda model
CCD	Central composite design
CCS	Carbon capture and storage
DFT	Density functional theory
DME	Dimethylether
DOE	Experimental design
EA	Elemental analysis
EDXA	Energy dispersive X-ray
ESI-MS	Electrospray ionization-mass spectroscopy
EtAc	Ethyl acetate
FA	Formic acid
FAO	Food and Agriculture Organization
FID	Flame ionization detectors
FT-IR	Fourier transform infrared spectroscopy
GC	Gas chromatography
GC-MS	Gas chromatography -Mass spectrometry
GPC	Gel permeation chromatography
H/C	Hydrogen to carbon ratio
HDO	Hydrodeoxygenation
HK	Horvath-Kawazoe model
HMF	Hydroxymethylfurfural
ICP-AES	Inductively couple plasma atomic emission spectroscopy
ICP-EOS	inductively coupled plasma optical emission spectroscopy
LPR	Liquid-phase reforming
LtL	Lignin to liquids
MAC	Magnetic activated carbon
M_w	Average molecular weight
NH_3-TPD	Temperature programmed desorption of ammonia
O/C	Oxygen to carbon ratio
PCA	Principal Component Analysis

PGM	Platinum-group metal
RSM	Response surface Methodology
SEC	Size exclusion chromatography
TCD	Thermal conductivity detector
THF	Tetrahydrofuran
TPR	Temperature-Programmed Reduction
UN-DESA	Department of Economic and Social Affairs of United Nations
UV	Ultraviolet
XRD	X-ray diffraction

Contents

PART I

Chapter 1. Introduction

Among all biomass sources, the lignocellulosic biomass derived from agricultural and forestry wastes is considered as the most adequate substitute for fossil sources due to its abundance, versatility and lack of competition with food resources. Yet, the efficient and economically feasible conversion of lignin into fuels and chemicals remains one of the major technology gaps for the development of lignocellulosic bio-refineries. Here, the chemical nature of the lignin biopolymers will be described based on their botanical origin and the isolation process. After summarizing the most relevant advances in the catalytic conversion of lignin, the recently developed Lignin-to-Liquids (LtL) process will be described and its major challenges addressed.

1.1 Energy transition: from crude oil to a biomass based energy system

According to the results of the *2015 Revision*[1] published by the Department of Economic and Social Affairs of United Nations (UN-DESA), the world population reached 7.3 billion as of mid-2015. The global population is expected to rise in the short-to-medium term, reaching between 8.4 and 8.6 billion in 2030 and between 9.5 and 13.3 billion by the end of the century[1]. Hence, the demand of natural resources for the production of food, energy and chemicals is expected to increase significantly in the course of the century. It is important, therefore, to develop an integrated production model that addresses the sustainable and environmentally friendly production and distribution of these three basic commodities: food, energy and raw materials (chemicals).

The challenge is of immense magnitude. In terms of food supply, the Food and Agriculture Organization (FAO) expects an steady growth of the total agricultural product consumption of 1.1 % per year until 2050[2]. The global energy demand is estimated to grow even faster, by 48 % between 2012 and 2040 (Figure 1.1, *above*); fossil fuels being the major contributor providing over 78 % of the demand[3]. The same trend is observed for the bulk chemicals, of which organic chemicals account for

47 % of the total shipment value (Figure 1.1, *below*): the value of bulk chemical shipments is expected to grow from $288 billion in 2013 to $454 billion in 2040[4].

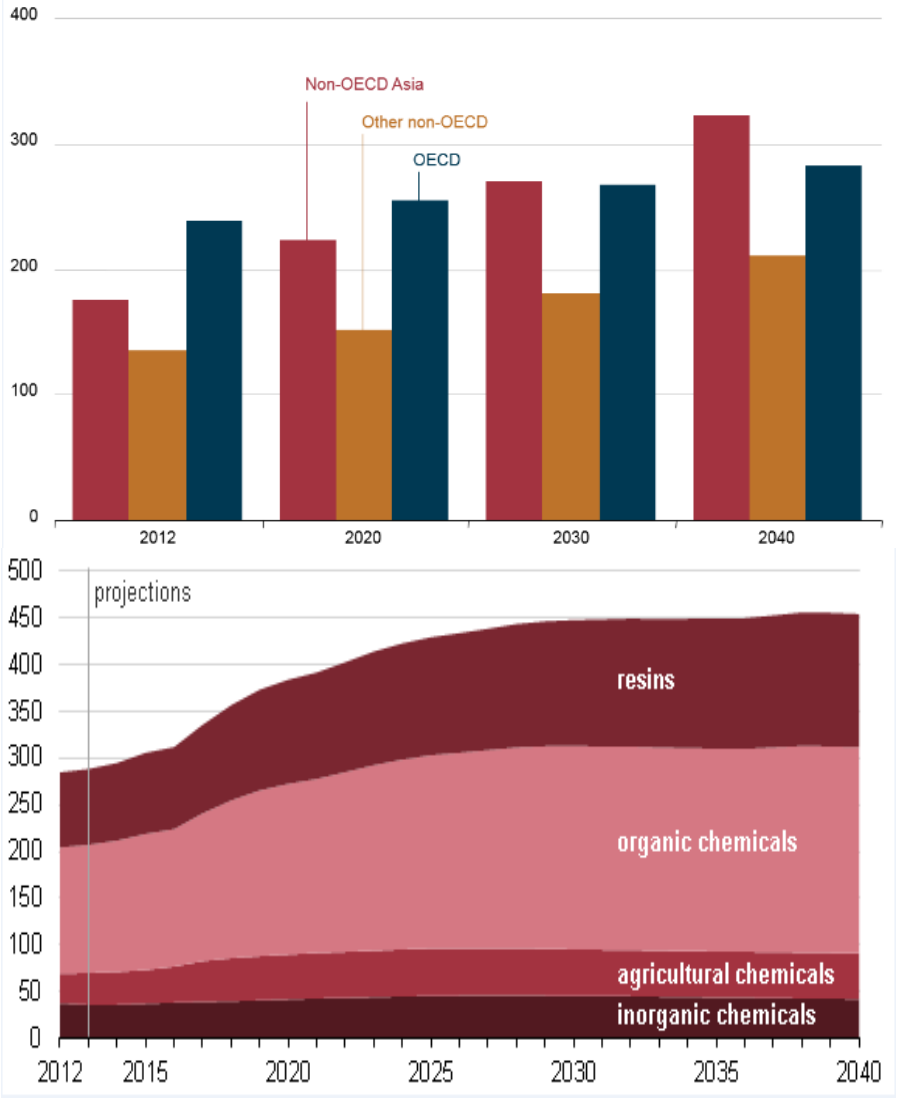

Figure 1.1: World energy consumption in quadribillion BtU (British thermal unit equivalent to 257 cal.) by country grouping 2012-40 [3] (*above*) and value of industrial bulk chemicals shipments 2012-40 (billion 2009 dollars)[4] (*below*)

Today's energy and organic chemical production model basically relies on fossil sources. Among them, crude oil has displaced coal as the most important energy and organic chemical resource in both industrial and post-industrial countries. The major amount of the crude oil is consumed for energy applications although around 16 % is employed for the production of oil-derived products and chemicals[5]. However, the excessive consumption of oil-based commodity products (i.e. energy, transportation fuel, materials, plastics and chemicals) is causing an extreme environmental impact all over the world. Moreover, the unbalanced geographical distribution of the crude oil reserves, which are often found in politically unstable regions, have led to military conflicts and the current oil price volatility has contributed to the rise and fall of local economies and global markets. Thus, the modern society needs to address as early as possible the transition towards a sustainable and environmentally friendly renewable model.

Based on these concerns, several countries and supranational entities have designed and in some cases implemented ambitious policies focused in long term sustainability, especially in the energy sector. The European Union has set a mandatory target of 20% for the renewable energy share of energy consumption by 2020 and a mandatory minimum target of 10% for biofuels for all member states[6]. Although the United States (U.S.) carries no mandatory renewable energy targets, the U.S. Department of Agriculture and U.S. Department of Energy have set the goal that by 2030 20% of transportation fuels and 25% of U.S. chemical commodities should be derived from biomass[7].The Chinese National Energy Administration has carried out a "National Twelfth Five-Year Plan" to reach a consumption of 12 million metric tons of biofuels by 2020, mainly ethanol and biodiesel[8].

While energy can be produced by different renewable sources (e.g. wind, solar systems, tidal power), the other crude oil based consumer products (e.g. chemicals) can only be made from biomass. Biomass is the fourth largest source of energy in the world (following oil, coal, and natural gas)[9] and the only renewable organic carbon resource in nature. Today, ethanol or ethanol blended petrol, as well as bio-diesel produced from energy crops, are the main fossil fuel substituents and the demand is

increasing. However, the production of the so-called first generation bio-fuels, those derived from potential alimentary resources, resulted in the rise of the energy crop prices and the subsequent outcry from world-wide consumers and livestock producers[10]. To avoid some of the mentioned concerns, the so-called second generation biofuels are attracting more and more attention from researchers, industry and policy makers.

Lignocellulosic material, found in both agricultural and forestry residues, is a very promising platform for the production of both second generation bio-fuels and renewable chemicals. Lignocellulose is the most abundant form of biomass, with an annual production of around 170 billion metric tons[11] and its use will not impose a direct negative impact on food supplies. However, the transition from a crude-oil model to a production system based on lignocellulosic biomass is still a huge challenge. The cost of bio-based products in many cases exceeds the cost of oil-refining and petrochemical processing, and the new products must be proven to perform at least as well as their petrochemical equivalents[12]. Novel and existing processes for the conversion of lignocellulosic feedstock need to be further developed and/or optimized in order to achieve the economically feasible biomass valorization. Moreover, these processes need to be further integrated mimicking the production system found in the refining and petrochemical industries. Hence, the key to the most efficient use of lignocellulosic biomass is to design suitable and sustainable integrated bio-refineries.

1.2 Lignocellulosic Bio-refineries: the lignin issue

Bio-refineries are classified on the basis of a number of key characteristics, mainly type of feedstock and platforms. Platforms are defined as the range of bio-refinery streams in which the selected feedstock can be processed: these include the syngas, biogas, C6 and C6/C5 sugar, plant-based oil, algae oil, organic solutions, lignin and pyrolysis oil platforms[12].

Lignocellulosic biomass is a heterogeneous feedstock comprising of three main components of different nature: hemicellulose, cellulose and lignin. Among them, hemicellulose (20−30%) and cellulose (40−50%) are the polymers containing both C5 and C6 sugars (hemicellulose) and only C6 sugars (cellulose), the rest being lignin[8]. Therefore, the development of the lignocellulosic bio-refinery concept should focus on the integration and optimization of the syngas, pyrolysis oil, C6 and C6/C5 sugar and lignin platforms.

Gasification (i.e. syngas production) and pyrolysis of lignocellulosic biomass have been extensively studied and are among the most mature biomass conversion technologies[13-14]. The objective of the syngas platform is to produce a mixture mainly of CO and H_2 that can be further converted into lower alcohols, fuel (e.g. Fischer Tropsh diesel) and chemical products such as methanol, dimethyl ether (DME) or ethanol[15]. The pyrolysis oil platform, on the other hand, is the thermal decomposition of biomass occurring in the absence of oxygen, yielding gas phase, a liquid bio-oil and a considerable amount of solid organic products[14]. In general, both syngas and pyrolysis platforms produce low quality fuels that need further processing (syngas-to-liquids) or up-grading (pyrolysis oils). Moreover, the narrow range of chemicals produced by these methods is insufficient to replace all the crude-oil based commodity products.

A more efficient and flexible way of valorizing lignocellulosic biomass is its fractionation into its cellulose, hemicellulose and lignin components and the integral conversion of each of these individual biopolymers into fuels and chemicals; i.e. the

integration of biomass-pretreatment methods with the C6 (cellulose) and C6/C5 (hemicellulose) sugar and lignin platforms.

After biomass fractionation, the hydrolysis products from cellulose and hemicellulose (i.e. carbohydrates such as glucose or xylose) can be further converted into value added chemicals in the so-called C6 and C6/C5 platform. Fermentation products such as bio-ethanol, formic acid or adipic acid[16]; and chemical transformation products such as sorbitol, furfural, hydroxymethylfurfural (HMF), levulinic acid are some examples of sugar-derived products[17-19]. The enormous potential of this bio-refinery platform and its flexibility to tune the fuel/chemical production ratio upon demand has attracted the interested of both researchers and private and public investors. Nevertheless, processing large quantities of sugars into fuel and chemicals will generate a huge amount of lignin waste, making the viability of the lignocellulosic bio-refineries highly dependent on the effective utilization of this lignocellulosic component[12].

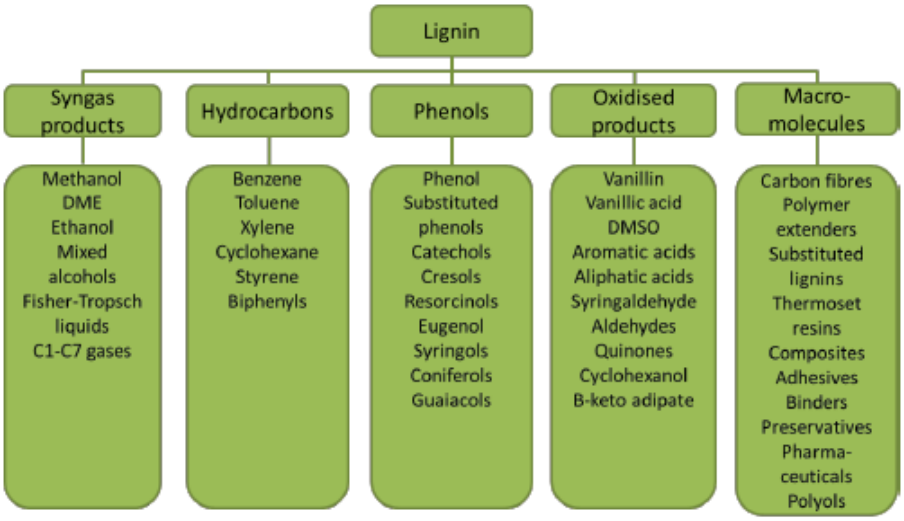

Figure 1.2: Summary of lignin platform products[20].

Lignin is an extremely abundant raw material contributing as much as 30 % of the weight and 40 % of the energy content of lignocellulosic biomass[12]. Its native aromatic structure represent the only direct source of renewable aromatics and its

conversion can also lead to the production of fuels and fuel-blends[21, 22]. A summary of the major lignin platforms products is given in Figure 1.2. Chemicals (e.g. phenols and other aromatic compounds), novel liquid biofuels[23] and lignin-based biomaterials such as resins, composites and fibers can be produced from this recalcitrant biopolymer. However, most of the lignin derived-products are not yet commercial on a large scale, mainly due to the high production costs associated with the difficulty of valorizing this highly stable and complex molecule.

1.3 Lignin: Chemical nature, reactivity and isolation methods

Lignin is a major constituent in structural cell walls of all higher vascular land plants. This highly complex cross-linked macromolecule forms part of the secondary cell walls of plants. It is responsible for the strength and rigidity of the cell walls and helps maintaining the integrity of the cellulose/hemicellulose/pectin matrix[8, 20, 24]. Lignin is vital for the survival of the plant species since its hydrophobic nature and insolubility in aqueous systems prevents the access for degrading chemicals and organisms[20].

The relative amount of lignin in the lignocellulosic material varies not only between species, but also between different tissues of an individual plant[25]. For example, the amount of lignin content in softwoods varies from 24 to 33%, in temperate zone hardwoods from 19 to 28%, and in tropical hardwoods from 26 to 35%. In non-wood fiber crops the lignin content is generally lower, ranging from 3% for cotton to around 11-15% for sisal and jute[20]. Grasses such as cereal straws, bamboo or sugar cane have higher lignin contents in the range of 15-25%[20].

1.3.1 Native lignin: Structure and reactivity

From a chemical point of view, lignin can be defined as a complex polyphenol-network. While its chemistry, biosynthesis and molecular biology are not fully understood, it is generally accepted that the lignin structure is built through the bonding of three basic phenol derivatives: the so-called monolignols[26-28]. These three basic units, namely p-coumaryl alcohol, coniferyl alcohol and sinapyl alcohol (Figure 1.3) are also known as p-hydroxyphenyl (H), guaiacyl (G) and syringyl (S)units,

respectively[29]. The content of each monolignol is related to plant taxonomy: (i) softwood lignin (gymnosperm) contains more G units, (ii) hardwood (angiosperm) lignin is mainly a mixture of G and S units, while (iii) grass lignin presents a mixture of all three aromatic units[24]. Based on the relative abundance of the monolignols, lignins can be classified as type-G (softwood lignin), type-GS (hardwood lignin), type-H-G-S (grass lignin), and type-H-G (compression wood lignin)[25].

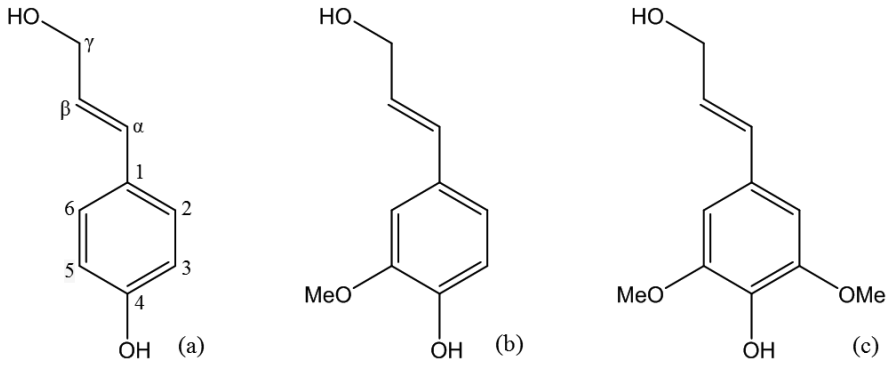

Figure 1.3: Lignin monomers: (a) *p*-coumaryl (H) , (b) coniferyl (G) and (c) sinapyl (S) alcohols[30]

Monolignols are predominantly linked either by ether or C-C bonds; in native lignin, ether bonds account for over two-thirds of the total linkages[8]. However, not all the ether or C-C bonds are of the same nature (Figure 1.4). The most abundant linkage is the β-O-4 accounting for 40-50% of the bonds found in softwood and 50-60 % found in hardwood. Other mayor lignin linkages are β-5 (pheylcoumaran) and β- β (resinol) bonds[31]. Additional linkages such as α-O-4 (α-aryl ether), 4-O-5 (diaryl ether), 5-5, α-O-γ (aliphatic ether) and β-1 (spirodienone) are also found at lower concentrations.

The linkages between monolignols are the key factor that determines the reactivity of the lignin biopolymer and its resistance to chemical digestion, especially the reactivity of the most frequent β-O-4 bond[8]. Another important factor that affects the reactivity of lignin is the functional groups attached both to the aromatic rings and the lignin ether and C-C linkages such as methoxyl, hydroxyl, and carbonyl groups. Among these, the hydroxyl groups and specially the aliphatic hydroxyl groups are

among the most abundant ones. In softwood lignin, for example the order of hydroxyl contents is as follows: aliphatic OH > phenolic OH > carboxylic OH[8]. This trend is also repeated for hardwood and grass lignin although the type and abundance of phenolic OH groups vary.

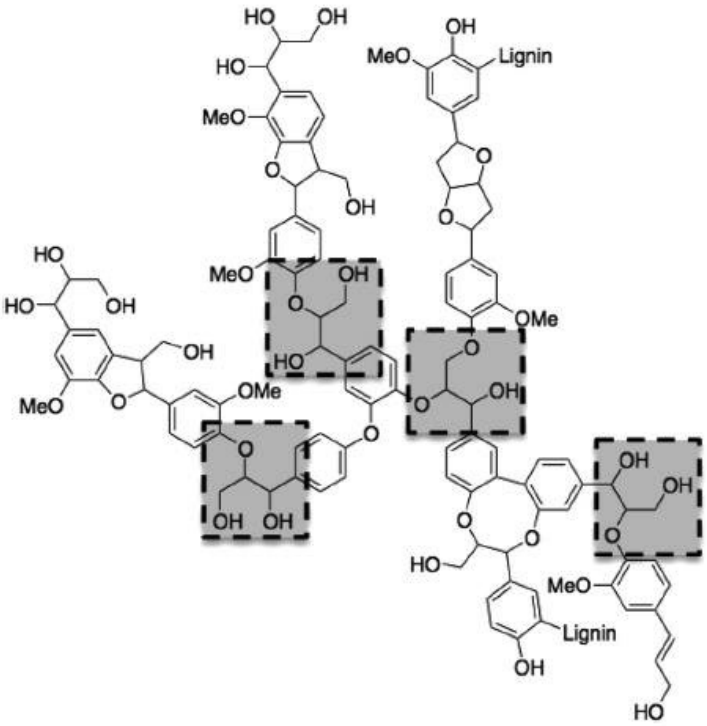

Figure 1.4: Representative structure of lignin showing four β-O-4 linkages highlighted by dashed rectangles[32]

1.3.2 Isolation methods: Types of lignin

The botanical species is not the only factor that affects the chemical structure of the lignin-macromolecule. The biomass pretreatment methods, i.e. those methods used for the isolation and extraction of lignin from the cellulose and hemicellulose components, also determine the nature and reactivity of the lignin bonds[33]. Furthermore, the impurities (minerals, organic acids) in natural biomass might also be solubilized with the lignin streams and can play a role in its reactivity, even in some cases causing the deactivation of those catalysts used in conversion processes.

In this section the most common lignin isolation methods are summarized, with a special focus on those processes used for the extraction of the lignins used in this dissertation. Other less common biomass fractionation methods such as ammonia fiber explosion (AFEX), oxidative delignification methods, biological methods and hot water processes are not considered.

1.3.2.1 *Kraft lignin*

Kraft pulping is the most common chemical process used for the fractionation of lignocellulosic biomass. Wood is treated in the presence of sodium sulfide under alkaline conditions (Na_2S/NaOH). The mixture reacts at temperatures of 155-175 °C for several hours yielding a solid (cellulose) and a lignin containing fluid (black liquid) fraction[34]. The lignin is partially cleaved and thiol groups are introduced in the lignin structure as shown in Figure 1.5 (*left*). Traditionally the lignin is precipitated by neutralization of the black liquor. Kraft lignin is water-insoluble and its molecular mass is lower than that of the original lignin[8]. The lignin is further redissolved in water and acid to overcome conventional filtering and sodium separation problems.

An additional technology for the extracting high quality lignin from a kraft pulp mill is the LignoBoost processes. The lignin is obtained by the evaporation of the black liquor and its neutralization with CO_2[35].

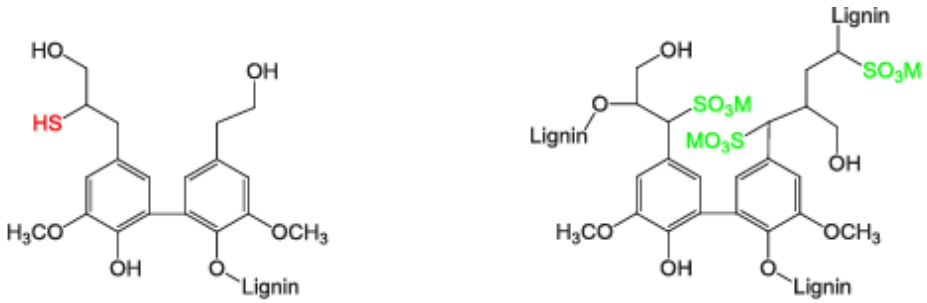

Figure 1.5: Simplified structures of Kraft lignin (*left*) and lignosulfonate (*right*)

1.3.2.2 *Sulfite process lignin*

Lignosulfonates are produced through the so-called sulfite process. These processes consist on the impregnation of biomass with and aqueous solution of sulfur dioxide at different pHs. Sulfonate groups are incorporated within the lignin structure (Figure 1.5, *right*) yielding a water-soluble lignin[33].

1.3.2.3 *Organosolv lignin*

In the organosolv process lignin is extracted from biomass in the presence of an organic solvent (e.g. ethanol) or a mixture of water and an organic solvent. The process is conducted at high temperatures and pressures[24]. Organosolv pulping or fractionation enables the production of high quality cellulose and lignin[20]. This type of lignin has a less modified structure than Kraft lignin and is largely sulfur-free. To date, only Alcell® and Organocell lignins are commercially available[24].

1.3.2.4 *Steam explosion*

This process consists of two main stages. First wood is treated with steam at high temperatures (between 180 °C and 240 °C) and pressures (1 to 3.5 MPa) for short reaction times. Then, the pressure is reduced rapidly and the biomass explodes at atmospheric pressure in the presence of different chemicals. The sudden pressure release defibrillates the cellulose bundles making the cellulose more accessible for subsequent hydrolysis treatments[8]. Lignin is later recovered as the solid residue from the combination of the steam explosion and hydrolysis processes. The nature of the steam exploded lignin is highly hydrophobic, with a low level of carbohydrate and wood-extractive impurities. Its molecular mass is relatively low since some acid hydrolysis of lignin takes place during the steam explosion process[24].

1.3.2.5 *Alkali-pulping lignin*

Soda pulping is the most common technology to produce alkali-pulping lignin. Soda (NaOH) is used as the main pulping chemical although other additives such as anthraquinone might be used to decrease the carbohydrate degradation. In soda-pulping lignin is recovered by and alternative recovery process consisting in an acid precipitation-maturation-filtration process. This type of lignin is sulfur-free[36-37].

1.3.2.6 *Acid-hydrolysis lignin*

Dilute and concentrated acid treatments are among the most effective pretreatment methods for the fractionation of lignocellulosic biomass. Both inorganic and organic acids such as sulfuric, oxalic or per-acetic acid can be used[38]. Depending on the concentration of the acid used in the process, the acid fractionation methods are divided into weak and strong acid hydrolysis.

Strong hydrolysis of biomass is normally conducted in the presence of strong and concentrated mineral acids (e.g. H_2SO_4, H_3PO_4 or HCl) at temperatures lower than 160 °C. Batch reaction systems are preferred and high biomass loading can be processed, between 10 and 40 % in weight[39-40]. However, this process requires large amounts of acids causing corrosion problems to the equipment. Very little is known about the structural change of the lignin upon the acid hydrolysis process. Evstigneyev et al.[41] studied the structure of a lignin produced by the industrial acid hydrolysis in a H_2O_2-H_2SO_4 system. This process leads to an opening of aromatic rings and probable formation of muconic acid derivatives. However, the chemical process has little effect on alkyl-aryl ether linkages (β-O-4 bonds) between lignin phenyl-propane subunits.

Dilute acid treatment is considered as a cheap and effective pretreatment method due to the low cost and easy availability of the acids[38]. The method is especially suitable for the fractionation of biomass with low lignin content[42]. In general, dilute sulfuric acid is sprayed on raw biomass which is then heated up to 160-220 °C for few minutes. Low acid (e.g. concentration of H_2SO_4 < 4 wt.%) and biomass (around 5-10 %)[43] concentrations are used. Unlike for strong acid hydrolysis, only hemicelluloses are completely converted into sugars and other organic compounds

(e.g. furfural and HMF), whereas cellulose and lignin are unaffected[38]. The dilute acid hydrolysis of biomass is often combined with enzymatic hydrolysis to produce fermentable carbohydrates for the production of bio-ethanol. During acid hydrolysis of biomass, lignin can undergo chemical and structural changes, the most relevant being the cleavage of a fraction of the β-O-4 and the shift of the S/G units ratios[42].

1.3.2.7 *Enzymatic-hydrolysis lignin:*

As mentioned above enzymatic hydrolysis of biomass is normally performed after a first steam explosion or dilute hydrolysis step. In enzymatic hydrolysis, cellulolytic enzymes are used to hydrolyze the carbohydrate fraction, leaving behind a cellulose-enzyme-lignin residue. This process occurs at mild conditions producing some slight structural changes in lignin: decrease of the phenolic hydroxyl group content, increase of the β-O-4 linkages and increase the molecular weight of lignin[44]. In addition, enzymatic hydrolyzed lignin contains a considerable amount of protein and carbohydrate impurities[45].

1.4 Lignin catalytic conversion

As mentioned in the previous section, lignin is a highly stable and cross-linked biopolymer with distinct chemical and physical properties depending on the botanical species and the pretreatment method used for its isolation. Numerous strategies have been investigated for the valorization of this raw material into fuels and chemicals; however, valorization of lignin still remains as one of the most challenging tasks in the development of the bio-refinery concept.

In the present section the most recent advances in the catalytic valorization of lignin with heterogeneous catalysts will be summarized. Among the catalytic methods, reductive lignin processes will be analyzed further in detail. The summary is based on a recent published review on catalytic conversion of lignin for fuels and chemicals[8]. Five main conversion techniques will be described: Hydrolytic methods (both basic and acid catalyzed), pyrolytic methods, liquid-phase methods, oxidative methods and reductive or hydro-processing methods. In most research papers, lignin model

compounds have been used in an attempt to decrease the complexity of the reaction system.

1.4.1 Hydrolytic methods

Hydrolytic methods can be further divided regarding the type of catalyst used (i.e. acid or base). Base-catalyzed de-polymerization (BCD) refers to those lignin conversion processes were a base is used as the catalyst. The main advantage of these methods is their ability to produce simple aromatic chemicals under mild conditions[8]. Traditionally, cheap and commercially available bases such as LiOH, NaOH and KOH are used. The base is able to catalyze the cleavage of the weaker ether bonds in lignin, yielding aromatic-rich oil and high amounts of organic solid products[46-48]. However, the quality of the oil obtained with such processes is low and additional bio-oil up-grading steps are required[49]. Other types of catalysts such as organic bases or homogenous metal catalysts have been extensively studied[8, 50]; however, the development of heterogeneous basic catalysts has attracted little attention. Bata et al.[51] studied the conversion of Kraft lignin into aromatics in the presence of MgO-modified La_2O_3, CeO_2 and ZrO_2. MOF-based catalysts or chemically modified layered double hydroxides (LDHs) are two of the most recently studied heterogeneous based-catalysts[49, 52].

Acid-catalyzed conversion of lignin, on the other hand, refers to those techniques were the catalyst is of acid nature. Homogeneous mineral acids (e.g. HCl) and several homogeneous Lewis acids ($FeCl_3$, $ZnCl_2$, BF_3 and $AlCl_3$) have been used extensively for the acid-catalyzed conversion of lignin[53-55]. In the last years, acidic ionic liquids have proven to be effective catalysts for the cleaving of the β-O-4 bonds; however, their high cost, downstream separation issues and high viscosity hampers their use on a commercial scale[8, 56-57]. Little research has been carried out on the catalytic conversion of lignin with solid acids; different types of alumino-silicates being among the most studied solids[58].

1.4.2 Pyrolytic methods

This concept differs from the above described biomass pyrolytic platform. Pyrolysis of lignin refers to the rapid heating of this biopolymer at high temperatures (450-600 °C) often in the absence of oxygen. Catalytic pyrolysis of lignin has been widely studied for the direct conversion of lignin into bio-oil. The product consists of a non-condensable gas mixture, a low quality and high viscosity bio-oil and a fraction of organic solid products[59]. The proportion of each pyrolysis product depends on the process variables; for example, in the case of fast pyrolysis the production of bio-oil is favored [60-61].

In lignin pyrolysis, catalysis is applied to tune the product distribution towards the production of hydrocarbons[62-63]. Zeolites (e.g. HZSM-5 and H-USY) are the preferred catalyst used in fast pyrolysis for this aim[64-66]. Zeolites have two main effects in the process: their acid sites can catalyze the de-polymerization of lignin into desirable and stable products, while their porous structure prevents the re-polymerization of the reaction intermediates. Still, catalytic pyrolysis presents some drawbacks: (i) low oil yields, (ii) rapid catalyst deactivation due to intense charring and (iii) instability of the zeolites under hydrothermal conditions[8, 67]. That is why recent investigations center their attention on improving the activity and hydrothermal stability of zeolites by chemical modification (Ce, Na) and/or by tuning their synthesis methods[8, 68].

1.4.3 Liquid-phase or steam reforming methods

The liquid-phase reforming (LPR) refers to the conversion of lignin at low temperatures in the presence of a solvent, enhancing the heat and mass transfer and thus improving the process homogeneity and selectivity. The main differences of LPR with respect to pyrolysis are the use of the solvent and the milder reaction temperatures[69]. Various liquids and liquid mixtures such as water, ethanol/water, supercritical ethanol and liquid ammonia have been used in LPR of lignin at low/moderate pressures[70-75]. Ethanol and ammonia can easily dissolve the lignin feedstock although water is normally preferred for its low cost and green nature. Very

little work has been done in catalytic LPR. Jongerious et al.[76] developed a sequential approach consisting of a first catalytic LPR step on an ethanol/water media in the presence of a Pt/Al_2O_3 catalyst. Ekhe et al.[77] demonstrate that lignin could be efficiently converted on subcritical methanol in the presence of H-ZSM5. In many cases liquid-phase methods are conducted in reductive environments; these methods are further discussed in *Section 1.4.5*.

1.4.4 Oxidative methods

Oxidative methods rely on different oxidizing agents -O_2, H_2O_2, nitrobenzene and metal oxides- to cleave aryl ether bonds, carbon-carbon bonds, aromatic rings or other linkages within lignin. The oxidative de-polymerization of lignin focuses on the production of poly-functional aromatic compounds[8]. A wide variety of aromatic aldehydes and carboxylic acids can be obtained through the catalytic oxidation of lignin: vanillin, syringaldehyde, muconic acid, etc.

Base and acid catalysts do not only act as efficient reagents for lignin hydrolysis; they also exhibit remarkable activity in lignin oxidation. In the case of the base catalyzed oxidation, NaOH, KOH and Na_2CO_3 are typically used[78-80]. The acid-catalyzed oxidation of lignin mainly focuses on the production of vanillin from Kraft lignin[81-82]. Polyoxometalate $H_3PMo_{12}O_{40}$ is one of the most active homogenous catalysts investigated for the oxidative lignin conversion.

Homogeneous catalysis with metal salts are also widely used for the selective oxidation of lignin and lignin model compounds. Methyltrioxo rhenium (MTO), salen complexes, biomimetic metal complexes, metal-free organo-catalytic systems and other type of metal salts have been investigated for this purpose[21, 83-87].

In photocatalytic and electrocatalytic oxidation of lignin, on the other hand, heterogeneous catalysts are preferred over homogeneous. Heterogeneous photocatalysis has been explored as a way to minimize the organic pollutants in the gas al liquid phases[88-89]. The TiO_2- based catalysts are the most frequently used oxides because of their high activity, chemical stability, commercial availability and low cost. Other semiconductor materials such as ZnO_2 and CdS have also been used.

The photo-oxidative lignin conversion is initiated when TiO_2 absorbs ultraviolet (UV) light[8].

In electrocatalytic oxidation IrO_2-based electrodes were originally studied for the conversion of lignin into mainly vanillin and vanillic acid[90]. Non-IrO_2-based electrodes such as Ti/TiO_2NT/PbO_2[91] and more complex systems such as flow cells bearing Ni, Au and PbO_2 anodes have also been studied[92]. Ionic liquids are used as electronic mediator systems due to their high conductance, and in some cases, their potential to solubilize lignin. Despite the potential of this electrochemical technique, the high cost and the electrode fouling issues limit its industrial application[8].

1.4.5 Reductive methods

Reductive lignin conversion is one of the most popular and efficient strategies applied in deconstruction of lignin into components such as phenols and other valuable chemicals. It is also a widely used strategy for the upgrading of lignin derived bio-oils and the production of hydrocarbons from lignin compounds. The method involves the thermocatalytic reduction of lignin in the presence of hydrogen (hydroprocessing) or a hydrogen donor molecule (e.g. formic acid, iso-propanol, tetralin)[8]. Hydrogen donor molecules are thought to convert lignin through catalytic transfer hydrogenation mechanisms or act as an in situ hydrogen source for lignin hydroprocessing[93-94]. In some cases a solvent is used to improve the heat and mass transfer rates and enhance the miscibility of the reaction mixture[93, 95-96]. Low molecular weight alcohols, such as ethanol, methanol and isopropanol, ionic liquids and water are among the preferred choices[8]. Alcohols can also act as hydrogen donor molecules as reported in the literature[95].

The type of catalysts used in the reductive methods can be classified into: (i) iron-group-based catalysts, (ii) the group VI metal-based catalysts, (iii) the platinum-group-based catalyst, (iv) bimetallic catalysts and (v) bifunctional catalyst. These metal-based systems can catalyzed a wide variety of reductive reactions among which hydrogenolysis, hydrodexoygenation and hydrogenation are the most relevant.

1.4.5.1 *Hydrogenolysis*

Lignin hydrogenolysis reactions involve mainly the cleavage of etheric C-O bonds[95]. For the conversion of lignin into bio-oil, the selective hydrogenolysis of aliphatic C-O bonds over aryl C-O is preferred. The latter are way more stable bonds and they demand higher temperatures and/or pressures for their cleavage. This reaction usually takes place in the presence of supported metal catalyst such as Pt, Ru, Ni, Pd, and Cu[97-98]. In the case of real lignin feedstock, the addition of tiny amounts of mineral acids or solid acids enhances the de-polymerization efficiency and allows its conversion at milder reaction conditions[99-100].

Ni-based catalysts -both in homogenous and heterogeneous forms- have been the most widely used type of catalysts for lignin hydrogenolysis[101]. Heterogeneous Ni in the form of Raney nickel or supported over metal oxides and activated carbons have been systematically investigated[102-104]. The introduction of a second metal in the supported Ni catalyst has been proven to be an effective strategy to enhance their activity. Zang et al.[105] proved that carbon supported Ni-W_2C can convert not only cellulose but also lignin yielding 46 % of monophenols. Similar synergistic effects have also been reported for Ni-TiN, NiAu, NiRh, NiRu, NiPd bimetallic systems[106-108].

The more expensive platinum-group metals (PGMs) exhibit even higher intrinsic activities than Ni and therefore are widely used in direct hydrogenolysis of raw and pretreated lignins. Generally mild conditions are preferred to avoid ring hydrogenation and thus preserve the aromatic nature of the resulting bio-oil[109]. PGMs have been supported on a wide variety of inorganic oxides (e. g. Al-SBA-15, Al_2O_3) and activated carbon supports[8].

1.4.5.2 *Hydrodeoxygenation*

Hydrodeoxygenation (HDO) involves the simultaneous addition of hydrogen and removal of oxygen from the lignin and lignin model compounds. It is considered the most efficient method for the up-grading of lignin bio-oil, but is also used in the direct lignin conversion[8]. In conventional HDO the conversion of lignin proceeds through two main routes: hydrogenation-deoxygenation or direct deoxygenation[110-111]. The

HDO catalysts can be divided in three different types: monometallic, bimetallic and bifunctional.

Mo-based *monometallic catalysts* in their oxide, sulfide, nitride and carbide forms have been studied for the HDO reaction of lignin and lignin model compounds since the 80s. Smith et al.[112] proved that the MoP is the more active for the HDO of 4-methylphenol followed than the MoS_2, MoO_2, and MoO_3 phases. Additional transition metal phosphides and sulfides (e.g. Ni_2P, Fe_2P, Co_2P, WP and FeS_2) and noble metals supported over a wide variety of solids (e.g. Al_2O_3, SiO_2, zeolites ZrO_2, activated carbon, zeolites) have also been studied[8]. Platinum group metals alone, however, are not good catalysts for the HDO of lignin model compounds if the aromatic nature is to be retained[113]. Most of the studies that focus on the HDO of lignin are, however, carried out over lignin model compounds; thus, the HDO of real lignin with *monometallic* catalysts has not been deeply investigated.

The addition of a second metal to the catalytic system -*bimetallic systems*- offers the possibility to improve the stability and activity of the catalyst and to tailor its selectivity to a particular product[8]. Some reports report that the addition of Co or Ni to Mo catalyst could strongly enhance the direct deoxygenation pathway versus the hydrogenation-deoxygenation pathway[110], while others reported that the improvement of HDO performance can be attributed to the enhancement of demethoxylation and deoxygenation pathways[114-115]. Traditionally mixed sulfides of Co, Ni, Mo, and W are the most used HDO catalysts[8]. Other *bimetallic catalyst* systems, such as PtSn [116], PtRh [117], NiRe [118], PtRe [119], and ZnPd [120] have also been evaluated in the lignin HDO. However, there are still several challenges to overcome: (i) the deactivation of the catalyst due to acid-catalyzed carbon deposition[121], (ii) the deactivation of the sulfur phases due to the high oxygen content of the bio-oil [122] and (iii) the unknown effect of the lignin impurities on the catalyst activity[8].

Bifunctional catalysts containing both metal and acid components were developed to solve the deactivation problem of the conventional sulfide-based HDO catalysts. Unlike in HDO, in bifunctional catalysis metal-catalyzed hydrogenation and acid catalyzed hydrolysis/dehydration are supposed to couple together [123-125] [126-127].

Several combinations of hydrogenating (e.g. Ni Raney, Pd/C, Pt/Al_2O_3) and Brønsted solid-acid catalysts (e.g. HZSM-5 and $Nafion/SiO_2$)[128-130]; or even bifunctional hydrogenation/hydrolysis catalysts (e.g. Ru/HZSM-5, Ni-HZSM-5)[125, 131] have been studied.

1.4.5.3 *Hydrogenation*

Hydrogenation is a chemical reaction which employs a pair of hydrogen atoms to reduce or saturate organic compounds increasing their H/C ratio. Generally, hydrogenation occurs together with hydrogenolysis and deoxygenation (HDO) in lignin conversion and bio-oil upgrading processes. The selectivity for hydrogenation toward the type of bond (i.e. aromatic C=C, linear C=C or C=O) varies drastically depending on the nature of the catalyst[132]. For example, zerovalent metals (Al, Fe, Mg, and Zr) are suitable catalysts for the selective hydrogenation of the C=O groups at ambient temperature and pressure and are widely used to increase the chemical stability (pH) of the bio-oil[133].

Other advanced approaches for the hydrogenation of lignin derived components have recently been reported. A catalytic tandem strategy was recently developed were noble- based supported catalysts such as Ru/C and Pt/C were employed to hydrogenate pyrolysis oils into polyols and alcohols. These were later converted into light olefins and aromatic hydrocarbons over zeolites [134]. Pang and co-workers[135] reported the effective hydrogenation of naphthalene into tetralin in the presence of noble pseudo-precious metal Mo_2C/C prepared via microwave irradiation. Electrocatalytic hydrogenation is a new technique that has been recently developed for the stabilization and upgrading of biomass-derived bio-oil. Ru/C [136] and RANEY Nickel [137]were proven to be effective cathodic catalysts for the hydrogenation and partial HDO of phenolic compounds.

In summary, most of the hydroprocessing catalysts described in this section consist of a metal –or a bimetallic system- and a metal oxide or activated carbon support. Ni, Co and noble metals alone or in combination mainly with Mo and W are the preferable metallic systems; whereas in the case of the support, metal oxides with

acidic properties are preferred. These catalyst formulations are repeated for all the hydroprocessing reaction types described above.

Thus, in lignin catalytic reductive methods hydrogenolysis, HDO and hydrogenation (even hydrolytic cleavage of lignin) might occur simultaneously in the so-called "integrated lignin hydrogenprocessing". Hence, a catalyst that exhibits high activity for all the reactions involved in the integrated lignin hydroprocessing would be the preferred candidate. This integrated approach will not only benefit the economy of the system, but also increase the possibility to scale up lignin conversion processes.

1.5 Lignin-to-Liquid concept (LtL)

A promising and relatively new lignin reductive conversion methodology is the Lignin-to-Liquid (LtL) process. In the LtL process the lignin is converted at moderate temperatures in the presence of two additional compounds: (i) *formic acid* (FA) as a substitute of molecular hydrogen, and (ii) a solvent, mostly ethanol or water.

Formic acid has been proved to be more active than molecular hydrogen in the reductive conversion of lignin[138]. This hydrogen donor molecule decomposes mainly into molecular hydrogen and CO_2 under the LtL conditions creating a reductive environment (low amounts of CO and H_2O are also produced). Most of the researchers believe that formic acid act either as an *in-situ* hydrogen source or a hydrogen donor molecule through catalytic-hydrogen transfer reactions[93, 96, 138-140]. However, its role in the lignin conversion process is not fully understood and there are no published mechanisms that can explain why formic acid is more active than other hydrogen donors.

The *solvent* is added to create a more homogeneous reaction environment and increase the mass and heat transfer rates. This allows operating at milder reaction conditions and increases the selectivity towards the production of bio-oil. *Water* is considered as a promising reaction media due to its abundance, low cost and green nature, although it has a low ability to solubilize most type of lignins. *Ethanol* has also been identified as one of the most promising alternatives due to is very good solvent

properties for biomass and low critical temperature; furthermore, it is one of the main fuel type products obtained from the conversion of lignocellulosic feedstock. Other alternatives such as iso-propanol and methanol have been studied as well[138].

Overall, the LtL-reaction system combines de-polymerization, deoxygenation and hydrogenation of the biopolymer in one step. Lignin is mainly converted into a liquid and an organic solid fraction (Figure 1.6). Depending on the solvent used the liquid fraction consists of: (i) only one organic phase (ethanol), or (ii) a biphasic system (water) composed of a dark- brown organic phase and a water phase. The organic bio-oil has a high H/C and low O/C ratio and can be described as a complex mixture of aromatic monomers; typically alkylated phenols, guaiacols and catechols. Some low molecular weight hydrocarbons, esters and ketones that are thought to be derived from the bridging units of the polymer together with the solvents are also found; especially when using ethanol as solvent.

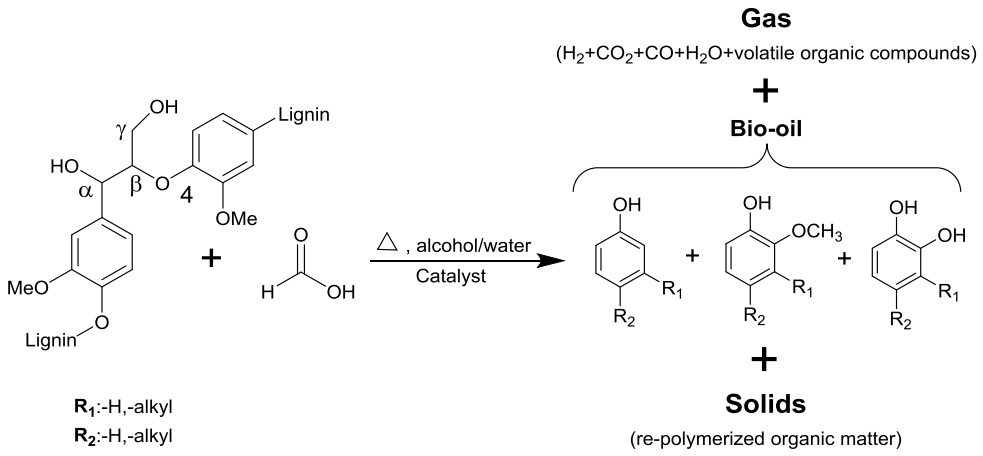

Figure 1.6: A simplified scheme of lignin and its degradation products in the LtL reaction approach

With temperatures typically of 350–400 °C and reaction times of 8–16 h, lignin from spruce, pine, birch and aspen wood has been converted into a chemically stable LtL bio-oil. Nevertheless, in order to make this bio-oil competitive with fuels and chemicals obtained from crude oil, some important process parameters need to be improved: (i) shorter reaction times, (ii) lower reaction temperatures and (iii) the

reduction of low-value side streams i.e., gas and solid phases. Additional strategies for the valorization of the low-value side streams such as the production of activated carbons from the solid products could also benefit the overall process economics.

1.5.1 Catalytic LtL conversion

One possibility to address these challenges is the use of heterogeneous catalysts in the process. As mentioned in *Section 1.4.5*, catalytic hydrotreatment of lignin has already been explored extensively and several catalysts have been evaluated mostly based on lignin model compounds. However, very little research has been carried out on the catalytic conversion of real lignin feedstock in a formic acid/solvent media:

- ✓ Ligouri and Barth showed that the reaction time and temperature could be reduced dramatically when using heterogenous a Pd/C catalyst together with Nafion SAC-13[100]. Nonetheless the use of two types of catalyst present some drawbacks form and industrial and economical point of view.

- ✓ In a similar approach alkali lignin was subjected to depolymerization in subcritical water at 265 °C in the presence of formic acid and a Pd/C catalyst. A maximum oil yield of 33.1 % was obtained when the lignin was reacted in the presence of formic acid alone[141].

- ✓ Jones et al.[140] studied the de-polymerization and hydrodeoxygention of organosolv switchgrass lignin in a formic acid/ethanol solvent. They claimed that the combination of formic acid and Pt/C promotes the production of lower molecular weight compound in the liquid products; after 20 h of reaction time the lignin was significantly depolymerized to form liquid products with a 76 % reduction in the weighted average molecular weight. The combination of formic acid and Pt/C is found to promote the production of larger fractions of lower molecular weight compound in the liquid products.

✓ Heeres et al. studied the catalytic conversion of Alcell® lignin in iso-propanol/formic acid mixtures in a batch set-up using Ru/C as the catalyst. Beside iso-propanol, ethanol and methanol in combination with formic acid were also explored. Lignin oils were obtained in good yields (71 % relative to lignin input) consisting on a mixture of mainly aromatics.

✓ Sanhua Huang et al.[142] studied a different solvent approach combining both water and ethanol (50/50 v/v) for the conversion of Kraft lignin. Several catalyst systems such as Ru/C, FHUDS-2 (W-Mo-Ni), Ni/Zeolite and Ni/Al_2O_3) were evaluated.

However, the aim of most of these studies was to evaluate the effect of individual catalyst in the final oil yield and quality. No systematic catalyst-screening approach has been conducted to evaluate the effect of the type of metal (base or noble metal) and nature of the support (activated carbon, Al_2O_3, ZrO_2) on the LtL conversion of lignin. Additional information on the effect of key reaction parameters (i.e. temperature and reaction time) in the oil yield and properties is also lacking. Furthermore, the specific role of formic acid in the LtL reaction mechanism and its synergistic interactions with the catalyst and the solvent has not been thoroughly investigated.

1.6 Objectives of the thesis

The aim of the thesis is to systematically explore the use of heterogeneous catalysts in the LtL conversion, and to develop new and improved catalyst formulations. Catalyst development is, however, a challenging task that involves previous fundamental knowledge of the specific chemical reaction and significant catalyst screening effort; a scientific background that was not available before this work was initiated. Basic studies on the role of formic acid in the LtL conversion mechanism have therefore also been included in this study.

Chapter 2. Experimental procedures & methods

The following chapter shortly introduces the general LtL experimental procedures and main analytical methods and tools used in this thesis. In the experimental section the LtL process and work-up procedure is summarized and a short description of the reaction systems, lignins and catalysts used is also presented. The method section, on the other hand, focusses on the catalyst and bio-oil characterization techniques employed and the mathematical data processing methods applied in this project.

2.1 Experimental procedures

In most cases- papers **A, B, D** and **E** - the LtL experiments were conducted in SS316 25 mL 4742 non-stirred Parr reactors. A detail description of the amount of reactants and the exact reaction conditions are given in the *Experimental Section* of each paper.

Briefly summarized: lignin, formic acid, the solvent and the catalyst (10 % by weight relative to the amount of lignin) were first added into the reactor. The Parr reactor was then heated in a Carbolite LHT oven to the desired temperature; the reaction time was monitored from the moment the reactor was introduced in the oven.

- Different type of lignins, solvents (mainly water or ethanol) and catalysts were evaluated in the course of the project. The type and nature of lignins and catalysts used are described in more detail later in the section.

After completed the reaction time, the reactor was cooled down to ambient temperature and the amount of produced gases determined by weighting the reactor before and after ventilating the gas. The reactor was opened and the liquid mixture extracted with a solution of ethyl acetate (EtAc): tetrahydrofuran (THF) (90:10). The solids (unreacted lignin, organic solid products and catalysts) were filtered off. The work-up procedure varied at this point depending on the solvent used:

- When *ethanol* was selected as the solvent the extracted mixture consisted of one organic dark-brown phase. In this case, the liquid phase was directly dried over Na_2SO_4.

- When *water* was selected as the solvent a two well-separated liquid phases were obtained, an organic top phase and an aqueous bottom phase. The phases were separated by decanting: the water phase was stored in a fridge while the dark-brown organic phase was dried over Na_2SO_4.

After dewatering the organic phase over Na_2SO_4, the solution was filtered to eliminate the solids and then concentrated at reduced pressure (at 40 °C) to yield a dark brown to black liquid. The yields were determined by weight and the oil and solids characterized by several analytic techniques that are further described in *Section 2.2*.

In paper **C** the LtL residual organic solids (hydrochars) were chemically activated to produce lignin derived magnetic activated carbons (MACs). Thus, large quantities of hydrochar had to be produced using a 5-L stainless steel reactor (ESTANIT GmbH). The experimental procedure is described in detail in paper **C.**

2.1.1 Experiments carried out at the University of the Basque Country (UPV-EHU)

Most of the experiments described in paper **F** were conducted in a 300 mL SS316 stainless steel stirred-reactor from Autoclave Engineers (Figure 2.1). Unlike the non-stirred 4742 Parr reactor, this reaction system had two gas inlets, a liquid inlet, a gas outlet, a liquid outlet, a stirring system, a heating mantle and a pressure and temperature control system. In addition, a Wilson HPLC 307 pump was connected to the reactor what allows feeding liquids at high pressures. This reaction system made it possible not only to pressurize the reactor with different gases (H_2, CO_2) but also to pump liquid mixtures (formic acid, ethanol) continuously into the reactor (Figure 2.1). A more detailed description of the different experimental procedures is described in detailed in paper **F**. The reaction time started when the mantle temperature reached the desired working temperature.

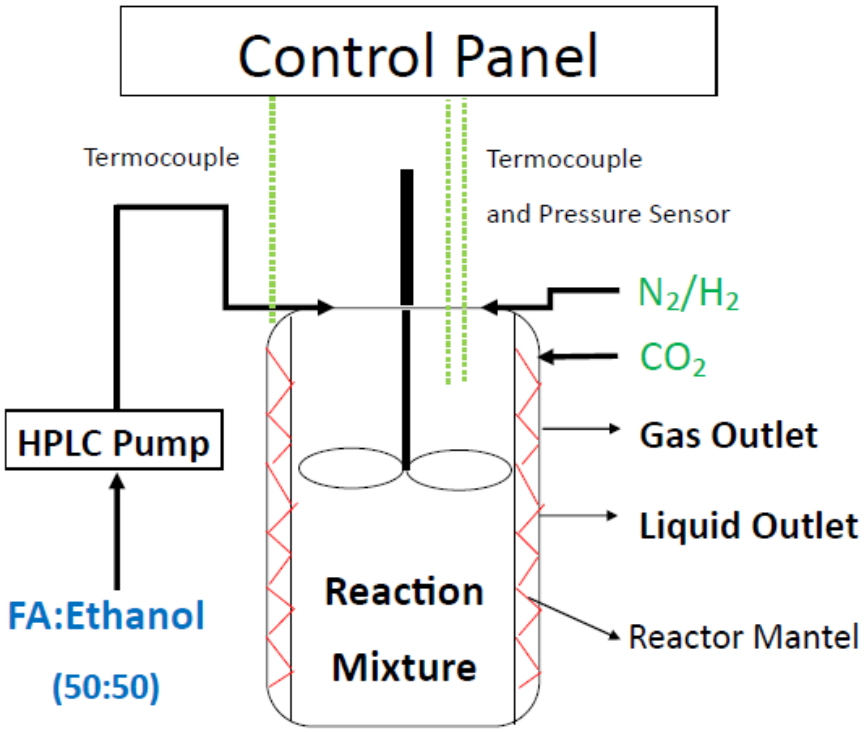

Figure 2.1: Schematic 300 mL stirred-reactor systems. **FA:** formic acid

2.1.2 Lignin starting materials

Various lignins from different botanical origin and isolation methods were employed in the course of the thesis. The elemental analysis and inorganic ash content is given in Table 2.1 The lignins are classified according to their botanical species and isolation method.

Table 2.1: botanic species, isolation method, elemental analysis and ash content of the lignin used in this work.

Lignin	Botanical species	Isolation method	Elemental analysis (wt. %)			Ash (wt.%)
			C	H	O	
KL	-	Kraft pulping process	48.1	5.1	46.7	-
AL	Norwegian Spruce	Strong acid hydrolysis	62.0	5.5	32.3	1.51
RL	Rice straw	Strong acid hydrolysis	46.1	5.0	33,4	14.9
EL	Norwegian Spruce	Weak acid hydrolysis + enzymatic hydrolysis	51.9	5.8	41.9	-
SL	Eucalyptus	Steam explosion + enzymatic hydrolysis	47,6	5,6	41,3	4.4

[a] Inorganic ash content

Kraft lignin (KL): a commercial low sulfonate alkali lignin (4 wt. % S content), namely KL, was purchased from Sigma Aldrich and used as bought. This lignin was used to evaluate the effect of the type of lignin in the catalytic LtL; the results are presented in paper **A**.

Strong acid hydrolysis lignins (AL and *RL):* the Technical College of Bergen provided two types of lignins of different botanical origin: Norwegian spruce and rice straw. They were obtained through strong acid carbohydrate dissolution biomass pre-treatment processes. In all cases, the lignins were ground, and sieved (<500 μm) prior to use.

- Lignin from Norwegian Spruce (Picea abies), namely AL, was the main lignin used for the evaluation of the effect of several process parameters; the results are present in papers **A** and **B**.

- Rice straw lignin (*Oryza sativa*), namely RL, was employed to evaluate the effect of different type of catalysts in the LtL process. The results are presented in papers **D** and **E** and *Section 3.2.3*.

Enzymatic hydrolysis lignins (EL and *SL):* two different providers supplied enzymatic hydrolysis lignins using different biomass pretreatment processes. Both lignins were ground, and sieved (<500 μm) prior to use:

- The Norwegian University of Life Science in Ås used a combination of weak acid hydrolysis and enzymatic hydrolysis process to obtain lignin from Norwegian Spruce (Picea abies), namely EL. The effect of the type of lignin was evaluated for the catalytic conversion of lignin; the results are presented in paper **A**.

- The bioethanol production facility, SEKAB, used a combination of steam explosion and enzymatic hydrolysis processes to isolate eucalyptus lignin, namely SL. This lignin was employed to investigate the role of formic acid in the LtL processes; the results are presented in paper **F**.

2.1.3 Catalyst screening

The activity of several types of catalyst was examined in the course of the Ph.D project. This can be summarized as follows:

✓ *Commercial catalysts purchased from Sigma-Aldrich:* Pd/Al2O3, Rh/Al2O3 and Ru/Al_2O_3 were used to evaluate the interaction of the catalyst and different process parameters such as temperature and reaction time. The results obtained are presented in papers **A** and **B**.

✓ C*atalyst synthesized* at the University of Bergen (UiB):

- NiMo catalyst supported on activated carbons: Ni and Mo were supported on a commercial activated carbon (AC) and two different type of magnetic activated carbons (MACs). The synthesis procedure and the results obtained are presented in paper **D**.

- NiMo catalyst supported on metal oxides: Ni and Mo were supported on different sulfated and non-sulfated γ-Al_2O_3 and ZrO_2. The synthesis procedure and the results obtained are presented in paper **E**.

- Ru on activated carbon (Ru-AC): an additional Ru-AC catalyst was synthesized to evaluate the effect of the type of metal, either noble or base metal, in the catalytic LtL. The synthesis procedure is further described in *ANEX I*.

2.2 Methods

2.2.1 Catalyst Characterization

In the present Section, a brief description of the chemical and physical fundaments of the most relevant catalyst characterization methods is given. Those less relevant or rarely used techniques are therefore not considered. The detailed experimental procedures employed are described in the *Experimental* and/or *Supplementary Information* sections in each paper.

2.2.1.1 *Physisorption of gases (N_2-adsorption)*

The physical adsorption, or physisorption, of gases is an analytical technique used to determine the textural properties of a solid. It is based in the interaction between a gas (adsorbate), N_2 in this case, and the solid that is being characterized (adsorbent). The result of this analysis is the adsorption-desorption isotherm. Its interpretation through different mathematical models allows obtaining the textural properties of the solid (e.g. specific surface area, total pore volume and pore size distribution). The *specific surface are*a is normally obtained at the intermediate pressure range and the preferred mathematical model for its determination is the so-called BET (Brunauer-Emmett-Teller) model. The *total pore volume refers* to the volume occupied by the adsorbate inside the adsorbent at a particular pressure; in this project it was defined as p/p_0=0.99. The *pore size distribution* is an indirect measurement obtained by applying more complex mathematical models. While models such as the Horvath-Kawazoe model (HK) or the Barret-Joyner-Halenda model (BJH) are only suitable to determine the pore size distribution of micropores or mesoporous, respectively; those models based on the density functional theory (DFT) can be applied to evaluate both micro- and mesopores simultaneously[143].

2.2.1.2 *X-ray powder diffraction (XRD)*

X-ray diffraction (XRD) relies on the dual wave/particle nature of X-rays to obtain information about the structure of crystalline materials. A primary use of this technique is the identification and characterization of compounds based on their diffraction pattern. X-ray diffraction is based on constructive interference of monochromatic X-rays and a crystalline sample. These X-rays are generated by a cathode ray tube, filtered to produce monochromatic radiation, collimated to concentrate, and directed towards the sample. The interaction of the incident rays with the sample produces constructive interference (and a diffracted ray) when conditions satisfy Bragg's law (Equation 2.1, Figure 2.2):

$$n\lambda = 2d\sin\theta \qquad \text{(Equation 2.1)}$$

where ***n*** (an integer) is the "order" of reflection, ***λ*** is the wavelength of the incident X-rays, ***d*** is the interplanar spacing of the crystal and ***θ*** is the angle of incidence.

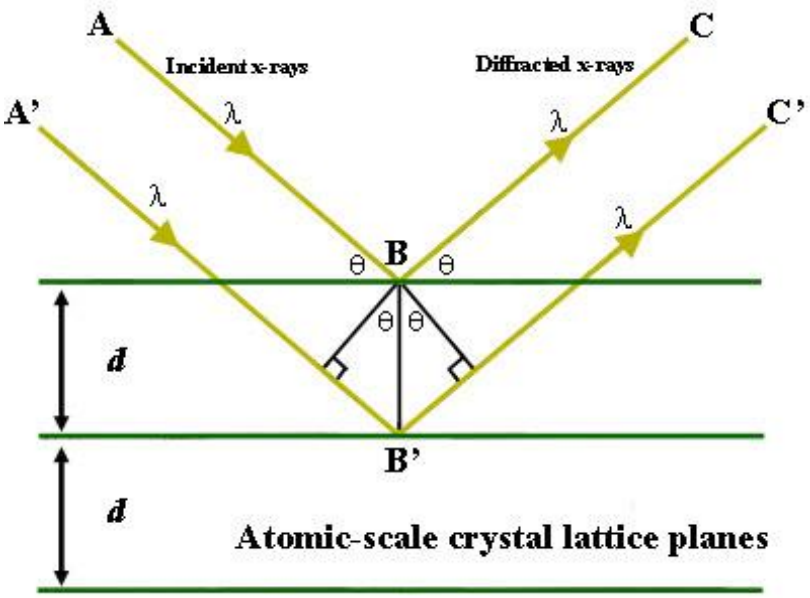

Figure 2.2: schematic representation of X-ray constructive interference[144]

In *X-ray powder diffraction* the sample is scanned through a range of 2θ angles; thus, all possible diffraction directions of the lattice are attained due to the random orientation of the powdered material. As the crystallites (coherently scattering domains, not necessarily the same size as the particles) get smaller, the diffraction peaks get wider, and if the crystallites get as small as 30-50 Å (3-5 nm) the peaks are hard to observe[145].

2.2.1.3 *Analysis of the surface acidity*

It is well known that the catalytic activity of solids and of some transition-metal oxides is essentially determined by the presence of surface acid sites. Consequently, studies on the nature of these sites and accurate determination of their amount and strength are of major importance[146]. In the present work the characterization surface acid sites was conducted through a combination of two analytical techniques: (i) *Fourier transform infrared spectroscopy (FT-IR)* of absorbed pyridine is preferred for the determination of the nature (Brønsted or Lewis) of acid sites while (ii) *temperature-programmed-desorption of ammonia (NH_3-TPD)* is preferred to determine their abundance and strength.

FTIR spectroscopy of adsorbed probe molecules is one of the most widely available and well developed methods for studying the composition and structure of the surface functional groups of supported metal catalysts. As the vibrational spectrum reflects both the properties of the molecule as a whole and the characteristic features of separate chemical bonds, FTIR spectroscopy offers the fullest possible information on the perturbation experienced by a molecule on contract with the solid surface, and often determines the structure of adsorption complexes and of surface compounds[147]. *Pyridine* is one of the most widely used probe molecules for the characterization of Lewis and Bronsted acid sites. Its vibration bands in the 1400-1600 cm^{-1} regions of the IR spectrum of the chemisorbed pyridine can distinguish between the Brønsted and the Lewis acidity[148].

NH_3-TPD is one of the most widely used and flexible techniques for determining the quantity and strength of the surface acid sites in a solid. During this analysis the sample is submitted to an increasing temperature with constant rate and it is swept by an inert gas such as helium, argon or nitrogen. The sample surface desorbs the NH_3 that has been previously chemisorbed and a suitable detector monitors the process (thermal conductivity detector (TCD) or mass spectrometer (MS))[149]. The greater the strength of the acid sites, the stronger is the adsorption of the ammonia and the higher is the corresponding desorption temperature. The amount and distribution of the surface acid sites –relative to their strengths- can also be determined through the analysis of the NH_3-profile intensity.

2.2.1.4 *Temperature-programmed-reduction (TPR)*

Temperature-Programmed Reduction (TPR) determines which are the reducible species present on the catalyst surface and reveals the temperature at which the reduction of each species occurs. An important aspect of TPR analyses is that the samples need not to have any special characteristics other than containing reducible metals. The TPR analysis begins by the flow of an analysis gas -typically hydrogen in an inert carrier gas such as nitrogen or argon- through the sample, usually at ambient temperature. While the gas is flowing, the temperature of the sample is increased linearly with time and the hydrogen uptake monitored[150].

This technique is used for the quantitative and qualitative determination of the supported mono- and bimetallic species [149]. It can provide evidence of the interaction between two different metallic species; furthermore, the area under the TPR peak reflects the concentration of that component in the catalyst surface[151]. It is also employed to find the most efficient reduction conditions[149].

2.2.1.5 *Inductively couple plasma atomic emission spectroscopy (ICP-AES)*

The ICP-AES technique, also referred as *inductively coupled plasma optical emission spectroscopy (ICP-EOS)* is widely regarded as the most versatile analytical technique in the inorganic chemistry laboratory. After dissolving the solid sample, the solution is introduced into the spectrometer and it becomes atomized into a mist-like cloud. This mist is carried into the argon plasma through an argon gas stream. The plasma (ionized argon) produces temperatures close to 7000 °C, which thermally excites the outer-shell electrons of the elements in the sample. The relaxation of the excited electrons as they return to the ground state is accompanied by the emission of photons of light with a certain energy characteristic of the element. Because the sample contains a mixture of elements, spectra of light wavelengths are emitted simultaneously. The spectrometer uses a grating to disperse the light, separating the particular element emission and directing each to a dedicated photomultiplier tube detector. The more intense this light is, the more concentrated the element[152].

In the present thesis this technique was used to determine the elemental composition of the catalysts and lignin ashes. Prior to the analysis the ashes and catalysts were dissolved in a mixture of different mineral acids in a microwave oven.

2.2.2 Chemical characterization of bio-oil products

The major bio-oil characterization techniques used for this work are described below. Less central characterization techniques such as FT-IR or *electrospray ionization-mass spectroscopy* (ESI-MS) are only described in the individual papers.

2.2.2.1 *Elemental analysis*

This technique was employed to determine the C, H and O content of the bio-oils. The N and S content was not considered in this thesis. The bio-oil sample is first placed in an oven and combusted in the presence of oxygen excess at high temperatures (900 °C). During combustion the C, H, N and S elements produce, in addition to molecular nitrogen, O_2, H_2O, NO_x, SO_2 and SO_3 gases. The combustion is carried out in the presence a tungsten trioxide catalyst, that binds alkaline or earth alkaline elements and

avoids non-volatile sulfates. The nitrogen oxides (NO_x) and sulfur oxides (SO_2/SO_3) are later reduced in to N_2 and SO_2 respectively in the present of copper; thus, the remaining gas stream contains only CO_2, H_2O, SO_2 and N_2. The gases are then separated in specific adsorption columns and each gas is individually analyzed by a thermal conductivity detector (TCD).

2.2.2.2 *Gas chromatography (GC)*

The separation of the individual components of gas and liquid mixtures is often performed using gas chromatography. The individual components are separated based on their volatility and their affinity to a stationary and mobile phase (chemically inert gas). The column containing the stationary phase is inside a heating chamber and is connected on one side to an injector system and on the other side to a detector. Typical detectors used in gas chromatography are flame ionization (FID), and the more simple thermal conductivity (TCD) detectors[153]. The former detector is preferred for quantifying the eluting compounds. In papers **A** and **B** a gas chromatograph coupled to a FID detector was used for the identification and quantification of several bio-oil components. The bio-oil was first silylated to facilitate the analysis.

Silylation is a derivatization technique consisting on the introduction of a silyl group substituent (R_3Si) by reaction with a specific functional group within a molecule; in this case to the hydroxyl substituents of the lignin mono-aromatics. The introduction of the silyl group gives derivatives with enhanced volatility and reduced polarity, making them more suitable for GC analysis. The compounds were identified and quantified with the aid of different silylated standards.

Most of the GC analyses were carried out in a chromatograph coupled to a mass spectrometry detector (GC-MS). Mass spectrometry (MS) detectors are descriptive detectors that consist of an ionization source, a mass separator and a mass analyzer. The ionized molecules fragment to give characteristic fragmentation patterns, the study of which can aid the identification of the parent molecules. In GC applications, the molecules are ionized when they elute from the column after chromatographic

separation. Large databases, enabling matching of such fragmentation patterns to parent molecules in a library based approach are widely established[153].

2.2.2.3 *Gel permeation chromatography- size exclusion chromatography (GPC-SEC)*

Gel permeation chromatography (GPC) is a term used for a type of size exclusion chromatography (SEC) that separates analytes on the basis of size. Although normally applied to the characterization of polymers, this method is also widely used in the characterization of lignin derived bio-oils[154].

GPC-SEC uses the liquid present in the pores of beads as the stationary phase, and a flowing liquid as the mobile phase. The separation of the components within the mixture occurs via the use of porous beads packed in a column (Figure 2.3, *left*). The smaller analytes can enter the pores more easily and therefore spend more within pores, increasing their retention time. Conversely, larger analytes spend little if any time in the pores and are eluted quickly, thus showing the distribution of molecular sizes in the sample[155]. As the components exit the column they are detected (e.g. by an UV-detector) and the elution behavior of the sample is displayed in a chromatogram. The time it takes for a group of molecules of the same size (a fraction) to emerge from the column is called its retention time.

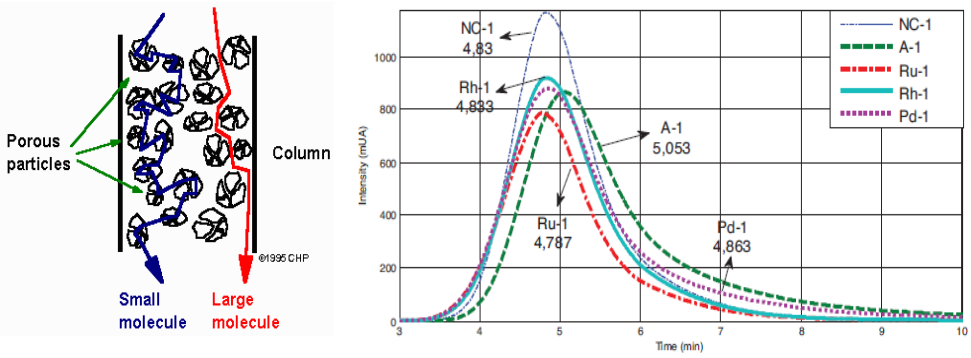

Figure 2.3: Graphical representation of a GPC-SEC column (*left*)[156] and a typical GPC-SEC chromatogram of a selection of lignin derived LtL bio-oils labeled by the type of catalyst used for its production (*right*)[36]

When a bio-oil is analyzed by GPC-SEC the chromatogram consist in most cases of a broad and asymmetric single peak (Figure 2.3, *right*). By comparing its retention time -the point at which peak shows its maximum height- with a calibration curve of previously analyzed standards, the average molecular weight of the mixture (M_w) can be calculated. This value represents a rough indirect measurement of the depolymerization degree achieved during the lignin conversion process. The analysis of the peak shape can provide additional information about the molecular weight distribution of the bio-oil sample.

2.2.3 Chemometric evaluation of LtL reaction systems

2.2.3.1 *Experimental design (DOE)*

Screening of many variables with a limited amount of experimental effort, and to extract the maximum possible amount of information from a limited set of experiments, is the first step in a sequential chemometrics approach[153]. The design of experiments (DOE) is an efficient procedure for planning the minimum amount of experiments needed so that the data obtained can be analyzed to yield valid and objective conclusions[157]. Coupled with statistical and mathematical evaluation, DOE can be used to establish relationships among input and response variables optimize different reaction parameters and evaluate if a certain input factor has a significant effect in the system.

When applying design of experiments (DOE), choosing the most adequate design is a crucial aspect that depends largely on the type of reaction system studied and the focus of the investigation[153]. Full-factorial designs, for example, allow complete and systematical evaluation of the interaction between all the input variables, whereas other designs, such as the Plackett-Burman design, are preferred for screening purposes when only the main effects are of interest. Within this thesis, *DOE* was used to evaluate the effect of the type of catalytic system, temperature and reaction time on several response factors. In paper **B**, a two-level-full-factorial design was first used for catalyst-screening purposes; while in a later step process, optimization was conducted based on a central composite design (CCD).

2.2.3.2 *Response surface methodology (RSM)*

Response surface Methodology (RSM) is a set of mathematical and statistical techniques that can be used to define the relationships between the input and response variables[158]. The experimental data is used to derive an empirical (approximation) model allowing a more graphical (Figure 2.4) and quantitative interpretation of the main effects in the reaction system.

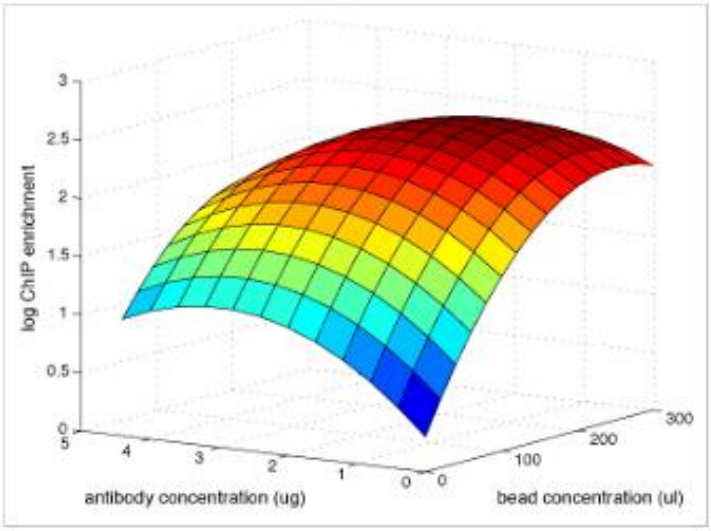

Figure 2.4: Graphical representation of a second-order regression model[159]

Depending on the goal and the complexity of the system simpler or more complex regression models can be built. For example, for screening purposes less data demanding first-order models (linear) with interaction terms are the preferred choice. However, often in more complex systems, quadratic terms need to be considered in order to build statistically significant regression models. In those cases second-order regression models (quadratic) are the best option. In paper **B**, both linear and quadratic regression models with interaction factors were built, the former for catalyst screening purposes while the latter for optimization purposes.

2.2.3.3 *Principal Component Analysis (PCA)*

PCA is a mathematical procedure that allows visualizing correlations between sets of independent and dependent variables. In PCA, a new set of linear combinations of orthogonal vectors with suitable vector parameters describe the variance present in the dataset. The new vectors, or principal components (Figure 2.5), are oriented along the maximal residual variance in the data and are completely dependent on the data set[153, 160]. The goal is to explain the maximum amount of variance with the fewest number of principal components.

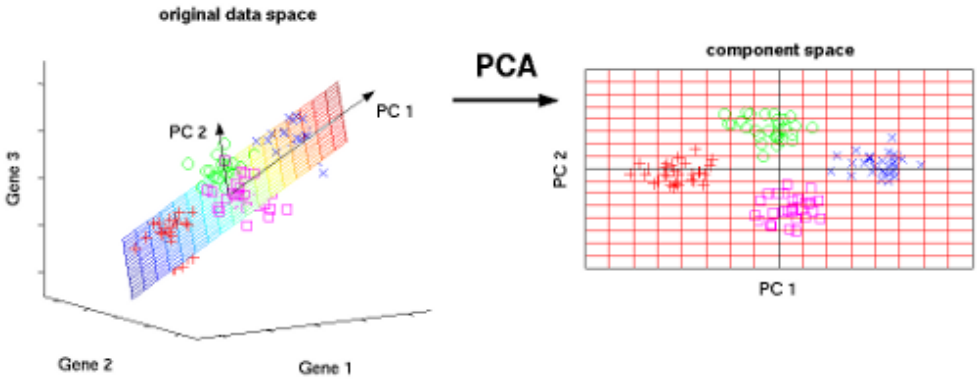

Figure 2.5: graphical representation of PCA procedure[161]

PCA has been already used in the past to discriminate the effect of reaction conditions and reactant concentrations in the properties of the LtL oils[162] . In paper **B**, PCA was used to evaluate the possible correlations among several process parameters (type of catalytic system, reaction temperature and time), and response variables (oil and solid yields, and several properties that define the quality of the oils such as H/C ratio, O/C ratio and average molecular weight (M_w)).

Chapter 3. Summary & main results

This chapter summarizes the main results of the attached papers presented in Part II. To simplify the reader´s understanding of the overall work approach strategy, the papers have been grouped and their presentation subdivided into three sections.

Section 3.1 focuses on the catalytic LtL conversion in *water media* and includes papers **A** and **B**. The activity of three different noble metal catalysts (i.e. Rh/Al_2O_3, Pd/Al_2O_3 and Ru/Al_2O_3) is evaluated. In addition, the influence of several other reaction parameters on the LtL results is investigated using in some cases experimental design and chemometric approaches.

In *Section 3.2* different metal-support catalyst combinations are investigated in the LtL conversion in *ethanol media* and includes papers **D** and **E**. The investigated catalyst can be grouped into: (i) NiMo catalyst on magnetic activated carbons (*Section 3.2.1*), (ii) NiMo on metal oxide catalysts (*Section 3.2.2*) and (iii) a Ru on carbon (Ru-AC) catalyst (*Section 3.2.3*).

One off the key characteristic of the LtL conversion is using formic acid as a substitute of molecular hydrogen or a different hydrogen-donor molecule. Our previous experience suggests that formic acid is the most active hydrogen source for the conversion of the lignin bio-polymer; however, the reason behind this higher activity is not fully understood. Thus, in *Section 3.3*, the role of formic acid in the complex LtL system is addressed (Paper **F**). Additional aspects such as the role of the catalyst, the type of solvent and their synergistic interactions with formic acid are also discussed.

3.1 Water System

The development of stable and active heterogeneous catalysts is a challenging task that involves both fundamental knowledge of the specific chemical reaction and extensive experimental effort (i.e. catalyst screening). The LtL process, however, is a relatively novel and intricate reaction system and limited number of heterogeneous catalysts have been evaluated for it (*see Section 1.5.1*). Moreover, most efforts focused on the effect of such catalysts on the oil yield and properties paying little attention to the synergistic interactions between the catalysts and the other process variables (e.g. type of catalyst, temperature and reaction time).

Therefore, the effects of several process parameters on the catalytic LtL reaction were first evaluated to gain fundamental understanding of this complex reaction system. These initial tests were carried out in a formic acid/water media in non-catalyzed systems and in the presence of γ-Al_2O_3 and different *commercial catalysts* (Ru/Al_2O_3, Rh/Al_2O_3 and Pd/Al_2O_3). Noble metal base catalysts were selected since other base metals such as Ni and Mo proved to be inactive in water media[163]. The results are presented in papers **A** and **B**.

The composition of the feed was held constant for all the experiments described in this section. Lignin from strong acid hydrolysis of Norwegian spruce was used if not otherwise specified. The aluminas used to synthesize the different *commercial catalysts* were not of the same nature; hence, their acid properties were characterized by NH_3-TPD and FT-IR of absorbed pyridine to evaluate the effect of the support acidity in the LtL reaction. Additional experiments using only γ-Al_2O_3 as a catalysts and non-catalyzed experiment were also carried out.

In paper **A**, the effect of several process parameters on the oil, solid and gas phases were investigated. The yields and characteristics of the oil, solid and gas phases were highly dependent on the reaction conditions, type of lignin and the presence of γ-Al_2O_3 or of a *commercial catalyst*. The bio-oil contained mainly monoaromatics such as phenol, cresol, guaiacol, methylguaiacol, catechol, ethylcatechol, syringol and *o*-vanillin. The most relevant results are summarized below:

- ✓ Effect of the *commercial catalysts* (Ru/Al_2O_3, Rh/Al_2O_3 and Pd/Al_2O_3): The presence of the catalysts considerably increased the oil yield while decreasing the amount of solid products (hydrochar). The bifunctional catalysts simultaneously increased the de-polymerization rate of the lignin biopolymer and the hydrodeoxygenation (HDO) rate of the depolymerized lignin monomers. The oil yield increase was believed to be a consequence of the kinetic control induced by the *commercial catalysts* in the lignin degradation pathway (Figure 3.1). The stabilization of the depolymerized lignin monomers through HDO reactions (k_2) decreased their re-polymerization tendency hindering the production of solid products; the re-polymerization rate of the primary monomers (k_3) is faster than the re-polymerization rate of the HDO monomers (k_4)[96]. However, later studies proved that the higher bio-oil yields obtained in the presence of the catalysts is mainly due to the their activity in the formic acid aided aliphatic ether bond cleavage, as described in *Section 3.3*. This is further discussed in *Chapter 4*.

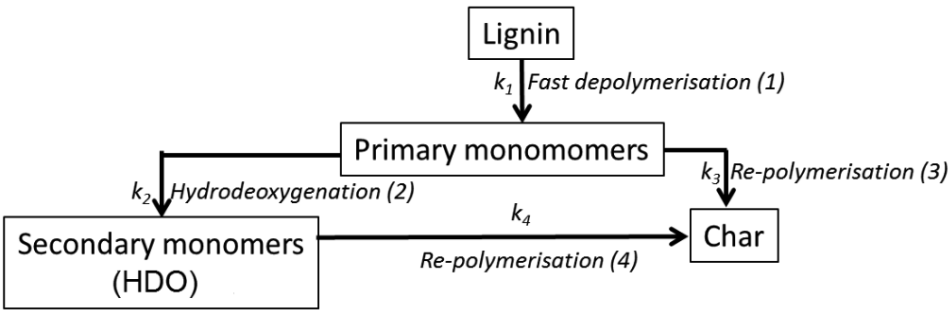

Figure 3.1: Simplified reaction scheme of lignin degradation[36]

The *alumina support* played a vital role in the de-polymerization of the lignin biopolymer and in the re-polymerization of the depolymerized lignin-monomers. The presence of temperature-stable Lewis acid sites increased the de-polymerization (k_1) degree of the bio-oils; the higher number of strong acid sites[IV], the lower the average molecular weight (M_w) of the oils. The effect of the alumina support in the re-polymerization mechanism (k_3) was also determined by the elemental and FTIR analysis of the solid products. The *type of noble metal* (Ru, Rh, Pd) also has an influence on the final oil, solid and gas yields. Ru exhibited higher activity towards the productions of bio-oil while the Pd catalyst was the most effective in the reduction of the solid phase. The composition of the gas phase was also affected: The Ru catalyst was able to induce a higher production of H_2 from formic acid, which could have favored the conversion towards bio-oil over solid phase.

✓ Catalytic effect of the reactor surface: the catalytic effect of the SS316 stainless steel in the LtL process was evaluated in the presence and absence of the Ru catalyst. To isolate the reactor surface from the reaction media a quartz insert was used. The results showed that the reactor surface exhibited considerable catalytic activity: for the non-catalyzed experiments a higher oil yield - 8.7 wt % units higher with respect to lignin input- and a lower solid yield - 12.6 wt % units lower with respect to lignin input- was obtained in the absence of the quartz insert. However, in the presence of the Ru catalyst comparable results were obtained with or without the quartz insert, so no catalytic effect of the reactor surface was observed. This confirmed that the activity of the Ru catalyst is considerably higher than the activity of the reactor surface. The Energy Dispersive X-ray (EDXA) analysis of the reactor surface suggested that Ni and Mo species could be behind the catalytic activity of the SS316 stainless steel.

[IV] This concept is referred as active acidity in paper **A**.

✓ Influence of the type of lignin: the type of lignin was a key factor when analyzing the catalytic activity of the *commercial catalyst*. Three type of lignin were tested for this purpose: Kraft lignin (KL), lignin from enzymatic hydrolysis of Norwegian spruce (EL) and lignin of strong hydrolysis of Norwegian spruce (AL). The *commercial catalyst*s were found to be active only for the EL and AL lignins. Comparable oil and solid yields were obtained for the KL lignin in the presence and absence of catalysts. The basicity of the reaction media was thought to neutralize the effect of the surface acidity of the alumina support and the activity of the catalyst; however, these results were not conclusive and will be further discussed in *Chapter 4*.

Paper **B** focuses on the effect of temperature and reaction time on the LtL process using a step-wise approach. *Initially* the effect of the temperature (300-380 °C) and reaction time (2-10 h) were evaluated for three different *commercial catalysts* (Ru/Al_2O_3, Rh/Al_2O_3 and Pd/Al_2O_3). The aim of these screening tests was to evaluate the differences and similarities among the selected *commercial catalysts* in a broader experimental space. A two-level full-factorial design with three center points was devised for each catalyst and the oil and solid yield fitted into a first-order regression model with an interaction factor. The surface response models confirmed that the Ru, Pd and Rh catalyst behaved similarly for both the oil and the solid yield, with regression coefficients that were of the same sign and comparable magnitude. The highest oil yields were obtained for the Ru catalysts, followed by the Pd and the Rh system. In terms of solid yield the lowest amount was obtained for the Pd catalysts, followed by the Ru and the Rh. The effect of the type of catalysts on the H/C ratio, O/C ratio and average molecular weight (M_w) in the whole experimental space was further assessed by principal component analysis (PCA). The PCA analysis showed that the type of catalyst had the strongest effect on the M_w value; the higher number of strong acid sites[V] of the catalysts, the lower the M_w value of the oil. An additional PCA analysis on the composition of the bio-oil was carried out. The results indicated that guaiacol and methyl-guaicaol were primary reaction products, catechol was found to

[V] This concept is referred as active acidity in paper **A**.

be an intermediate while phenol and cresol were end products. It can be noted that this degradation pathway had been previously observed for the non-catalyzed LtL [96, 164].

In a second step, the influence of temperature (283-397 °C) and reaction time (21 min- 700 min) was evaluated for the Ru catalysts and the results compared with the non-catalyzed (NC) and the γ-Al_2O_3 catalyzed systems. Among the *commercial catalyst* Ru was chosen for the higher oil yields obtained. Previous screening tests suggested that the introduction of the quadratic term was necessary to build significant regression models. Therefore, in this second step, a central composite design (CCD) with axial (α=1.41) and three centre points was devised for each system (NC, Ru/Al_2O_3 and γ-Al_2O_3), and the oil and solid yield were fitted into a second-order regression model with an interaction factor. The aim of this study was to further assess the role of the alumina support and the role of the noble metal in a broader experimental space.

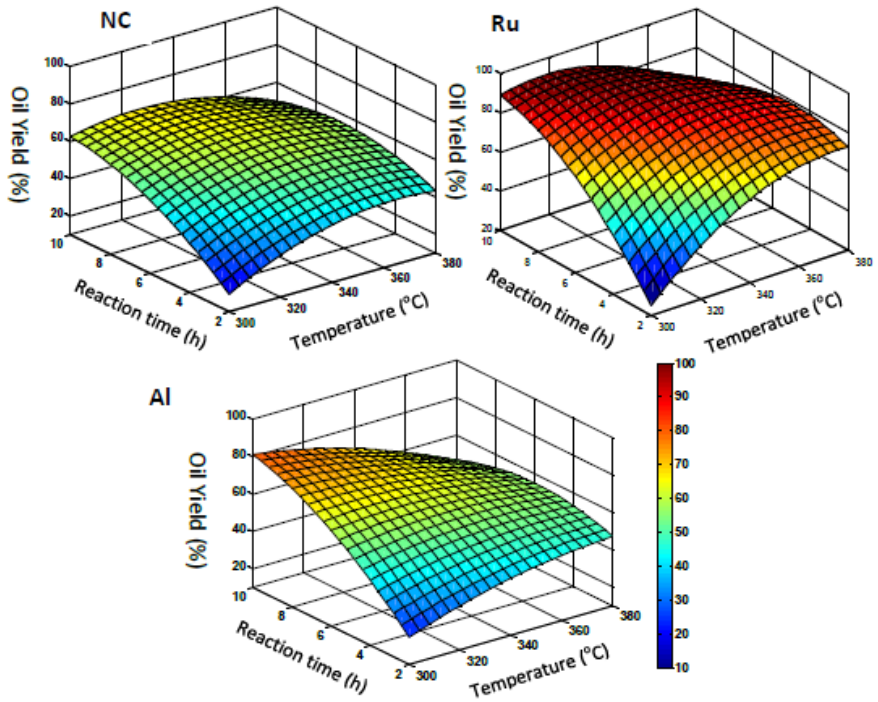

Figure 3.2: Response surface models for the oil yield. **NC:** non-catalyzed system, **Ru:** Ru/Al_2O_3 catalyzed system, **Al:** γ-Al_2O_3 catalyzed system

The response surface for the oil (Figure 3.2) and the solid phases suggests that the presence of Al and Ru somehow alters the reaction mechanisms relative to the non-catalyzed system. In paper **A** it was already reported that the γ-alumina is able to catalyze both the de-polymerization and re-polymerization reactions. In the present paper this theory was confirmed, although the exact Lewis-catalyzed lignin hydrolysis mechanism could not be elucidated. In any case, the results clearly showed that at low temperatures the lignin de-polymerization was favored over the re-polymerization of the lignin monomers, while at high temperatures the effect of the Lewis-catalyzed de-polymerization could be neutralized by a combination of other phenomena. Firstly, increasing the temperature is known to favor re-polymerization reactions of the unstable lignin monomers. Secondly, the higher solid yield observed at high temperatures and long reaction times could also be a consequence of the non-stable activity of the alumina support: the surface acidity could cause intense coke deposition over the alumina surface leading to the coverage of acid sites. The incorporation of the Ru phase seemed to hinder the re-polymerization of the lignin monomers – induced kinetic control- and to hinder the deactivation of the catalyst especially at high temperatures. Noble metals are known to catalyze HDO reactions; thus, stabilizing the lignin monomers and preventing their re-polymerization and the formation of coke deposits. However, as mentioned above, later studies proved that the higher bio-oil yields obtained by the catalysts are due to their activity in the formic acid aided aliphatic ether bond cleavage (*see Section 3.3*). This is further discussed in *Chapter 4*.

In a third step the recyclability of the Ru catalyst was evaluated: no deactivation was observed after 3 separate runs. The RSM and PCA assessment of the experimental results obtained in *step one* and *step two* led to further conclusions about the relationship between the reaction parameters -temperature, reaction time and type of catalyst- and response variables -oil yield, solid yield, properties of the oil (H/C, O/C and M_w) and composition of the oil. Surprisingly, only the M_w value of the oil was significantly affected by the type of catalyst; the O/C and H/C ratios and the composition of the oil were more temperature and reaction time dependent.

Based on the statistically significant second order models and the chemometric supported analysis the best results were obtained at 340 °C and 6 h in the presence of the Ru/Al_2O_3 catalyst: high oil yields coupled with relatively high H/C ratios and low O/C ratios and M_w values. In an overall perspective, the results show the potential for improving the yields of oil by the use of catalysts which are quite stable, and suggest a good potential for tuning the quality and composition of the oil to specific requirements.

3.2 Ethanol system

Ethanol is another strong solvent candidate for the catalytic LtL. It is a major fuel type product obtained from the conversion of lignocellulosic feedstock and therefore a widely available and cheap resource in future bio-refineries. In comparison to water, ethanol has been proven to be a more effective solvent in the LtL conversion of lignin. Recent studies show that ethanol as solvent systematically gives higher oil yields than water-based systems[165]. Moreover, ethanol could provide a more suitable environment for the stability of cheaper hydrotreating catalysts based on base metals (i.e. NiMo catalysts)[166].

In this thesis, the activities of several hydrotreating catalysts synthesized at the University of Bergen (UiB) were evaluated in the conversion of lignin in a formic acid/ethanol media. The lignin used was produced from the strong acid hydrolysis of rice straw. The composition of the feed was held constant in all cases. The activity of the catalyst was evaluated at two different reaction conditions: 340 °C and 6 h, and 300 °C and 10 h.

3.2.1 NiMo catalyst supported on magnetic activated carbons (MAC)

Many lignin conversion processes suffer from significant production of solids (hydrochar). Transforming these solid products into functional material would give additional value to the lignin and would also reduce its environmental footprint. Paper **C** describes the production of magnetic activated carbons (MAC) by KOH chemical activation of two different LtL hydrochars: hydrochar from eucalyptus and hydrochar

from spruce lignin (*see Section 2.1.3*). MACs are potentially relevant to carbon capture and storage (CCS) and gas purification processes.

The pore size distribution, surface area, and the ultramicropore volume of the renewable MACs could be varied by changing the temperature of the chemical activation. When activated at 700 °C, the MACs displayed very high ultramicropore volume and correspondingly large uptake of CO_2. These properties are important for their potential use as CO_2 sorbents. After being activated at 800 °C, the MACs displayed high specific surface areas and broad pore size distributions (PSD). Such properties could be suitable in water purification processes or as catalyst supports. The MACs contained significant amounts of embedded nanoparticles of iron oxide (magnetic) that displayed soft magnetic behavior with coercivities below 100 Oe^{-}. The magnetic properties of MACs may be used to facilitate their separation from liquids and have the potential to reduce desorption time, and therefore cycling time of CO_2 temperature swing processes through the application of electromagnetic fields.

In addition to their sorbent properties, the renewable MACs could also be considered as potential catalyst supports. In paper **D**, two of the previously produced MACs were evaluated: (i) a MAC produced from the KOH activation at 800 °C of eucalyptus hydrochar (MACE) and (ii) a MAC produced from the KOH activation at 700 °C of Norwegian spruce hydrochar (MACS). These renewable MACs were used to synthesize NiMo-based catalysts (C-MACE and C-MACS) and their catalytic activity in the LtL conversion was evaluated. Additionally, the activity of the C-MACE and C-MACS was compared with the activity of a NiMo catalyst supported on a commercial activated carbon (C-AC).

At 340 °C and 6 h, all the catalysts exhibited considerable activity towards lignin conversion (Figure 3.3, *left*): higher oil yields coupled to lower solids yields were obtained in comparison to the non-catalyzed experiment. The best results were obtained for the C-MACS catalyst (Spruce hydrochar): 72.2 % of oil –relative to the lignin input- and 21.1 % of solids. The commercial based C-AC catalyst yielded comparable oil (67.6 %) and solid (20.1 %) amounts, whereas the C-MACE produced 65.6 % of oil and 27.7 % of solids. Moreover, the oil produced by the C-MACS

catalyst was the most upgraded: the C-MACS produced the oil with highest H/C and the lowest O/C ratios.

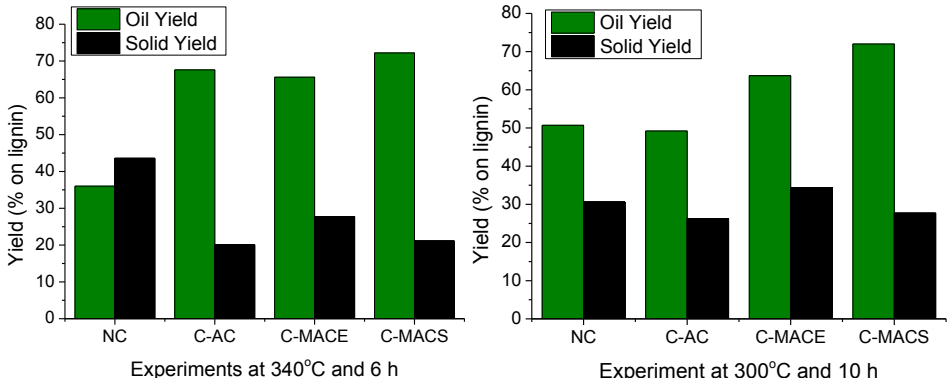

Figure 3.3: oil and solid yields for the experiments NC, C-AC, C-MACE and C-MACS at 340 °C and 6 h (left) and at 300 °C and 10 h (right).

At 300 °C and 10 h, all the catalysts generated comparable solid amounts (Figure 3.3, *right*). However, the oil yields obtained for the MAC based catalysts, C-MACE and C-MACS, were considerably higher. Furthermore, the oil generated by the C-MACE and C-MACS catalysts had a higher H/C and lower O/C ratio than the C-AC and the non-catalyzed bio-oil. It appears that the NiFe bimetallic species in the C-MACE and C-MACS catalysts, as observed by XRD, increased the HDO rate of the bio-oil components at this temperature, enhancing their stability toward re-polymerization during the work-up procedure (Paper **D**). Hence, higher oil amounts were recovered.

The magnetism exhibited by the C-MACS catalyst enables its separation from the solid products and the evaluation of its recyclability. The activity of the catalyst was evaluated upon three consecutive runs. The catalyst deactivated faster at 340 °C than at 300 °C as depicted in Figure 3.4. The loss of magnetism and the leaching of the metals seemed to be the most relevant factors that affected the recyclability and activity of the catalysts. The recovered solids seemed to be a combination of leached catalyst and other lignin derived solid products (hydrochar). The renewable MACs are therefore perfect candidates to synthesize NiMo catalyst with outstanding HDO

properties for the conversion of lignin into highly up-graded bio-oil; improving their stability and recyclability, however, should be further considered.

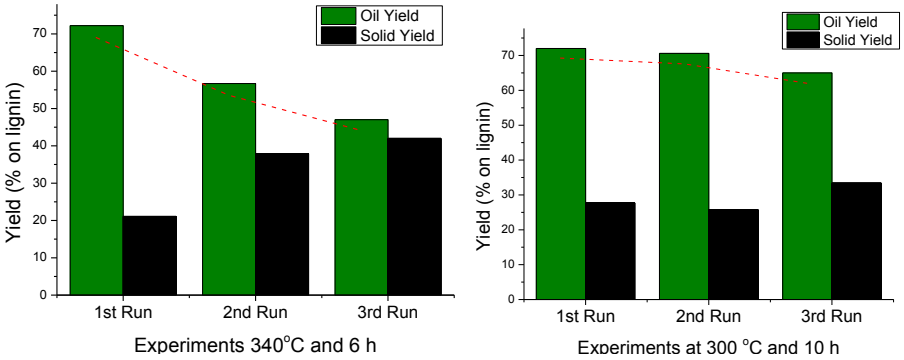

Figure 3.4: Oil and solid yield for the recycling experiments at 340 °C and 6 h (*left*) and at 300 °C and 10 h (*right*).

3.2.2 NiMo catalysts supported on metal oxides

Metal oxides are extensively used in a wide range of catalytic applications. γ-Al_2O_3 is largely studied as catalytic support due to its low cost, stable chemical nature and thermal and textural stability. It is therefore a suitable candidate for the synthesis of LtL-active catalyst as already demonstrated in *Section 3.1*. Its Lewis acid sites proved to be active towards the de-polymerization and re-polymerization of the lignin monomers in formic acid/water media.

Another suitable candidate for the synthesis of active NiMo catalyst is zirconium oxide. ZrO_2-based catalysts are known to be highly active HDO catalyst for the valorization of phenol type compounds[114]. Nevertheless, the zirconia supports exhibit typically weak acidities and low surface areas. Sulfated zirconias, on the contrary, exhibit stronger surface acidities and higher surface areas than their non-sulfated counterparts[167]. Sulfated-zirconia is obtained by treating its corresponding hydroxide ($Zr(OH)_4$) with a H_2SO_4 solution. The dried solid is later calcined at the desired temperature to produce the sulfated- ZrO_2 (SZR). The sulfation process can also be applied to the γ-Al_2O_3 support to further boost its acid properties[167]. The sulfated alumina (SAR) is, however, obtained using a different process: the γ-Al_2O_3 is

directly impregnated with a solution of H_2SO_4, dried and calcined at the desired temperature.

In paper **E**, several NiMo catalysts supported on different sulfated and non-sulfated aluminas and zirconias were studied for the catalytic LtL conversion. The bare support and calcined and pre-reduced catalysts were tested:

✓ *Bare supports:* Four different supports were studied: γ-alumina (AL), sulfated γ-alumina (SAL), zirconia (ZR) and sulfated zirconia (SZR).

✓ *Calcined catalysts:* the supports were impregnated with Ni and Mo precursors and calcined at 570 °C. Four different calcined catalysts were tested: NiMo supported on γ-alumina (NiMo-AL), NiMo supported on sulfated alumina (NiMo-SAL), NiMo supported on zirconia (NiMo-ZR) and NiMo supported on sulfated zirconia (NiMo-SZR).

✓ *Pre-reduced catalysts:* The calcined catalysts were pre-reduced at 550 °C under a hydrogen flow. Four different pre-reduced catalysts were tested: H-NiMo-AL, H-NiMo-SAL, H-NiMo-ZR and H-NiMo-SZR. Two additional monometallic Ni (H-Ni-SAL) and Mo (H-Mo-SAL) catalyst were also tested.

The experiments were carried out at 340 °C and 6 h and 300 °C and 10 h. Surprisingly, none of the *pre-reduced catalysts* tested (H-NiMo-AL, H-NiMo-SAL, H-NiMo-ZR and H-NiMo-SZR) displayed any activity at 300 °C. The *pre-reduced* NiMo catalyst supported on sulfated alumina (H-NiMo-SAL) exhibited the highest activity at 340 °C and 6 h yielding 76.5 % of oil and 19.3 % of solid (R1-NiMo-SAL experiment, *see* paper **E**). This value was close to complete lignin conversion since the amount of lignin inorganic ashes was of 14.9 %. The oil contained a high number of mono-aromatics, mainly alkylated phenols although a small number of alkoxy-substituted compounds were also found. The recyclability of the H-NiMo-SAL catalyst was also studied: no deactivation was observed upon three consecutive runs.

At 340 °C and 6 h, only the Lewis acid sites of the alumina-based *bare supports* (AL and SAL) displayed activity towards the hydrolytic cleavage of lignin ether bonds, none of the zirconia-based *bare supports* displayed (ZR and SZR) any activity (Figure 3.5, *above*). *Calcined catalyst* bearing Ni and Mo oxides (i.e. NiMo-AL, NiMo-SAL, NiMo-ZR and NiMo-SZR) exhibited a higher activity than their corresponding *bare supports* (i.e. AL, SAL, ZR and SZR).

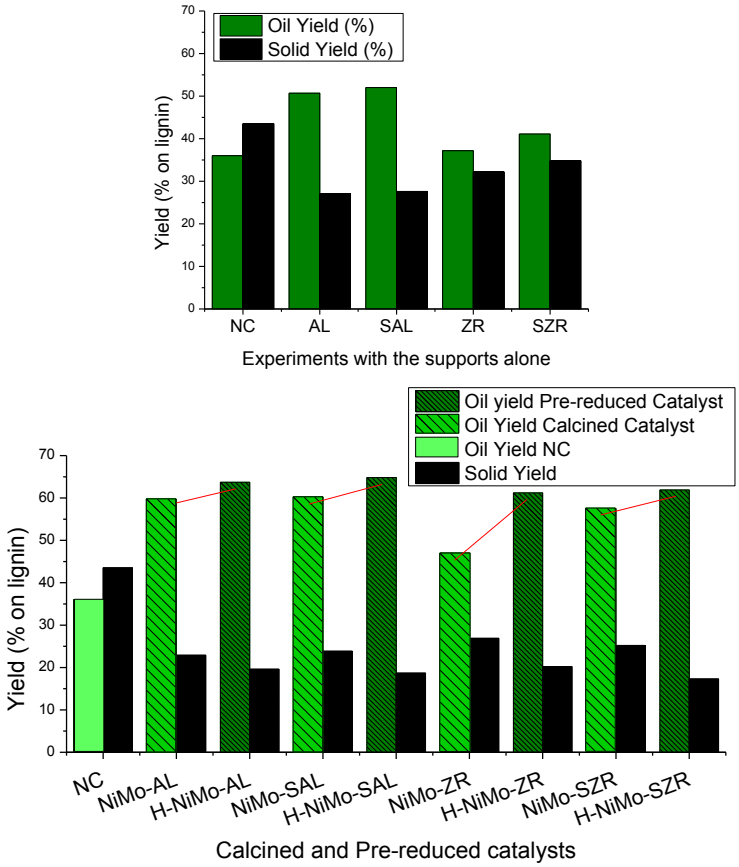

Figure 3.5 Oil and solid yield for the bare supports (NC, AL, SAL, ZR and SZR experiments), *above*; and oil and solid yield for the calcined and pre-reduced catalysts (NC, NiMo-AL, H-NiMo-AL, NiMo-SAL, H-NiMo-SAL, NiMo-ZR, H-NiMo-ZR, NiMo-SZR and H-NiMo-SZR experiments), *below*. The experiments were carried out at 340 °C and 6 h.

It was also observed that at 340 °C and 6 h those *calcined catalysts* based on acidic supports (NiMo-AL, NiMo-SAL and NiMo-SZR) were significantly more active than the non-acidic NiMo-ZR *calcined catalyst* (Figure 3.5, *below*). Upon pre-reduction all the catalysts increased their activity (Figure 3.5, *below*). The *pre-reduced*

catalysts exhibited comparable activities, despite exhibiting different acidities, surface area and number of Ni active sites. Pre-reduction was particularly positive in the case of the zirconia (ZR) catalysts: The H-NiMo-ZR *pre-reduced catalyst* displayed a considerably higher activity than the NiMo-ZR *calcined catalysts.* The higher activity was a consequence of the higher number of reduced Ni species and higher surface area exhibited by the *pre-reduced* H-NiMo-ZR catalysts.

The experiments carried out at 340 °C and 6 h indicate that the overall reaction mechanism of the catalytic LtL conversion was especially complex. The oil yield and its properties are a consequence of a combination of several catalytic reactions: catalytic ether bond hydrogenolysis, Lewis catalyzed ether bond hydrolytic cleavage, catalytic HDO and catalytic alkylation of the lignin monomers. The most relevant mechanism for the production of LtL oil was found to be the Ni(0)-catalyzed ether bond cleavage (hydrogenolysis), as it can be deduced from the results presented in Figure 3.5 (*below*). The CO-chemisorption and BET analysis also suggested that this reaction is mainly catalyzed by those Ni species found over the outer surface of the catalyst; the Ni species within the pores seem not to have a significant effect on the final oil and solid yield.

HDO and alkylation reactions, in addition, favor the stabilization of the lignin monomers and contribute to the oil yields, although to lesser extent than aliphatic ether bond hydrogenolysis. Mo was found to be the most active species towards the catalytic HDO of the lignin monomers at 340 °C. The Lewis acids sites also catalyze the hydrolytic aliphatic ether bond cleavage, but this mechanism is not relevant in the case of the *calcined* and *pre-reduced* catalysts. The results suggest that the presence of Mo does not significantly increase the final oil yield at these reaction conditions despite its HDO activity.

3.2.3 Ru/C catalyst and overall catalyst screening results

Noble metals, such as Ru, Rh and Pd, are known to have higher intrinsic hydrogenolysis activity than Ni and are widely used in direct reductive conversion of raw and pretreated lignins. Already in *Section 3.1* we reported the remarkable activity of different noble metal catalysts in a formic acid/water media. These catalysts exhibited high activities even at temperatures close to 300 °C; among them, Ru displayed the highest activity for the conversion of lignin into bio-oil.

Thus, in this section, the activity of a noble metal based catalyst for the LtL conversion of lignin in ethanol media is investigated: a Ru on carbon catalyst (Ru-AC) has been chosen for this purpose. The activated carbon used to synthesize the Ru-AC catalyst is the same *commercial activated carbon* described in *Section 3.2.1*. The Ru content of the catalyst, on the other hand, was calculated so that the number of moles of Ru was equivalent to the number of moles of Ni supported on those catalysts described *Section 3.2.1* and *Section 3.2.2*. The synthesis procedure and characterization results for the Ru-AC catalyst are described in detailed in *ANNEX I.*

Table 3.1: oil yield, solid yield, elemental analysis and average molecular weight (M_w) of the oils for the Ru-AC, H-SA and C-MACS catalyst at different reaction conditions.

Catalyst[a]	Temp. (°C)[b]	Reaction time (h)	Oil Yield (%)[c]	Solid Yield (%)[c]	Elemental analysis Oil		M_w[d] (Da)
					H/C	O/C	
NC	340	6	36.0	43.5	1.27	0.13	347
Ru-AC	340	6	75.2	20.3	1.32	0.17	479
C-MACS	340	6	72.2	21.1	1.33	0.12	331
H-NiMo-SAL	340	6	76.5	19.3	1.22	0.15	397
NC	300	10	49.3	28.2	1.18	0.18	552
Ru-AC	300	10	75.8	23.9	1.33	0.20	498
C-MACS	300	10	72.0	27.7	1.27	0.18	515
H-NiMo-SAL	300	10	51.2	27.0	1.17	0.19	441

[a] **NC:** non-catalyzed experiment, **Ru-AC:** Ru on commercial activated carbon **C-MACS:** calcined NiMo catalyst on MACS support **H-NiMo-SAL:** pre-reduced NiMo catalyst on sulfated alumina. [b] **Temp:** reaction temperature [c] wt% respect to the lignin input [d] Average molecular weight of the oil

The activity of the Ru-AC catalyst is further compared with the activity of the C-MACS and H-NiMo-SAL catalysts (Table 3.1). C-MACS and H-NiMo-SAL were the most active catalyst among the ones studied in *Section 3.2.1* and *Section 3.2.2*, respectively. The Ru-AC results are only described in this section, and are not included in the papers.

At 340 °C and 6 h all the catalyst exhibited comparable activities for the conversion of lignin (Figure 3.6, *left*). The highest oil and lowest solid yields were obtained for the H-NiMo-SAL catalyst, followed closely by the Ru-AC and the C-MACS catalyst. The C-MACS catalyst, however, produced the oil with the best quality: the highest H/C ratio (1.33) and lowest O/C ratio (0.12) and M_w values (331 Da) were obtained in the presence of C-MACS.

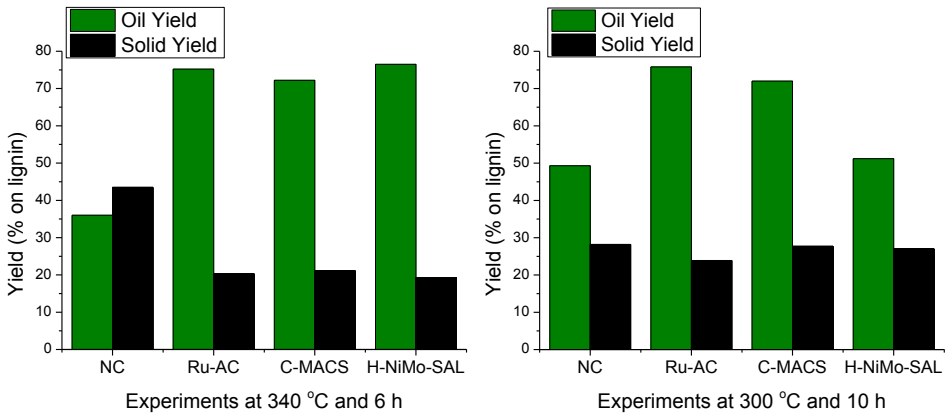

Figure 3.6: oil and solid yields for the NC, Ru-AC, C-MACS and H-SA catalyst at 340 °C and 6 h (*left*) and oil and solid yields for the NC, Ru-AC, C-MACS and H-SA catalyst at 300 °C and 10 h (*right*)

At low temperatures (Figure 3.6, *right*), however, there were significant differences among the results obtained for the different catalysts. The H-NiMo-SAL catalyst exhibited no catalytic activity as reported in *Section 3.2.2*. The C-MACS catalyst yielded a higher amount of oil when compared to the H-NiMo-SAL catalyst; the solid yield was, however, comparable to the one obtained for the NC and H-NiMo-SAL experiments. As mentioned in *Section 3.2.1*, the NiFe species within the C-MACS are more active than the NiMo species present in the H-NiMo-SAL for the

HDO of the bio-oil components at his temperature. This hinders their re-polymerization during the work-up procedure; thus, a higher amount of oil is recovered. The best results were obtained for the Ru-AC catalyst: the highest oil yield (75.8 %) and lowest solid yield (23.9 %) was obtained.

3.3 LtL reaction mechanism: the role of formic acid

Few studies have focused their attention on comparing the effect of formic acid with molecular hydrogen or other hydrogen donor molecules in the de-polymerization of lignin. Kloekhorst et al.[138] studied the effect of substituting formic acid for isopropanol, a well-known hydrogen donor molecule; but the reaction conditions chosen in all cases led to oil yields close to full conversion, what makes impossible to draw any clear conclusion. Ma et al.[168] studied the effect of molecular hydrogen and different hydrogen donor molecules in the catalytic solvolysis of lignin with little focus on the role of the different species in the reaction mechanism.

In recent years different research groups have suggested novel reaction pathways involving lignin model compounds and formic acid [169-170] or lignin model compounds and similar organic acids, such as acetic acid [171]. However, these hypotheses have never been verified with real lignin feedstock. The experiments carried out in paper **F** are aimed at gaining a better understanding on the role of formic acid in the LtL process. Additionally, the role of the catalyst, the type of solvent and their synergistic interactions with the formic acid is examined. The catalyst used in this paper is the NiMo supported on sulfated alumina (H-NiMo-SAL) studied in *Section 3.2.2*. The experimental procedures, reactant amounts and reaction conditions are described in the *Experimental Section* of paper **F**.

Initially, the role of formic acid as a possible *in situ* hydrogen source or hydrogen donor molecule was studied by replacing formic acid either totally or partially with H_2, a H_2/CO_2 (1:1) gas mixture or isopropanol, a well know hydrogen donor molecule. When substituting formic acid for molecular hydrogen or isopropanol, lower oil yields and higher solid yields were obtained and the properties of the oils also differed significantly. In contrast, molecular hydrogen and isopropanol generated comparable yields and type of oils. These results suggest that both iso-propanol and molecular hydrogen follow the same type of reaction mechanism, which is different than the one followed by formic acid.

Blank experiments carried out in the absence of lignin showed that the H-NiMo-SAL catalyst increased the decomposition rate of formic acid. For the non-catalyzed blank 57.0 % of formic acid was still present in the system after 51 minutes, while in the case of the catalyzed blank only 12.4 % of formic acid was present after the same reaction time. In an attempt to determine whether the continuous presence of formic acid during the 6 h reaction time could be beneficial to increase the oil yield, two additional semi-batch reaction configurations (SB^{VI}) were tested:

(i) a semi-batch experiment where part of the formic acid is introduced initially and the rest continuously ($SB1^{VI}$)

(ii) a second semi-batch experiment where formic acid is only introduced continuously along the course of the reaction ($SB2^{VI}$)

Both the catalytic and non-catalytic systems were considered and the results compared with the batch counterparts (B^{VI}), where all the formic acid is introduced initially in the reactor. For the non-catalyzed experiments, Figure 3.7 (*left*) similar oil and solid yields are obtained regardless of whether formic acid is added at the beginning (B^{VI} experiment) or continuously ($SB1^{VI}$ and $SB2^{VI}$ experiments). For the catalyzed experiments (C-B^{VI}, C-$SB1^{VI}$ and C-$SB2^{VI}$), however, the highest oil and lowest solid yield was obtained by far for the batch configuration as depicted in Figure 3.7 (*right*).

[VI] Note that the coding used in this section does not coincide with the coding used in paper **F**

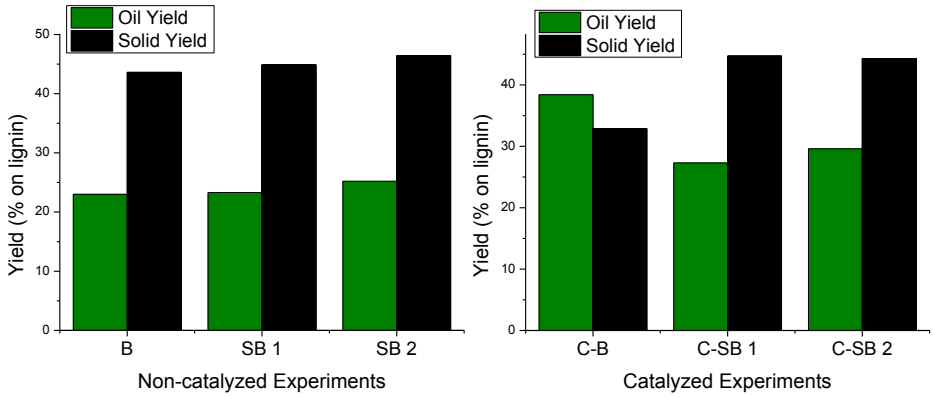

Figure 3.7: oil and solid yield for the non-catalyzed batch (**B**) semi-batch SB1 (**SB1**) and semi-batch (**SB2**) experiments (*left*) oil and solid yield for the catalyzed batch (**C-B**) semi-batch SB1 (**C-SB1**) and semi-batch (**C-SB2**) experiments (*right*)

The results described above suggest that there is a competing reaction between the decomposition of formic acid and its interaction with the lignin biopolymer. In the catalyzed experiments (Figure 3.7, *right*), significant higher oil yields were obtained when all the formic acid was present from the beginning in the reactor (C-B[VII] experiment). This indicates that a higher contact time between the lignin and the formic acid during the heating and the initial isothermal period favors the conversion of lignin. On the other hand, in the catalyzed semi-batch experiments (C-SB1[VII] and C-SB2[VII]) formic acid is slowly added into the reactor, which seems to disfavor the lignin-formic acid interaction and favor its decomposition into H_2 and CO_2: a higher amount of formic acid will be decomposed before it can react with the lignin. Regarding the non-catalyzed systems, comparable amount of oil and solid were obtained with the batch (B[VII]) and semi-batch configurations (SB1[VII] and SB2[VII]). In the absence of a catalyst, formic acid is decomposed slowly thus enabling a sufficient amount of formic acid to react continuously with the lignin throughout the duration of the reaction regardless of the reactor configuration.

[VII] Note that the coding used in this section does not coincide with the coding used in paper **F**

Based on the existing literature[169-171] and the experimental results a formylation-deformylation-hydrogenolysis mechanism is proposed for the lignin ether bonds cleavage (Figure 3.8). The deformylation step would be catalyzed by an *in situ* generated *alkoxide* that would act as the based needed for the abstraction of the proton in the C_β; leading to the elimination of the formate attached to the C_γ and the formation of an unsaturated bond. The alkoxide could be generated by two different mechanisms: (i) the adsorption of alcohols over MoO_3 and (ii) the interaction between alcohols and Lewis acid sites. The cleavage of the aliphatic ether bond is thought to happen through a catalytic hydrogenolysis mechanism, although the less likely hydrolysis and solvolysis mechanisms are not fully rejected.

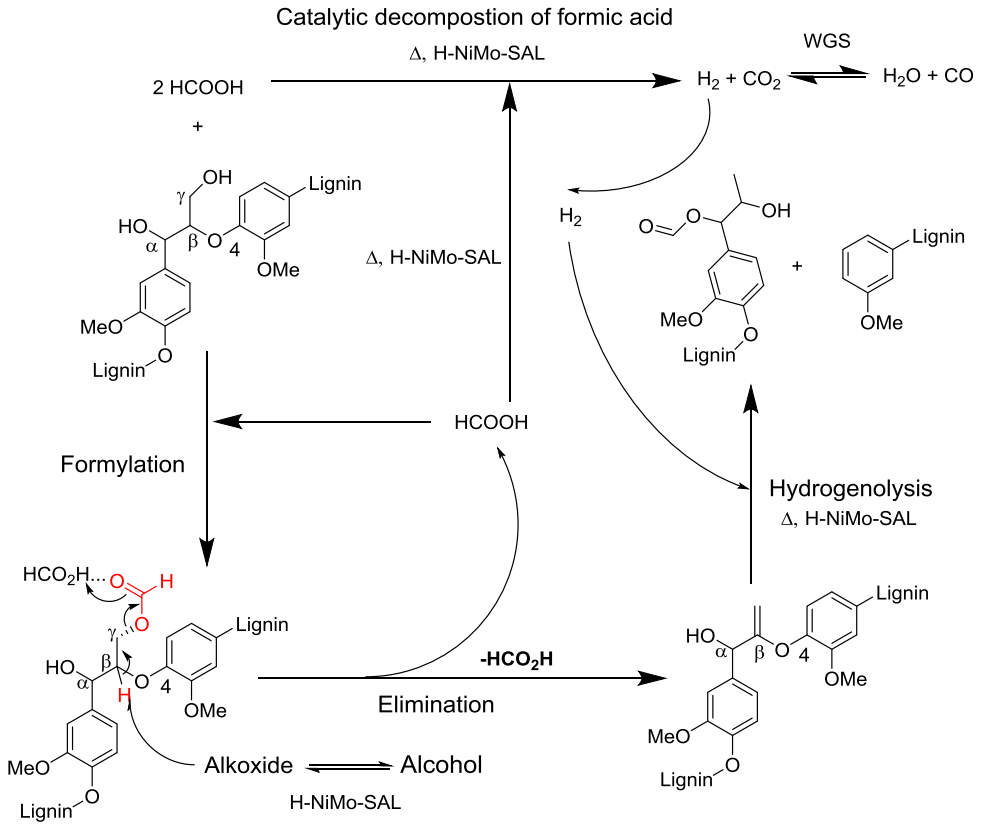

Figure 3.8: Proposed mechanism for formic acid-aided depolymerization of lignin through a formylation, elimination, hydrogenolysis

The effect of different solvents (i.e. ethanol, methanol and isopropanol) on the reaction system was also analyzed in paper **F**. The results indicated that the primary effect of the solvents was the stabilization of the lignin monomers; hindering their re-polymerization into higher molecular weight products (i.e. hydrochar). The most effective solvent for the production of bio-oil was ethanol. This solvent displayed a better activity towards etherification (O-alkylation) of highly reactive phenolic intermediates and alkylation (C-alkylation) of the aromatic rings.

Chapter 4. Discussion

The results detailed in *Chapter 3* -particularly the ones described in *Section 3.3*- justify an additional revision of some of the conclusions reported in the papers presented in Part II.

The results described in *Section 3.1* prove that *commercial* noble metal-alumina catalysts were active in the LtL conversion in *water* as reaction medium. According to the results, the *commercial catalysts* induce a kinetic control in the lignin degradation pathway that favors the conversion of lignin into bio-oil. The stabilization of the depolymerized lignin monomers through HDO reactions is believed to decrease their re-polymerization tendency increasing the amount of low molecular weight stable lignin monomers (bio-oil). Nevertheless, the latter mechanistic elucidation described in *Section 3.3* (Paper **F**) suggests that the effect of the catalyst in the overall reaction mechanism is more complex. The catalyst is able to increase the HDO rate of the lignin monomers contributing to their stabilization. However, this reaction is not so relevant for the production of bio-oil - as described in *Section 3.2.2* (Paper **E**) and *Section 3.3* (Paper **F**) - as the catalytic aliphatic ether bond cleavage. Thus the *commercial catalysts* would increase the reaction rate of the aliphatic ether bond cleavage, which is believed to happen through a formylation-deformylation(elimination)-hydrogenolysis mechanism.

The exact mechanistic pathways for the aliphatic ether bond cleavage when working in an ethanol medium cannot be entirely transferred, however, to explain the mechanism in water media. The *deformylation* step, for instance, cannot be catalyzed by an alkoxide, due to the lack of alcohols in the reaction media. Nonetheless, water is known to interact with alumina forming stable surface hydroxyl groups[172-173]. Furthermore, in the case of the *commercial catalysts* water could also dissociate over the metals forming hydroxyl groups attached to the metal surface[174-175]. This hydroxyl species could act as the base needed for the abstraction of the proton in the C_{β}, although there is no enough experimental evidence to confirm this theory. On the other hand, the activity of the alumina catalyst at low temperatures described in *Section 3.1*

(Paper **B**) indicates that the aliphatic ether bond cleavage could also occur in the absence of metallic species. Thus, the prevalent reaction pathway in the presence of bare γ-alumina support appear to be a *formylation-deformylation-hydrolysis mechanism*, as suggested by Rahimi and co-workers[169]; although *hydrogenolysis* reactions catalyzed by the reactor metallic surface could occur simultaneously. The Lewis acid sites of the γ-alumina could catalyze the hydrolytic cleavage of lignin at low temperatures. At high temperatures, on the contrary, the catalytic effect of the γ-alumina would be neutralized by the re-polymerization tendency of the monomers and the deactivation of the catalyst due to excess coking. The noble metals within the *commercial catalysts* could have a combined effect. On the one hand, they could catalyze the de-polymerization of lignin polymer by promoting a formylation-elimination-hydrogenolysis mechanism. On the other hand, they could hinder the re-polymerization of the monomers and the production of coke through catalytic HDO reactions hindering the deactivation of the catalyst at high temperatures.

The effect of the type of alumina in the LtL process in water media described in *Section 3.1* (Paper **B**) needs also to be revised. The type of alumina is thought to influence the pH of the reaction media; thus, in some cases like the alkaline KL lignin, the activity of the catalyst could be neutralized. However, the mechanistic studies described in *Section 3.3* suggest that the nature of the aliphatic ether bond could also affect the reaction mechanism. The isolation process employed to extract the lignin from the lignocellulosic biomass has an effect on the nature of the aliphatic ether bond in the lignin, especially on the abundance of aliphatic hydroxyl (OH-) groups attached to the β-O-4 bond (*see Section 1.3*). The abundance of aliphatic hydroxyl groups would have an effect in the formylation step and would influence the aliphatic ether bond cleavage rate; nevertheless, there is not enough experimental evidence to evaluate this phenomenon.

Noble metals such as Ru were active for the conversion of lignin both in *ethanol* and *water system*. They exhibited significant catalytic activity for all the reaction conditions studied. NiMo based catalysts, however, were only active in *ethanol*, and exhibited scarce catalytic activity at low temperatures (i.e. 300 °C), as described in *Section 3.2*. Furthermore, the results obtained for the monometallic H-Ni-SAL and H-Mo-SA catalysts in *Section 3.2.1* suggested that the Mo does not have a significant effect in the bio-oil yield at 340 °C. On the other hand, the results obtained for the NiMo catalysts at 300 °C could be improved by the presence of Fe on the surface of the catalysts (C-MACE and C-MACS catalysts); the stabilization of the bio-oil through HDO reactions induced by NiFe species resulted in a higher bio-oil recovery. Additional screening experiments based on NiFe catalyst are recommended to further investigate their effect in the final oil and solid yield.

The role of support in ethanol is secondary when comparing with the role of the metal phases: comparable oil and solid yields were obtained regardless the textural and chemical properties of the different supports studied. In contrast, the oil and solid yield are highly dependent on the type of monometallic and bimetallic species. The dispersion of the active sites seems not to affect the activity of the catalyst indicating that the aliphatic ether bond cleavage is mainly catalyzed by the metal species found in the outer surface of the catalyst.

The type of support used is, however, crucial when evaluating the recyclability of the catalysts. The alumina based catalysts could be easily recycled and their activity and stability is maintained upon 3 consecutive tests, both for the *water* (Ru/Al_2O_3) and *ethanol system* (H-NiMo-SAL). The renewable MACs, however, are recovered with difficulty despite their magnetism and they exhibited considerable loss of activity, particularly at 340 °C, most probably due to metal leaching.

In summary, the best results using *water* as solvent were obtained for the Ru/Al_2O_3 catalysts at 340 °C and 6 h. Practically all the lignin was converted into bio-oil (86.8 wt%), while only 3.7 % into solids. Furthermore, the Ru/Al_2O_3 was easily recycled and exhibited no deactivation after 3 consecutive runs. In *ethanol* system, it is more difficult to stablish which catalyst gives the best results. At 340 °C and 6 h, the

highest oil (76.5 wt %) and lowest solid yield (19.3 wt%) were obtained for the H-NiMo-SAL catalysts; the catalyst was easily recycled and exhibited no deactivation after 3 consecutive runs. At 300 °C and 10 h, however, the H-NiMo-SAL exhibited no activity. The highest oil yield (75.8 %) and lowest solid yield (23.9 %) were obtained for the Ru-AC catalyst, although the C-MACS catalyst generated comparable oil (72.0 %) and solid (27.7 %) yields. Thus, the Ru-AC can be considered as the most active catalyst in ethanol media, although its recyclability needs to be assessed.

Overall, the results indicate that the non-catalytic and catalytic LtL reaction systems are of great complexity. Several reactions are simultaneously involved in the lignin conversion process: aliphatic ether bond hydrogenolysis, aliphatic ether bond hydrolysis, alkylation and HDO of the de-polymerized monomers, re-polymerization of the lignin monomers and decomposition of formic acid. The most relevant reaction mechanism for the *production of bio-oil* seems to be the formic acid-aided aliphatic ether bond cleavage. In *ethanol media*, this reaction is thought to happen through a formylation-deformylation-hydrogenolysis mechanism and could be catalyzed by Ru and bimetallic NiMo catalysts. The deformylation step requires the presence of basic species such as alkoxides, that can be generated from the interaction between the ethanol and the different metallic species (Ru[176], Ni[177], Mo[178]), and/or by the interaction between the ethanol and Lewis acid sites[179]. When the reaction is carried out in water media, the ether bond cleavage could be catalyzed solely by *γ-alumina*, which is thought to induce a mechanism involving formylation, deformylation – catalyzed by hydroxyl groups attached to the surface of the catalyst- and hydrolysis steps. HDO and alkylation reactions further contribute to the production of bio-oil by stabilizing the lignin monomers; thus, hindering their re-polymerization. Alkylation reactions could be further favored by selecting the right solvent: ethanol was a better candidate than methanol and isopropanol since it favored the etherification (O-alkylation) of phenolic intermediates and the alkylation (C-alkylation) of the aromatic rings.

Chapter 5. Conclusions & outlook

The activity of several noble metal and base metal supported catalysts was evaluated for the conversion of lignin in a formic acid/solvent media. The experiments were carried out using both ethanol and water as solvents.

Noble metal catalysts such as Ru were proven more active than base metals (Ni, Mo), particularly in *water media* and/or at low reaction temperatures (i.e. 300 °C). The performance of monometallic Ni species at low temperatures (i.e. 300 °C), however, could be considerably promoted by the addition of Fe. In fact, the NiFe bimetallic system should be considered as a cheaper alternative to the more active Ru catalyst when working in *ethanol*. Future investigations should focus on the reduction of the metal loading for the Ru and NiFe catalysts. Furthermore, the optimum Ni/Fe ratio should be determined and alternative catalyst synthesis strategies evaluated to increase the number of NiFe bimetallic species.

The effect of the reaction support in the catalytic activity was also studied; although the type of support (alumina, zirconia, activated carbon) did not significantly affect the activity of the catalyst. Thus, the support should be chosen based on its cost and the stability of the resulting catalyst. Magnetic activated carbons (MACs) produced by chemical activation of lignin organic phases were found to be suitable supports for the synthesis of highly active LtL catalyst. Moreover, the valorization of the solid products into valuable products is a positive strategy to enhance the process-economics in a larger perspective. However, their stability could be further improved. Increasing the calcination temperature could partially hinder the leaching of the metals and improve the stability of the MAC-based catalysts. The effect of different parameters (e.g. type of hydrochar, O/C, H/C ratio and Fe content) on the stability of MAC-based catalyst could be also determined. ZrO_2 catalysts also constitute a cheap and suitable alternative despite their low surface area and low acidity. Among the supports studied, alumina was found to be the best candidate. Cheap and chemically stable, it is active for the conversion of lignin in water media and the resulting

supported catalysts were found to be stable and easy to recycle. Sulfating the ZrO_2 and γ-alumina, however, does not significantly increase the activity of the resulting solid.

Additional reaction parameters such as temperature, reaction time and type of lignin significantly affect the final LtL results. The effect of both temperature and reaction time in the oil yield and quality has been thoroughly investigated. The best results both in *ethanol* and *water systems* are obtained at 340 °C and 6 h where high oil yields coupled with good quality oil- high H/C and low O/C ratio and M_w value- are generated. The effect of the type on lignin in the catalytic LtL, on the other hand, is still uncertain. Additional experiments are recommended to stablish the relationship between the abundance of aliphatic OH- groups – by FTIR or solid state NMR techniques- and the ether bond cleavage rate.

The LtL process is a highly complex reaction system that involves different chemical reactions. Formic acid aided aliphatic ether bond cleavage was found to be the most relevant reaction for the production of liquid bio-oil. Formic acid induces a lignin degradation mechanism different to the one induced by other hydrogen sources such as H_2 or isopropanol. The exact reaction mechanism is not fully understood but is believed to happen through a formylation-deformylation-hydrogenolysis/hydrolysis mechanism, depending on the solvent and the catalyst used. HDO and alkylation reactions contribute to a lesser extent to the production of bio-oil by stabilizing the lignin monomers and hindering their re-polymerization. The HDO activity of the catalyst is particularly important when working at lower temperatures: the HDO of the bio-oil components hinders the re-polymerization of the more unstable compounds and would prevent the formation of downstream solid residues in future bio-refineries. All the reactions described above could be catalyzed by different noble metal and base metal catalysts. Furthermore, alkylation reactions could also be favored by selecting the right solvent.

From a basic research perspective, the formic acid aided ether bond cleavage mechanism should be further investigated. Using lignin model compounds instead of real lignin feedstock would reduce the complexity of the system and could aid in the elucidation of the exact reaction mechanism. The results presented in this work also suggest that the fast decomposition of formic acid is detrimental for the LtL conversion of lignin. Thus, future investigations should focus in those catalytic formulations that exhibit little or no activity towards the decomposition of the acid. The exchange of formic acid for a more thermally stable organic acid (i.e. acetic acid) could also overcome such problems. In the case of acetic acid, however, H_2 or another hydrogen donor molecule should be introduced in the reactor to facilitate the hydrogenolysis step.

In conclusion, applying heterogeneous catalysts is a promising option to overcome some of the major challenges associated with the LtL process. Reaction temperature and time could be reduced by applying different catalytic formulations, still producing good quality oil in high yields. Additionally, the catalysts are able to stabilize the lignin monomers preventing their re-polymerization into solid products. Nevertheless, although the reduction of this low value side stream is in theory beneficial for the overall process economics, its conversion into value-added magnetic activated carbons (MACs) could be regarded as a better alternative. Moreover, the catalyst screening approach presented in this thesis is a step towards the understanding of the LtL reaction system, particularly the mechanism of the formic acid-aided aliphatic ether bond cleavage. This is especially relevant to develop new and improved catalytic formulations.

References

1. United Nations, Department of Economic and Social Affairs, Population Division. *World Population Prospects: The 2015 Revision, Key Findings and Advance Tables;* Working Paper No. ESA/P/WP.241, 2015.

2. Alexandratos, N. B., J. , Food and Agricultur Organization of the United Nations (FAO), *World agriculture towards 2030/2050: the 2012 revision*; ESA No. 12-03, 2012.

3. Li, B.; Lv, W.; Zhang, Q.; Wang, T.; Ma, L., Pyrolysis and catalytic pyrolysis of industrial lignins by TG-FTIR: Kinetics and products. *Journal of Analytical and Applied Pyrolysis* **2014,** *108*, 295-300.

4. U. S. Energy Information Administration. http://www.eia.gov/todayinenergy/detail.cfm?id=21432 (accesed June 1, 2016).

5. Park, Y.; Doherty, W. O. S.; Halley, P. J., Developing lignin-based resin coatings and composites. *Industrial Crops and Products* **2008,** *27* (2), 163-167.

6. European Commision. Energy. Renewable energy. https://ec.europa.eu/energy/en/topics/renewable-energy (accessed June 12 2016).

7. Zakzeski, J.; Bruijnincx, P. C. A.; Jongerius, A. L.; Weckhuysen, B. M., The Catalytic Valorization of Lignin for the Production of Renewable Chemicals. *Chemical Reviews* **2010,** *110* (6), 3552-3599.

8. Li, C.; Zhao, X.; Wang, A.; Huber, G. W.; Zhang, T., Catalytic Transformation of Lignin for the Production of Chemicals and Fuels. *Chemical Reviews* **2015,** *115* (21), 11559-11624.

9. International Energy Agency, *World Energy Outlook 2012. Executive Summary;* WEO-2012, 2012.

10. Martin, M. A., First generation biofuels compete. *New Biotechnology* **2010,** *27* (5), 596-608.

11. Amidon, T. E.; Liu, S., Water-based woody biorefinery. *Biotechnology Advances* **2009,** *27* (5), 542-550.

12. Jong, de E.; Higson, A.; Walsh, P.; Wellisch, M. IEA Bioenergy. *Bio-based Chemicals. Value Added Products from Biorefineries*, 2012.

13. Jahangiri, H.; Bennett, J.; Mahjoubi, P.; Wilson, K.; Gu, S., A review of advanced catalyst development for Fischer-Tropsch synthesis of hydrocarbons from biomass derived syn-gas. *Catalysis Science & Technology* **2014,** *4* (8), 2210-2229.

14. Bridgwater, A. V., Review of fast pyrolysis of biomass and product upgrading. *Biomass and Bioenergy* **2012,** *38*, 68-94.

15. George, E.; Huber, W. University of Massachusetts Amherst. National Science Foundation (NSF). Chemical, Bioengineering, Environmental, and Transport Systems Division. *Breaking the Chemical and Engineering Barriers to Lignocellulosic Biofuels: Next Generation Hydrocarbon Biorefineries*; 180 pWashington D.C., 2008.

16. Song, H.; Lee, S. Y., Production of succinic acid by bacterial fermentation. *Enzyme and Microbial Technology* **2006,** *39* (3), 352-361.

17. Mondal, D.; Chaudhary, J. P.; Sharma, M.; Prasad, K., Simultaneous dehydration of biomass-derived sugars to 5-hydroxymethyl furfural (HMF) and reduction of graphene oxide in ethyl lactate: one pot dual chemistry. *RSC Advances* **2014,** *4* (56), 29834-29839.

18. Ooms, R.; Dusselier, M.; Geboers, J. A.; Op de Beeck, B.; Verhaeven, R.; Gobechiya, E.; Martens, J. A.; Redl, A.; Sels, B. F., Conversion of sugars to ethylene glycol with nickel tungsten carbide in a fed-batch reactor: high productivity and reaction network elucidation. *Green Chemistry* **2014,** *16* (2), 695-707.

19. Obregón, I.; Gandarias, I.; Miletić, N.; Ocio, A.; Arias, P. L., One-Pot 2-Methyltetrahydrofuran Production from Levulinic Acid in Green Solvents Using Ni-Cu/Al2O3 Catalysts. *ChemSusChem* **2015,** *8* (20), 3483-3488.

20. Suhas; Carrott, P. J. M.; Ribeiro Carrott, M. M. L., Lignin – from natural adsorbent to activated carbon: A review. *Bioresource Technology* **2007,** *98* (12), 2301-2312.

21. Lange, H.; Decina, S.; Crestini, C., Oxidative upgrade of lignin – Recent routes reviewed. *European Polymer Journal* **2013,** *49* (6), 1151-1173.

22. Aresta M. , D. A., Dumeignil, F., *Biorefinery - From Biomass to Chemicals and Fuels*. De Gruyter: 2012.

23. Zmierczak, W.; Miller, J. Processes for catlaytic conversion of lignin to liquid bio-fuels and novel bio-fuels. US20080050792 A1, February 28, 2008.

24. Calvo-Flores, F. G.; Dobado, J. A., Lignin as Renewable Raw Material. *ChemSusChem* **2010,** *3* (11), 1227-1235.

25. Lewin, M. G., I.S., Wood Structure and Composition. *CRC Press: Boca Raton* **1991**, 183-261.

26. Boerjan, W.; Ralph, J.; Baucher, M., Lignin biosynthesis. *Annual Review of Plant Biology* **2003,** *54* (1), 519-546.

27. Ralph, J.; Brunow, G.; Boerjan, W., Lignins. In *eLS*, John Wiley & Sons, Ltd: 2001.

28. Whetten, R. W.; MacKay, J. J.; Sederoff, R. R., Recent advances in understanding lignin biosynthesis. *Annual Review of Plant Physiology and Plant Molecular Biology* **1998,** *49* (1), 585-609.

29. Vanholme, R.; Morreel, K.; Ralph, J.; Boerjan, W., Lignin engineering. *Current Opinion in Plant Biology* **2008,** *11* (3), 278-285.

30. Yinghuai, Z; Yuanting, K. T.; Hosmane, N. S. Applications of Ionic Liquids in Lignin Chemistry, Ionic Liquids - New Aspects for the Future; Kadokawa, J., Ed.; InTech, 2013.

31. Yue, F.; Lu, F.; Sun, R.; Ralph, J., Synthesis and Characterization of New 5-Linked Pinoresinol Lignin Models. *Chemistry – A European Journal* **2012,** *18* (51), 16402-16410.

32. Strassberger, Z.; Alberts, A. H.; Louwerse, M. J.; Tanase, S.; Rothenberg, G., Catalytic cleavage of lignin [small beta]-O-4 link mimics using copper on alumina and magnesia-alumina. *Green Chemistry* **2013,** *15* (3), 768-774.

33. Lora, J., Chapter 10 - Industrial Commercial Lignins: Sources, Properties and Applications A2 - Belgacem, Mohamed Naceur. In *Monomers, Polymers and Composites from Renewable Resources*, Gandini, A., Ed. Elsevier: Amsterdam, 2008; pp 225-241.

34. Tedder, D. W. Albright's Chemical Engineering Handbook; Albright, L., Ed.; CRC Press: Boca Raton, 2008.

35. Valment Forward. Lignin Spearation. LignoBoost - lignin from pulp mill black liquor. http://www.valmet.com/products/pulping-and-fiber/chemical-recovery/lignin-separation/ (accessed Jun 17, 2016).

36. Oregui Bengoechea, M.; Hertzberg, A.; Miletić, N.; Arias, P. L.; Barth, T., Simultaneous catalytic de-polymerization and hydrodeoxygenation of lignin in water/formic acid media with Rh/Al2O3, Ru/Al2O3 and Pd/Al2O3 as bifunctional catalysts. *Journal of Analytical and Applied Pyrolysis* **2015,** *113*, 713-722.

37. Zhao, E.; Isaev, Y.; Sklyarov, A.; Fripiat, J. J., Acid centers in sulfated, phosphated and/or aluminated zirconias. *Catalysis Letters* **1999,** *60* (4), 173-181.

38. Chaturvedi, V.; Verma, P., An overview of key pretreatment processes employed for bioconversion of lignocellulosic biomass into biofuels and value added products. *3 Biotech* **2013,** *3* (5), 415-431.

39. Sun, Y.; Cheng, J., Hydrolysis of lignocellulosic materials for ethanol production: a review. *Bioresource Technology* **2002,** *83* (1), 1-11.

40. Fevolden, A. TOP-NEST. Value chain analysis of biofuels: Weyland. http://www.topnest.no/attachments/article/12/Value%20Chain%20Analysis%20Weyland.pdf (accesed Sep 3, 2016).

41. Evstigneyev, E. I.; Yuzikhin, O. S.; Gurinov, A. A.; Ivanov, A. Y.; Artamonova, T. O.; Khodorkovskiy, M. A.; Bessonova, E. A.; Vasilyev, A. V., Study of Structure of Industrial Acid Hydrolysis Lignin, Oxidized in the H2O2-H2SO4 System. *Journal of Wood Chemistry and Technology* **2016,** *36* (4), 259-269.

42. Pu, Y.; Hu, F.; Huang, F.; Davison, B. H.; Ragauskas, A. J., Assessing the molecular structure basis for biomass recalcitrance during dilute acid and hydrothermal pretreatments. *Biotechnology for Biofuels* **2013,** *6* (1), 1-13.

43. González, G.; López-Santín, J.; Caminal, G.; Solà, C., Dilute acid hydrolysis of wheat straw hemicellulose at moderate temperature: A simplified kinetic model. *Biotechnology and Bioengineering* **1986,** *28* (2), 288-293.

44. Abdulkhani, A.; Karimi, A.; Mirshokraie, A.; Hamzeh, Y.; Marlin, N.; Mortha, G., Isolation and chemical structure characterization of enzymatic lignin from populus deltoids wood. *Journal of Applied Polymer Science* **2013,** *130* (1), 710-710.

45. Holtman, K. M.; Chang, H.-m.; Kadla, J. F., Solution-State Nuclear Magnetic Resonance Study of the Similarities between Milled Wood Lignin and Cellulolytic Enzyme Lignin. *Journal of Agricultural and Food Chemistry* **2004,** *52* (4), 720-726.

46. Roberts, V.; Fendt, S.; Lemonidou, A. A.; Li, X.; Lercher, J. A., Influence of alkali carbonates on benzyl phenyl ether cleavage pathways in superheated water. *Applied Catalysis B: Environmental* **2010,** *95* (1–2), 71-77.

47. Yuan, Z.; Cheng, S.; Leitch, M.; Xu, C., Hydrolytic degradation of alkaline lignin in hot-compressed water and ethanol. *Bioresource Technology* **2010,** *101* (23), 9308-9313.

48. Lavoie, J.-M.; Baré, W.; Bilodeau, M., Depolymerization of steam-treated lignin for the production of green chemicals. *Bioresource Technology* **2011,** *102* (7), 4917-4920.

49. Sturgeon, M. R.; O'Brien, M. H.; Ciesielski, P. N.; Katahira, R.; Kruger, J. S.; Chmely, S. C.; Hamlin, J.; Lawrence, K.; Hunsinger, G. B.; Foust, T. D.; Baldwin, R. M.; Biddy, M. J.; Beckham, G. T., Lignin depolymerisation by nickel supported layered-double hydroxide catalysts. *Green Chemistry* **2014,** *16* (2), 824-835.

50. Jia, S.; Cox Blair, J.; Guo, X.; Zhang, Z. C.; Ekerdt John, G., Decomposition of a phenolic lignin model compound over organic N-bases in an ionic liquid. In *Holzforschung*, 2010; Vol. 64, p 577.

51. Narani, A.; Chowdari, R. K.; Cannilla, C.; Bonura, G.; Frusteri, F.; Heeres, H. J.; Barta, K., Efficient catalytic hydrotreatment of Kraft lignin to alkylphenolics using supported NiW and NiMo catalysts in supercritical methanol. *Green Chemistry* **2015,** *17* (11), 5046-5057.

52. Stavila, V.; Parthasarathi, R.; Davis, R. W.; El Gabaly, F.; Sale, K. L.; Simmons, B. A.; Singh, S.; Allendorf, M. D., MOF-Based Catalysts for Selective Hydrogenolysis of Carbon–Oxygen Ether Bonds. *ACS Catalysis* **2016,** *6* (1), 55-59.

53. Jia, S.; Cox, B. J.; Guo, X.; Zhang, Z. C.; Ekerdt, J. G., Hydrolytic Cleavage of β-O-4 Ether Bonds of Lignin Model Compounds in an Ionic Liquid with Metal Chlorides. *Industrial & Engineering Chemistry Research* **2011,** *50* (2), 849-855.

54. Hepditch, M. M.; Thring, R. W., Degradation of solvolysis lignin using Lewis acid catalysts. *The Canadian Journal of Chemical Engineering* **2000,** *78* (1), 226-231.

55. Constant, S.; Basset, C.; Dumas, C.; Di Renzo, F.; Robitzer, M.; Barakat, A.; Quignard, F., Reactive organosolv lignin extraction from wheat straw: Influence of Lewis acid catalysts on structural and chemical properties of lignins. *Industrial Crops and Products* **2015,** *65*, 180-189.

56. Bu, Q.; Lei, H.; Zacher, A. H.; Wang, L.; Ren, S.; Liang, J.; Wei, Y.; Liu, Y.; Tang, J.; Zhang, Q.; Ruan, R., A review of catalytic hydrodeoxygenation of lignin-derived phenols from biomass pyrolysis. *Bioresource Technology* **2012,** *124*, 470-477.

57. Creary, X.; Willis, E. D.; Gagnon, M., Carbocation-Forming Reactions in Ionic Liquids. *Journal of the American Chemical Society* **2005,** *127* (51), 18114-18120.

58. Deepa, A. K.; Dhepe, P. L., Solid acid catalyzed depolymerization of lignin into value added aromatic monomers. *RSC Advances* **2014,** *4* (25), 12625-12629.

59. Goyal, H. B.; Seal, D.; Saxena, R. C., Bio-fuels from thermochemical conversion of renewable resources: A review. *Renewable and Sustainable Energy Reviews* **2008,** *12* (2), 504-517.

60. Cho, J.; Chu, S.; Dauenhauer, P. J.; Huber, G. W., Kinetics and reaction chemistry for slow pyrolysis of enzymatic hydrolysis lignin and organosolv extracted lignin derived from maplewood. *Green Chemistry* **2012,** *14* (2), 428-439.

61. Wright, M. M.; Daugaard, D. E.; Satrio, J. A.; Brown, R. C., Techno-economic analysis of biomass fast pyrolysis to transportation fuels. *Fuel* **2010,** *89, Supplement 1*, S2-S10.

62. Mullen, C. A.; Boateng, A. A., Catalytic pyrolysis-GC/MS of lignin from several sources. *Fuel Processing Technology* **2010,** *91* (11), 1446-1458.

63. Lu, Q.; Zhang, Y.; Tang, Z.; Li, W.-z.; Zhu, X.-f., Catalytic upgrading of biomass fast pyrolysis vapors with titania and zirconia/titania based catalysts. *Fuel* **2010,** *89* (8), 2096-2103.

64. Li, X.; Su, L.; Wang, Y.; Yu, Y.; Wang, C.; Li, X.; Wang, Z., Catalytic fast pyrolysis of Kraft lignin with HZSM-5 zeolite for producing aromatic hydrocarbons. *Frontiers of Environmental Science & Engineering* **2012,** *6* (3), 295-303.

65. Ma, Z.; Troussard, E.; van Bokhoven, J. A., Controlling the selectivity to chemicals from lignin via catalytic fast pyrolysis. *Applied Catalysis A: General* **2012,** *423–424*, 130-136.

66. Ma, Z.; van Bokhoven, J. A., Deactivation and Regeneration of H-USY Zeolite during Lignin Catalytic Fast Pyrolysis. *ChemCatChem* **2012,** *4* (12), 2036-2044.

67. Hicks, J. C., Advances in C–O Bond Transformations in Lignin-Derived Compounds for Biofuels Production. *The Journal of Physical Chemistry Letters* **2011,** *2* (18), 2280-2287.

68. Neumann, G. T.; Hicks, J. C., Novel Hierarchical Cerium-Incorporated MFI Zeolite Catalysts for the Catalytic Fast Pyrolysis of Lignocellulosic Biomass. *ACS Catalysis* **2012,** *2* (4), 642-646.

69. Cortright, R. D.; Davda, R. R.; Dumesic, J. A., Hydrogen from catalytic reforming of biomass-derived hydrocarbons in liquid water. *Nature* **2002,** *418* (6901), 964-967.

70. Zakzeski, J.; Weckhuysen, B. M., Lignin Solubilization and Aqueous Phase Reforming for the Production of Aromatic Chemicals and Hydrogen. *ChemSusChem* **2011,** *4* (3), 369-378.

71. Kudo, S.; Hachiyama, Y.; Takashima, Y.; Tahara, J.; Idesh, S.; Norinaga, K.; Hayashi, J.-i., Catalytic Hydrothermal Reforming of Lignin in Aqueous Alkaline Medium. *Energy & Fuels* **2014,** *28* (1), 76-85.

72. Zakzeski, J.; Jongerius, A. L.; Bruijnincx, P. C. A.; Weckhuysen, B. M., Catalytic Lignin Valorization Process for the Production of Aromatic Chemicals and Hydrogen. *ChemSusChem* **2012,** *5* (8), 1602-1609.

73. Jongerius, A. L.; Copeland, J. R.; Foo, G. S.; Hofmann, J. P.; Bruijnincx, P. C. A.; Sievers, C.; Weckhuysen, B. M., Stability of Pt/γ-Al2O3 Catalysts in Lignin and Lignin Model Compound Solutions under Liquid Phase Reforming Reaction Conditions. *ACS Catalysis* **2013,** *3* (3), 464-473.

74. Huang, X.; Korányi, T. I.; Boot, M. D.; Hensen, E. J. M., Catalytic Depolymerization of Lignin in Supercritical Ethanol. *ChemSusChem* **2014,** *7* (8), 2276-2288.

75. Strassberger, Z.; Prinsen, P.; Klis, F. v. d.; Es, D. S. v.; Tanase, S.; Rothenberg, G., Lignin solubilisation and gentle fractionation in liquid ammonia. *Green Chemistry* **2015,** *17* (1), 325-334.

76. Jongerius, A. L.; Bruijnincx, P. C. A.; Weckhuysen, B. M., Liquid-phase reforming and hydrodeoxygenation as a two-step route to aromatics from lignin. *Green Chemistry* **2013,** *15* (11), 3049-3056.

77. Singh, S. K.; Nandeshwar, K.; Ekhe, J. D., Thermochemical lignin depolymerization and conversion to aromatics in subcritical methanol: effects of catalytic conditions. *New Journal of Chemistry* **2016,** *40* (4), 3677-3685.

78. Araújo, J. D. P.; Grande, C. A.; Rodrigues, A. E., Vanillin production from lignin oxidation in a batch reactor. *Chemical Engineering Research and Design* **2010,** *88* (8), 1024-1032.

79. Azarpira, A.; Ralph, J.; Lu, F., Catalytic Alkaline Oxidation of Lignin and its Model Compounds: a Pathway to Aromatic Biochemicals. *BioEnergy Research* **2014,** *7* (1), 78-86.

80. Wu, A.; Lauzon, J. M.; Andriani, I.; James, B. R., Breakdown of lignins, lignin model compounds, and hydroxy-aromatics, to C1 and C2 chemicals via metal-free oxidation with peroxide or persulfate under mild conditions. *RSC Advances* **2014,** *4* (34), 17931-17934.

81. Voitl, T.; Rohr, P. R. v., Demonstration of a Process for the Conversion of Kraft Lignin into Vanillin and Methyl Vanillate by Acidic Oxidation in Aqueous Methanol. *Industrial & Engineering Chemistry Research* **2010,** *49* (2), 520-525.

82. Werhan, H.; Assmann, N.; Rudolf von Rohr, P., Lignin oxidation studies in a continuous two-phase flow microreactor. *Chemical Engineering and Processing: Process Intensification* **2013,** *73*, 29-37.

83. Tang, K.; Zhou, X.-F., Co(salen) catalysed oxidation of synthetic lignin-like polymer: Pyridine effects. *Theoretical Foundations of Chemical Engineering* **2015,** *49* (6), 877-883.

84. Hofrichter, M., Review: lignin conversion by manganese peroxidase (MnP). *Enzyme and Microbial Technology* **2002,** *30* (4), 454-466.

85. Sbiai, A.; Kaddami, H.; Sautereau, H.; Maazouz, A.; Fleury, E., TEMPO-mediated oxidation of lignocellulosic fibers from date palm leaves. *Carbohydrate Polymers* **2011,** *86* (4), 1445-1450.

86. Weinstock, I. A.; Atalla, R. H.; Reiner, R. S.; Moen, M. A.; Hammel, K. E.; Houtman, C. J.; Hill, C. L.; Harrup, M. K., Catalysis in WaterA new environmentally benign technology for transforming wood pulp into paper. Engineering polyoxometalates as catalysts for multiple processes. *Journal of Molecular Catalysis A: Chemical* **1997,** *116* (1), 59-84.

87. Zhu, Y.; Chuanzhao, L.; Sudarmadji, M.; Hui Min, N.; Biying, A. O.; Maguire, J. A.; Hosmane, N. S., An Efficient and Recyclable Catalytic System Comprising Nanopalladium(0) and a Pyridinium Salt of Iron Bis(dicarbollide) for Oxidation of Substituted Benzyl Alcohol and Lignin. *ChemistryOpen* **2012,** *1* (2), 67-70.

88. Pu, Y.; Anderson, S.; Lucia, L.; Ragauskas, A. J., Investigation of the photo-oxidative chemistry of acetylated softwood lignin. *Journal of Photochemistry and Photobiology A: Chemistry* **2004,** *163* (1–2), 215-221.

89. Uğurlu, M.; Karaoğlu, M. H., Removal of AOX, total nitrogen and chlorinated lignin from bleached Kraft mill effluents by UV oxidation in the presence of hydrogen peroxide utilizing TiO2 as photocatalyst. *Environmental Science and Pollution Research* **2009,** *16* (3), 265-273.

90. Tolba, R.; Tian, M.; Wen, J.; Jiang, Z.-H.; Chen, A., Electrochemical oxidation of lignin at IrO2-based oxide electrodes. *Journal of Electroanalytical Chemistry* **2010,** *649* (1–2), 9-15.

91. Pan, K.; Tian, M.; Jiang, Z.-H.; Kjartanson, B.; Chen, A., Electrochemical oxidation of lignin at lead dioxide nanoparticles photoelectrodeposited on TiO2 nanotube arrays. *Electrochimica Acta* **2012,** *60*, 147-153.

92. Parpot, P.; Bettencourt, A. P.; Carvalho, A. M.; Belgsir, E. M., Biomass conversion: attempted electrooxidation of lignin for vanillin production. *Journal of Applied Electrochemistry* **2000,** *30* (6), 727-731.

93. Ouyang, X.; Huang, X.; Zhu, Y.; Qiu, X., Ethanol-Enhanced Liquefaction of Lignin with Formic Acid as an in Situ Hydrogen Donor. *Energy & Fuels* **2015,** *29* (9), 5835-5840.

94. Ferrini, P.; Rinaldi, R., Catalytic Biorefining of Plant Biomass to Non-Pyrolytic Lignin Bio-Oil and Carbohydrates through Hydrogen Transfer Reactions. *Angewandte Chemie International Edition* **2014,** *53* (33), 8634-8639.

95. Tyrone Ghampson, I.; Sepúlveda, C.; Garcia, R.; García Fierro, J. L.; Escalona, N.; DeSisto, W. J., Comparison of alumina- and SBA-15-supported molybdenum nitride catalysts for hydrodeoxygenation of guaiacol. *Applied Catalysis A: General* **2012,** *435–436*, 51-60.

96. Gasson, J. R.; Forchheim, D.; Sutter, T.; Hornung, U.; Kruse, A.; Barth, T., Modeling the Lignin Degradation Kinetics in an Ethanol/Formic Acid Solvolysis Approach. Part 1. Kinetic Model Development. *Industrial & Engineering Chemistry Research* **2012,** *51* (32), 10595-10606.

97. Barta, K.; Warner, G. R.; Beach, E. S.; Anastas, P. T., Depolymerization of organosolv lignin to aromatic compounds over Cu-doped porous metal oxides. *Green Chemistry* **2014,** *16* (1), 191-196.

98. Warner, G.; Hansen, T. S.; Riisager, A.; Beach, E. S.; Barta, K.; Anastas, P. T., Depolymerization of organosolv lignin using doped porous metal oxides in supercritical methanol. *Bioresource Technology* **2014,** *161*, 78-83.

99. Yan, N.; Zhao, C.; Dyson, P. J.; Wang, C.; Liu, L.-t.; Kou, Y., Selective Degradation of Wood Lignin over Noble-Metal Catalysts in a Two-Step Process. *ChemSusChem* **2008,** *1* (7), 626-629.

100. Liguori, L.; Barth, T., Palladium-Nafion SAC-13 catalysed depolymerisation of lignin to phenols in formic acid and water. *Journal of Analytical and Applied Pyrolysis* **2011,** *92* (2), 477-484.

101. Brewer, C. P.; Cooke, L. M.; Hibbert, H., Studies on Lignin and Related Compounds. LXXXIV. The High Pressure Hydrogenation of Maple Wood: Hydrol Lignin1. *Journal of the American Chemical Society* **1948,** *70* (1), 57-59.

102. Song, Q.; Wang, F.; Xu, J., Hydrogenolysis of lignosulfonate into phenols over heterogeneous nickel catalysts. *Chemical Communications* **2012,** *48* (56), 7019-7021.

103. He, J.; Zhao, C.; Lercher, J. A., Ni-Catalyzed Cleavage of Aryl Ethers in the Aqueous Phase. *Journal of the American Chemical Society* **2012,** *134* (51), 20768-20775.

104. Wang, X.; Rinaldi, R., Corrigendum: Solvent Effects on the Hydrogenolysis of Diphenyl Ether with Raney Nickel and their Implications for the Conversion of Lignin. *ChemSusChem* **2012,** *5* (8), 1335-1335.

105. Li, C.; Zheng, M.; Wang, A.; Zhang, T., One-pot catalytic hydrocracking of raw woody biomass into chemicals over supported carbide catalysts: simultaneous conversion of cellulose, hemicellulose and lignin. *Energy & Environmental Science* **2012,** *5* (4), 6383-6390.

106. Song, Q.; Cai, J.; Zhang, J.; Yu, W.; Wang, F.; Xu, J., Hydrogenation and cleavage of the C-O bonds in the lignin model compound phenethyl phenyl ether over a nickel-based catalyst. *Chinese Journal of Catalysis* **2013,** *34* (4), 651-658.

107. Zhang, J.; Asakura, H.; van Rijn, J.; Yang, J.; Duchesne, P.; Zhang, B.; Chen, X.; Zhang, P.; Saeys, M.; Yan, N., Highly efficient, NiAu-catalyzed hydrogenolysis of lignin into phenolic chemicals. *Green Chemistry* **2014,** *16* (5), 2432-2437.

108. Zhang, J.; Teo, J.; Chen, X.; Asakura, H.; Tanaka, T.; Teramura, K.; Yan, N., A Series of NiM (M = Ru, Rh, and Pd) Bimetallic Catalysts for Effective Lignin Hydrogenolysis in Water. *ACS Catalysis* **2014,** *4* (5), 1574-1583.

109. Nagy, M.; David, K.; Britovsek George, J. P.; Ragauskas Arthur, J., Catalytic hydrogenolysis of ethanol organosolv lignin. In *Holzforschung*, 2009; Vol. 63, p 513.

110. Romero, Y.; Richard, F.; Brunet, S., Hydrodeoxygenation of 2-ethylphenol as a model compound of bio-crude over sulfided Mo-based catalysts: Promoting effect and reaction mechanism. *Applied Catalysis B: Environmental* **2010,** *98* (3–4), 213-223.

111. Romero, Y.; Richard, F.; Renème, Y.; Brunet, S., Hydrodeoxygenation of benzofuran and its oxygenated derivatives (2,3-dihydrobenzofuran and 2-ethylphenol) over NiMoP/Al2O3 catalyst. *Applied Catalysis A: General* **2009,** *353* (1), 46-53.

112. Whiffen, V. M. L.; Smith, K. J., Hydrodeoxygenation of 4-Methylphenol over Unsupported MoP, MoS2, and MoOx Catalysts. *Energy & Fuels* **2010,** *24* (9), 4728-4737.

113. Ardiyanti, A. R.; Gutierrez, A.; Honkela, M. L.; Krause, A. O. I.; Heeres, H. J., Hydrotreatment of wood-based pyrolysis oil using zirconia-supported mono- and bimetallic (Pt, Pd, Rh) catalysts. *Applied Catalysis A: General* **2011,** *407* (1–2), 56-66.

114. Bui, V. N.; Laurenti, D.; Delichère, P.; Geantet, C., Hydrodeoxygenation of guaiacol: Part II: Support effect for CoMoS catalysts on HDO activity and selectivity. *Applied Catalysis B: Environmental* **2011,** *101* (3–4), 246-255.

115. Bui, V. N.; Laurenti, D.; Afanasiev, P.; Geantet, C., Hydrodeoxygenation of guaiacol with CoMo catalysts. Part I: Promoting effect of cobalt on HDO selectivity and activity. *Applied Catalysis B: Environmental* **2011,** *101* (3–4), 239-245.

116. González-Borja, M. Á.; Resasco, D. E., Anisole and Guaiacol Hydrodeoxygenation over Monolithic Pt–Sn Catalysts. *Energy & Fuels* **2011,** *25* (9), 4155-4162.

117. Lin, Y.-C.; Li, C.-L.; Wan, H.-P.; Lee, H.-T.; Liu, C.-F., Catalytic Hydrodeoxygenation of Guaiacol on Rh-Based and Sulfided CoMo and NiMo Catalysts. *Energy & Fuels* **2011,** *25* (3), 890-896.

118. Feng, B.; Kobayashi, H.; Ohta, H.; Fukuoka, A., Aqueous-phase hydrodeoxygenation of 4-propylphenol as a lignin model to n-propylbenzene over Re-Ni/ZrO2 catalysts. *Journal of Molecular Catalysis A: Chemical* **2014,** *388–389*, 41-46.

119. Ohta, H.; Feng, B.; Kobayashi, H.; Hara, K.; Fukuoka, A., Selective hydrodeoxygenation of lignin-related 4-propylphenol into n-propylbenzene in water by Pt-Re/ZrO2 catalysts. *Catalysis Today* **2014,** *234*, 139-144.

120. Parsell, T. H.; Owen, B. C.; Klein, I.; Jarrell, T. M.; Marcum, C. L.; Haupert, L. J.; Amundson, L. M.; Kenttamaa, H. I.; Ribeiro, F.; Miller, J. T.; Abu-Omar, M. M., Cleavage and hydrodeoxygenation (HDO) of C-O bonds relevant to lignin conversion using Pd/Zn synergistic catalysis. *Chemical Science* **2013,** *4* (2), 806-813.

121. Vogelaar, B. M.; Eijsbouts, S.; Bergwerff, J. A.; Heiszwolf, J. J., Hydroprocessing catalyst deactivation in commercial practice. *Catalysis Today* **2010,** *154* (3–4), 256-263.

122. Wang, W.; Yang, Y.; Luo, H.; Peng, H.; He, B.; Liu, W., Preparation of Ni(Co)–W–B amorphous catalysts for cyclopentanone hydrodeoxygenation. *Catalysis Communications* **2011,** *12* (14), 1275-1279.

123. Zhao, C.; Kou, Y.; Lemonidou, A. A.; Li, X.; Lercher, J. A., Highly Selective Catalytic Conversion of Phenolic Bio-Oil to Alkanes. *Angewandte Chemie International Edition* **2009,** *48* (22), 3987-3990.

124. Güvenatam, B.; Kurşun, O.; Heeres, E. H. J.; Pidko, E. A.; Hensen, E. J. M., Hydrodeoxygenation of mono- and dimeric lignin model compounds on noble metal catalysts. *Catalysis Today* **2014,** *233*, 83-91.

125. Zhang, W.; Chen, J.; Liu, R.; Wang, S.; Chen, L.; Li, K., Hydrodeoxygenation of Lignin-Derived Phenolic Monomers and Dimers to Alkane Fuels over Bifunctional Zeolite-Supported Metal Catalysts. *ACS Sustainable Chemistry & Engineering* **2014,** *2* (4), 683-691.

126. Furimsky, E., Catalytic hydrodeoxygenation. *Applied Catalysis A: General* **2000,** *199* (2), 147-190.

127. Girgis, M. J.; Gates, B. C., Reactivities, reaction networks, and kinetics in high-pressure catalytic hydroprocessing. *Industrial & Engineering Chemistry Research* **1991,** *30* (9), 2021-2058.

128. Zhao, C.; Lercher, J. A., Selective Hydrodeoxygenation of Lignin-Derived Phenolic Monomers and Dimers to Cycloalkanes on Pd/C and HZSM-5 Catalysts. *ChemCatChem* **2012,** *4* (1), 64-68.

129. Zhao, C.; Kou, Y.; Lemonidou, A. A.; Li, X.; Lercher, J. A., Hydrodeoxygenation of bio-derived phenols to hydrocarbons using RANEY[registered sign] Ni and Nafion/SiO2 catalysts. *Chemical Communications* **2010,** *46* (3), 412-414.

130. Laskar, D. D.; Tucker, M. P.; Chen, X.; Helms, G. L.; Yang, B., Noble-metal catalyzed hydrodeoxygenation of biomass-derived lignin to aromatic hydrocarbons. *Green Chemistry* **2014,** *16* (2), 897-910.

131. Singh, S. K.; Ekhe, J. D., Towards effective lignin conversion: HZSM-5 catalyzed one-pot solvolytic depolymerization/hydrodeoxygenation of lignin into value added compounds. *RSC Advances* **2014,** *4* (53), 27971-27978.

132. Divakar, D.; Manikandan, D.; Rupa, V.; Preethi, E. L.; Chandrasekar, R.; Sivakumar, T., Palladium-nanoparticle intercalated vermiculite for selective hydrogenation of α,β-unsaturated aldehydes. *Journal of Chemical Technology & Biotechnology* **2007,** *82* (3), 253-258.

133. Liu, W.-J.; Zhang, X.-S.; Qv, Y.-C.; Jiang, H.; Yu, H.-Q., Bio-oil upgrading at ambient pressure and temperature using zero valent metals. *Green Chemistry* **2012,** *14* (8), 2226-2233.

134. Vispute, T. P.; Zhang, H.; Sanna, A.; Xiao, R.; Huber, G. W., Renewable Chemical Commodity Feedstocks from Integrated Catalytic Processing of Pyrolysis Oils. *Science* **2010,** *330* (6008), 1222-1227.

135. Pang, M.; Liu, C.; Xia, W.; Muhler, M.; Liang, C., Activated carbon supported molybdenum carbides as cheap and highly efficient catalyst in the selective hydrogenation of naphthalene to tetralin. *Green Chemistry* **2012,** *14* (5), 1272-1276.

136. Li, Z.; Garedew, M.; Lam, C. H.; Jackson, J. E.; Miller, D. J.; Saffron, C. M., Mild electrocatalytic hydrogenation and hydrodeoxygenation of bio-oil derived phenolic compounds using ruthenium supported on activated carbon cloth. *Green Chemistry* **2012,** *14* (9), 2540-2549.

137. Lam, C. H.; Lowe, C. B.; Li, Z.; Longe, K. N.; Rayburn, J. T.; Caldwell, M. A.; Houdek, C. E.; Maguire, J. B.; Saffron, C. M.; Miller, D. J.; Jackson, J. E., Electrocatalytic upgrading of model lignin monomers with earth abundant metal electrodes. *Green Chemistry* **2015,** *17* (1), 601-609.

138. Kloekhorst, A.; Shen, Y.; Yie, Y.; Fang, M.; Heeres, H. J., Catalytic hydrodeoxygenation and hydrocracking of Alcell® lignin in alcohol/formic acid mixtures using a Ru/C catalyst. *Biomass and Bioenergy* **2015,** *80*, 147-161.

139. Huang, S.; Mahmood, N.; Tymchyshyn, M.; Yuan, Z.; Xu, C., Reductive de-polymerization of kraft lignin for chemicals and fuels using formic acid as an in-situ hydrogen source. *Bioresource Technology* **2014,** *171*, 95-102.

140. Xu, W.; Miller, S. J.; Agrawal, P. K.; Jones, C. W., Depolymerization and Hydrodeoxygenation of Switchgrass Lignin with Formic Acid. *ChemSusChem* **2012,** *5* (4), 667-675.

141. Onwudili, J. A.; Williams, P. T., Catalytic depolymerization of alkali lignin in subcritical water: influence of formic acid and Pd/C catalyst on the yields of liquid monomeric aromatic products. *Green Chemistry* **2014,** *16* (11), 4740-4748.

142. Huang, S. Reductive Depolymerization of Kraft Lignin for Chemicals and Fuels Using Formic Acid as In-Situ Hydrogen Source. Ph.D. Dissertation, The University of Wester Ontario, Ontario, Canada, 2014.

143. Rey Juan Carlos University. Laboratory of spectrocospical techniques (LABTE). http://www.labte.es/index.php/es/2013-11-03-19-54-23/propiedades-texturales/adsorcion-fisica-de-gases (accessed Jun 28, 2016). .

144. Integrating Research and Education. Geochemical Instrumentation and Analysis. http://serc.carleton.edu/research_education/geochemsheets/BraggsLaw.html (accessed Jun 24, 2016).

145. Poly Cristallography, Inc. An Introduction to X-ray Powder Diffractrion Analysis. http://www.polycrystallography.com/XRDanalysis.html (accessed Jun 29, 2016).

146. Barzetti, T.; Selli, E.; Moscotti, D.; Forni, L., Pyridine and ammonia as probes for FTIR analysis of solid acid catalysts. *Journal of the Chemical Society, Faraday Transactions* **1996,** *92* (8), 1401-1407.

147. Belskaya, O. B.; Danilova, I.G; Kazalov, M. O.; Mironenko, R. M.; Lavrenov, A. V.; Likholobov, V.A. FTIR Spectroscopy of Adsorbed Probe Molecules for Analyzing the Surface Properties of Supported Pt (Pd) catalysts. In *Infrared Spectroscopy-Materials Science, Engineering and Technology*; Theophanides, T. Ed; Intech: 2012; Caphter 7; p 151.

148. Parry, E. P., An infrared study of pyridine adsorbed on acidic solids. Characterization of surface acidity. *Journal of Catalysis* **1963,** *2* (5), 371-379.

149. Fadoni, M.; Lucarelli, L., Temperature programmed desorption, reduction, oxidation and flow chemisorption for the characterisation of heterogeneous catalysts. Theoretical aspects, instrumentation and applications. In *Studies in Surface Science and Catalysis*, Dąbrowski, A., Ed. Elsevier: 1999; Vol. Volume 120, Part A, pp 177-225.

150. Micromeritics. Autochem II 29020. Technique: Temperature Programmed Reduction (TPR). http://www.micromeritics.com/Repository/Files/Autochem%20II%202920%20technique%20TPR.pdf (accessed Jun 23, 2016).

151. Huang, Y. J.; Xue, J.; Schwarz, J. A., Analysis of temperature-programmed reduction profiles from metal-supported catalysts. *Journal of Catalysis* **1988,** *111* (1), 59-66.

152. USGS. Science for Changing the World. Understanding Our Planet Through Chemistry. ICP-AES Technique Description. http://minerals.cr.usgs.gov/gips/na/5process.html (accessed Jul 08, 2016).

153. Gasson, J. R. Solvolytic lignin degradation in an alcohol/formic acid medium. Ph.D. Dissertation, University of Bergen, Bergen, Norway, 2012.

154. Wenshan, Z., Lignins and Derivatives: GPC/SEC Analysis. In *Encyclopedia of Chromatography, Third Edition*, Taylor & Francis: 2009; Vol. null, pp 1359-1368.

155. Radboud University. Faculty of Science. Bio-organic chemistry. http://www.ru.nl/bio-orgchem/instrumentation/chromatography/gel-permeation-gpc/ (accesed Jul 2, 2016).

156. PREMEDHQ. Size-exclusion Chromatography. https://www.premedhq.com/size-exclusion-chromatography (accessed Jul 1, 2016).

157. Engineering Statistics Handbook. Process Improvment. Introduction. http://www.itl.nist.gov/div898/handbook/pri/section1/pri11.htm (accessed Jun 23, 2016).

158. Ates, F.; Erginel, N., Optimization of bio-oil production using response surface methodology and formation of polycyclic aromatic hydrocarbons (PAHs) at elevated pressures. *Fuel Processing Technology* **2016,** *142*, 279-286.

159. J's blog. Factorial and response surface optimization of chromatin immunoprecipitation protocol. http://blog-di-j.blogspot.com.es/2007/10/factorial-and-response-surface.html (accessed Jul 8, 2016).

160. Fahmi, R.; Bridgwater, A. V.; Donnison, I.; Yates, N.; Jones, J. M., The effect of lignin and inorganic species in biomass on pyrolysis oil yields, quality and stability. *Fuel* **2008,** *87* (7), 1230-1240.

161. Scholz, M. Approaches to analyse and interpret biological profile data. Ph.D Dissertation, University of Potsdam, Germany, 2006.

162. Kleinert, M.; Gasson, J. R.; Barth, T., Optimizing solvolysis conditions for integrated depolymerisation and hydrodeoxygenation of lignin to produce liquid biofuel. *Journal of Analytical and Applied Pyrolysis* **2009,** *85* (1–2), 108-117.

163. Rossebø, L. R. D. Undersøkelse av effekten av katalysator og støttematerialer på omdanningen av lignin til LtL-biooljer ved forskjellige betingelser. Master Thesis, Universitity of Bergen, Bergen, Norway, 2014.

164. Forchheim, D.; Gasson, J. R.; Hornung, U.; Kruse, A.; Barth, T., Modeling the Lignin Degradation Kinetics in a Ethanol/Formic Acid Solvolysis Approach. Part 2. Validation and Transfer to Variable Conditions. *Industrial & Engineering Chemistry Research* **2012,** *51* (46), 15053-15063.

165. Løhre, C.; Barth, T.; Kleinert, M., The effect of solvent and input material pretreatment on product yield and composition of bio-oils from lignin solvolysis. *Journal of Analytical and Applied Pyrolysis* **2016,** *119*, 208-216.

166. Laurent, E.; Delmon, B., Deactivation of a Sulfided NiMo/γ-Al2O3 during the Hydrodeoxygenation of Bio-Oils: Influence of a High Water Pressure. In *Studies in Surface Science and Catalysis*, Delmon, B.; Froment, G. F., Eds. Elsevier: 1994; Vol. Volume 88, pp 459-466.

167. Guzmán-Castillo, M. L.; López-Salinas, E.; Fripiat, J. J.; Sánchez-Valente, J.; Hernández-Beltrán, F.; Rodríguez-Hernández, A.; Navarrete-Bolaños, J., Active sulfated alumina catalysts obtained by hydrothermal treatment. *Journal of Catalysis* **2003,** *220* (2), 317-325.

168. Ma, R.; Hao, W.; Ma, X.; Tian, Y.; Li, Y., Catalytic Ethanolysis of Kraft Lignin into High-Value Small-Molecular Chemicals over a Nanostructured α-Molybdenum Carbide Catalyst. *Angewandte Chemie International Edition* **2014,** *53* (28), 7310-7315.

169. Rahimi, A.; Ulbrich, A.; Coon, J. J.; Stahl, S. S., Formic-acid-induced depolymerization of oxidized lignin to aromatics. *Nature* **2014,** *515* (7526), 249-252.

170. Qu, S.; Dang, Y.; Song, C.; Guo, J.; Wang, Z.-X., Depolymerization of Oxidized Lignin Catalyzed by Formic Acid Exploits an Unconventional Elimination Mechanism Involving 3c–4e Bonding: A DFT Mechanistic Study. *ACS Catalysis* **2015,** *5* (11), 6386-6396.

171. Lohr, T. L.; Li, Z.; Marks, T. J., Selective Ether/Ester C–O Cleavage of an Acetylated Lignin Model via Tandem Catalysis. *ACS Catalysis* **2015,** *5* (11), 7004-7007.

172. Ionescu, A.; Allouche, A.; Aycard, J.-P.; Rajzmann, M.; Hutschka, F., Study of γ-Alumina Surface Reactivity: Adsorption of Water and Hydrogen Sulfide on Octahedral Aluminum Sites. *The Journal of Physical Chemistry B* **2002,** *106* (36), 9359-9366.

173. Lodziana, Z.; Topsoe, N.-Y.; Norskov, J. K., A negative surface energy for alumina. *Nat Mater* **2004,** *3* (5), 289-293.

174. Desai, S. K.; Neurock, M., First-principles study of the role of solvent in the dissociation of water over a Pt-Ru alloy. *Physical Review B* **2003,** *68* (7), 075420.

175. Pozzo, M.; Carlini, G.; Rosei, R.; Alfè, D., Comparative study of water dissociation on Rh(111) and Ni(111) studied with first principles calculations. *The Journal of Chemical Physics* **2007,** *126* (16), 164706.

176. Gazdzicki, P.; Jakob, P., Reactions of Methanol on Ru(0001). *The Journal of Physical Chemistry C* **2010,** *114* (6), 2655-2663.

177. Demuth, J. E.; Ibach, H., Observation of a methoxy species on Ni(111) by high-resolution electron energy-loss spectroscopy. *Chemical Physics Letters* **1979,** *60* (3), 395-399.

178. Groff, R. P., An infrared study of methanol and ammonia adsorption on molybdenum trioxide. *Journal of Catalysis* **1984,** *86* (1), 215-218.

179. Cai, S.; Sohlberg, K., Adsorption of alcohols on γ-alumina (1 1 0 C). *Journal of Molecular Catalysis A: Chemical* **2003,** *193* (1–2), 157-164.

PART II

A

Paper A

Simultaneous catalytic de-polymerization and hydrodeoxygenation of lignin in water/formic acid media with Rh/Al_2O_3, Ru/Al_2O_3 and Pd/Al_2O_3 as bifunctional catalysts

Authords:
Oregui Bengoechea, M.; Hertzberg, A.; Miletić, N.; Arias, P. L.; Barth, T.

Published in:
Journal of Analytical and Applied Pyrolysis **2015,** *113*, 713-722

Journal of Analytical and Applied Pyrolysis 113 (2015) 713–722

Contents lists available at ScienceDirect

Journal of Analytical and Applied Pyrolysis

journal homepage: www.elsevier.com/locate/jaap

Simultaneous catalytic de-polymerization and hydrodeoxygenation of lignin in water/formic acid media with Rh/Al_2O_3, Ru/Al_2O_3 and Pd/Al_2O_3 as bifunctional catalysts☆

Mikel Oregui Bengoechea[a,*], Agnethe Hertzberg[a], Nemanja Miletić[b], Pedro L. Arias[b], Tanja Barth[a]

[a] Department of Chemistry, University of Bergen, Norway, Allegaten 41, N-5007 Bergen, Norway
[b] Department of Chemical and Environmental Engineering, School of Engineering, University of the Basque Country (EHU/UPV), C/Alameda Urquijo s/n, 48013 Bilbao, Spain

ARTICLE INFO

Article history:
Received 31 July 2014
Received in revised form 20 April 2015
Accepted 25 April 2015
Available online 28 April 2015

Keywords:
Catalytic hydrotreatment
Solvolysis
Lignin
Noble metals
Alumina
Bifunctional heterogeneous catalysis

ABSTRACT

The catalytic solvolysis of 3 lignins of different sources in a formic acid/water media using bifunctional Ru/Al_2O_3, Rh/Al_2O_3, Pd/Al_2O_3 catalysts was explored in a batch set-up at different temperatures and reaction times (340–380 °C and 2–6 h, respectively). Blank experiments using only gamma–alumina as catalysts and non-catalyzed experiments were also performed and compared with the supported catalysts results. All the supported catalysts significantly improved the oil yields on a lignin basis, with yields up to 91.5 wt% using the Ru catalyst. The main components phenol, cresol, guaiacol, methylguaiacol, catechol, ethylcatechol, syringol and *o*-vanillin are found in different concentrations depending on the catalytic system. The stable Lewis acidity in the alumina support has been found to be active in terms of de-polymerization of lignin, leading to lower average molecular weight oils. In addition, it was found that alumina plays a significant role in the re-polymerization mechanism of the monomers. The effect of the type of lignin on the final oil and solid yields was also established, demonstrating that lignins produced by basic pretreatment of biomass do not show significant increase in oil yield when catalysts on an acid support like alumina are used. The interpretation is that acid conditions are needed for efficient de-polymerisation of the lignin.

1. Introduction

In the biofuel sector, the concept of a "biorefinery" describes all the processes and technologies involved in converting biomass to a range of fuels and value-added chemicals. Among the biomass sources, lignocellulosic biomass (wood, grasses and agricultural residues) has been identified as a promising alternative for this purpose [1], since unlike vegetable oil and sugar crops the lignocellulose feedstock avoid the negative side effect of intense farming [2] and ethical concerns about the use of food as fuel raw materials [3]. For lignocellulosic biomass conversion, most of the research has been focused on the conversion of cellulose and hemi-cellulose to biofuels and value added chemicals, and major breakthroughs have been achieved. However, valorization of lignin, an amorphous polymer that accounts for 15–30% of the feedstock by weight, and 40% by energy [1], is still a challenge. Only approximately 2% of the lignin residues available from the pulp and paper industry are used commercially, with the remaining volumes burned as low value fuel [4]. Nevertheless, lignin has a significant potential as a feedstock for the sustainable production of fuels and bulk chemicals, and indeed lignin can be regarded as the major aromatic resource of the bio-based economy [1].

Various pathways have been explored for the conversion of lignin-rich residual material for fuels or phenols [1,5–7]. Among them, thermochemical conversion by fast pyrolysis is one of the central techniques, but the resulting "oil" has a high O/C and low of H/C ratio. These bio-oils are very acidic and corrosive and often chemically unstable, making it necessary to further upgrade them to produce motor fuels and chemicals to be used in the petrochemical industry [8–10]. In comparison to fast pyrolysis, solvolysis provides the advantages of milder conditions and a single phase environment due to the miscibility of the organic products in the (supercritical) solvent. Further advantages of solvolysis performed in

☆ Selected Paper from Pyrolysis 2014, Birmingham, U.K. 19–23 May 2014.
* Corresponding author. Tel.: +47 46230671.
E-mail address: mikel.oregui@kj.uib.no (M. Oregui Bengoechea).

http://dx.doi.org/10.1016/j.jaap.2015.04.020
0165-2370/

polar solvents such as ethanol or iso-propanol [11] over fast pyrolysis are a less oxygenated oil fraction and almost no solid residue (<5%) [12,13]. A promising and relatively new lignin conversion methodology involves the use of a hydrogen donor solvent instead of molecular hydrogen [14]. A well-known hydrogen donor is formic acid (FA), which is converted *in situ*, either thermally or catalytically, to molecular hydrogen and CO/CO_2. Commonly used solvents are alcohols (methanol, ethanol) and water, the latter being a preferred system for biofuel conversion since it is a "green" solvent.

With temperatures typically of 350–400 °C and reaction times of typically 8–16 h, lignin from spruce, pine, birch and aspen wood has been converted to a chemically stable bio-oil through a solvolysis process using formic acid as hydrogen donor. The molar H/C ratio of the product was between 1.3 and 1.8, and the O/C ratio between 0.05 and 0.1, indicative of a substantial reduction in the oxygen content compared with the fast pyrolysis process [2,14,15]. However, in order to make this bio-oil fuel competitive with fuels and chemicals obtained from petroleum, some important process parameters need to be improved: (i) shorter reaction times, (ii)lower reaction temperatures and (iii) the reduction of low-value side streams *i.e.*, gas and solid residues.

One possibility to address these challenges is the use of catalysts in the process. Catalytic hydrotreatment of lignin has already been explored extensively and involves the reaction of lignin in the presence of a (heterogeneous) catalyst with molecular hydrogen at elevated temperatures. Several catalytic systems have been evaluated both with model compounds and lignin [5,6]. Catalysts such as $Co–Mo/Al_2O_3$ and $Ni–Mo/Al_2O_3$ and noble metals on different supports, Rh/C, Rh/Al_2O_3, Pd/C, Rh/ZrO_2, Ru/C [1] have extensively been evaluated for this purpose. Although very effective when using model compounds, only low levels of lignin conversion is achieved in such lignin based systems [5]. Recent research by Ligouri and Barth showed that the reaction time and temperature can be reduced dramatically when using heterogeneous (Pd/C) catalyst together with Nafion SAC-13 as solid superacid in a formic acid/water media (2011) [16]. The Pd/C catalyst increases the hydrogenation rate, while the Nafion SAC-13, a Brønsted acid, activates the lignin aryl ether sites (de-polymerization) and promotes their hydrogenolysis to phenols [17]. The lignin was converted at a reaction temperature of 300 °C and a reaction time of 2 h, and high conversions into oil were achieved. Nonetheless, the use of two types of catalyst presents some drawbacks from an industrial and economical point of view. In this perspective, the use of a bifuntional catalyst were a cheap acid support is used could have the potential to improve the industrial and economic performance without lowering the lignin conversion values. Alumina could be an adequate alternative, although the role of its Lewis acidity in the lignin de-polymerization and re-polymerization needs investigation.

In this study, several noble metals supported on alumina, Ru/Al_2O_3, Rh/Al_2O3 and Pd/Al_2O_3 are investigated as bifunctional catalyst in a formic acid/water media for the simultaneous de-polymerization and hydrodeoxygenation of three different types of lignins. The conversion of lignin to oil and solids (coke) and the effect of the alumina as a support with Lewis acid properties are investigated at different temperatures (340–380 °C) and reaction times (2–6 h), in terms of bulk yields and chemical composition of the products.

2. Materials and methods

2.1. Chemicals

N,O- Bis(trimethylsilyl) trifluoroacetamide (BSTFA) with trimethylchlorosilane (TMCS) and pyridine (>99.5 %) was purchased from Fluka and used as bought. Pentane (>99%), formic acid (>98%), tetrahydrofuran (>99.9%) and ethyl acetate (99.8%) were purchase from Sigma–Aldrich and used as bought.

2.2. Catalysts

Ruthenium on alumina (5 wt%), Rhodium on alumina (5 wt%) and Palladium on alumina (10 wt%) were obtained from Sigma–Aldrich, and gamma-alumina (97 wt%) was obtained from Strem Chemicals Inc. These were dried at 80 °C for 24 h prior to use.

2.3. Acidity measurements (NH_3-TPD and DRIFT)

Temperature-programmed desorption of ammonia, NH_3-TPD, was performed to determine the total acidity of the samples. The measurements were carried out in chemisorption analyzer AutoChem II equipped with a thermal conductivity detector (Micromeritics, USA). The samples (50 mg) were flushed with helium at 650 °C for 30 min, then cooled down to 40 °C and loaded with ammonia for 30 min. Complete removal of physically adsorbed ammonia was carried out by purging the saturated samples with helium at 100 °C until no further desorption was recorded. Under constant flow of helium, the samples were heated up from 100 to 650 °C at a heating rate of 10 °C/min, and the release of ammonia was recorded. The total acidity was determined by using calibration data.

Diffuse reflectance infrared Fourier transform, DRIFT, was used to distinguish Lewis and Brønsted acid sites of noble-metal containing catalysts and γ-Al_2O_3. The analyses were done using a VERTEX 70 spectrometer coupled with an external sample chamber that enables measurements under vacuum (Bruker, Germany). The samples were dried *in situ* under vacuum for 1 h at 250 °C and later cooled down to 40 °C in order to record the background spectra. The main measurement features were a spectral range from 1650 to 1350 cm^{-1}, 200 scans, and a resolution of 4 cm^{-1}. Initially, the catalyst was brought in direct contact with pyridine vapor at 40 °C for 15 min. Analysis where obtained by heating the sample up to 100, 200, or 300 °C for 15 min.

2.4. Type of lignins

Low sulfonate alkali lignin (KL lignin) was purchase from Sigma–Aldrich. Lignin from Norway spruce from strong acid carbohydrate dissolution pre-treatment (AL) was received from Technical College of Bergen, and lignin from Norway spruce from weak acid and enzymatic hydrolysis biomass pre-treatment (EL) was received from the Norwegian University of Life Science in Ås. The two latter lignins were ground and sieved (<500 μm). All the lignins were dried at 80 °C for 24 h prior to use.

2.5. Experimental conditions

2.5.1. Experimental set-up

A detailed description is given elsewhere by Kleinert and Barth [14]. Briefly summarised, lignin (2 g), formic acid (3.075 g), water (5 g) and the catalyst (0.2 g) were added to a stainless steel reactor (Parr 4742 non-stirred reactor, 25 ml volume). The amounts of reactants are based on previous experiments for maximising oil yields. The reactor was closed and heated in a Carbolite LHT oven to the desired conditions (340 °C or 380 °C) for a given reaction time (2 or 6 h). The experimental conditions for all the experiments are summarized in Supplementary material Table S1.

2.5.2. Sample work-up

After completed reaction time, the reactors were taken out of the oven and cooled in an air stream to ambient temperature. The amount of produced gases was determined by weighting the reactor before and after ventilating the gas. After opening the reaction container, the liquid reaction mixture was extracted with a solution of ethyl acetate: tetrahydrofuran (90:10) and the solid phase (unreacted lignin, reaction products and catalyst) were filtered. Two well-separated liquid phases were obtained (organic top phase and aqueous bottom phase). They were separated by decanting, and the pH and the weight of the aqueous phase was determined. The organic phase was dried over Na_2SO_4 and concentrated at reduced pressure (ca. 250 mm bar) at 40 °C to yield a dark brown to black liquid. The yield was determined by weight. The solids were characterized by Fourier-transformed infrared spectroscopy (FT-IR) and elemental analysis. The oil fraction was characterized by gas chromatography (GC-FID), gel permeation chromatography-size exclusion chromatography (GPC–SEC) and electrospray soft ionization mass spectroscopy (ESI-MS).

2.6. GC-FID analysis

The oil was sylilated with BSTFA prior to the GC-FID analysis. Typically 3 mg of oil was dissolved in 100 μL of pyridine and latter 100 μL of BSTFA with TMS was added. The samples were heated to 70 °C for 20 min. After cooling the mixture was dissolved with pentane (3 mg of oil/ml of pentane) and analysed by GC-FID.

The samples were analysed on a Thermo Finnigan TRACE GC Ultra with a FID- detector equipped with a chromatographic HP-ULTRA2 [(5%-phenyl-methylpolysiloxane], 25 m, 0.200 ID column from Agilet Technologies. The following heating programme was applied: 30 °C for one minute, and then heating at 10 °C/min up to 250 °C. The injector temperature was 250 °C, and the detector temperature was 320 °C. Identification of the peaks was made by comparison with retention times of authentic commercially available reference compounds that were also sylilated prior to the analysis. The quantitative data was obtained using hexadecane as internal standard. Calibration curves were prepared for the following compounds: phenol, cresol, guiacol, methylguaiacol, catechol, ethylcatechol, syringol, *o*-vanillin.

2.7. Elemental analysis

All samples were analysed for their elemental composition in the CHNS mode with a Vario EL III instrument using helium as carrier gas. The amount of oxygen was calculated by difference.

2.8. GPC-SEC

The sample (1 mg) was dissolved in 1 ml of THF. The solution (20 μL) was injected into a GPC-SEC system equipped with a PLgel 3ìm Mini MIX-E column, and analysed at a flow rate of 0.5 ml/min of THF at 21.1 °C, and the detection was performed with UV at 254 and 280 nm, as well as with RI. The set of columns was calibrated with a series of polystyrene standards covering a molecular-mass range of 162–2360 Da.

2.9. FT-IR

The FTIR spectra were recorded by applying the sample to an attenuated total reflectance (ATR) crystal. The main measurement features were a spectral range from 4000 to 400 cm^{-1}, 16 scans, and a resolution of 4 cm^{-1}.

Table 1
Total acidity, acidity retention and active acidty of γ-alumina, Rh/Al_2O_3, Ru/Al_2O_3 and Pd/Al_2O_3.

	Total acidity[a] (mmol NH_3/g cat.)	Acidity retention[b] (%)	Active acidity (mmol NH3/g cat.)[a]
γ-Alumina	1.51	100 (100 °C)	1.51 (100 °C)
		92 (200 °C)	1.39 (200 °C)
		92 (300 °C)	1.39 (300 °C)
Rh/Al_2O_3	1.34	100 (100 °C)	1.34 (100 °C)
		71 (200 °C)	0.95 (200 °C)
		49 (300 °C)	0.66 (300 °C)
Ru/Al_2O_3	0.78	100 (100 °C)	0.78 (100 °C)
		77 (200 °C)	0.60 (200 °C)
		51 (300 °C)	0.40 (300 °C)
Pd/Al_2O_3	0.76	100 (100 °C)	0.76 (100 °C)
		99 (200 °C)	0.75 (200 °C)
		98 (300 °C)	0.74 (300 °C)

[a] Data obtained from NH3-TPD.
[b] Data obtained from DRIFT.

2.10. ESI-MS

Each sample (120 μg/ml) was dissolved in methanol and analysed by full-scan mass spectrometry (m/z range from 100 to 1000 with 1 scan/s) on an Agilent 6420 Triple Quad LC/MS system (Agilent Technologies, Inc., Palo Alto, CA). Samples of 2 μL were injected by direct injection into the ESI-MS. Both positive and negative electrospray ionization was used to detect different compounds.

2.11. Gas phase GC

Gas phase GC analysis was performed on a GC-FID/TCD (HP 7890A) and a 30 m Porapak Q Molsieve column equipped with a FID front detector and a TCD back detector, which was controlled by an HPChem laboratory data system. The heating programme was as follows: Initial temperature was 50 °C for 22 min after which, the temperature was raised at a rate of 20 °C/min up to 150 °C. 15 min after reaching this temperature it was again raised at a rate of 50 °C/min up to 220 °C. This temperature was held for 5 min. The injection port had a temperature of 250 °C, the pressure was kept constant at 255 kPa and the FID was at 300 °C.

2.12. Energy dispersive X-ray analysis (EDXA)

Compositional analysis of the reactor surface was carried out with an EDX spectrometer equipped with an SEM system (JEOL, JSM-5610LVS). The measurement duration of SEM-EDX analysis was set to 300 s. The energies of the obtained EDX spectra were calibrated by Cu·Lα and Kα lines of a copper (99.96%) plate.

3. Results

3.1. Acidity results

Acidity measurements on the Ru/Al_2O_3, Rh/Al_2O_3, Pd/Al_2O_3 and γ-alumina were carried out to determine the type of acidity (Lewis or Brønsted), the acidity retention and total acidity of the samples. Table 1 shows the total acidity data recorded by NH_3-TPD in the 100–650 °C temperature range. The highest acidity was obtained for the γ-Al_2O_3 (1.51 mmol NH_3/g cat.), with significantly lower acidities for the supported catalysts ($Rh/Al_2O_3 > Ru/Al_2O_3 > Pd/Al_2O_3$).

The DRIFT spectra (see Supplementary material Fig. S1) of all the catalysts show sharp IR bands at 1445 and 1610 cm^{-1}, that are assigned to Lewis acid sites [18]. IR bands assigned to Brønsted acid sites (1545 and 1638 cm^{-1}) were not detected in any of the samples [18]. Based on the IR band at 1445 cm^{-1}, acidity reten-

Table 2
Elemental composition of the altered and non-altered T316 stainless steel reactor surface.

	Altered surface (%)	Non-altered surface (%)
C	32–45	0–4.8
O	28.5–32.5	0
Si	1.5–2.3	1
Fe	11–13	64–65
Cr	9.3–11.5	17
Ni	1.19–2.5	9–12
Mo	4.1–5.8	2.14–2.5
Mn	-	2–2.6

tion was also calculated as [peak area (T)/peak area (100 °C)] × 100 (Table 1). Increasing the temperature did not influence the Lewis acid-bound pyridine in Al_2O_3 and Pd/Al_2O_3, as peak areas are not altered. In contrast, increased temperature causes pyridine desorption in Rh/Al_2O_3 and Ru/Al_2O_3 samples, which suggests that their acidity is rather weak. Given the reaction temperature, only the acidity obtained above 300 °C could actively participate in the reaction, due to its capability to retain pyridine or similar molecules at the given reaction temperatures. Therefore the active acidity, define as the fraction of total acidity that actually plays a significant role in the reaction was calculated (active acidity (T) = acidity retention (T) × total acidity) and the results are shown in Table 1. The catalyst with the highest active acidity is γ-Al2O3 followed by Pd/Al_2O_3, Rh/Al_2O_3 and Ru/Al_2O_3.

3.2. Influence of the reaction surface

3.2.1. Analysis of the reactor surface

The composition of the reactor surface can affect the final results of our system. The reactor used is a T316 stainless steel Parr reactor. The metals present in the reactor surface could in principle catalyze the hydrodeoxygenation reactions and therefore affect the final product distribution [19]. Furthermore, when the reactor is used for repeated solvolysis reactions, alterations in the reactor surface are observed, and the metallic surface turns black. Previous experience in our group shows an improvement in the oil yields obtained after the reactor was submitted to 3–4 reaction cycles, suggesting that these alterations in the reactor surface are beneficial for the overall process.

To evaluate these changes and the possible metals that could have a catalytic effect in the reaction system, an EDXA analysis of the non-altered and the altered reactor surface was carried out. The results are shown in Table 2.

The composition of the non-altered surface is in accordance to the data provided by the producer, which confirms the suitability of this method to analyze the surface composition. When comparing both surfaces, several differences in the composition are observed. The content of Fe, Cr and Mn decreases significantly, while the O,C and Ni and Mo content increases.

3.2.2. Effect of the reactor surface in the non-catalyzed and catalyzed system

With the aim of evaluating the effect of the reactor surface, four experiments at a temperature of 340 °C and 6 hours were performed. Two of the experiments, NC-Q and NC-1, were carried out without the catalyst, with and without a quartz insert to prevent contact between the system and the reactor surface. Subsequently, the equivalent experiments were carried out using Ruthenium on alumina (Ru/Al_2O_3) as catalyst (Ru-Q and RU-1).

Table 3 shows the results for these experiments. When the contact between the system and the reactor surface is reduced by using the quartz insert, the oil yield decreases by 11 wt% and the solid yield increases by 13 wt%. However, when the analogous experiments are done in the presence of the Ru catalyst, no significant difference is observed. Actually, when using the quartz liner, the oil yield is slightly higher and the solid yield is slightly lower.

3.3. Screening of Rh (Rh/Al_2O_3), Ru (Ru/Al_2O_3) and Pd (Pd/Al_2O_3) on alumina

3.3.1. Reproducibility and mass balance

Table 3 shows the yields as a function of the inputs for the first replicate of each system. The lignin mass balance accounts for the amount of solids and oil (g) divided by the amount of lignin introduced, while the water recovery percentage accounts for the ratio of water phase recovered (g) with respect to the water phase introduced (g). All the experiments show a total mass balance of nearly a 100%, only the gamma-alumina (γ-Al_2O_3) system has a value around 94,8%, which can be assigned to the low water recovery percentage.

Table 3 shows that the solvolysis approach comprises of four major products: a gas phase, a solid phase, an aqueous liquid phase and an organic liquid phase (bio-oil). The amount of gas recovered after the reaction is very close to the values of the formic acid introduced, which supports that the main components of the gas phase are the decomposition products of the formic acid. As mentioned above, the liquid phase obtained after the reaction can be divided into the clear water phase and the organic oil product. The water phase recovered mostly accounts for slightly higher amounts than the one introduced (see Table 3), which suggests that the water does not act as a reactant, but rather a solvent in the reaction media. Some water-soluble organics and water produced in deoxygenation reactions [20,21] could account for the increased amounts of water recovered, and also for the mass loss in the quantified products relative to the lignin input. The solid yield for the catalyzed systems is calculated after subtracting the amount of catalyst introduced. The sum of this value and the oil yield accounts for over 80 % of the lignin introduced for all experiments, and is even higher, 95%, for the Ru catalyst. This supports that the solid and oil are the main products of the lignin de-polymerization and hydrodeoxygenation.

Table 3
Mass balance of the selected experiments at 340 °C.

Name of experiment	Oil yield (% on lignin)	Solid yield (% on lignin)	Gas phase (% total input)	Water recovery (% inital input)	Lignin mass balance (%)	Total mass balance (%)
NC-Q[a]	49.5	35.0	29.5	103.7	84.5	97.3
NC-1[a]	58.2	22.4	30.5	103.6	80.6	97.9
Ru-Q[a]	91.2	3.5	29.9	88.2	94.7	93.3
Ru-1[a]	90.0	5.1	29.1	102.6	95.0	99.3
A-1[a]	63.1	22.0	30.0	94.8	85.1	94.8
Rh-1[a]	81.0	4.8	30.0	106.3	85.7	99.9
Pd-1[a]	81.7	2.8	30.8	101.1	84.4	98.1

NC: non-catalyzed experiment. A: γ-alumina (0.2 g). Rh: rhodium on alumina (0.2 g). Ru: ruthenium on alumina (0.2 g). Pd: palladium on alumina (0.2 g). Q: A quartz insert was used to suppress the effect of the reactor wall.

[a] Reaction conditions: 340 °C and 6 h. 2 g of acid hydrolysis lignin, 5.0 g of water and 3.075 g of formic acid.

Table 4
Average oil and solid yields for the selected replicates.

Name of experiment	Oil yield (% on lignin)	Average oil yield and standard deviaton (%)	Solid yield (% on lignin)	Average solid yield and standard deviaton (%)
NC-1[a]	58.2	61.6 ± 3.0	22.4	20.6 ± 3.4
NC-2[a]	62.3		23.0	
NC-3[a]	64.2		16.5	
A-1[a]	63.1	62.8 ± 3.9	22.0	21.6 ± 4.3
A-2[a]	58.7		25.7	
A-3[a]	66.5		17.1	
Rh-1[a]	81.0	80.5 ± 3.7	4.8	4.6 ± 0.5
Rh-2[a]	83.9		4.0	
Rh-3[a]	76.6		5.0	
Ru-1[a]	90.0	91.5 ± 6.3	5.1	4.2 ± 1.0
Ru-2[a]	98.4		4.4	
Ru-3[a]	86.2		3.2	
Pd-1[a]	81.7	82.9 ± 2.2	2.8	2.7 ± 0.3
Pd-2[a]	85.4		2.4	
Pd-3[a]	81.6		2.9	

NC: non-catalyzed experiment. A: γ-alumina (0.2 g). Rh: rhodium on alumina (0.2 g). Ru: ruthenium on alumina (0.2 g). Pd: palladium on alumina (0.2 g).
[a] Reaction conditions: 340 °C and 6 h. 2 g of acid hydrolysis lignin, 5.0 g of water and 3.075 g of formic acid.

Table 5
Quantification of the main oil components by GC-FID and molecular weight distributions by GPC-SEC.

GC-FID	NC-1[a]	A-1[a]	Ru-1[a]	Rh-1[a]	Pd-1[a]	NC-4[b]	Ru-4[b]	A-4[b]
Phenol (wt% oil)	1.68	1.44	1.99	1.41	2.47	2.70	1.52	1.56
Cresol (wt% oil)	3.62	3.16	4.27	2.94	5.22	5.90	3.17	3.41
Guaiacol (wt % oil)	2.53	2.18	3.21	2.03	3.44	4.22	2.28	2.42
Methyl guaiacol (wt % oil)	2.38	2.29	2.80	1.91	3.38	3.92	2.13	2.58
Catechol (wt % oil)	2.00	3.15	1.91	1.35	2.05	3.68	1.70	3.35
Ethylcatechol (wt % oil)	1.36	3.24	1.44	0.99	1.69	2.33	1.36	3.76
Syringol (wt % oil)	0.19	0.20	0.22	0.12	0.23	0.47	0.19	0.26
o-Vanillin (wt % oil)	1.81	1.32	1.9	1.33	0	3.00	1.45	0
GPC-SEC	NC-1[a]	A-1[a]	Ru-1[a]	Rh-1[a]	Pd-1[a]	NC-4[b]	Ru-4[b]	A-4[b]
Average molecular weight (Da)	346	215	397	344	323	294	497	211

NC: non-catalyzed experiment. A: γ-alumina (0.2 g). Rh: rhodium on alumina (0.2 g). Ru: ruthenium on alumina (0.2 g). Pd: palladium on alumina (0.2 g).
[a] Reaction conditions: 340 °C and 6 h. 2 g of acid hydrolysis lignin, 5.0 g of water and 3.075 g of formic acid.
[b] Reaction conditions: 380 °C and 2 h. 2 g of acid hydrolysis lignin, 5.0 g of water and 3.075 g of formic acid.

Table 4 shows a summary of the results for the three different replicates carried out for each system, the average of the oil and solid yield for each system, and the standard deviation from the average values. It can be observed the Ru system shows the highest standard deviation in terms of oil yield (6.3 wt%) while the alumina system shows the highest standard deviation in terms of solid yield (4.3 wt%).

3.3.2. Effect of the catalyst on the oil and solid yields

From the results in Table 4 we can clearly see the effect of the catalysts in our reaction system. For the non-catalyzed system the average oil yield accounts for 61.6 ± 3.0 wt% and the solid for 20.6 ± 3.4 wt% of the lignin input. These results are comparable to the ones obtained in the gamma-alumina catalyzed system (62.8 ± 3.9 wt% oil yield and 21.6 ± 4.3 wt% solid yield). However, when comparing these systems with the supported catalyst systems, Rh/ Al_2O_3, Pd/ Al_2O_3, Ru/ Al_2O_3, a substantial increase in the oil yield together with a decrease in the solid yield is observed. The best result in terms of oil yield is obtained for the Ru catalyst with an increase of 29.9 wt%. Both the Pd and the Rh catalyst show comparable oil yield with 82.9 ± 2.2 wt% and 80.5 ± 3.7 wt%, respectively. In terms of solid yield the best values are obtained for the Pd catalyst, where nearly no solid is found (2.7 ± 0.3 wt%). In the case of the Ru and Rh systems, slightly higher amounts of solids are obtained, with an average of 4.2 ± 1.0 wt% and 4.6 ± 0.5 wt%, respectively.

3.3.3. Oil phase composition

The main components in the oil have been quantitatively analyzed by GC-FID as the tri-methyl silyl (TMS) derivatives. The results of the quantification are summarized in Table 5. The Ru-catalyzed system shows the higher abundance of highly hydrogenated and lower oxygenated compounds such as phenol (1.99%) and cresol (4.27%), followed by the Pd catalyst, the non-catalyzed system, the alumina catalyzed system and the Rh system. Less hydrogenated compounds such as catechol and ethyl-catechol are more abundant in the alumina system (3.15 and 3.24%, respectively), followed by the palladium, non-catalyzed, ruthenium and Rh systems.

Table 6
Results of the elemental analysis of the lignin, oils and solids

	C (%wt)	H (%wt)	O (%wt)	N(%wt)	(O/C)	(H/C)
AL lignin	61.27	5.74	32.82	0.16	0.40	1.12
NC-1 Oil[a,b]	73.78	7.37	18.09	0.76	0.18	1.19
A-1 Oil[a,b]	71.47	7.21	20.07	0.32	0.21	1.21
Ru-1 Oil[a,b]	74.29	7.31	17.86	0.54	0.18	1.17
Rh-1 Oil[a,b]	76.97	7.83	14.13	1.07	0.14	1.21
Pd-1 Oil[a,b]	76.97	7.83	14.13	1.07	0.14	1.21
NC-1 Solid[a,c]	73.63	4.98	21.18	0.21	0.22	0.81
A-1 Solid[a,c]	42.60	3.46	53.82	0.12	0.95	0.97

NC: non-catalyzed experiment. A: γ-alumina (0.2 g). Rh: rhodium on alumina (0.2 g). Ru: ruthenium on alumina (0.2 g). Pd: palladium on alumina (0.2 g). AL: acid hydrolysis lignin.
[a] Reaction conditions: 340 °C and 6 h. 2 g of acid hydrolysis lignin, 5.0 g of water and 3.075 g of formic acid.
[b] Elemental analysis of the oil.
[c] Elemental analysis of the recovered solids.

Table 6 gives the elemental composition of the oil. The H/C ratio is highest when using the Pd, Rh and γ-alumina catalyst, although comparable results are obtained for all the experiments. However when analyzing the O/C ratio, significant differences are observed. The Pd and Rh catalyzed oils clearly has the lowest O/C ratio (0.14), the Ru and the non-catalyzed systems have comparable values, and the highest value is obtained for the alumina catalyzed system.

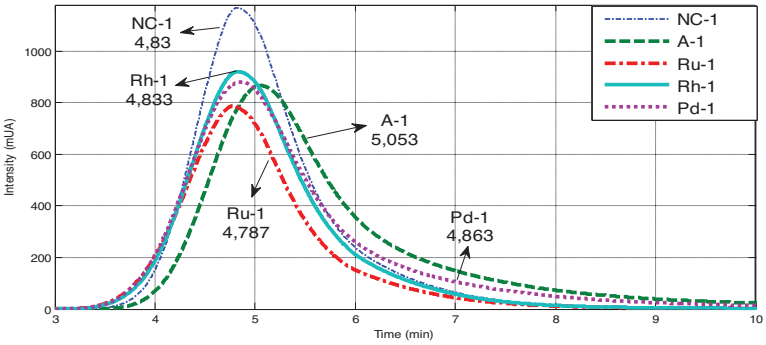

Fig. 1. GPC spectras of the oils for the NC-1, A-1, Ru-1, Rh-1 and Pd-1 experiments. Analytical conditions are given in Section 2.8.

According to the GPC-SEC analysis presented in Table 5, the γ-alumina catalyst generates the oil with the lowest average molecular weight (215 Da), followed by the Rh, Pd, non-catalyzed and Ru systems. When analyzing the GPC-SEC spectras in Fig. 1, more information about the product distribution of the oils can be obtained. The shape of the peaks are narrower, nearly symmetric for the Rh and the non-catalyzed oils, but in the case of the Al and Pd the right side of the curve is less steep implying a higher concentration of lower molecular weight compounds.

The ESI-MS spectra show a clear difference in the composition of the oils (see Supplementary material Fig. S2a–e). The alumina system shows the narrowest product distribution, with high intensity peaks in the low molecular range, 100–300 Da. The Ru, Pd and Rh catalyst show high intensity peaks in both low molecular range (100–300 Da) and medium molecular range (300–600 Da) which could explain the lower proportion of quantified compounds obtained by the GC-FID. In the case of the non-catalyzed system, a very wide product distribution is observed, with a high concentration of medium molecular range products (300–600 Da) and intense peaks even in the high molecular mass range.

Overall, the more hydrodeoxygenated oils are obtained in the case of the supported systems, as shown in the GC-FID and elemental analysis data, while lower average-molecular-weight oils are obtained in the γ-alumina and Pd systems. The reason for these results will be further discussed in Section 4.

3.3.4. Solid phase composition

The amount of solid phase obtained in the Ru, Rh and Pd catalyst was insignificant, preventing any analysis. However, higher amounts of solid were recovered in the non-catalyzed and γ-alumina catalyzed systems. In Fig. 2, the FT-IR spectras of the AL lignin, non-catalyzed solid phase products and gamma alumina solid phase products are compared with the aim of gaining insight into the nature of the solids, and the re-polymerization mechanism.

Two main observations can be made: (i) the proportion of functional groups in the Al solids is much lower than in the non-catalyzed solid and the lignin; (ii) there are significant differences between the solid obtained in the Al and the non-catalyzed system. It can be observed that the OH—stretching signal is broad (3500–3400 cm^{-1}) for both non-catalyzed and lignin spectra, while a much narrow signal is found in the alumina solid, suggesting that a lower abundance of intramolecular H—bonding in the latter. In addition, the CH— stretching signal for methyl and methylene peak (2940–2930 cm^{-1}) is not found in the Al experiment, which suggests an absence of these functional groups compared to the non-catalyzed system and the lignin. The same trend is seen for the carbonyl function above 1700 cm^{-1}, it is quite intense in the lignin with a peak at 1705 cm^{-1} which is typical for carboxylic acid. In the non-catalyzed oil there is a less intense peak at 1788 cm^{-1}, indicating ester groups and the carbonyl peak is inexistent in the alumina catalyzed solids. Some of the aromatic nature is retain in the alumina solid, as seen when analyzing the 1605–1600, 1515–1505 and the 1430–1425 cm^{-1} ranges, although this peaks are less intense than in the lignin and non-catalyzed solid [22]. The guaiacyl pattern is present in the lignin spectra, and the syringyl pattern in both the lignin and the non-catalyzed system. However, both the lignin and the alumina catalyzed solids spectra has a strong peak at around 1065 cm^{-1}, which can be assign to the C—O ether stretching (all band indexing is summarized in the Supplementary material Table S2).

The results of the elemental analysis of the lignin and solid phases confirme the differences between these solids (Table 6). The non-catalyzed solids have a high content of carbon (73.63 wt%), followed by the lignin (61.27 wt%) and the alumina solids (42.6 wt%), while the content in O is higher for the alumina (53.82 wt%) and less than half for the non-catalyzed system (21.18 wt%).

3.3.5. Gas phase

The gas phase was analyzed for the non-catalyzed and the supported catalyzed systems, and the concentration of CO_2, CO, H_2 and some light alkanes (methane, ethane, propane and butane) were measured, see Table 7.

No water was determined in the gas phase due to the inability to measure this by the selected method. Nevertheless, the analysis of the mass balance suggests that the water produced through the decomposition of the formic acid and the water-gas-shift-reaction (WGS) mainly condenses in the liquid water phase.

The main gas product in all cases is CO_2, produced mainly by the decomposition of the formic acid but also through decarboxylation and gasification reactions of the lignin and its monomers. The component with the second highest concentration is H_2, which can have a strong influence in the hydrogenation rate of the depolymerized lignin monomers. The hydrogen seen in these measurements does not account for all the hydrogen produced from decomposition of formic acid in the course of the reaction, since considerable quantities are used for the hydrogenation of the monomers, especially in the catalytic systems, as suggested by the higher oil yields (Table 3).

When comparing the different systems the following conclusion can be stated: (i) the catalytic systems enhance the production of CO_2 (especially Pd and Rh), (ii) the amount of hydrogen is higher in the Ru system, (iii) the amount of CO is lower in all the catalytic sys-

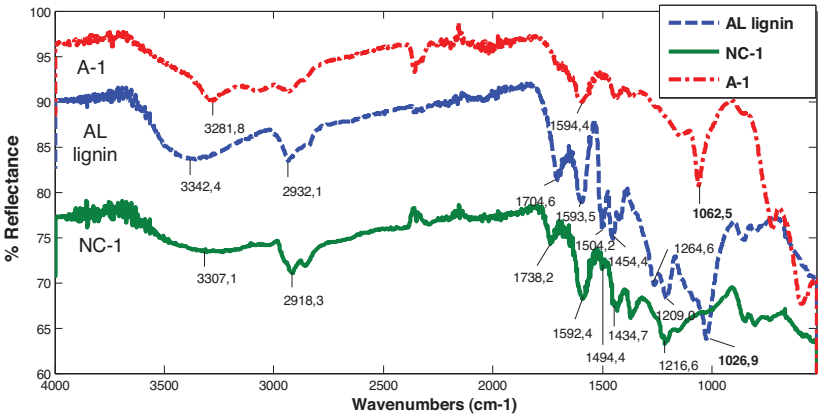

Fig. 2. FT-IR spectra for the AL lignin and the solids obtained in the A-1 and NC-1 experiments. For experimental conditions, see Table 1.

tems (especially Ru) and the concentration of light hydrocarbons which are Fischer–Tropsch type reaction products are higher when using the Pd and Rh.

3.4. Influence of the type of lignin

Three different types of lignins were tested to evaluate the influence of the lignin type in the non-catalyzed and catalyzed systems. To ensure sufficient oil yields in all systems, the experiments were carried out at 380 °C and 2 h reaction time. In total nine experiments were done, one non-catalyzed and two catalyzed (Rh and Ru) experiments for each lignin. The results obtained are summarized in Table 8.

The most obvious difference between the three lignins is in the pH of the recovered water phase. While the KL lignin, which is a low sulfonate lignin derived from a kraft pretreatment process, yields a water phase with a basic pH, the EL and the AL lignin yield acidic water phases. This is highly correlated with the performance of the catalyst in the different lignin systems. For the KL lignin, with final water phases pH from 8–9, there is no significant difference between the non-catalyzed and catalyzed systems. The best results are obtained for the Rh catalyst, with an oil yield of 52.3 wt% and a solid yield of 9.99 wt%, but these differences are not significant, and even lower oil yields are obtained in the case of the Ru catalyst. In contrast, significant differences in the oil yield values are observed for those lignins with a final water phase pH lower than 7. Here, the oil yield is increased and the solid yield decreased when using the catalysts. In the case of the acid lignin there is an increased of the oil yield in 30 wt% when using the Ru catalyst, while in the enzymatic lignin we obtained an increase of 19 wt%. In both cases the solid yield were reduced.

To further evaluate the role of the alumina support in the AL and EL lignin, three additional experiments using only the γ-alumina as catalyst where carried out at a temperature of 380 °C and 2 h reaction time (experiments A-4, A-KL and A-EL). These results are compared with the non-catalyzed and Ru catalyzed results in Table 8. For both lignins, at this reaction conditions, there is moderate increase in the oil yield when using the alumina compared to the non-catalyzed system, with a 3.4 wt% increase for the AL lignin and a 13.7 wt% increase for the EL lignin.

To further confirm the effect of the alumina catalyst in the AL lignin, the oils obtained were submitted to GPC-SEC and ESI-MS analysis (see Supplementary material Fig. S3a–c). As shown in Section 3.3.3, the average molecular weight of the oil is lower in the case of the alumina catalyzed experiment than in the case of the non-catalyzed system (Table 5). Furthermore, when analyzing the ESI-MS results, it can be observed that the Ru and alumina oil spectrograms show a narrower product distribution of the oils, mostly below the 500 Da, while in the non-catalyzed experiments the product distribution goes up to over 800 Da.

Another aspect that can be evaluated in these results is the nature of the solids when using the supported catalysts. In the case of the El lignin, enough solids are recovered to analyze the non-catalyzed and the Ru supported catalyzed solid phase. In Fig. 3, FT-IR spectrograms of the solids obtained in the Ru and non-catalyzed system are compared with the FT-IR spectra of the EL lignin. We can clearly see that the Ru solids shows the same reduced OH stretching peak, the lack of the methylene and methyl peak, the low intensity peaks in the aromatic region and the strong ether peak that appeared in the alumina solids FT-IR spectra in Section 3.3.4. The non-catalyzed solids also show comparable spectra to the solids analyzed previously (see Fig. 2).

Table 7
Composition of the gas phase for the selected experiments.

	CO_2 (%mol)	CO (% mol)	H_2 (% mol)	CH_4 (% mol)	C_2H_6 (% mol)	C_3H_8 (% mol)	C_4H_{10} (% mol)
NC-1[a]	59.50	7.95	31.33	1.01	0.12	0.04	0.05
Ru-1[a]	60.69	2.97	34.74	1.35	0.13	0.06	0.06
Pd-1[a]	62.80	3.34	31.39	2.11	0.15	0.08	0.13
Rh-1[a]	63.99	3.67	29.88	2.10	0.16	0.09	0.12

NC: non-catalyzed experiment. A: γ-alumina (0.2 g). Rh: rhodium on alumina (0.2 g). Ru: ruthenium on alumina (0.2 g). Pd: palladium on alumina (0.2 g).
[a] Reaction conditions: 340 °C and 6 h. 2 g of acid hydrolysis lignin, 5.0 g of water and 3.075 g of formic acid.

Table 8
Mass balance and aqueous pH of experiment with different lignins at 380 °C

Name of experiment	Type of lignin	pH (water phase)	Oil yield (% on lignin)	Solid yield (% on lignin)	Total Mass balance (%)	Lignin mass balance (%)
NC-4[a]	AL	4–5	54.0	26.3	99.1	80.2
Rh-4[a]	AL	3–4	74.0	5.2	95.8	79.2
Ru-4[a]	AL	4	83.9	8.2	102.3	92.1
A-4[a]	AL	3–4	57.4	24.5	97.0	81.9
NC-KL[a]	KL	8–9	47.9	10.4	90.2	58.3
Rh-KL[a]	KL	8–9	52.3	10.0	92.8	52.3
Ru-KL[a]	KL	8–9	44.7	6.9	89.0	51.6
A-KL[a]	KL	8–9	47.0	11.7	92.8	58. 7
NC-EL[a]	EL	5	28.3	25.5	91.3	53.8
Rh-EL[a]	EL	5	45.3	2.9	90.1	48.2
Ru-EL[a]	EL	5	47.7	15.3	91.9	63.0
A-EL[a]	EL	5	42.0	27.1	91.3	69.1

NC: non-catalyzed experiment. A: γ-alumina (0.2 g). Rh: rhodium on alumina (0.2 g). Ru: ruthenium on alumina (0.2 g). Pd: palladium on alumina (0.2 g). AL: acid hydrolysis lignin. KL: kraft lignin. EL: enzymatic hydrolysis lignin.

[a] Reaction conditions: 380 °C and 2 h. 2 g of acid hydrolysis lignin, 5.0 g of water and 3.075 g of formic acid.

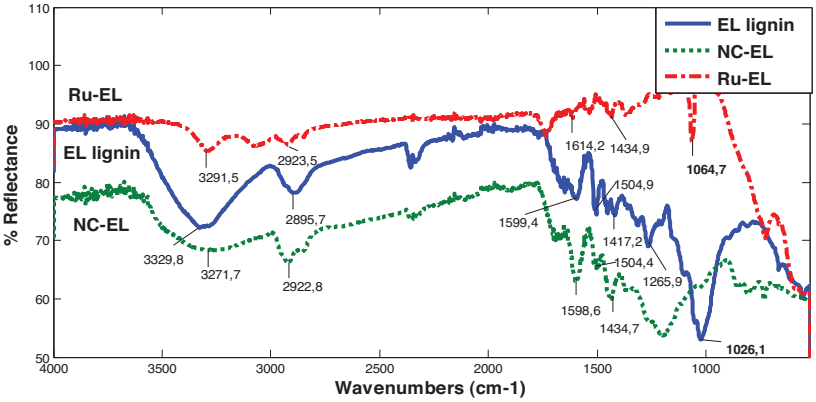

Fig. 3. FT-IR spectras for the EL lignin and the solids obtained in the Ru-EL and NC-EL experiments.

3.5. Influence of the hydrogen partial pressure

To evaluate the influence of the total reaction pressure of the system in the final oil and solid yield two extra experiments were carried out, one without catalyst and one with the Ru/Al_2O_3 catalyst. The proportions of the reactants were held constant, but the amount of each reactant was reduced to half for the NC-LP and the Ru-LP experiments. A lower amount of reactant, specially a lower amount of formic acid, will generate less of gases when the reactor is heated. Since the reactor volume is constant, a lower total pressure will result, for the same temperature, in a lower hydrogen partial pressure.

In Table 9, we compare the results of the low pressure experiments with their higher pressure counterparts. For the non-catalyzed experiments, with reduced pressure, the oil yield is decreased to nearly the half, from 58.2 wt% to 29.9 wt%. The solid yields is correspondingly higher, increasing from 22.4 wt% to 44.9 wt%. However when the supported Ru catalyst is used this effect is partially neutralized. The oil yield is lower, but the decrease is less than in previous case, from 90.0 wt% to 73.7 wt%. In the case of the solid yield, the increase is not significant, from 5.1 wt% to 6.6 wt%.

Another relevant result is the amount of gas obtained in the low-pressure experiments. Both for the NC-LP and the Ru-LP the gas percentage recovered is 3% higher than for their high pressure counterparts. This increase is observed together with a reduction in the values of the lignin mass balance percentage, suggesting that more lignin is gasified at these conditions.

Table 9
Gas oil and solid yield for the high pressure and low pressure (LP) and reducted catalyst loading (LC) experiments.

Name of experiment	Oil yield (% on lignin)	Solid yield (% on lignin)	Gas phase (% total)	Lignin mass balance (%)
NC-1[a]	58.2	22.4	30.5	80.6
NC-LP[b]	29.9	44.9	33.4	74.7
Ru-1[a]	90.0	5.1	29.1	95.0
Ru-LP[b]	73.7	6.6	32.4	80.3
Ru-LC[a,c]	85.2	4.5	30.0	89.7

NC: non-catalyzed experiment. Ru: ruthenium on alumina (0.2 g). LP: low pressure. LC: low catalyst content.

[a] Reaction conditions: 340 °C and 6 h. 2 g of acid hydrolysis lignin, 5.0 g of water and 3.075 g of formic acid.

[b] Reaction conditions: 340 °C and 6 h. 1 g of acid hydrolysis lignin, 2.5 g of water and 1.5375 g of formic acid and 0.1 g of catalyst.

[c] 0.1 g of catalyst.

3.6. Influence of the catalyst concentration

The amount of catalyst in the Ru system was reduced to 5 wt% on lignin (Ru-LC) to evaluate the effect of the catalyst concentration.

Even when the amount of catalyst was reduced to the half, the oil and solid yield does not vary significantly (Table 9). This suggests that the catalyst concentration could be reduced to 5 wt% on lignin without inducing major changes in the catalyst efficiencies.

4. Discussion

Replicate experiments in Table 4 show low standard deviation values, from 0.3 to 6% ($n = 3$) for the oil and solid yields, which support that the reactions and workup are reproducible. The deviations that are observed can be caused by inhomogeneity in the lignins, evaporation of volatile compounds and experimental errors during the work-up procedure. The consistency of the reaction process and work-up procedure is further confirmed by mass balances shown in Table 3, with a total mass recovery above 95 wt% for all the cases, and higher than 98 wt% for the supported-catalyzed systems.

The effect of the selected catalysts (Ru/Al_2O_3, Rh/Al_2O_3 and Pd/Al_2O_3) is positive for all the experimental conditions tested, as described in Section 3.3.2. This could be due to kinetic control of the lignin degradation mechanism by the catalysts. Gasson and Forchheim [22,23] suggest that the primary reaction in lignin solvolysis is a fast de-polymerization step, followed by competing reactions giving hydrodeoxygenation or repolymerisation of the de-polymerized monomers. The apparent activation energy values obtained for this kinetic model show that the probability of re-polymerisation of the lignin monomers is reduced when the monomers are hydrodeoxygenated and/or alkylated (see the simplified reaction scheme in Fig. 4).

This effect is further confirmed by the results described in Sections 3.2.2, 3.3.3 and 3.5. Section 3.2.2 shows that the presence of a metalic reaction surface containing among other metals Ni and Mo, can increase the oil yield and reduce the solid yield. These metals are well known catalysts for hydrodeoxygenating reactions [19], and can also provide the kinetic enhancement discussed above. Nevertheless, the quantitative results indicate that the activity of the metallic reaction surface is significantly lower than the activity of the Ru/Al_2O_3 catalyst. Section 3.3.3 shows how the Ru, Rh and Pd systems have the highest H/C and lower O/C ratios in the oil phase products (Table 6) and the Ru and Pd systems the higher concentrations of highly hydrodeoxygenated compounds (Table 5). Finally, the results in Section 3.5 also confirm this kinetic enhancement. The lower hydrogen partial pressure of the system lowers the hydrogenation rate, which significantly affects the oil and solid yield in the un-catalyzed system, while the Ru system is not as strongly affected. The oil yield is reduced to half in the case of the un-catalyzed system as opposed to only 17 wt % reduction in the case of the Ru system, and the solid yield is doubled in the un-catalyzed system while it remains nearly stable for the Ru system. All this suggests that the Ru, Pd and Rh active phases will catalyze the hydrodeoxygenation reactions (see Fig. 4), increasing the oil yield and reducing the solid yield.

Another point for evaluation is to what degree the bifunctionality of the catalyst is important. The role of the hydrogenating active site (Ru, Rh and Pd) has already been discussed, but the support materials may also play an important role in the lignin degradation mechanism. Previous work suggests that acid heterogeneous catalysts are able to catalyzed the cleavage of ether bonds and cause de-polymerization of lignin [17,24], the polymerization of alcohols to ethers (re-polymerization) [25,26] and the deoxygenation of hydroxyl and methoxy aromatics [19,20]. Therefore an effect of the alumina support due to its acid nature could be expected. The results given in Table 4 show that alumina alone had no significant effect on the oil and solid yields, which may be due to the ability of alumina to catalyze both the de-polymerization and re-polymerization reactions. However, the composition of the oil shows a clear difference between the non-catalyzed and alumina catalyzed systems.

Table 5 indicates that the lowest values of average molecular weight are obtained for the oils from the γ-alumina and Pd systems. The ESI-MS analyses show that the γ-alumina has the highest concentration of low molecular weight compounds, followed by the Pd, Ru and Rh systems. The un-catalyzed system is the only one that shows high concentration of high molecular weight compounds. These results are in agreement with the acidity measurement in Section 3.1. The γ-alumina sample shows the highest stable acidity and consequently the oil obtained is the one with the lowest average molecular weight (215 Da). On the other hand, the oils in the noble metal containing catalysts have significantly higher average molecular weight in the following order: Pd/Al_2O_3 (323 Da) < Rh/Al_2O_3 (344 Da) < Ru/Al_2O_3 (397 Da). Since this order is inversely proportional to the active acidity of the catalysts, we can conclude that stable -strong Lewis acid sites play an important role in the de-polymerization of lignin into monomers. The acid alumina support could also be able to catalyze the re-polymerization of the lignin monomers, which can be confirmed by comparing the FT-IR spectra for the AL lignin, the non-catalyzed and the alumina system. As described in Section 3.3.4, the solid phase from the γ-aluna system has limited or no presence of methylene and carbonyl functionalities, very low concentration of intramolecular H-bonding of the hydroxyl groups, low intensity of aromatic bands and quite intense ether functionalities. In addition to this, the elemental composition data (Table 6) show that the solid phase has a high O/C ratio, which suggests that the O atoms have been retained in polyphenolic or aryl ether dominated solids. On the other hand, the lack of ether functionalities and low O/C ratio in the un-catalyzed system suggest a more graphite like structure of the solid phase for this system. We can conclude that the alumina support directs the reactions towards an aryl ether type structure through acid-catalyzed condensation reactions of the hydroxyl groups present in the depolymerized lignin monomers. The same comparison was done for reactions with EL lignin, where solids from the Ru and the non-catalyzed system were compared. In Fig. 3, the most intense IR peak for the Ru solid also corresponds to C—O stretching, again indicating a predominance of ether moieties in the solid products. The importance of the acidity of the reaction system for the final oil and solid yield can also be evaluated by comparing experiments with different pH values in the reaction medium. As shown in Section 3.4, when the recovered water phase pH is >7 (KL lignin), no significant effect of the catalyst on the oil or solid yield is observed. There are two possible explanations for this observation; either the acid sites of the solid are deactivated, or the influence of the basicity of the lignin is just through the pH of the reaction mixture. The increased oil yields obtained from the acidic AL and EL lignins in the catalyzed systems suggest that the latter mechanism is the main reason for the lack of effect of the catalyst. Furthermore, if the γ-alumina system is compared with the non-catalyzed system, we can clearly see that the presence of alumina at 380 °C and 2 h icreases the amount of oil in acidic reaction media (marginally significant increase of 3.4 wt% for the A-4 experiment and a significant increase of 13.7 wt% for the A-EL experiment). This effect is higher for the EL lignin, which might be due to the higher pH of the reaction system. In the AL lignin, this increase is not so significant, but the GPC-SEC (Table 5) and the ESI-MS analysis confirms the higher amount of low molecular weight compounds in the alumina system. All this implies that the properties of the selected lignin are a key factor when selecting the most efficient catalyst.

Finally, the effect of the catalysts in the composition of the gas phase should also be mentioned. The complexity of the reaction mechanisms producing the gas phase makes it complicated to analyze the reasons behind the disparity in the concentration of the components. It is clear that the lower CO values of the catalyzed

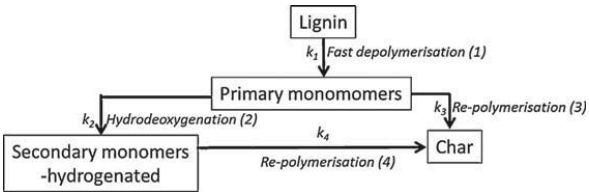

Fig. 4. Simplified reaction scheme of lignin degradation.

systems (see Section 3.3.5), can be caused by on the one hand, the displacement of the WGS equilibria towards the production of H_2, predominant in the Ru catalyst, and on the other hand to the Fishcer–Tropsch type reactions to low molecular weight hydrocarbons like methane, mainly in the Rh and Pd catalyst. The first mechanism is supported by the observation that higher H_2 amounts are found in the Ru system even though higher quantities of hydrogen are incorporated into the liquid products in the course of the reaction. The later mechanism is based on the observation that higher amounts of volatile alkanes are present in the Pd and Rh systems. Together, this indicates an effect of the catalyst in the final composition of the gas phase. In any case, the higher amount of hydrogen in the Ru system could be a reason for the highest oil yields obtanied in this system.

5. Conclusion

The simultaneous catalytic de-polymerization and hydrodeoxygenation of KL, EL and AL lignings was carried out in a formic acid/water media and their results were compared with the non-catalytized and a gamma-alumina support catalyzed system. Three bifunctional catalysts were screened, Rh, Pd and Ru on alumina, and evaluated in terms of the conversion of the lignin to oil and solids. A central focus of this paper was to identify the role of the alumina support and to evaluate its effect on the process. As a summary, the following conclusions can be made:

- The effect of the supported catalyst (Rh/Al_2O_3, Ru/Al_2O_3, Pd/Al_2O_3) is positive with regard to an increase on oil yield and a decrease on solid yield. The best result in terms of oil yield is for the Ru system, while the most effective one for the reduction of the solid yield was the Pd system.
- When analyzing the composition of the oils, 8 major components are identified and quantified: phenol, cresol, guaiacol, methyl guaiacol, catechol, ethylcathecol, syringol and *o*-vanilin. Ru shows the highest amount of highly hydrodeoxygenated monomers, followed by the Pd catalysts. However, when analyzing the average elemental composition of the oils, Pd and Rh show lower O/C and higher H/C ratios.
- The alumina support plays a vital role in the de-polymerization of lignin. This has been proved by analyzing the yields and composition of the oil and by changing the type of lignin and consequently the pH of the reaction media. The presence of temperature-stable Lewis acid sites seems to increase the amount of low molecular weight compounds in the oils.
- The alumina support plays also a role in the re-polymerization of the lignin monomers. The elemental and FTIR analysis of the solids suggest an alternative re-polymerization mechanism when the alumina support is present in the system.
- The type of lignin is a key factor when analyzing the effect of the selected catalyst. Only lignins that provide acid reaction media are suitable for this type of bifunctional catalysts.
- The pressure has a strong influence in the final oil and solid yield. Under reduced pressure conditions, the oil yield is reduced while the solid yield is increased. This effect is partially neutralized when using a catalyst. In both cases the amount of lignin gasified increases.
- The reactor surface has a positive effect on the oil and solid yield. This is due to mainly its Ni and Mo content, which can catalyze hydrodeoxygenation reactions.
- The catalyst also affects the decomposition of the formic acid into molecular H_2 and CO/CO_2. The Ru catalyst is able to induce a higher production of H_2, while the Rh and Pd catalyst are responsible for a higher production of low molecular weight compounds.

Acknowledgements

We gratefully acknowledge financial support from the Lignoref project group, including The Research Council of Norway(grant no. 190965/S60), Statoil ASA, Borregaard AS, Allskog BA, Cambi AS, Xynergo AS/Norske Skog, Hafslund ASA and Weyland AS.

Appendix A. Supplementary data

Supplementary data associated with this article can be found, in the online version, at http://dx.doi.org/10.1016/j.jaap.2015.04.020

References

[1] J. Zakzeski, P.C.A. Bruijnincx, A.L. Jongerius, B.M. Weckhuysen, Chem. Rev. 110 (2010) 3552.
[2] M. Kleinert, J.R. Gasson, T. Barth, J. Anal. Appl. Pyrolysis 85 (2009) 108.
[3] A. Limayem, S.C. Ricke, Prog. Energy Combust. Sci. 38 (2012) 449.
[4] R.J.A. Gosselink, E. de Jong, B. Guran, A. Abächerli, Ind. Crops Prod. 20 (2004) 121.
[5] Q. Bu, H. Lei, A.H. Zacher, L. Wang, S. Ren, J. Liang, Y. Wei, Y. Liu, J. Tang, Q. Zhang, R. Ruan, Bioresour. Technol. 124 (2012) 470.
[6] A.L. Jongerius, P.C.A. Bruijnincx, B.M. Weckhuysen, Green Chem. 15 (2013) 3049.
[7] B. Li, W. Lv, Q. Zhang, T. Wang, L. Ma, J. Anal. Appl. Pyrolysis 108 (2014) 295.
[8] A.V. Bridgwater, Chem. Eng. J. 91 (2003) 87.
[9] S. Czernik, A.V. Bridgwater, Energy Fuels 18 (2004) 590.
[10] D.C. Elliott, Energy Fuels 21 (2007) 1792.
[11] N.P. Vasilakos, D.M. Austgen, Ind. Eng. Chem. Process Des. Dev. 24 (1985) 304.
[12] E. Dorrestijn, M. Kranenburg, D. Poinsot, P. Mulder, Holzforschung – Int. J. Biol. Chem. Phys. Technol. Wood (1999) 611.
[13] D. Mohan, C.U. Pittman, P.H. Steele, Energy Fuels 20 (2006) 848.
[14] M. Kleinert, T. Barth, Energy Fuels 22 (2008) 1371.
[15] M. Kleinert, T. Barth, Chem. Eng. Technol. 31 (2008) 736.
[16] L. Liguori, T. Barth, J. Anal. Appl. Pyrolysis 92 (2011) 477.
[17] C. Zhao, Y. Kou, A.A. Lemonidou, X. Li, J.A. Lercher, Chem. Commun. 46 (2010) 412.
[18] M. Tamura, K. Shimizu, A. Satsuma, Appl. Catal. A: General 433 (2012) 135.
[19] E. Furimsky, Appl. Catal. A: General 199 (2000) 147.
[20] C. Zhao, D.M. Camaioni, J.A. Lercher, J. Catal. 288 (2012) 92.
[21] C. Zhao, J. He, A.A. Lemonidou, X. Li, J.A. Lercher, J. Catal. 280 (2011) 8.
[22] J.R. Gasson, D. Forchheim, T. Sutter, U. Hornung, A. Kruse, T. Barth, Ind. Eng. Chem. Res. 51 (2012) 10595.
[23] D. Forchheim, J.R. Gasson, U. Hornung, A. Kruse, T. Barth, Ind. Eng. Chem. Res. 51 (2012) 15053.
[24] J. He, C. Zhao, D. Mei, J.A. Lercher, J. Catal. 309 (2014) 280.
[25] S.R. Kirumakki, N. Nagaraju, S. Narayanan, Appl. Catal. A: Gen. 273 (2004) 1.
[26] R. van Grieken, J.A. Melero, G. Morales, J. Mol. Catal. A: Chem. 256 (2006) 29.

Paper B

B

Analysis of the effect of temperature and reaction time on yields, compositions and oil quality in catalytic and non-catalytic lignin solvolysis with formic acid using experimental design

Authords:
Oregui Bengoechea, M.; Miletíc, N.; Vogt, M. H.; Arias, P.L.; Barth, T.

Submitted to:
Biomass & Bioenergy, **2016**.

Analysis of the effect of temperature and reaction time on yields, compositions and oil quality in catalytic and non-catalytic lignin solvolysis with formic acid using experimental design.

Mikel Oregui Bengoechea[a*] (double family name), Nemanja Miletíc[b], Mari H. Vogt[a], Pedro L. Arias[b], Tanja Barth[a]

[a] *Department of Chemistry, University of Bergen, Norway, Allegaten 41, N-5007 Bergen, Norway*

[b] *Department of Chemical and Environmental Engineering, School of Engineering, University of the Basque Country (EHU/UPV), C/Alameda Urquijo s/n, 48013 Bilbao, Spain*

Keywords: lignin conversion, formic acid, noble metal catalyst, alumina, response surface modeling (RSM), principal component analysis (PCA)

Abstract

The catalytic solvolysis of Norway spruce (*Picea abies* L.) lignin in a formic acid/water media using bifunctional Ru/Al_2O_3, Rh/Al_2O_3, Pd/Al_2O_3 catalysts was explored in a batch set-up at different temperatures and reaction times (283-397 °C and 21 min-700 min, respectively). Blank experiments using only γ–alumina as catalyst and non-catalyzed experiments were also carried out and compared with the supported catalysts results. Surface response methodology (RSM) and principal component analysis (PCA) were used to evaluate the effect of the reaction conditions and type of catalyst on the oil yield, solid residue yield, oil quality and composition. The optimum reaction conditions were found to be around 340 °C and 6 h using Ru/Al_2O_3 as a catalyst, where nearly complete conversion of lignin into oil is achieved (83.8 %), while still having high H/C ratios (1.21) coupled with low O/C ratios (0.19) and M_w values (500 Da). No correlations between the oil yield and the quality of the oil were found. The oil yield strongly depends on the presence of the catalyst, temperature and reaction time, while the oil quality is mainly dependent on the reaction conditions (reaction temperature and time). The recycling of the catalyst proved that the deactivation of the Ru/Al_2O_3 catalyst was negligible after two separate recycling tests. The results show the potential for improving the yields of oil by the use of catalysts which are easily recovered, and suggest a good potential for tuning the oil composition to specific composition depending on the requirements of the oil product.

1. Introduction

Global warming, volatile oil prices and world political instability point toward the necessity of new localized and environmentally friendly ways of producing fuels and oil derived products from non-alimentary biomass sources[1]. The development of economically feasible biomass-based bio-refineries is recognized as one of the best alternatives to meet all these ongoing challenges[2]. Among the biomass sources, lignocellulosic biomass (wood, grasses and agricultural residues) has been identified as a promising resource for this purpose[3], since unlike vegetable oil and sugar crops, the lignocellulose feedstocks avoid the negative side effect of intense farming[4] and ethical concerns about the use of food as fuel raw materials[5].

Extensive work has been carried out on the chemical and enzymatic fractionation of lignocellulose, and the subsequent conversion of the cellulose and hemicellulose fractions into bioethanol[5-6]. However, the third component, lignin, comprising between 10-30 % of the feedstock, is mostly considered as waste[7]. Several thermochemical processes have been explored as suitable for the conversion of lignin-rich residual materials into fuels or phenols[3, 8]. A promising and relatively new lignin conversion approach, known as lignin-to liquids (LtL), involves the use of formic acid (FA) together with a solvent. The solvent can be either ethanol or water, though the latter is preferred due to its lower cost and greener nature. High oil yields, with high H/C and low O/C ratios are obtained, still retaining the phenol-type structure of the bio- oil components. Therefore this versatile process can be used for the production of both a bio-oil that can be blended with conventional fuels and aromatic compounds such as phenol, catechol and guaiacol[9].

One of the major research challenges of the LtL method is to obtain high oil yields and good quality while decreasing the temperature and the reaction time of the process. Good oil quality can be defined as a high energy content, stable, non-acidic and low viscous oils[10], with high H/C and low O/C ratios and low average molecular weight distribution (M_w). One alternative to address this challenge is the use of a catalyst in order to increase the lignin conversion rate[11]. Previously in our group, Ru/Al_2O_3 (Ru), Rh/Al_2O_3 (Rh) and Pd/Al_2O_3 (Pd) have been shown to be active catalysts toward the conversion of lignin with formic acid in an aqueous media[12]. Among other aspects, the activity of the alumina support and the influence of the type of noble metal in the oil quality and yield were discussed.

However, the results were not conclusive since those effects were mainly studied only at a specific reaction conditions, i.e. 340 °C during 6 h.

A more systematic approach based on experimental design can be used, not only to confirm the effect of the alumina support and type of noble metal in the oil yield and quality in a wider experimental space, but also to address other aspects that could be interesting from an industrial perspective: (*i*) the optimal reaction conditions, (*ii*) possible correlations between the oil yield and the oil quality, (*iii*) the influence of reaction temperature and time in the composition of the oil, and (*iv*) activity of the catalysts upon recycling.

Here, a step-wise approach based on experimental design will be presented. Initially the effect of the temperature (300-380 °C) and reaction time (2-10 h) for three different catalytic systems (Ru, Rh, Pd) will be evaluated using a full factorial design. Response surface methodology (RSM) and principal component analysis (PCA)[10, 13] will be used to evaluate the influence of the reaction conditions and type of catalyst on the oil yield, solid residue yield, oil quality and composition. An additional aim of this screening study is to assess both the similarities and differences within the catalytic systems.

In a second step, the influence of temperature (283-397 °C) and reaction time (21 min-700 min) on three different reaction systems (non-catalyzed (NC), γ-Al_2O_3 (Al) and Ru catalyzed systems) will be studied based on a central composite design[14]. Again RSM and PCA will be used to evaluate the influence of the reaction conditions and type of system on the oil yield, solid residue yield, oil quality and composition. In addition, the role of the noble metal and the γ-alumina support in the lignin de-polymerization and hydrodeoxygenation will be evaluated.

In a third step, the activity of one of the catalysts will be evaluated upon two recycling cycles in terms of oil yield and quality.

2. Materials and Methods

2.1 Chemicals

Formic acid (>98%), tetrahydrofuran (THF) (>99.9%) and ethyl acetate (99.8%) were purchased from Sigma Aldrich and used as supplied. Lignin from Norway spruce (*Picea abies L.*) from strong acid carbohydrate dissolution pre-treatment was received from Technical College of Bergen. The lignin was ground, sieved (<500μm) and dried at 80 °C for 24 h prior to use.

2.2 Catalysts

Ruthenium on alumina (5 wt%), rhodium on alumina (5wt%), and palladium on alumina (10 wt%), were obtained from Sigma Aldrich (MO, USA), and γ-alumina (97 wt%) of similar of different nature to the one used for the preparation of the Sigma-Aldrich catalysts was purchased from Strem Chemicals Inc (MA, USA). These were dried at 80 °C for 24 h prior to use.

2.3 Catalyst characterization

The Al_2O_3 used to synthesize the supported catalyst (Ru/Al_2O_3, Rh/Al_2O_3, Pd/Al_2O_3) and the γ-alumina provided by Strem Chemicals Inc are of different nature. Therefore acidity measurements were carried out to evaluate the catalytic activity of the acid sites within the aluminas. The type of acidity (Lewis or Brønsted), the total acidity, the acidity retention and the active acidity of the Ru/Al_2O_3, Rh/Al_2O_3, Pd/Al_2O_3 and γ-alumina catalysts were analysed by NH_3-TPD and DRIFT of adsorbed pyridine.The active acidity is defined as the fraction of total acidity that actually plays a significant role in the reaction (active acidity (T) = acidity retention (T) x total acidity).

Temperature-programmed desorption of ammonia, NH_3-TPD, was performed to determine the total acidity of the samples. The measurements were carried out in a chemisorption analyzer AutoChem II equipped with a thermal conductivity detector (Micromeritics, USA). A detailed description of the analysis procedure is given elsewhere by Oregui Bengoechea *et al.*[12].

Diffuse reflectance infrared Fourier transform, DRIFT, was used to distinguish Lewis and Brønsted acid sites of noble-metal containing catalysts and γ-Al_2O_3. The analyses were done using a VERTEX 70 spectrometer coupled with an external sample chamber that enables measurements under vacuum (Bruker, Germany). A detailed description on the analysis procedure is given elsewhere by Oregui Bengoechea *et al.*[12].

2.4 Experimental conditions

2.4.1 Experimental set-up

A detailed description is given elsewhere by Oregui Bengoechea *et al.*[12]. Briefly summarised, lignin (2 g), formic acid (3.075 g), water (5 g) and the catalyst (0.2 g) were added to a stainless steel reactor (Parr 4742 non-stirred reactor, 25 ml volume). The amounts of reactants are based on previous experiments for maximising oil yields. The reactor was closed and heated in a Carbolite LHT oven up to the desired conditions (283-397 °C) for a given reaction time (21 min-11 h 40 min).

2.4.2 Sample work-up

A detailed description is given elsewhere by Oregui Bengoechea *et al.*[12]. Briefly summarized, after the reactor was cooled down to the ambient temperature, the produced gas was vented and the gas quantity was determined. The reactor was opened and the liquid reaction mixture was extracted with a solution of ethyl acetate: tetrahydrofuran (90:10). The solid phase (unreacted lignin, reaction products and catalyst) was filtered and dried at ambient conditions for 2 days before weighing. Two well-separated liquid phases were obtained (organic top phase and aqueous bottom phase). The phases were separated by decantation and the organic phase was dried over Na_2SO_4 and concentrated at reduced pressure (ca. 250 mmbar) at 40 °C. The final oil and solid yield was determined by weight (amount of oil/char (g.)/amount of introduced lignin (g.)). The solid yield for the catalyzed systems is calculated after subtracting the amount of catalyst introduced. Therefore the solid yield refers to the organic solids (char) and the inorganic lignin ashes.

2.4.3 Recycling of the catalyst

2.4.3.1 Ash content of lignin: Three crucibles were calcined at 575 °C and weighed to the nearest 0.1 mg until constant weight (less than ±0,3 mg after one 1 h of heating at 575 °C). Once the weight of each crucible is recorded, between 0.5 and 2.0 g of lignin was weighed into each tared crucible. The lignin was calcined using the following temperature programme: hold the temperature at 105 °C for 12 min, increase the temperature until 250 °C at 10 °C /min, hold the temperature at 250 °C for 30 min, increase the temperature until 575 °C at 20 °C /min, and hold it at that temperature for 180 min. After cooling, the samples were weighed to the nearest 0.1 mg until constant weight. The final ash content is calculated as the mean of the three crucibles.

2.4.3.2 Recycling procedure: The residual solids recovered after the work-up described in Section 2.4.2, were subjected to a thermal treatment at 360 °C for two hours with a heating ramp of 2 °C /min to eliminate the organic (char) residues. After the thermal treatment the resulting solids, catalyst and ashes, were re-used at 340 °C and 6 h following the experimental set-up described in Section 2.4.1. The oil and solid yields were calculated by weight and the oil was analysed. This procedure was repeated again to evaluate the activity of the catalyst upon two recycling-cycles.

2.5 Characterization of the oils

2.5.1 GC-FID analysis

A detailed description is given elsewhere by Oregui Bengoechea *et al.*[12]. Briefly, the samples were first silylated with *N,O*-bis(trimethylsilyl)trifluoroacetamide (BSTFA) prior to the GC-FID analysis. The samples were analysed on a Thermo Finnigan TRACE GC Ultra with a FID-detector equipped with a chromatographic HP-ULTRA2 column from Agilent Technologies. The following heating programme was applied: 30 °C for one minute, and then heating at 10 °C /min up to 25 °C. The injector temperature was 250 °C, and the detector temperature was 320 °C. Identification of the peaks

was carried out by comparison with retention times of authentic commercially available reference compounds that were also silylated prior to the analysis. The quantitative data was obtained using hexadecane as internal standard. Calibration curves were prepared for the following compounds: phenol (Ph), cresol (Cr), guaiacol (Gu), methyl-guaiacol (M-Gu), catechol (Ca) and syringol (Sy), and their concentrations were calculated as % weight in the oil.

2.5.2 Elemental analysis

All samples were analysed for their elemental composition in the CHNS mode with a Vario EL III instrument using helium as carrier gas. The oxygen content was calculated by difference.

2.5.3 GPC-SEC

The sample (1 mg) was dissolved in 1 mL of THF. The solution (20 µL) was injected into a GPC-SEC system equipped with a PLgel 3 µm Mini MIX-E column, and analysed at a flow rate of 0.5 mL/min of THF at 21.1 °C, and the detection was performed with UV at 254 and 280 nm, as well as with IR at 4000-400 cm^{-1} range. The set of columns was calibrated with a series of polystyrene standards covering a molecular-mass range of 162–2360 Da.

2.6 Data analysis

2.6.1 Screening Experiments

A two-level full-factorial design with three center points was used to evaluate the influence of the temperature (x_1) and reaction time (x_2) in each of the three different supported catalysts (Ru/Al_2O_3, Rh/Al_2O_3, Pd/Al_2O_3). The experimental design was done separately for each catalytic system and different responses were examined: oil and solid yield, H/C and O/C ratio, average molecular weight distribution (M_w) and oil composition (see Section 2.6.1). The selected control variables (temperature and reaction time) and their levels for each system are described in Table 1. The relation between the coded and the actual values is the following:

$$x_i = \frac{X_i - X_0}{\Delta X}$$

Where X_i is the actual value of the variable, X_0 is the actual value of X_i at the center point, and ΔX is the step change of the variable.

Table 1: experimental design for catalyst screening

Experiment	X_1 Temperature (°C)		X_2 Reaction time (h)	
	Actual	**Coded**	**Actual**	**Coded**
X[a]-1	300	-1	10	+1
X[a]-2	380	+1	10	+1
X[a]-3	300	-1	2	-1
X[a]-4	380	+1	2	-1
X[a]-5	340	0	6	0
X[a]-6	340	0	6	0
X[a]-7	340	0	6	0

[a]**X:** refers to either Ru (Ru/Al_2O_3 catalyst), Rh (Rh/Al_2O_3 catalyst) or Pd (Pd/Al_2O_3 catalyst)

2.6.1.1 *Response surface methodology (RSM) for the oil and solid yield:* Response Surface Methodology (RSM) is a set of mathematical and statistical techniques that can be used to define the relationships between the response and the independent variables, and the objective is to maximize this response[10, 15]. In the present study oil and solid yields were selected as response variables and fitted in a first order polynomial regression model with an interaction factor (*see below*). First order models were selected to screen different supported catalyst (Ru/Al_2O_3, Rh/Al_2O_3, Pd/Al_2O_3) with the minimum number of experiments:

$$Y = \beta_0 + \sum \beta_i x_i + \sum\sum \beta_{ij}\ x_i x_j \quad (1)$$

Where Y is the predicted response variable (oil or solid yield); β_0, β_i, β_{ij} are constant regression coefficients of the model, and x_i, x_j (ij= 1,2; $i \neq j$) represent the coded values of independent variables that are used in statistical calculations. For each system separate oil and solid regression models were calculated and their response surface model built. After the regression model was obtained, the significance of the regression model was evaluated by the analysis of variance (ANOVA)[16].

2.6.1.2 *Principal component analysis (PCA) to evaluate the quality of the oil:* Principal component analysis (PCA) is a commonly used technique in statistics for simplifying the data by reducing multivariable to a 2-D plot in order to characterise the results. The use of principal component analysis allows identifying the factors which influence the data so that relationships can be established on a qualitative analysis. PCA uses complex matrix transformation which does not impose fixed vectors, and is completely dependent on the data set[17]. PCA has been used in the past to discriminate the effect of reaction conditions and reactant compositions in the quality of the LtL oils [4] . In the present study, the variables studied to evaluate the quality of the oils are: reaction temperature, reaction time, type of catalyst, oil and solid yield, H/C and O/C ratio of the oil and average molecular weight distribution (M_w). The variable named catalyst is added to visualize the effect of the type of catalyst. This is a three level variable where Ru is represented by the coded level +1, Rh by 0, and Pd by -1. No cross-term is considered in this analysis to maximize the explained variance.

2.6.1.3 *Principal component analysis (PCA) to evaluate the oil composition:* Eight variables were submitted to PCA analysis. Three process variables, reaction temperature, reaction time and type of catalyst; and five response variables, named concentration of phenol (Ph), guaiacol (Gu), catechol (Ca), cresol (Cr) and methyl-guaiacol (M-Gu) in the oils. No cross-term is considered in the analysis to maximize the explained variance.

2.6.2 Optimization experiments

A central composite design (CCD) with axial (α=1.41) and three centre points was used to evaluate the influence of the temperature (x_1) and reaction time (x_2) in three different reaction systems (NC: the non-catalysed system, Al: the γ-alumina catalysed system and the Ru catalysed system). The Ru system represents the best catalytic system in terms of oil yield. CCD allows determining both linear and quadratic models and is a good alternative of a three level full factorial design as it provides comparable results with a smaller number of experiments[18]. The experimental design was carried out separately for each catalytic system and different responses were examined: oil and solid yield, H/C and O/C ratio, and M_w and oil composition (see Section 2.6.1). The selected control variables (temperature and reaction time) and their levels for each system are described in Table 2. The relation between the coded and the actual values is the following:

$$x_i = \frac{X_i - X_0}{\Delta X}$$

Where X_i is the actual value of the variable, X_0 is the actual value of X_i at the centre point, and ΔX is the step change of the variable. For each system separate oil and solid regression models were calculated and their response surface model was built. After the regression model of experimental data was obtained, the significance of the regression model was evaluated by the analysis of variance (ANOVA)[16].

Table 2: experimental design for system optimization

Experiment	X_1 Temperature (°C)		X_2 Reaction time (h)	
	Actual	Coded	Actual	Coded
X[a]-1	300	-1	10	+1
X[a]-2	380	+1	10	+1
X[a]-3	300	-1	2	-1
X[a]-4	380	+1	2	-1
X[a]-5	340	0	6	0
X[a]-6	340	0	6	0
X[a]-7	340	0	6	0
X-[a]S1	397	+1.41	6	0
X-[a]S2	283	-1.41	6	0
X-[a]S3	340	0	21 min	-1.41
X-[a]S4	340	0	11 h 40 min	+1.41

[a]**X:** refers to either the Ru catalyzed system (Ru), γ-Al_2O_3 catalyzed system (Al) or the non-catalyzed system (NC) **S:** refers to the axial points were α=1.41

2.6.2.1 *Response surface methodology (RSM) for the oil and solid yield:* Previous screening tests suggested that the introduction of the quadratic term was necessary to build significant regression models. Therefore, in this section the oil and solid yields were selected as response variables and fitted to second-order (quadratic) models in the form of quadratic polynomial equation:

$$Y = \beta_0 + \sum \beta_i x_i + \sum \beta_{ii} x_i^2 + \sum \sum \beta_{ij}\ x_i x_j \qquad (2)$$

Where Y is the predicted response variable (either oil or solid yield); β_0, β_i, β_{ii} ,β_{ij} are constant regression coefficients of the model, and x_i, x_j (ij= 1,2; i ≠ j) represent the coded values of independent variables that are used in statistical calculations. For each system separate oil and solid second order regression models were calculated and their response surface model was built. After the regression model of experimental data was obtained, the significance of the regression model by analysis of variance (ANOVA).

2.6.2.2 *Principal component analysis (PCA) to evaluate the quality of the oil:* The variables studied to evaluate the quality of the oils are: reaction temperature, reaction time, type of system, oil and char yield, H/C and O/C ratio of the oil and average molecular weight distribution (M_w). The variable named system is added to visualize the effect of the type of system. This is a three level variable where Ru is represented by the coded level +1, NC by 0, and Al by -1. No cross or quadratic term is considered in the analysis to maximize the explained variance.

2.6.2.3 *Principal component analysis (PCA) to evaluate the oil composition:* Initially eight variables were submitted to PCA analysis. Three process variables, reaction temperature, reaction time and type of system; and five response variables, named concentration of Ph, Gu, Ca, Cr and M-Gu in the oils

(see Section 2.5.1). No cross or quadratic term is considered in either analysis to maximize the explained variance.

3. Results and Discussion

3.1 Acidity Results of Ru/Al_2O_3, Rh/Al_2O_3, Pd/Al_2O_3 and γ-alumina

Table 3 summarizes the results obtained for the DRIFT and NH_3-TPD analysis. IR bands assigned to Brønsted acid sites (1545 and 1638 cm^{-1}) were not detected in any of the samples[19], suggesting that only Lewis acidity (1448 cm^{-1}) is present (see *Figure S1, Supplementary Information*).

Table 3: Total acidity, acidity retention and active acidity of γ-alumina, Rh/Al_2O_3, Ru/Al_2O_3 and Pd/Al_2O_3.

	Total acidity[a] (mmol NH_3/g cat.)	Acidity retention[b] (%)	Active acidity (mmol NH_3/g cat.)
γ-alumina	1.51	100 (100 °C) 92 (200 °C) 92 (300 °C)	1.51 (100 °C) 1.39 (200 °C) 1.39 (300 °C)
Rh/Al_2O_3	1.34	100 (100 °C) 71 (200 °C) 49 (300 °C)	1.34 (100 °C) 0.95 (200 °C) 0.66 (300 °C)
Ru/Al_2O_3	0.78	100 (100 °C) 77 (200 °C) 51 (300 °C)	0.78 (100 °C) 0.60 (200 °C) 0.40 (300 °C)
Pd/Al_2O_3	0.76	100 (100 °C) 99 (200 °C) 98 (300 °C)	0.76 (100 °C) 0.75 (200 °C) 0.74 (300 °C)

[a] Data obtained from NH_3-TPD [b] Data obtained from DRIFT

The highest total acidity measured by NH_3-TPD was obtained for the γ-Al_2O_3 (1.51 mmol NH_3/g catalyst), with significantly lower acidities for the supported catalysts (Rh/Al_2O_3 > Ru/Al_2O_3 > Pd/Al_2O_3). Based on the IR band at 1445 cm^{-1}, acidity retention was also calculated as [peak area (T) / peak area (100 °C)] x 100 (Table 3). Increasing the temperature did not influence the Lewis acid-bound pyridine in Al_2O_3 and Pd/Al_2O_3, but caused pyridine desorption in the case of Rh/Al_2O_3 and Ru/Al_2O_3. This suggests that the Lewis sites present in Rh/Al_2O_3 and Ru/Al_2O_3 samples are rather weak compared to the ones present in Al_2O_3 and Pd/Al_2O_3. Therefore the catalyst with the highest active acidity is γ- Al_2O_3 followed by Pd/Al_2O_3, Rh/Al_2O_3 and Ru/Al_2O_3.Note that the calculated active acidity is an approximation of the absolute active acidity of the solids since the acid sites titrated by NH_3 and pyridine are not strictly of the same nature.

3.2. Screening experiments: effect of the type of catalyst

3.2.1 Effect of the catalyst, temperature and time on the oil and solid yield

The main goal of this experimental set was to determine which catalyst performs best in the terms of high oil and low solid yield. For this purpose three analogous experimental sets for the Pd, Rh and Ru catalysts were subjected to surface response modelling. The experiments were performed randomly to minimize the systematic error. The results obtained for the oil and solid yield are summarized in Table 4.

Table 4: Experimental design for screening experiments and oil and solid yields

Exp.	Oil Yield (%)	Solid Yield (%)	H/C	O/C	Mw	Ph*	Gu*	Ca*	Cr*	M-Gu*
Pd-1	86.1	12.8	1.19	0.21	444	2.6	4.2	1.1	5.8	3.8
Pd-2	57.1	6.2	1.18	0.1	305	2.8	3.3	0.7	5.3	3.7
Pd-3	38.2	60.3	1.24	0.26	538	2.3	3.7	0.3	0.0	3.4
Pd-4	78.5	7.5	1.15	0.16	404	2.0	2.9	1.7	4.3	2.8
Pd-5	81.7	2.8	1.21	0.14	323	2.5	3.4	2.0	5.2	3.4
Pd-6	85.4	2.4	1.19	0.17	332	1.9	2.8	2.0	3.9	2.6
Pd-7	81.6	2.9	1.21	0.18	340	2.2	3.1	2.0	4.6	3.0
Rh-1	83.0	16.5	1.22	0.22	556	2.0	3.4	1.1	4.6	3.1
Rh-2	58.9	5.7	1.18	0.1	187	2.0	2.6	0.6	4.3	2.9
Rh-3	38.4	56.4	1.25	0.26	561	3.4	5.3	0.3	0.0	5.0
Rh-4	74.0	5.2	1.15	0.16	296	1.7	2.5	1.1	3.6	2.4
Rh-5	81.0	4.8	1.21	0.14	344	1.4	2.0	1.3	2.9	1.9
Rh-6	83.9	4.0	1.2	0.16	388	1.3	1.9	1.7	2.8	1.8
Rh-7	76.6	5.0	1.2	0.16	420	1.4	2.0	1.5	2.9	1.9
Ru-1	91.8	10.1	1.23	0.18	688	2.4	4.0	1.3	5.2	3.5
Ru-2	60.7	5.0	1.19	0.09	359	2.5	2.7	0.4	4.4	0.0
Ru-3	37.0	61.9	1.25	0.26	721	2.1	3.4	0.3	4.7	3.1
Ru-4	83.9	8.2	1.17	0.17	497	1.5	2.3	1.7	3.2	2.1
Ru-5	90.0	5.1	1.21	0.19	490	1.6	4.5	2.4	6.7	4.4
Ru-6	84.2	3.3	1.21	0.19	522	1.3	3.9	2.1	5.5	1.7
Ru-7	86.2	3.2	1.21	0.19	487	2.0	3.2	1.9	4.3	2.8

Pd: Pd/Al_2O_3 was used as catalyst **Rh:** Rh/Al_2O_3 was used as catalyst **Ru:** Ru/Al_2O_3 was used as catalyst. The experimental conditions are given in Table 1. *: Phenol (Ph), cresol (Cr), guaiacol (Gu), methyl-guaiacol (M-Gu), catechol (Ca) and syringol (Sy) yields as %(weight) in the oil

Table S1, *Supplementary Information*, shows the results of the analysis of variance (ANOVA) of the fitted models for the oil and solids yields. The ANOVA results illustrate that none of the models are significant for a 90 % confidence interval. Nevertheless, the aim of this section is not to build significant models, but to evaluate the effect of the type of catalyst, temperature and reaction time in the response variables.

Figure 1 and Figure 2 show the surface response models for each catalyst system. The former describes the oil yields while the latter the solid yields. Note that the temperature and reaction time axes are in different position for the oil and solid yield. The fitted equations for the oil and char yield are presented in Table 5. From the results depicted, one main conclusion is obtained: the Ru, Pd and Rh systems behave similarly for both the oil and solid yield, with regression coefficients that are of the same sign and comparable magnitude.

Table 5: Fitted equations for the oil and solid yield

System		Equation
Pd[a]	**Oil Yield (%)**[d]	$Y = 72.66 + 2.83X_1 + 6.63X_2 - 17.33X_1X_2$
Rh[b]		$Y = 70.83 + 2.88X_1 + 7.38X_2 - 14.93X_1X_2$
Ru[c]		$Y = 76.25 + 3.95X_1 + 7.9X_2 - 19.5X_1X_2$
Pd[a]	**Solid Yield (%)**[e]	$Y = 13.56 - 14.85X_1 - 12.2X_2 + 11.55X_1X_2$
Rh[b]		$Y = 13.94 - 15.5X_1 - 9.85X_2 + 10.1X_1X_2$
Ru[c]		$Y = 13.83 - 14.7X_1 - 13.75X_2 + 12.15X_1X_2$

Pd: Pd/Al_2O_3 system **Rh:** Rh/Al_2O_3 system **Ru:** Ru/Al_2O_3 system **Oil Yield (%):** regression model built for the oil yield (%) **Solid Yield:** regression model built for the solid yield (%)

According to the fitted equations, high temperatures or long reaction times increase the oil and decreases the solid yield, while the sign of the cross-term coefficient suggests that the maximum is found out of the experimental space, toward the corners. This is confirmed by the analysis of the surface response models in Figure 1, which shows that the highest oil yields are found at low temperatures and long reaction times and/or at high temperatures and short reaction times. When comparing the oil yields, it is clear that the Ru system gives the highest values, followed by Pd and Rh system. Lesser differences are seen in terms of solid yield, with the best results being obtained for the Pd catalyst, followed by the Ru and Rh. Therefore, Ru is selected as the best overall catalyst in terms of oil and solid yield. The behavior of this catalyst in the experimental space, together with the Al and NC system, will be quantitatively analyzed in Section 3.3.1.

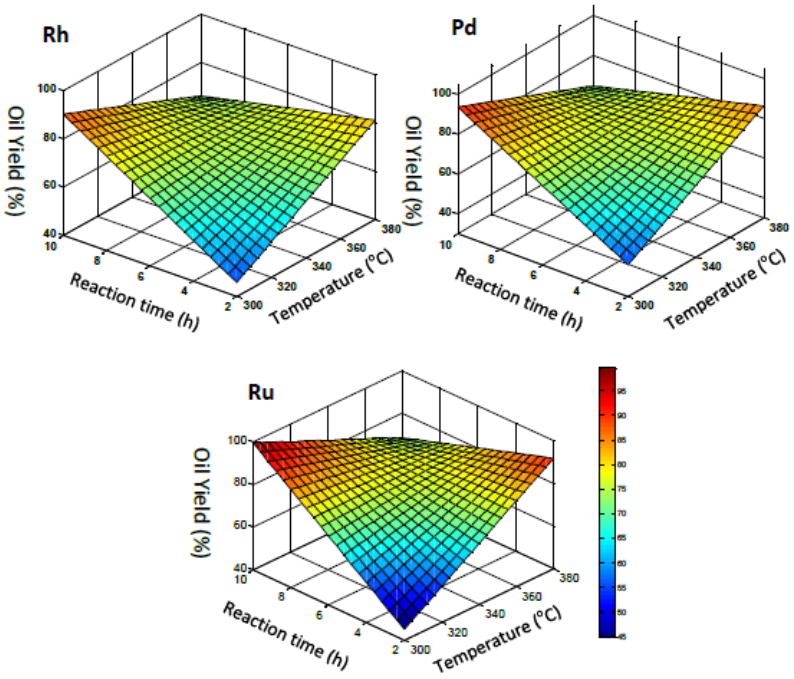

Figure 1: Response surface models for the oil yields. **Rh:** Rh/Al_2O_3 catalyzed system, **Pd:** Pd/Al_2O_3 catalyzed system , **Ru:** Ru/Al_2O_3 catalyzed system

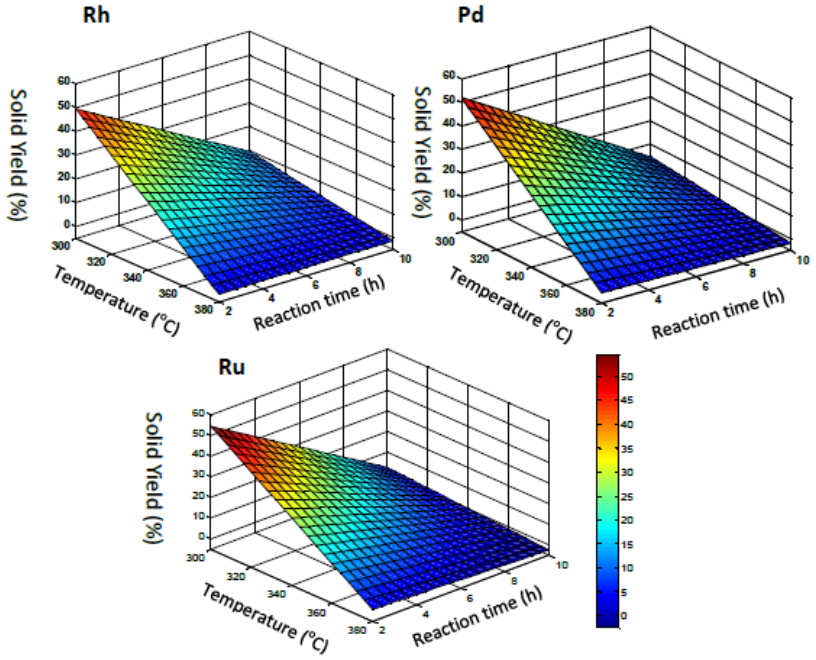

Figure 2: Response surface models for the solid yields. **Rh:** Rh/Al_2O_3 catalyzed system, **Pd:** Pd/Al_2O_3 catalyzed system , **Ru:** Ru/Al_2O_3 catalyzed system

3.2.2 Effect of type of catalyst, temperature and reaction time in the quality of the oil (PCA)

The aim of this section is mainly to establish the effect of the type of supported catalyst (Ru,Rh and Pd) on the quality of the oil, although correlations between reaction time, temperature and oil quality will also be discussed. The values of the variables studied are summarized in Table 4. 85 % of the explained variance is described by three principal components (PCs). When analyzing the score plots (Figure 3a), it can be observed that the objects are somehow grouped together according to the type of catalyst (Ru in red, Rh in blue and Pd in green) and reaction conditions. Thus there is a correlation between the oil quality, oil and solid yield, the type of catalyst and the reaction conditions.

When analyzing the loading plots (Figure 3b), some correlations between the design variables and the oil quality variables can be observed. The most obvious observation is that the M_w is positively correlated to the catalyst variable in all cases. This means that the Ru catalyst gives the oils with the highest average molecular weight distributions followed by the Rh and Pd catalysts. Previous results obtained in our group [12] suggest that the average molecular weight is dependent on the active acidity of the alumina support (see Section 3.1), since lowering the active acidity resulted in an increase in the average molecular weight within the oils. This correlation is therefore confirmed by the data present in this study. M_w is negatively correlated to the temperature and reaction time on PC1, which explains up to 52.5 %. Further analysis of the data in Table 4 confirms this correlation: increasing the temperature and prolonging the reaction time resulted in oils with lower molecular weight. For a given reaction temperature, lower M_w values are obtained at longer reaction times.

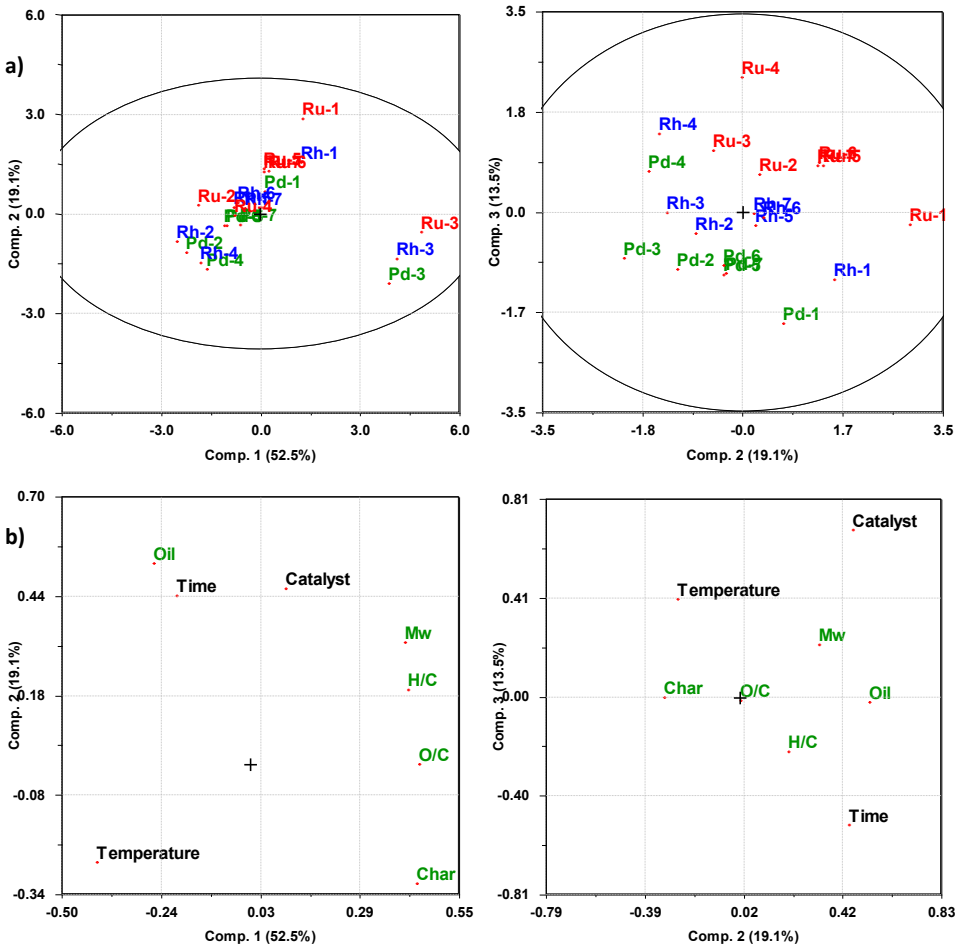

Figure 3: Score and loading plots for the quality of the oil. a) Score plots of the PCA analysis for the catalyst screening. Pd experiments in green, Rh experiments in blue, Ru experiments in red b) Loading plots of the PCA analysis for the catalyst screening. Factors describing the reaction conditions in black, factors describing the oil yield (oil), solid yield (char) and quality of the oil (H/C, O/C and M_w) in green. Coding for the response variables is given in Table 1.

A strong negative correlation is found between the temperature and the H/C ratio, while no or weak correlations are found between the catalyst and the H/C ratio. When analyzing the data in Table 4 three trends can be identified: (*i*) at low temperatures the H/C ratio decreases with the reaction time, (*ii*) at high temperatures the H/C ratio increases with the reaction time, and (*iii*) slightly higher H/C ratios are obtained for the Ru system. In terms of O/C ratio, there is a clear negative correlation between this variable and the temperature and reaction time, while no correlation is found between the O/C ratio and the catalyst variable. This is confirmed when analyzing the raw data in Table 4, illustrating that high temperatures and long reaction times are the most beneficial conditions in terms of low O/C ratio. Hence the data show two different behaviors in the elemental analysis of the oils depending on the temperature level. At low temperature both the O/C and H/C ratios decrease, while at high temperatures the O/C decrease and the H/C increases.

Another interesting result is the lack of correlation between the oil yield and the quality of the oil (H/C ratio, O/C ratio and M_w value). This is confirmed by both the loading plots and the analysis of the raw data. High H/C, O/C ratios and M_w values are obtained at low oil yields. Hence, the best reaction conditions are found around the center points: high oil yields coupled with relatively low M_w values and O/C ratios and relatively high H/C ratios.

3.2.3 Influence of the type of catalyst on the concentration of selected compounds

The values submitted to PCA are given in Table 4. In the data analysis 71.55 % of the variance is explained by three PCs. Figure 4 shows the score and loading plots. From the loading plots it can be observed that those compounds bearing methoxy-groups, such as Gu and M-Gu, show only a strong negative correlation with the temperature. Ca, a compound with two hydroxy-groups, is positively correlated to the catalyst variable and non-correlated with the temperature and reaction time. Coumpounds with only one hydroxy-group, such as Ph and Cr, are positively correlated with the reaction time. The former, Ph, is also negatively correlated to the catalyst, and while the latter, Cr, is positively correlated to the reaction time and catalyst variable.

These observations are in accordance with the behaviour of the elemental analysis of the oils presented in Section 3.2.2. At low temperatures the H/C and O/C ratios decrease with time suggesting that at this temperature level de-methoxylation and dehydration reactions of methoxy- and hydroxyl-bearing compound are the prevailing reactions. However, at high temperatures, low amount of methoxy- bearing compounds are found at low reaction times and the prevailing reaction seems to be the alkylation of the monomers, which would justify both the increase of the H/C ratio and the decrease of the O/C ratio.

Previous works[20] proposed the following mechanism. Lignin is initially depolymerized into primary products bearing methoxy groups such as syringol and different guaiacols. These react further accompanied by an increase in the degree of demethoxylation and deoxygenation of the different substituted species to yield catechols and thereafter phenols as stable products. Unlike this kinetic study, our experimental set is held at different temperatures. This might have distorted the actual correlations, but the loading plots still support the mechanism. At low temperatures, when the conversion rate is slow, Gu and M-Gu are at high concentrations. Ca is not correlated with any of the reaction conditions, which could indicate that this compound is an intermediate. Finally, at long reaction times the concentrations of Ph and Cr are the highest which suggests them as the end products. In terms of type of catalyst, Ru seems to favor the abundance of both catechol and cresol, while Pd seems to be the most suitable catalyst when oils with a high concentration in phenol are preferred.

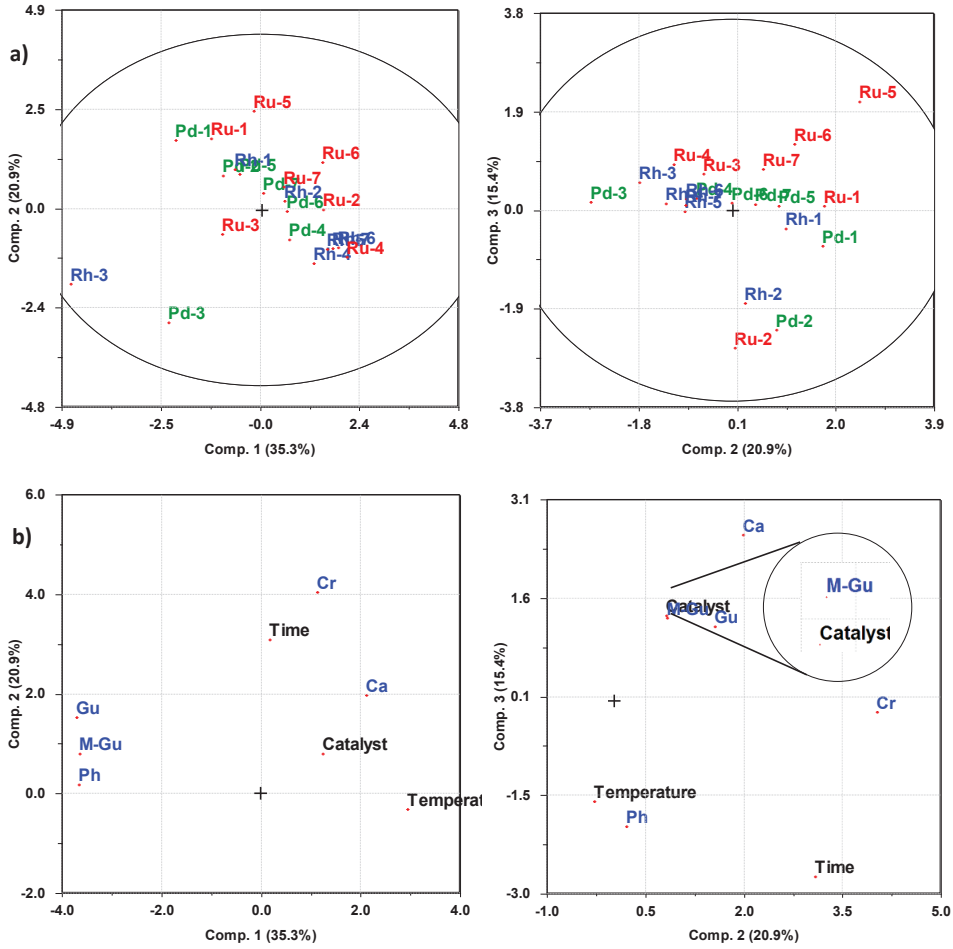

Figure 4: Score and loading plots for the composition of the oil. a) Score plots of the PCA analysis for the catalyst screening. Pd experiments in green, Rh experiments in blue, Ru experiments in red b) Loading plots of the PCA analysis for the catalyst screening. Factors describing the reaction conditions in black, factors describing the concentration of certain components in blue. Coding for the response variables is given in Table 1

3.3 Optimization experiments: Effect of the type of system

3.3.1 Influence of the type of system, temperature and reaction time on the oil and solid yields

In Section 3.2 several first order response surface models were built to analyze the effect of the type of catalyst, temperature and time, but none of them were statistically significant. In this section, the best catalyst in terms of oil and solid yield, Ru, is compared to additional reaction systems NC (non-catalyzed) and Al (γ-alumina catalyst) to evaluate which is the effect of the alumina support and the noble metal (Ru) in the reaction in a central composite design with a wider experimental basis for the modelling. The results obtained for the oil and solid yield are summarized in Table 6.

Table 6: Experimental design for optimization experiments and oil and solid yields

Experiment	Oil Yield (%)	Solid Yield (%)	H/C	O/C	Mw	Ph*	Gu*	Ca*	Cr*	M-Gu*
NC-1	64.8	31.7	1.13	0.2	431	1.9	3.3	1.5	4.2	2.8
NC-2	50.2	16.2	1.17	0.08	206	2.9	3.7	0.5	5.9	4.3
NC-3	32.1	57.5	1.17	0.24	553	1.7	3.4	0.6	3.9	2.7
NC-4	54.0	26.3	1.11	0.17	294	2.7	4.2	3.7	5.9	3.9
NC-5	58.2	22.4	1.19	0.18	346	1.7	2.5	2.0	3.6	2.4
NC-6	62.3	23.0	1.21	0.21	327	1.8	2.6	2.9	3.6	2.4
NC-7	64.2	16.5	1.21	0.2	339	2.1	3.0	2.8	4.3	2.8
NC-S1	41.4	21.3	1.1	0.15	95	2.8	2.4	0.5	4.2	3.5
NC-S2	31.0	63.6	1.17	0.29	928	2.1	3.7	0.8	0.0	3.2
NC-S3	13.5	83.4	1.29	0.33	548	2.2	3.3	0.4	5.1	3.0
NC-S4	63.2	16.6	1.11	0.16	258	2.4	3.0	1.4	4.7	3.0
Ru-1	91.8	10.1	1.23	0.18	688	2.4	4.0	1.3	5.2	3.5
Ru-2	60.7	5.0	1.19	0.09	359	2.5	2.7	0.4	4.4	0.0
Ru-3	37.0	61.9	1.25	0.26	721	2.1	3.4	0.3	4.7	3.1
Ru-4	83.9	8.2	1.17	0.17	497	1.5	2.3	1.7	3.2	2.1
Ru-5	90.0	5.1	1.21	0.19	490	1.6	4.5	2.4	6.7	4.4
Ru-6	84.2	3.3	1.21	0.19	522	1.3	3.9	2.1	5.5	1.7
Ru-7	86.2	3.2	1.21	0.19	487	2.0	3.2	1.9	4.3	2.8
Ru-S1	59.3	5.5	1.11	0.11	91	2.7	4.5	0.6	6.2	2.2
Ru-S2	45.5	48.3	1.27	0.4	2150	1.5	2.6	0.2	3.6	0.0
Ru-S3	30.8	67.6	1.17	0.27	2049	2.5	4.7	0.4	5.9	3.9
Ru-S4	79.8	3.3	1.18	0.16	468	2.8	5.5	2.0	6.7	4.3
Al-1	84.8	16.1	1.18	0.23	276	1.2	2.3	1.2	2.8	2.3
Al-2	48.2	17.3	1.2	0.1	178	2.4	2.7	0.6	4.9	4.6
Al-3	36.8	61.8	1.22	0.27	318	2.3	4.2	0.5	0.0	4.0
Al-4	57.4	24.5	1.16	0.21	211	1.6	2.4	3.4	3.4	2.6
Al-5	63.1	22.0	1.2	0.21	215	1.4	2.2	3.1	3.2	2.3
Al-6	58.7	25.7	1.18	0.17	225	2.0	2.9	3.0	4.3	3.0
Al-7	66.5	17.1	1.19	0.19	210	2.5	3.6	2.9	5.5	3.8
Al-S1	43.3	21.0	1.12	0.12	108	2.8	3.0	0.5	5.6	4.5
Al-S2	49.8	52.1	1.19	0.25	1360	1.9	3.4	0.5	0.0	3.5
Al-S3	13.3	82.8	1.36	0.32	826	2.1	3.3	0.3	5.5	3.3
Al-S4	65.4	11.1	1.19	0.16	347	2.4	3.0	1.4	5.1	3.3

NC: non-catalysed experiments **Ru**: Ru/Al_2O_3 was used as catalyst **Al:** γ-Al_2O_3 was used as catalyst. **S:** refers to the axial points were α=1.41. The experimental conditions are given in Table 2. *: Phenol (Ph), cresol (Cr), guaiacol (Gu), methyl-guaiacol (M-Gu), catechol (Ca) and syringol (Sy) yields as %(weight) in the oil

The analysis of the variance (ANOVA) (Table S2, *Supplementary Information*), shows that all the models are significant for a confidence level of 90 %, which allows a quantitative analysis of the results. Table 7 displays the second order regression models for the oil and solid yield. The surface response models for the oil and solid yield are presented in Figures 5 and 6 respectively.

Ru gives higher oil and lower solid yields in the experimental space. The maximum oil and minimum solid yield is found around the center of the experimental space, and more precisely toward the area of low temperatures and long reaction times. This model differs from the one obtained in Section 3.2.1 where the maximum was not found within the experimental space. Hence, quadratic terms are important to provide significant models of the systems.

Table 7: Regression second order models for the oil yield and solid yield

Syst		Equation
NC[a]	Oil Yield (%)[d]	$Y = 61.56 + 2.75X_1 + 12.40X_2 - 9.43X_1^2 - 8.36X_2^2 - 9.13X_1X_2$
Ru[b]		$Y = 86.79 + 4.41X_1 + 12.61X_2 - 19.5X_1^2 - 13.57X_2^2 - 12.12X_1X_2$
Al[c]		$Y = 62.76 - 3.15X_1 + 14.06X_2 - 4.64X_1^2 - 8.25X_2^2 - 14.3X_1X_2$
NC[a]	Solid Yield (%)[e]	$Y = 20.64 - 13.32X_1 - 16.30X_2 + 7.58X_1^2 + 11.36X_2^2 - 3.93X_1X_2$
Ru[b]		$Y = 3.87 - 14.92X_1 - 18.24X_2 + 12.15X_1^2 + 9.05X_2^2 + 12.32X_1X_2$
Al[c]		$Y = 21.6 - 10.01X_1 - 19.29X_2 + 4.52X_1^2 + 9.72X_2^2 + 9.63X_1X_2$

NC: non-catalysed reaction system **Ru:** Ru/Al_2O_3 was used as catalyst **Al:** γ-Al_2O_3 was used as catalyst **Oil Yield (%):** regression model built for the oil yield (%) **Solid Yield:** regression model built for the solid yield (%)

The NC tests give significantly lower oil yields than the Ru. However, the regression coefficients are of the same sign,the shape of the response surface is similar, and the maximum oil yield is found around the same area. In the case of the Al, on the other hand, the maximum oil yield is not found within the experimental space and the shape of the surface response model differs significantly from the ones obtained for the Ru and NC. This is because unlike Ru and NC, the Al system is negatively correlated to the temperature, shifting the maximum towards the area of low temperatures and long reaction times.

The analysis of the solid yields (Figure 6 and Table 7), confirms the conclusions described above. Note that the axes regarding the temperature and reaction time are on the opposite side to the ones in Figure 5. NC and Ru systems behave analogously, although considerably lower solid values are obtained for the Ru system. However in the case of the Al system, the lowest solid yields are obtained in the areas of low temperatures and long reaction times. This confirms that the presence of γ-alumina increases the oil yield at low temperatures, while the presence of the noble metal Ru supported on the alumina increases the oil yield in the experimental space.

The results indicate that the presence of Al and Ru alter somehow the original reaction mechanism. Our previous results [12] suggest that alumina is able to catalyze both the de-polymerization and re-polymerization reactions. Many research groups[21] have reported the hydrolysis of lignin ether bonds in the presence of homogenous Lewis acids. It is believed that Lewis acids in combination with water or low molecular alcohols yield Brønsted acids that are active for the hydrolytic conversion of lignin[22]. A similar mechanism could be expected in the case of Lewis solid acids, although the mechanism itself is still unclear. In any case, the results presented above clearly show that at low temperatures the lignin de-polymerization is favored over the re-polymerization of the monomers. At high temperatures, however, the activity towards the hydrolytic lignin conversion could be neutralized by a combination of two phenomena. Increasing the temperature is known to favor re-polymerization reactions of the unstable lignin monomers thus yielding a higher amount of solid residues (reference).

It is noteworthy that at 380 °C the oil yield is slightly higher for the Al system (57.4 %) than that of the NC system (54.0 %) when the reaction time is 2 h, while the oil yield is slightly higher for the NC system (50.2 %) than for the Al system (48.2 %) when the reaction time is 10 h. In addition, the higher solids yields observed at long reaction times could also be a consequence of the non-stable activity of the alumina support at high temperatures: the surface acidity could cause intense coke deposition over the alumina surface leading to a more rapid catalyst deactivation. The incorporation of the Ru phase seems to hinder the re-polymerization of the lignin monomers and deactivation of the catalyst. Noble metals are known to catalyze HDO reactions of lignin and lignin model compounds in the presence of H_2 or hydrogen molecular donors such as formic acid[23]. The active hydrogen species would thus stabilize the lignin monomers preventing their re-polymerization and the formation of coke deposits.

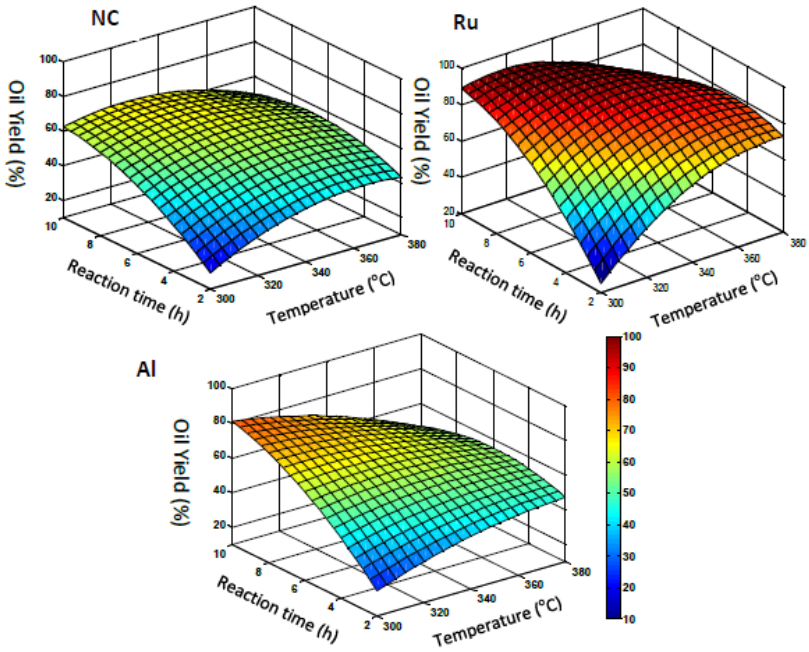

Figure 5: Response surface models for the oil yield. NC: non-catalyzed system, Ru: Ru/Al_2O_3 catalyzed system, Al: γ-Al_2O_3 catalyzed system

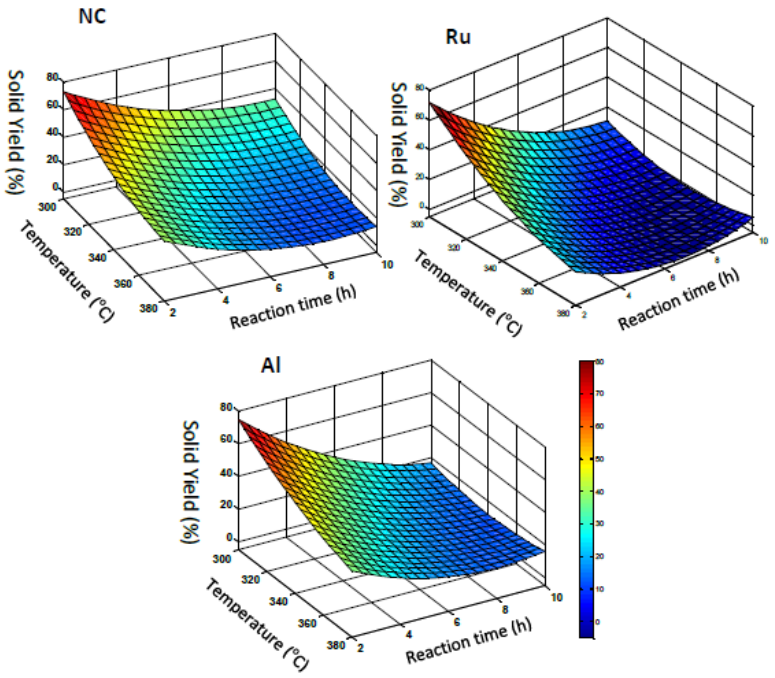

Figure 6: Response surface models for the solid yield. NC: non-catalyzed system, Ru: Ru/Al_2O_3 catalyzed system, Al: γ-Al_2O_3 catalyzed system

3.3.2 Effect of type of system, temperature and reaction time in the quality of the oil

The system variable, accompanied by the temperature, reaction time, oil yield, solid yield and the oil-quality responses are submitted to an exploratory PCA. Table 6 describes the values of the different responses. 81.5 % of the variance is explained by three PC. The score plots depicted in Figure 7a show that the objects are group in terms of system and reaction conditions, although this pattern is less clear than in Section 3.2.2. On the other hand, the loading plots in Figure 7b significantly resemble the corresponding plots in Section 3.2.2.

The most obvious correlation is again the one between the system variables and the Mw. This means that the Ru systems produce the oils with higher average molecular weights, while the lowest M_w values are obtained for the Al. In the absence of catalyst, the values of M_w are lower than the ones for the Ru, but higher than the ones for the Al systems. This phenomenon could be due the fact that the Ru catalyst, the Ru active phase, can stabilize high M_w oligomers thought hydrodeoxygenation[24] and alkylation reactions[25], while in the case of the Al and NC systems these compounds are re-polymerized into solid. The lowest values of M_w obtained in the Al system could be due to the high active acidity of the γ-alumina, a phenomenon already observed in Section 3.2.2. The loading plots and the raw data in Figure 7b suggest that the temperature and reaction time are negatively correlated to the M_w, and support that high temperatures and long reaction times favor lignin de-polymerization.

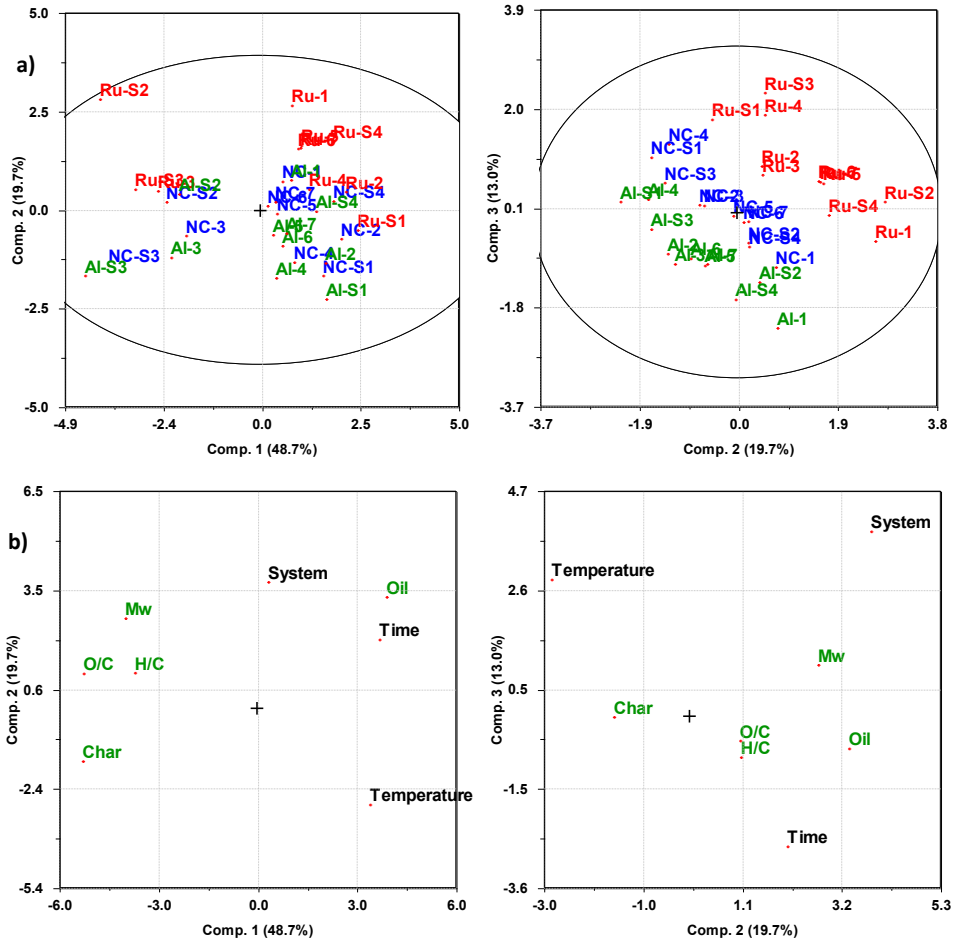

Figure 7: Score plots and loading plots for composition of the oil. a) Score plots of the PCA analysis for the catalyst optimization. Al experiments in green, NC experiments in blue, Ru experiments in red b) Loading plots of the PCA analysis for the optimization experiments. Factors describing the reaction conditions in black, factors describing the oil yield (oil), solid yield (char) and quality of the oil (H/C, O/C and M_w) in green. The coding for the response variables is given in Table 2.

The behavior of the H/C ratio with respect to the temperature and reaction time is in accordance with the results observed in Section 3.2.2. At low temperatures the H/C ratio decreases with the reaction time, while at high temperatures this value increases with the reaction time. From the loading plot (Figure 7a) no or weak correlations are found between the system, reaction time and H/C variables. However, the data in Table 6 clearly show that the Ru (+1) system gives higher H/C ratio oils, followed by the Al (-1) and the NC (0) system.

The O/C ratio is not considerably influenced by the type of system. Temperature is again negatively correlated to the O/C ratio, while the correlation with the reaction time is not that clear when analyzing the score plots. Nevertheless, the raw data again indicate that the higher the temperature and the longer the reaction time, the lower the O/C ratio.

As in Section 3.2.2 there is a lack of correlation between the oil yield and the variables selected to evaluate the quality of the oil. Some other aspects are also confirmed: (*i*) the active acidity of the catalysts decreases the M_w value, (*ii*) the H/C ratio is negatively correlated to the temperature, (*iii*) the O/C ratio is negatively correlated to temperature and reaction time, and (*iv*) the best results are found in the center of the experimental space. An additional observation is that the presence of the noble metal is positive for the H/C ratio, which can be explained by catalysis of the hydrogenation of the end products, as expected.

3.3.3 Analysis of the concentration of main compounds

Table 6 describes the values of the variables submitted to exploratory PCA. As in Section 3.2.3, five main components were selected (Ph, Gu, Ca, Cr, MGu). The first three PCs describe only 65.5 % of the variance. From the analysis of the score plot in Figure 8a, it can be observed that the objects are mainly grouped by the type of the system. The loading plots in Figure 8b show that the variance is largely explained by the system variable, especially on PC2. All this indicates that there are significant differences on the kinetic or mechanistic pathways between the systems.

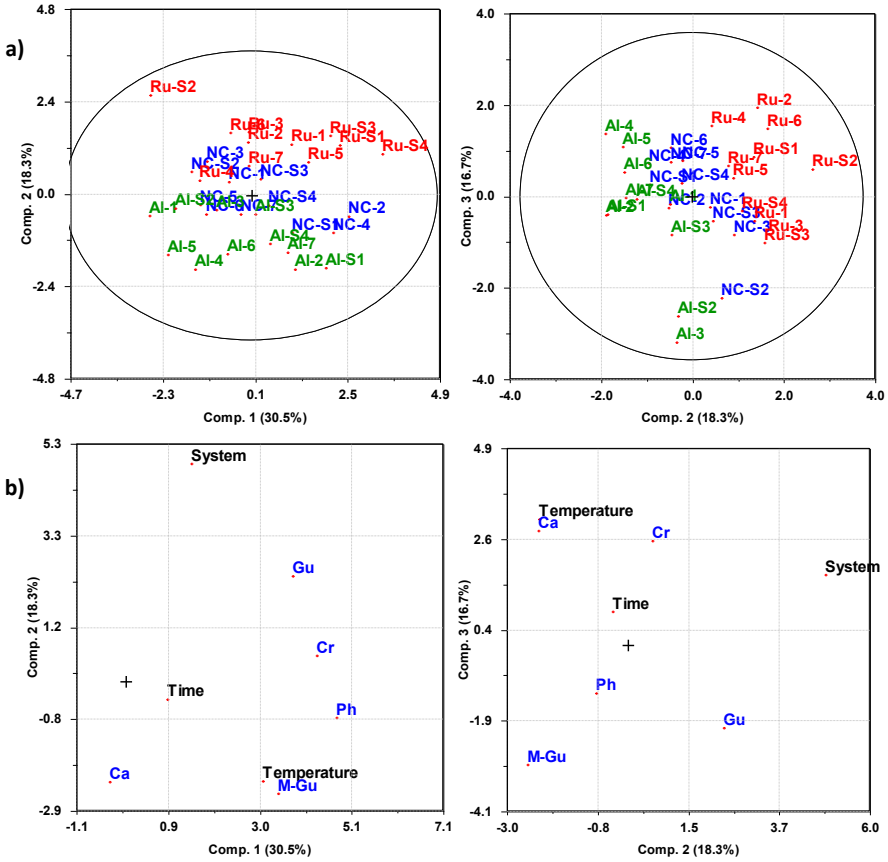

Figure 8: Score and loading plots of the composition of the oil. a) Score plots of the PCA analysis for the optimization experiments. Al experiments in green, NC experiments in blue, Ru experiments in red b) Loading plots of the PCA analysis for the optimization experiments. Factors describing the reaction conditions in black, factors describing the concentration of certain components in blue. The coding for the response variables is given in Table 2.

When analyzing the correlations for each compound, no clear patterns are observed. Each component is differently correlated to the temperature, reaction time and system variable depending on the PC. This shows that the significant difference in the reaction mechanisms prevents clear conclusions on how the experimental variables studied affect the composition of the oil using this multivariate approach.

3.4 Recycling of the catalyst

The inorganic ash content of the lignin used is 1.5 wt%. The average value of the recovered organic solids (char) and lignin-derived inorganic ashes for the Ru system, at 340 °C and 6 hours, is 2.7 wt%. This means that the solids recovered after the reaction mainly comprises the catalyst. After the thermal treatment the organic matter was eliminated, giving a recovered catalyst with a small amount of inorganic impurities derived from the lignin (ashes).

The catalyst was recycled twice, and its activity was evaluated in terms of oil and solid yields. For the first cycle three replicates were made (Ru-A1, Ru-A2 and Ru-A3), while two replicates were carried out for the second recycling cycle (Ru-B1 and Ru-B2).

Table 11 shows the results obtained for both cycles. Surprisingly, the average values show that the oil yield is maintained or increased upon recycling. The solid yield is comparable for all the reaction cycles. The variation could be assigned to experimental uncertainty during the work-up procedure and the catalytic effect of the inorganic lignin impurities (ashes).

Table 11: Oil yield, H/C and O/C ration of the oil and solid yield for the recycling experiments

Experiment Name	Oil Yield (% on lignin)	Average Oil Yield (% on lignin)	(H/C)	(O/C)	Solid Yield (% on lignin)	Average Solid Yield (% on lignin)
Ru-5	90.0	86.8	1.21	0.19	5.1	3.9
Ru-6	84.2		1.21	0.19	3.3	
Ru-7	86.2		1.21	0.19	3.2	
Ru-A1	84.9	86.8	1.20	0.19	2.7	2.6
Ru-A2	88.7		1.18	0.18	2.5	
Ru-A3	86.7		1.16	0.18	2.5	
Ru-B1	88.9	91.6	1.22	0.20	4.7	4.6
Ru-B2	94.2		1.22	0.19	4.6	

A: refers to the replicates for first recycling cycle **B:** refers to the replicates for the second recycling cycle. Conditions: 340 °C and 6 hours

Overall, the results show no deactivation of the catalyst in terms of oil and solid yield. The H/C and O/C ratio of the oils depicted in Table 11 confirm that there is no catalyst deactivation. The H/C ratios decrease slightly for some experiments in the first recycling cycle, but the results are comparable or higher for the second cycle. This means that the differences can be understood as a function of uncertainties during the work-up and/or the analytic procedures. The O/C ratio is also maintained within acceptable uncertainty limits.

4. Conclusion

Lignin from Norway spruce was successfully converted into aromatic based oil in the presence of several noble metal catalysts supported in alumina in a formic acid water media. Oils were produced over a range of reaction temperatures (283-397 °C) and reaction times (21 min-11 h 40 min). Response surface methodology (RSM) has been proven to be a successful tool to build significant models for the oil and solid yield within the studied experimental space. Principal component analysis (PCA) is proven to be a successful tool to evaluate the effect of the reaction variables on the oil quality and composition, and to extract qualitative data on the reaction mechanism. The recycling of the catalyst shows that the Ru catalyst fully retains its activity in two separate recycling tests.

This systematic approach improved the quantitative understanding of the process and successfully confirmed features previously noted from less extensive investigations [12]. For the catalysts, both the noble metal and the γ-alumina are active in the LtL process. The former increases the oil yield while decreasing the solid yield. The latter is active in the lignin de-polymerization and in the re-polymerization of the lignin monomers, and therefore increases the oil yield at low temperatures, where re-polymerization is not favored. Among the noble metals studied Ru gives the highest oil yield in the whole experimental space. A strong dependency between the active acidity of the alumina support and the M_w of the oil has been also confirmed.

No correlations between the oil yield and the quality of the oil has been found. The oil yield is strongly dependent on the presence of the catalyst, temperature and reaction time, while the oil quality is mainly dependent on the temperature and reaction time. Therefore, the optimum reaction conditions were found to be around 340 °C and 6 h, where nearly complete conversion of lignin into oil is achieved while still having high H/C ratios coupled with low O/C ratios and M_w values.

The study of the composition of the oil confirms that the reaction mechanism differs between the supported catalyst (Ru/Al_2O_3, Pd/Al_2O_3 and Rh/Al_2O_3) system, the γ-Al_2O_3 system and the non-catalyzed system. In the supported catalyst systems, the reaction comprises several steps. It starts with the de-polymerization of the lignin, followed by de-methoxylation, dehydration and alkylation of the monomers. At low temperatures de-methoxylation and dehydration reactions are predominant for the reaction times studied, while at high temperatures these reactions take place at short reaction times, followed by alkylation reactions. Thus, the final products obtained depend on the reaction temperature: at high temperature alkylated compounds such as cresol are favored, while at low temperatures non-alkylated compounds, such as phenol, are more abundant.

In an overall perspective, the results show the potential for improving the yields of oil by the use of catalysts which are easily recovered, and suggest a good potential for tuning the oil composition to specific compositions depending on the requirements for the product. Such processing of lignin residues to phenol-type product compositions could be a complementary process to the carbohydrate conversion in the utilization of lignocellulosic biomass in a bio-based refinery.

5. Acknowledgement

Some of this work has been performed as a part of the LignoRef project (“Lignocellulosics as a basis for second generation biofuels and the future biorefinery”). We gratefully acknowledge The Research Council of Norway (grant no. 190965/S60), Statoil ASA, Borregaard Industries Ltd., Allskog BA, Cambi AS, Xynergo AS, Hafslund ASA and Weyland AS for financial support. The authors would also like to thank I. J. Fjellanger for assisting with elemental analysis, Dr. Egil Nodland and Prof Bjørn Grung for their assistance on RSM and PCA, and the Technical College of Bergen for supplying lignin.

6. References

1. (a) Maher, K. D.; Bressler, D. C., Pyrolysis of triglyceride materials for the production of renewable fuels and chemicals. *Bioresource Technology* **2007,** *98* (12), 2351-2368; (b) Sastre, C. M.; González-Arechavala, Y.; Santos, A. M., Global warming and energy yield evaluation of Spanish wheat straw electricity generation – A LCA that takes into account parameter uncertainty and variability. *Applied Energy* **2015,** *154*, 900-911.
2. Kamm, B.; Kamm, M., Biorefinery-Systems. *Chemical and Biochemical Engineering Quarterly* **2004,** *18* (18), 1-6.
3. Zakzeski, J.; Bruijnincx, P. C. A.; Jongerius, A. L.; Weckhuysen, B. M., The Catalytic Valorization of Lignin for the Production of Renewable Chemicals. *Chemical Reviews* **2010,** *110* (6), 3552-3599.
4. Kleinert, M.; Gasson, J. R.; Barth, T., Optimizing solvolysis conditions for integrated depolymerisation and hydrodeoxygenation of lignin to produce liquid biofuel. *Journal of Analytical and Applied Pyrolysis* **2009,** *85* (1–2), 108-117.
5. Limayem, A.; Ricke, S. C., Lignocellulosic biomass for bioethanol production: Current perspectives, potential issues and future prospects. *Progress in Energy and Combustion Science* **2012,** *38* (4), 449-467.
6. (a) Chen, H.; Fu, X., Industrial technologies for bioethanol production from lignocellulosic biomass. *Renewable and Sustainable Energy Reviews* **2016,** *57*, 468-478; (b) Dias, M. O. S.; Junqueira, T. L.; Rossell, C. E. V.; Maciel Filho, R.; Bonomi, A., Evaluation of process configurations for second generation integrated with first generation bioethanol production from sugarcane. *Fuel Processing Technology* **2013,** *109*, 84-89; (c) Gonzalez, R.; Daystar, J.; Jett, M.; Treasure, T.; Jameel, H.; Venditti, R.; Phillips, R., Economics of cellulosic ethanol production in a thermochemical pathway for softwood, hardwood, corn stover and switchgrass. *Fuel Processing Technology* **2012,** *94* (1), 113-122; (d) Chum, H. L.; Overend, R. P., Biomass and renewable fuels. *Fuel Processing Technology* **2001,** *71* (1–3), 187-195.
7. Peng, C.; Zhang, G.; Yue, J.; Xu, G., Pyrolysis of lignin for phenols with alkaline additive. *Fuel Processing Technology* **2014,** *124*, 212-221.
8. (a) Jongerius, A. L.; Bruijnincx, P. C. A.; Weckhuysen, B. M., Liquid-phase reforming and hydrodeoxygenation as a two-step route to aromatics from lignin. *Green Chemistry* **2013,** *15* (11), 3049-3056; (b) Bu, Q.; Lei, H.; Zacher, A. H.; Wang, L.; Ren, S.; Liang, J.; Wei, Y.; Liu, Y.; Tang, J.; Zhang, Q.; Ruan, R., A review of catalytic hydrodeoxygenation of lignin-derived phenols from biomass pyrolysis. *Bioresource Technology* **2012,** *124*, 470-477; (c) Li, B.; Lv, W.; Zhang, Q.; Wang, T.; Ma, L., Pyrolysis and catalytic pyrolysis of industrial lignins by TG-FTIR: Kinetics and products. *Journal of Analytical and Applied Pyrolysis* **2014,** *108*, 295-300.
9. (a) Kleinert, M.; Barth, T., Towards a Lignincellulosic Biorefinery: Direct One-Step Conversion of Lignin to Hydrogen-Enriched Biofuel. *Energy & Fuels* **2008,** *22* (2), 1371-1379; (b) Holmelid, B.; Kleinert, M.; Barth, T., Reactivity and reaction pathways in thermochemical treatment of selected lignin-like model compounds under hydrogen rich conditions. *Journal of Analytical and Applied Pyrolysis* **2012,** *98*, 37-44.
10. Ates, F.; Erginel, N., Optimization of bio-oil production using response surface methodology and formation of polycyclic aromatic hydrocarbons (PAHs) at elevated pressures. *Fuel Processing Technology* **2016,** *142*, 279-286.
11. Liguori, L.; Barth, T., Palladium-Nafion SAC-13 catalysed depolymerisation of lignin to phenols in formic acid and water. *Journal of Analytical and Applied Pyrolysis* **2011,** *92* (2), 477-484.
12. Oregui Bengoechea, M.; Hertzberg, A.; Miletić, N.; Arias, P. L.; Barth, T., Simultaneous catalytic de-polymerization and hydrodeoxygenation of lignin in water/formic acid media with Rh/Al2O3, Ru/Al2O3 and Pd/Al2O3 as bifunctional catalysts. *Journal of Analytical and Applied Pyrolysis* **2015,** *113*, 713-722.
13. Focardi, S.; Ristori, S.; Mazzuoli, S.; Tognazzi, A.; Leach-Scampavia, D.; Castner, D. G.; Rossi, C., ToF-SIMS and PCA studies of Seggianese olives and olive oil. *Colloids and Surfaces A: Physicochemical and Engineering Aspects* **2006,** *279* (1–3), 225-232.
14. Ngo, T.-A.; Kim, J.; Kim, S.-S., Characteristics of palm bark pyrolysis experiment oriented by central composite rotatable design. *Energy* **2014,** *66*, 7-12.
15. Oramahi, H. A.; Wahdina; Diba, F.; Nurhaida; Yoshimura, T., Optimization of Production of Lignocellulosic Biomass Bio-oil from Oil Palm Trunk. *Procedia Environmental Sciences* **2015,** *28*, 769-777.
16. (a) Smichi, N.; Messaoudi, Y.; Gelicus, A.; Allaf, K.; Gargouri, M., Optimization of DIC technology as a pretreatment stage for enzymatic saccharification of Retama raetam. *Fuel Processing Technology* **2015,** *138*, 344-354; (b) Lee, H. V.; Yunus, R.; Juan, J. C.; Taufiq-Yap, Y. H., Process optimization design for jatropha-based biodiesel production using response surface methodology. *Fuel Processing Technology* **2011,** *92* (12), 2420-2428; (c) Hameed, B. H.; Lai, L. F.; Chin, L. H., Production of biodiesel from palm oil (Elaeis guineensis) using heterogeneous catalyst: An optimized process. *Fuel Processing Technology* **2009,** *90* (4), 606-610.
17. Fahmi, R.; Bridgwater, A. V.; Donnison, I.; Yates, N.; Jones, J. M., The effect of lignin and inorganic species in biomass on pyrolysis oil yields, quality and stability. *Fuel* **2008,** *87* (7), 1230-1240.

18. Sharif, K. M.; Rahman, M. M.; Azmir, J.; Mohamed, A.; Jahurul, M. H. A.; Sahena, F.; Zaidul, I. S. M., Experimental design of supercritical fluid extraction – A review. *Journal of Food Engineering* **2014,** *124*, 105-116.
19. Tamura, M.; Nishibayashi, H.; Ogura, M.; Uematsu, Y.; Itakura, T.; Mangin, J. F.; Régis, J.; Ikuta, S.; Yoshimitsu, K.; Suzuki, T.; Niki, C.; Muragaki, Y.; Iseki, H., MRI Based Sulcal Pattern Analysis for Diagnosis and Clinical Application in Neurosurgery. In *Computer Aided Surgery: 7th Asian Conference on Computer Aided Surgery, Bangkok, Thailand, August 2011, Proceedings*, Dohi, T.; Liao, H., Eds. Springer Japan: Tokyo, 2012; pp 135-143.
20. (a) Gasson, J. R.; Forchheim, D.; Sutter, T.; Hornung, U.; Kruse, A.; Barth, T., Modeling the Lignin Degradation Kinetics in an Ethanol/Formic Acid Solvolysis Approach. Part 1. Kinetic Model Development. *Industrial & Engineering Chemistry Research* **2012,** *51* (32), 10595-10606; (b) Forchheim, D.; Gasson, J. R.; Hornung, U.; Kruse, A.; Barth, T., Modeling the Lignin Degradation Kinetics in a Ethanol/Formic Acid Solvolysis Approach. Part 2. Validation and Transfer to Variable Conditions. *Industrial & Engineering Chemistry Research* **2012,** *51* (46), 15053-15063.
21. (a) Hepditch, M. M.; Thring, R. W., Degradation of solvolysis lignin using Lewis acid catalysts. *The Canadian Journal of Chemical Engineering* **2000,** *78* (1), 226-231; (b) Jia, S.; Cox, B. J.; Guo, X.; Zhang, Z. C.; Ekerdt, J. G., Hydrolytic Cleavage of β-O-4 Ether Bonds of Lignin Model Compounds in an Ionic Liquid with Metal Chlorides. *Industrial & Engineering Chemistry Research* **2011,** *50* (2), 849-855; (c) Vuori, A.; Niemelä, M., Liquefaction of Kraft Lignin. 2. Reactions with a Homogeneous Lewis Acid Catalyst under Mild Reaction Conditions. In *Holzforschung - International Journal of the Biology, Chemistry, Physics and Technology of Wood*, 1988; Vol. 42, p 327.
22. Li, C.; Zhao, X.; Wang, A.; Huber, G. W.; Zhang, T., Catalytic Transformation of Lignin for the Production of Chemicals and Fuels. *Chemical Reviews* **2015,** *115* (21), 11559-11624.
23. (a) Kloekhorst, A.; Shen, Y.; Yie, Y.; Fang, M.; Heeres, H. J., Catalytic hydrodeoxygenation and hydrocracking of Alcell® lignin in alcohol/formic acid mixtures using a Ru/C catalyst. *Biomass and Bioenergy* **2015,** *80*, 147-161; (b) Mu, W.; Ben, H.; Du, X.; Zhang, X.; Hu, F.; Liu, W.; Ragauskas, A. J.; Deng, Y., Noble metal catalyzed aqueous phase hydrogenation and hydrodeoxygenation of lignin-derived pyrolysis oil and related model compounds. *Bioresource Technology* **2014,** *173*, 6-10.
24. Huang, X.; Korányi, T. I.; Boot, M. D.; Hensen, E. J. M., Catalytic Depolymerization of Lignin in Supercritical Ethanol. *ChemSusChem* **2014,** *7* (8), 2276-2288.
25. Shu, R.; Long, J.; Xu, Y.; Ma, L.; Zhang, Q.; Wang, T.; Wang, C.; Yuan, Z.; Wu, Q., Investigation on the structural effect of lignin during the hydrogenolysis process. *Bioresource Technology* **2016,** *200*, 14-22.

7. Supplementary Information

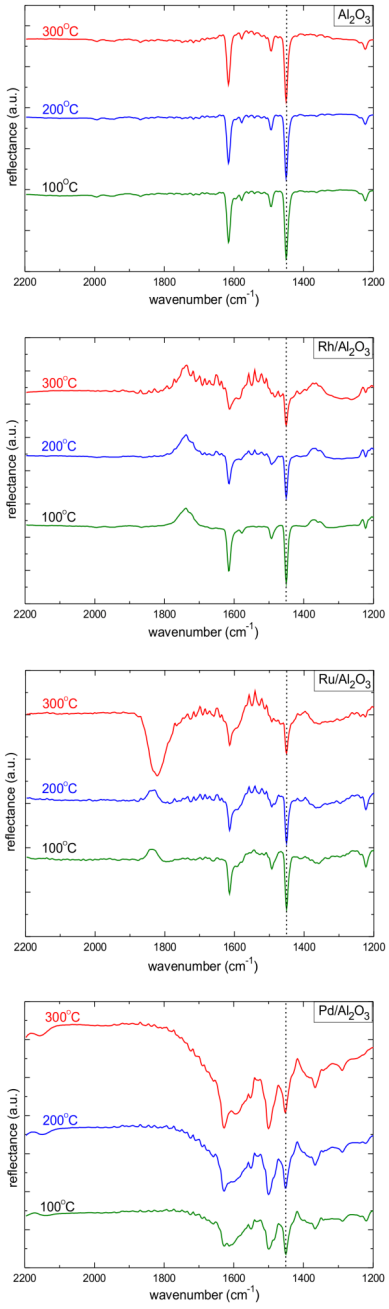

Figure S1: DRIFT spectra of pyridine adsorbed on Al_2O_3, Rh/Al_2O_3, Ru/Al_2O_3, and Pd/Al_2O_3.

Table S1: Analysis of the variance (ANOVA) of the built linear models

System-Product Yield (%)	Source of Variation	Degrees of Freedom	Summ of squares	Mean squares	F statistic	p-value
Pd[a]-Oil Yield (%)	Regression	3	1408.10	469.37	2.51	0.235
	Error	3	560.19	186.73		
	Total	6	1968.29			
Pd[a]-Solid Yield (%)	Regression	3	2011.10	670.35	3.25	0.180
	Error	3	619.00	206.33		
	Total	6	2630.10			
Rh[b]-Oil Yield (%)	Regression	3	1141.60	380.55	2.20	0.267
	Error	3	518.09	172.70		
	Total	6	1659.69			
Rh[b]-Solid Yield (%)	Regression	3	1757.10	585.71	3.83	0.150
	Error	3	458.83	152.94		
	Total	6	2215.93			
Ru[c]-Oil Yield (%)	Regression	3	1833.00	611.02	1.83	0.315
	Error	3	999.32	333.11		
	Total	6	2832.32			
Ru[c]-Solid Yield (%)	Regression	3	2211.10	737.03	4.41	0.127
	Error	3	501.17	167.06		
	Total	6	2712.27			

a) ANOVA analysis for the Pd/Al_2O_3 system **b)** ANOVA analysis for the Rh/Al_2O_3 system **c)** ANOVA analysis for the Ru/Al_2O_3 system

Table S2: ANOVA table for the second order regression models

System	Source of Variation	Degrees of Freedom	Summ of squares	Mean squares	F statistic	p-value
NC[a] Oil Yield (%)	**Regression**	5	2318.30	463.65	4.01	0.077
	Error	5	578.13	115.63		
	Total	10	2896.43			
NC[a] Solid Yield (%)	**Regression**	5	4443.80	888.77	5.35	0.045
	Error	5	830.38	166.08		
	Total	10	5274.18			
Ru[b] Oil Yield (%)	**Regression**	5	4398.00	879.60	7.12	0.025
	Error	5	617.79	123.56		
	Total	10	5015.79			
Ru[b] Solid Yield (%)	**Regression**	5	6197.10	1239.40	17.24	0.004
	Error	5	359.47	71.89		
	Total	10	6556.57			
Al[c] Oil Yield (%)	**Regression**	5	2892.90	578.59	5.05	0.050
	Error	5	572.39	114.48		
	Total	10	3465.29			
Al[c] Solid Yield (%)	**Regression**	5	4698.30	939.66	7.59	0.022
	Error	5	619.02	123.80		
	Total	10	5317.32			

a) ANOVA analysis for the non-catalysed system **b)** ANOVA analysis for the Ru/Al_2O_3 system **c)** ANOVA analysis for the γ-Al_2O_3 system

Paper F

Unraveling the role of formic acid and the type of solvent in the catalytic conversion of lignin: a holistic approach

Authords:
Oregui Bengoechea, M.; Gandarias, I.; Arias, P.L.; Barth, T.

Submitted to:
ChemSusChem ,**2016.**

F

Unraveling the role of formic acid and the type of solvent in the catalytic conversion of lignin: a holistic approach

Mikel Oregui-Bengoechea[a], Inaki Gandarias[b], Pedro L. Arias[b] and Tanja Barth[a]

[a] *Department of Chemistry, University of Bergen, N-5007 Bergen, Norway*

[b]*Department of Chemical and Environmental Engineering, School of Engineering, University of the Basque Country (EHU/UPV), C/Alameda Urquijo s/n,48013 Bilbao, Spain*

Keywords: lignin, formic acid, mechanism, catalyst, hydrogen, solvent.

Abstract

The role of formic acid together with the effect of the type of solvent and their synergic interactions with a NiMo catalyst were studied for the conversion of lignin into bio-oil in an alcohol/formic acid media. Replacing formic acid with molecular hydrogen or isopropanol decreased considerably the oil yield, increased the solid yield and altered the nature of the bio-oil. The differences induced by the presence of molecular hydrogen were comparable to the ones observed in the isopropanol system, suggesting similar lignin conversion mechanisms for both reacting systems. Additional semi-batch experiments confirmed that formic acid does not act merely as an *in situ* hydrogen source or hydrogen donor molecule. On the contrary, formic acid seems to react with lignin through a formylation-elimination-hydrogenolysis mechanism that leads to the de-polymerization of the biopolymer. This reaction competes with the formic acid decomposition mainly into H_2 and CO_2, forming a complex reaction system. To the best of our knowledge, this is the first time that the distinctive role/mechanism of formic acid has been observed in the conversion of real lignin feedstock. In addition, the solvent seems to play also a vital role in the stabilization of the de-polymerized monomers, especially ethanol, and in the elimination/deformilation step.

1. Introduction

In recent years the efficient valorization of lignin into a bio-oil rich in aromatic compounds has become a key issue within the development of the bio-refinery concept. This recalcitrant biomaterial accounts for 10-30 wt % of lignocellulosic biomass and can be obtained either from the cooking liquors produced in the paper-pulping industry, or as a by-product of biomass pretreatment processes for bio-ethanol production[1-2]. Hence, its efficient conversion into chemicals and fuels is crucial to make the processing of large quantities of lignocellulosic biomass economically viable[3]. Moreover, as lignin is the only renewable source of aromatic hydrocarbons, its conversion will also become important in the transition from fossil to renewable based economical models. .

Major challenges need to be addressed when valorizing lignin into chemicals or fuels. The production of lignin-derived value added chemicals requires the simultaneous de-polymerization of the biopolymer and the subsequent hydrodeoxygenation of the lignin monomers, but still avoiding the extensive hydrogenation of the aromatic rings[1]. Therefore a process that could combine the preservation of the aromatic structure with the production of low O/C, high H/C and stable oils in high yields would be the optimum approach.

A wide variety of chemical methods in the presence of different catalysts have been studied aiming to convert the highly cross-linked biopolymer into mono-aromatics. All these methods can be summarized into four main categories: cracking, hydrolytic, reductive and oxidative catalytic processes[3]. Catalytic cracking or hydrolytic processes, such as pyrolysis or base-catalyzed de-polymerization (BCD), produce highly viscous oils with a low pH and small heating values. Thus, an additional hydroprocessing step is necessary for further bio-oil upgrading. Similarly, oxidation processes are not suitable for converting lignin into fuel-blend or chemicals since they tend to produce more complex aromatic compounds with additional functionalities[3]. Lignin reductive de-polymerization can therefore be the preferred option to efficiently valorize lignin as long as the hydrogenation of the aromatic ring is avoided.

Among the reductive processes, solvent-aided catalytic conversion has attracted a great deal of attention in recent years. In these methods lignin is converted in the presence of a solvent (water, ethanol or methanol), a catalyst and either molecular hydrogen or a hydrogen donor molecule (formic acid, isopropanol or tetralin)[1, 3-7]. One of these promising lignin conversion methodologies, known as lignin-to liquids (LtL), involves the use of formic acid (FA) and a solvent, among which ethanol gives the best results[8]. High oils yield, with high H/C and low O/C ratios are achieved, still retaining the phenol-type structure of the bio-oil components. The catalytic LtL process has also been examined[7, 9-10], obtaining higher oil yields and still retaining its aromatic.

Nevertheless, very little is understood about the role of formic acid and its influence on the conversion of lignin into bio-oil. Formic acid is known to act as an *in situ* molecular hydrogen source or hydrogen donor molecule in several reactions and processes[11-18]. Few studies have focused their attention on comparing the effect of formic acid with molecular hydrogen or other hydrogen donor molecules in the de-polymerization of lignin. Kloekhorst *et al.*[7] studied the effect of substituting formic acid for isopropanol, a well-known hydrogen donor molecule; but the reaction conditions chosen led in all cases to oil yields close to full conversion, what makes impossible to drawn any clear conclusion. Ma *et al.*[19] studied the effect of different hydrogen donor molecules and molecular hydrogen in the catalytic solvolysis of lignin with little focus on the role of the different species in the reaction mechanism.

In recent years different research groups have suggested novel reaction pathways involving lignin model compounds and formic acid[20-21] or lignin model compounds and similar organic acids, such as acetic acid[22]. However, comparison of these hypotheses with the conversion of real lignin is lacking. Under this background, the present study aims to gain a better understanding on the role of formic acid in the LtL process via a holistic approach. Additionally, the role of the catalyst, the type of solvent and their synergistic interactions with the formic acid will be examined.

Initially, the role of formic acid as a possible *in situ* hydrogen source or hydrogen donor molecule was studied by replacing formic acid either totally or partially with H_2, H_2/CO_2 or a well know hydrogen donor molecule; isopropanol. Additional experiments were carried out feeding formic acid continuously along the course of the reaction, in order to evaluate the role of formic acid in the different reaction stages. Finally, the effect of different solvents such as ethanol, methanol and isopropanol on the reaction system was analyzed. Blank experiments were performed to determine the non-catalytic and catalytic degradation rates of formic acid under the different reaction conditions.

2. Material and Methods

2.1 Chemicals

Formic acid (>98%), ethanol (>99.5%), tetrahydrofuran (>99.9%) ethyl acetate (99.8%) and sulfuric acid (95-97%) were purchased from Sigma Aldrich and used as received. γ-Alumina (>97%), nickel (II) nitrate hexahydrate (99.9+%.Ni) and ammonium molybdate tetrahydrate (99.98%-Mo) were purchased from Strem Chemicals Inc and used as received. Eucalyptus lignin from enzymatic hydrolysis of biomass was provided by SEKAB. The lignin was ground, sieved (<500μm) and dried at 100°C for 24 h prior to use.

2.2 Catalyst synthesis and characterization

The catalyst was selected from a previous screening study among different NiMo catalysts supported on sulfated and non-sulfated γ-alumina and zirconium oxide [23-24]. For the synthesis of the selected catalyst 10 g of the γ-alumina were first subjected to a thermal treatment on air at 450 °C for 4 h with a heating ramp of 3 °C/min. 8 g of the calcined alumina were impregnated with 14 mL of a sulfuric acid solution (0.5 wt%) and stirred for 24 hours. The solution was dried and the resulting solid, was calcined at 600 °C for 4 h with a heating ramp of 3 °C/min, to obtain a sulfated alumina (AA). The NiMo catalyst was later prepared by successive incipient-wetness of the AA with an aqueous solution of ammonium molybdate ($(NH_4)_6Mo_7O_{24}\cdot 4H_2O$) followed by an aqueous solution of nickel nitrate ($NiNO_3\cdot 6H_2O$). The nominal loading of MoO_3 and NiO are 12 % and 5 % respectively. After impregnation the catalyst was dried at 105 °C for 20 min and calcined under static air at 570 °C for 2 h with a heating ramp of 2 °C/min. Finally, the calcined catalyst was subjected to thermal treatment under a hydrogen flow (10 v% and 10 mL/min) at 550 °C for 2 h with a heating ramp of 2 °C/min and used shortly after the treatment. The resulting solid is named as **NiMo/AA**.

The catalyst was characterized by N_2-adsorption, ICP-EOS, CO-Chemisorption and temperature-programmed desorption of ammonia (NH_3-TPD). The methods used for each technique are described in the *Supplementary Information*. The main physic-chemical characteristics of the catalyst are summarized in Table 1.

Table 1: BET surface area, nominal and real NiO and MoO_3 content, Ni dispersion and acidity of the NiMo/AA

S_{BET} (m^2/g)	NiO (%)[a]		Ni dispersion (%)[b]	MoO_3 (%)[a]		Acidity (mmol NH3/g cat)[c]
	Nominal	Real		Nominal	Real	
179.3	5.0	3.6	1.4	12.0	10.7	0,5468

[a] Calculated by ICP [b] Values obtained by CO-chemisorption [c] Calculated by NH_3-TPD for a temperature range of 85-340°C

2.3 Experimental procedure

2.3.1 Batch experiments

2.3.1.1 Batch experiments in stirred reactor (BS): Typically (ET-FA-BS experimental series), lignin(8.16 g), formic acid (7.14 g), ethanol (12.24 g) and the catalyst (0.816 g) if any, were added to an stainless steel (SS316) 300 mL stirred-reactor from Autoclave Engineers. The reactor was weighed and sealed. The reactor was pressurized with 40 bar of nitrogen to eliminate the residual oxygen and to check for leaks. After degassing the nitrogen the system was heated to 320 °C for 6 h with a stirring rate of 700 rpm. The temperature and pressure of the reactor were monitored during the whole process.

The reaction time started counting when the reactor mantle reached 320 ^{o}C. An additional catalyzed experiment (ET-FA-BS-C-R) was carried out to evaluate the reproducibility of the experiments.

In those experiments where formic acid was replaced by H_2 (ET-H_2-BS series) or a mixture of H_2:CO_2 (ET-H_2/CO_2-BS series), the system was pressurized with 17.5 bars of hydrogen or of a mixture of H_2:CO_2 (1:1) after purging with nitrogen. This is the pressure of the system found at room temperature when 7.14 g of formic acid decomposed into gas. When formic acid was partially replaced by hydrogen (ET-FA/H_2-BS series), 2.75 g of formic acid were added initially in the reactor together with the rest of the reactants and the reactor was pressurized with 10.5 bars of hydrogen for the same reason as before . In the case where formic acid is replaced by an isopropanol/H_2 mixture (ET-ISO/H_2-BS-C experiment), 3.59 g of isopropanol were added initially in the reactor and the reactor was pressurized with 10.5 bars of hydrogen. The number of moles of isopropanol in the ET-ISO/H_2-BS-C experiment were the same as the amount of moles of formic acid used in the ET-FA/H_2-BS series.

2.3.1.2 Batch experiments in non-stirred reactor (BNS): The experiments were carried out in a stainless steel reactor (Parr 4742 non-stirred reactor, 25 mL volume). The amounts of reactants were calculated considering the volume ratio between the stirred and the non-stirred reaction (the volume ratio is 25/300). The reactor was sealed, weighed and heated at 320 ^{o}C for 6 h in a Carbolite LHT oven; the reaction time started when the reactor was introduced in the oven.

2.3.2 Semi-batch experiments (SBS)

Two different semi-batch configurations were performed. For the ET-FA-SBS1 series lignin (8.16 g), formic acid (2.75 g), ethanol (9.75 g) and the catalyst (0.816 g) if any were added to the 300 mL stirred-reactor as described above. In this case, a solution of formic acid:ethanol (1:1 v/v) was continuously fed (0.02 mL/min) with a Wilson HPLC 307 pump during the 6 h reaction time. For the ET-FA-SBS2 series, lignin (8.16 g), ethanol (7.57 g) and the catalyst (0.816 g) if any were added to the reactor. In this case the formic acid:ethanol (1:1 v/v) solution was continuously fed at a 0.033 mL/min flow during the course of the reaction. The flows were calculated so that the amounts of formic acid and ethanol after the reaction time were equivalent to the amounts initially added for the ET-FA-BS series. The amount of reactants for all the experiments described above are summarized in Table S1, *Supplementary Information*.

2.3.3 Sample work-up

A detailed description is given elsewhere by Oregui Bengoechea *et al.*[9]. Briefly summarized, after reaction completion the reactor was cooled down overnight to ambient temperature,the produced gas was vented and the gas quantity determined. The reactor was opened and the liquid reaction mixture was extracted with a solution of ethyl acetate: tetrahydrofuran (90:10 v/v). The solid phase (unreacted lignin, reaction products and catalyst) was filtered and dried at ambient conditions for 2 days before weighing. A dark-brown organic phase was extracted, dried over Na_2SO_4 and concentrated at reduced pressure (ca. 160 mmbar) at 40^{o}C. The final oil and solid yields were determined by weight and are reported relative to lignin input (g of oil or char/g of introduced lignin). The solid yield for the catalyzed systems was calculated after subtracting the amount of catalyst introduced; therefore the solid yield refers to the organic solids (char) and the inorganic lignin ashes.

2.4 Experiments without lignin (blank experiments)

2.4.1 Stirred reactor

Three blank experiments ethanol and formic acid were carried out following the procedure described in Section *2.3.1.1:* a catalyzed (C) experiment -51 min reaction time- and two non-catalyzed (NC) experiments -51 min and 6 h reaction time After the reaction, the liquid inside the reactor was filtered and 1 mL of the solution was dissolved in 69 mL of distilled water. 30 mL of the resulting solution was titrated with a solution of NaOH (1 mL) to calculate the amount of unreacted formic acid.

2.4.2 Non-stirred reactor

Six catalyzed blank experiments with formic acid, the catalyst and a solvent (methanol, ethanol and isopropanol) were carried out following the procedure described in Section 2.3.1.2: for each solvent the blank was performed twice, for 40 and 68 min. After the reaction, the liquid inside the reactor was filtered and 0.5 mL of the solution was dissolved in 45.5 mL of distilled water. 25 mL of the resulting solution were titrated with a solution of NaOH (0.085 M) to calculate the amount of unreacted formic acid.

2.5 Characterization of the oils

2.5.1 Elemental Analysis

All samples were analyzed for their elemental composition in the CHNS mode with a Vario EL III instrument using helium as carrier gas. The amount of oxygen was calculated by difference.

2.5.2 GPC-SEC

The sample (1 mg) was dissolved in 1 mL of THF. The solution (20 µL) was injected into a GPC-SEC system equipped with a PLgel 3ìm Mini MIX-E column, and analyzed at a flow rate of 0.5 mL/min of THF at 21.1^{o}C. The detection was performed with UV at 254 and 280 nm, as well as with RI. The set of columns was calibrated with a series of polystyrene standards covering a molecular-mass range of 162–2360 Da.

2.5.3 GC-MS

The LtL-oil was analyzed on a 5977A Series GC/MSD System from Agilent Technologies. A EtAc:THF (90:10 v/v) mixture was used as solvent and the samples were analyzed using splitless injection at 280 °C (injector temperature) on a 30 m HP-5MS capillary column ((5% phenyl)-methylpolysiloxane), 0.250 mm ID from Agilent Technologies. A constant gas flow rate of 1 mL/min and the following GC oven temperature program were applied: 40^{o}C for 5 min, followed by a heating ramp of 6^{o}C/min from 40^{o}C to 280^{o}C and a heating ramp of 40^{o}C/min from 280^{o}C to 300^{o}C. The GC–MS inter phase valve delay was set to 5 min and the MS detector operated in positive mode at 70 eV with an ion-source temperature of 250 °C. Compounds were identified using the ChemStation software and the NIST 2.0 library.

2.5.4 FT-IR

The FTIR spectra were recorded on a Nicolet iS50 FT-IR Spectrometer from Thermo Scientific by applying the sample to an attenuated total reflectance (ATR) crystal. The main measurement features were a spectral range from 4000 to 400 cm^{-1}, 16 scans, and a resolution of 4 cm^{-1}.

3. Results

3.1 Reproducibility and effect of the reactors

Only the ET-FA-BS-C experiment was reproduced to evaluate the uncertainty of the reaction procedure. Table 2 (entry 4-5) shows the oil and solid yield for both replicates. For the first replicate, ET-FA-BS-C experiment, the oil yield accounts for 38.4 % of the initial lignin input while for the second replicate, ET-FA-BS-C-R experiment, the oil yield is 35.0 %. When it comes to the solid yield the difference between the experiments is of 2.4 points; 32.9 % for the ET-FA-BS-C and 35.3 % for the ET-FA-BS-C-R experiment. The values are therefore within around 3 points uncertainty on the yield, which confirms the reproducibility of the experiments.

In addition, two other experiments were carried out in the non-stirred 25 mL Parr reactor (entries 1-2, Table 2). The aim of these experiments was to evaluate the effect of the stirring and the reactor volume in the final outcome. Both reactors are made of the same material, 316 Stainless Steel, and thus both surfaces should present similar catalytic activity [9]. Overall, the experiments in the small system give higher lignin recovery yields, but the oil and solid yields are comparable (entries 1-4, Table 2). In both cases, a comparable increase in the oil yield, 14.1 for the non-stirred and 15.4 for the stirred reactor; together with a comparable decrease in the solid yield, 12.9 for the non-stirred and 10.7 for the stirred reactor, is observed between the catalyzed and the non-catalyzed counterparts. This suggests that the possible negative effect of having a bigger reactor volume such as the mass transfer and heat transfer limitations might be overcame by the effect of the stirring. This proves that the tested LtL procedure is reproducible and robust.

3.2 Influence of the source of hydrogen

The main aim of this paper is to understand the LtL reaction system; that is the interactions between the lignin, the formic acid, the catalyst and the solvent, and how they affect the characteristics and yield of the oil. As a first hypothesis, we studied the role of formic acid as a possible hydrogen source or hydrogen donor molecule. On the one hand, formic acid can decompose either into hydrogen and carbon dioxide, or water and carbon monoxide at high temperatures; although its decomposition kinetics can be modified by the presence of a catalyst[25-29]. Previous results in our group suggest that in the LtL process formic acid is mainly decomposed into hydrogen and carbon dioxide[9] .For this reason, the oil and solid yields of those experiments carried out with formic acid were compared with experiments where this molecule was substituted either partially (ET-FA/H_2-BS) or totally by molecular hydrogen or by a mixture of H_2:CO_2 (1:1) (entries 3-4, 6-11, Table 2). Both the catalytic and the non-catalytic systems were considered. On the other hand, formic acid can also act as a hydrogen donor molecule through a catalytic hydrogen transfer mechanism. Isopropanol is known to be a good hydrogen donor in catalytic transfer hydrogenation reactions; it decomposes into acetone and hydrogen through a reversible reaction[4, 30]. Hence, isopropanol can be regenerated *in situ* during the course of the reaction[31-32]. An experiment with isopropanol and hydrogen in the presence of the catalyst was performed, ET-ISO/H_2-BS-C (entry 12, Table 2) and the results compared with the ET-FA/H_2-BS-C experiment (entry 11, Table 2).

Table 2: oil, solid and lignin recovery yields together with the characterization of the oil and solids

Entry	Experiment (A^a-B^b-X^c-C^d)	Oil Yield (%)	Solid Yield (%)	Lignin Recovery Yield (%)	Oils		M_w (Da)
					(O/C)	(H/C)	
1	ET-FA-BNS-NC	27.5	47.3	74.7	-	-	-
2	ET-FA-BNS-C	41.6	34.4	76.0	-	-	-
3	ET-FA-BS-NC	23.0	43.6	66.7	0.15	1.28	313
4	ET-FA-BS-C	38.4	32.9	71.3	0.13	1.26	361
5	ET-FA-BS-C-R	35.0	35.3	70.3	-	-	-
6	ET-H_2-BS-NC	14.4	55.6	70.1	0.21	1.33	331
7	ET-H_2-BS-C	19.7	52.0	71.7	0.11	1.39	322
8	ET-H_2/CO_2-BS-NC	14.7	55.8	70.5	0.22	1.35	292
9	ET-H_2/CO_2-BS-C	17.8	54.2	71.9	0.13	1.40	327
10	ET-FA/H_2-BS-NC	18.3	51.9	70.2	0.20	1.30	532
11	ET-FA/H_2-BS-C	26.6	42.9	69.5	0.17	1.28	540
12	ET-ISO/H_2-BS-C	21.3	51.3	72.7	0.13	1.34	371
13	ET-FA-SBS1-NC	23.3	44.9	68.2	0.19	1.26	420
14	ET-FA-SBS1-C	27.3	44.7	76.5	0.15	1.29	467
15	ET-FA-SBS2-NC	25.2	46.4	71.5	0.22	1.24	513
16	ET-FA-SBS2-C	29.6	44.3	73.9	0.19	1.31	469
17	ISO-FA-BS-C	21.7	43.7	65.4	0.15	1.24	387
18	ME-FA-BS-C	23.8	44.1	67.8	0.17	1.24	364

[a]**A:** refers to the type of solvent [b]**B:** refers to the type of hydrogen source [c]**C:** refers to the type of reactor and reaction configuration [d]**Y:** refers weather the experiment is catalyzed or non-catalyzed reactor [e]**R:** refers to the replicate experiment [f]In this case refers to isopropanol instead of formic acid [g]In this case refers to isopropanol instead of ethanol [h]In this case refers to methanol instead of ethanol **ET:** ethanol **MET:** methanol **ISO:** isopropanol **FA:** formic acid **H:** molecular hydrogen **CO_2:** carbon dioxide **BS:** Batch experiments in stirred reactor **BNS:** Batch experiments in non-stirred reactor **SBS:** Semi-batch experiments

The evolution of the pressure depicted in Figure 1 shows that above a temperature of 200 ^oC, or reaction times longer than 50 minutes, the pressures of the systems behave similarly for all the experiments. The same happens with the lignin recovery yields that vary between 66.7 wt % (for the ET-FA-BS-NC) and 72.7 % (for the ET-ISO/H_2-BS-C); hence the reaction conditions are similar in all the cases, which allow comparing the modified parameters and drafting conclusions from the experimental results.

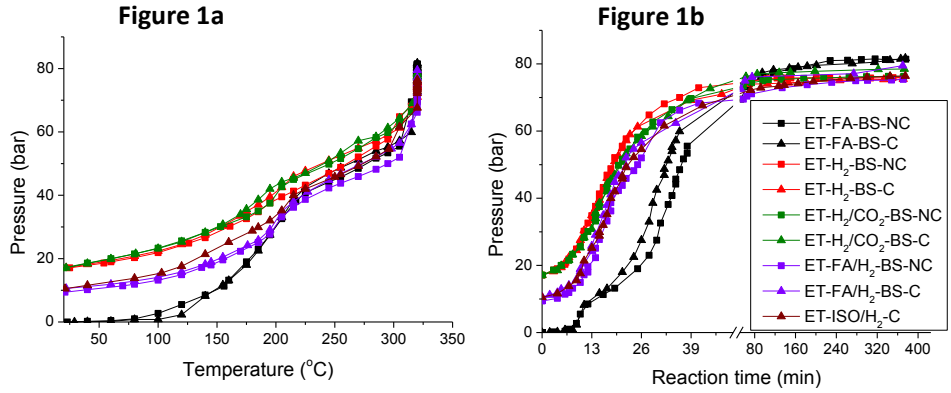

Figure 1a: Pressure vs Temperature for the ET-FA-BS, ET-H_2-BS, ET-H_2/CO_2-BS, ET-FA/H_2-BS and ET-ISO/H_2-BS-C series **Figure 1b:** Pressure vs Reaction time for the ET-FA-BS, ET-H_2-BS, ET-H_2/CO_2-BS, ET-FA/H_2-BS and ET-ISO/H_2-BS-C series

Figures 2a and 2b show the oil and solid yield for the above mentioned experiments. The analysis of the graph confirms that the presence of formic acid is positive when it comes to a higher oil and lower solid yield. In fact, those experiments with both formic acid and molecular hydrogen give better results than the experiments were only H_2, H_2:CO_2 or H_2/isopropanol is used. For the non-catalyzed systems the highest oil yield is obtained for the ET-FA-BS-NC experiment (23.0 %) followed by the ET-FA/H_2-BS-NC experiment (18.3 %) and the ET-H_2/CO_2-BS-NC and ET-H_2-BS-NC experiments (14.7 % and 14.4 %, respectively). All the catalyzed experiments give higher oil and lower solid yields than their non-catalyzed counterparts; nevertheless, the same trend as in the non-catalyzed systems is observed: the highest oil yield is obtained for the ET-FA-BS-C (41.6 %) followed by the ET-FA/H_2-BS-C (26.6 %), and the ET-H_2-BS-C and ET-H_2/CO_2-BS-C experiments (19.7 % and 17.8 % respectively). Interestingly, the oil and solid yields of the ET-ISO/H_2-BS-C experiment, 21.3 % and 51.3 %, are closer to the yields obtained for the ET-H_2-BS-C and ET-H_2/CO_2-BS-C experiments rather than for the ET-FA/H_2-BS-C experiment. This lower activity of isopropanol with respect to formic acid is in accordance with previous studies conducted by Toledano *et al.*[4].

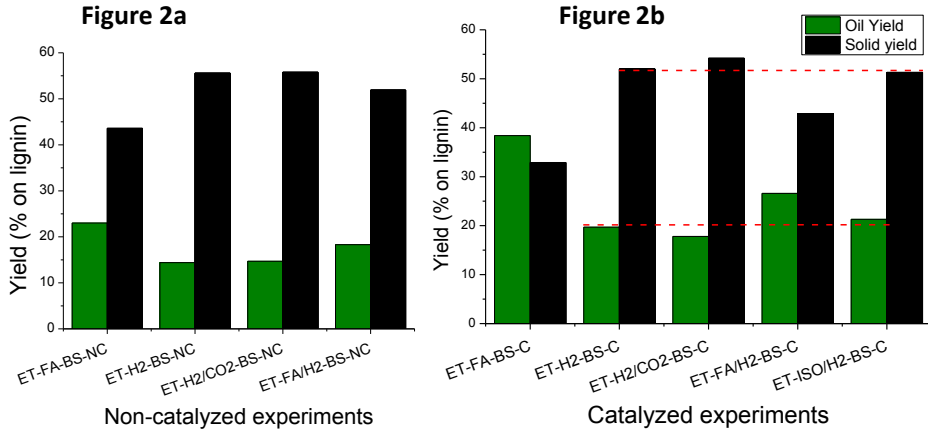

Figure 2a: oil and solid yield for the ET-FA-BS-NC, ET-H_2-BS-NC, ET-H_2/CO_2-BS-NC, ET-FA/H_2-BS-NC **Figure 2b:** oil and solid yield for the ET-FA-BS-C, ET-H_2-BS-C, ET-H_2/CO_2-BS-C, ET-FA/H_2-BS-C and ET-ISO/H_2-BS-C series

When comparing the results for the ET-H_2-BS and ET-H_2/CO_2-BS series it is clear that the partial pressure of hydrogen does not significantly affect the results in terms of oil and solid yield; at least for the pressure range studied. This is in accordance with the results obtained by Zhang *et al.*[33] and Li *et al.*[6] that claimed that above a certain hydrogen pressure the oil yield stabilizes.

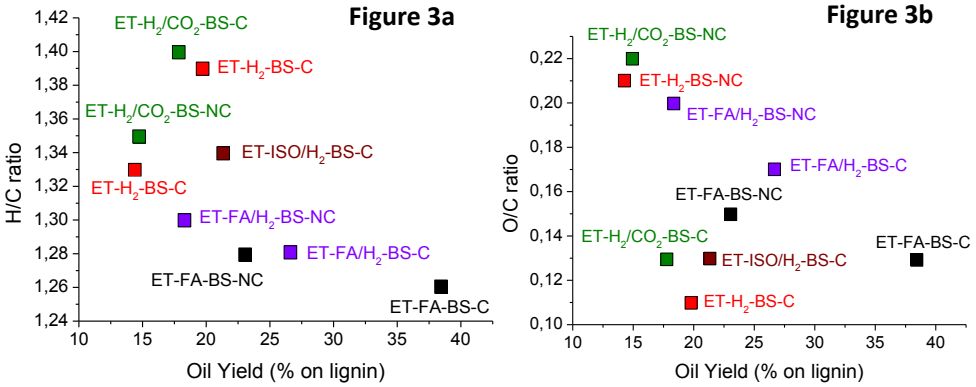

Figure 3a: H/C ratio vs oil yield for the ET-FA-BS (black), ET-H_2-BS (red), ET-H_2/CO_2-BS (green), ET-FA/H_2-BS (purple) and ET-ISO/H_2-BS series (maroon) **Figure 3b:** O/C ratio vs oil yield for the ET-FA-BS (black), ET-H_2-BS (red), ET-H_2/CO_2-BS (green), ET-FA/H_2-BS (purple) and ET-ISO/H_2-BS series (maroon)

To further confirm the difference between the role of hydrogen, isopropanol and formic acid in the lignin conversion, several oil properties were analyzed. The H/C and O/C ratio of the oils with respect to the oil yield are depicted in Figure 3a and 3b, respectively. The main conclusion that can be drawn from the graphs is that high H/C and low O/C oils do not necessarily mean a higher oil yield. Moreover, the oil yield is more affected by the presence of formic acid in the reaction system than by the presence of the catalyst. For those systems where no formic acid is used (ET-H_2-BS and ET-H_2/CO_2-BS series), the presence of the catalyst gives a significant increase in the H/C ratio while the oil yield just increases slightly. This indicates that for the experiments with molecular hydrogen the increase in the oil yield is an effect of the stabilization of the monomers either by hydrogenation or alkylation reactions (discussed below). On the contrary, in the systems where formic acid was used (ET-FA-BS and ET-FA/H_2-BS series), the presence of the catalyst significantly increases the oil yield but slightly decreases the H/C ratio; suggesting that the higher degree of lignin de-polymerization is achieved by other reaction mechanism than just a catalytic transfer hydrogenation.

This difference can also be observed when analyzing the O/C ratio. In all the cases the increase of the oil yield in the catalytic versions is accompanied by a decrease in the O/C ratio. However, this decrease is less significant when formic acid is present, with minimum differences between the ET-FA-BS-NC and ET-FA-BS-C experiments (0.15 and 0.13 respectively). Hence, the deoxygenation of the monomers might be an important mechanism for the stabilization of the lignin monomers for the experiments without formic acid, but is not so critical when formic acid is present in the reaction mixture. The elemental analysis results also confirm that the ET-ISO/H_2-BS-C and ET-H_2-BS-C oils are similar in terms of H/C and O/C ratios, whereas the ET-ISO/H_2-C and ET-FA/H_2-BS-C oils give significantly different H/C and O/C ratios.

Regarding the average molecular weight of the oils (Mw), all the experiments except for the ET-FA/H_2-BS series give oils with low average molecular weight distribution (entries 3-4, 6-11, Table 2), suggesting that the components within the oils are fully depolymerized and stable. This again shows the disparity between the ET-ISO/H_2-BS-C and the ET-FA/H_2-BS-C experiment, since the Mw values of the oil are significantly different, 371 Da and 540 Da, respectively.

The GC-MS analysis confirms the results obtained by the elemental analysis. Typically all the oils contain methoxy-, hydroxyl- and alkyl-substituted benzenes, although the abundance and type of compounds differs between the oils. In those experiments carried out in the absence of formic acid, the catalytic experiments give oils with lower frequency of methoxy- and higher frequency of alkyl-substituted groups, which explains the higher H/C and lower O/C ratios found by the elemental analysis. The GC-MS chromatogram for the ET-H_2-BS-NC and ET-H_2-BS-C is depicted in Figure 4, the behavior of the ET-H_2/CO_2-BS-NC and ET-H_2/CO_2-BS-C is analogous and their chromatograms are shown in Figure S1, Supplementary information. According to Hensen *et al.*[1], ethanol acts also as a capping agent which can stabilize the highly reactive phenolic intermediates by O-alkylation of hydroxyl groups and by C-alkylation of the aromatic rings. Our results suggest that the alkylation together with the decrease of the methoxy groups, probably through hydrogenolysis, are the mechanisms that contribute to the oil yield increase caused by the catalyst for the ET-H_2-BS and ET-H_2/CO_2-BS series. The partial pressure of hydrogen, however, has no significant effect in the results what suggest that there is an excess of hydrogen in the reaction.

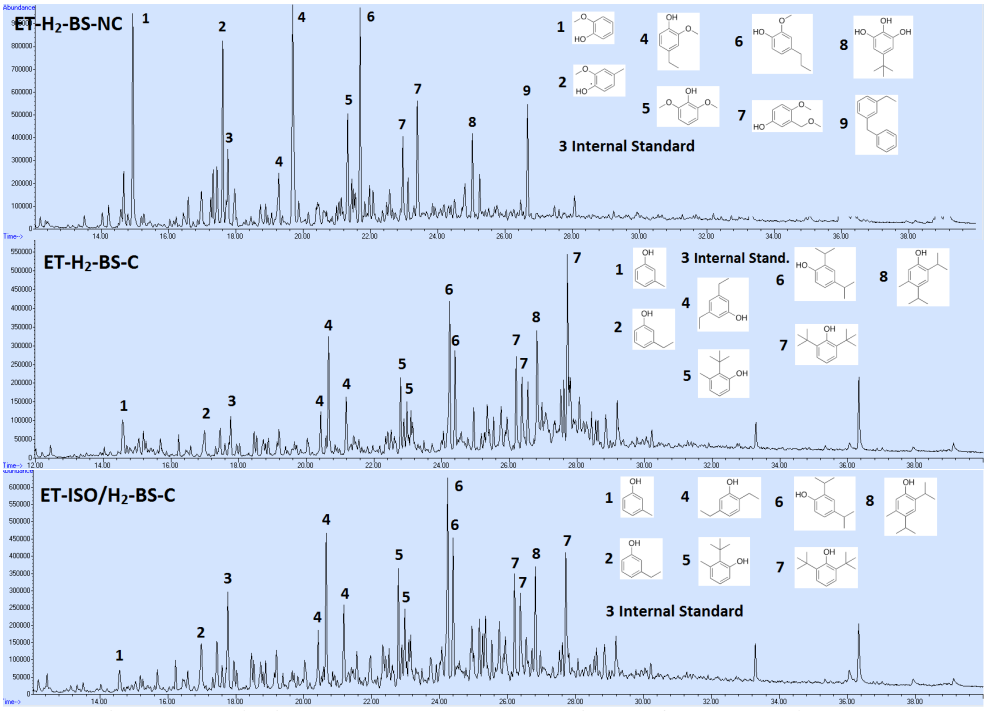

Figure 4: Chromatograms for the ET-H_2-BS-NC, ET-H_2-BS-C and ET-ISO/H_2-BS-C experiments

On the contrary, for the ET-FA-BS series only little differences can be observed between the catalyzed and the non-catalyzed counterparts; only slightly higher amounts of alkylated compounds are found as shown in Figure 5, which is in accordance with the elemental analysis. For both the un-catalyzed and catalyzed counterparts methoxy substituted phenols are the most abundant type of compounds; meaning that in this case the presence of the catalyst does not increase significantly the de-methoxylation rate of the lignin monomers. For the ET-FA/H_2-BS series, there is not so good correlation between the elemental analysis and the GC-MS results (Figure S2, Supplementary Information). In the ET-FA/H_2-BS-C oil slightly lower amounts of methoxy and higher amount of hydroxyl- and alkyl substituents are found: this could justify the lower O/C ratio but would imply that the H/C ratio should be higher. Nevertheless, the higher Mw values found in this series indicates the presence of compounds in the oil that are not detected by GC-MS; and therefore this analysis may not be as representative for the oil as in the case of the ET-FA-BS, ET-H_2-BS and ET-H_2/CO_2-BS series.

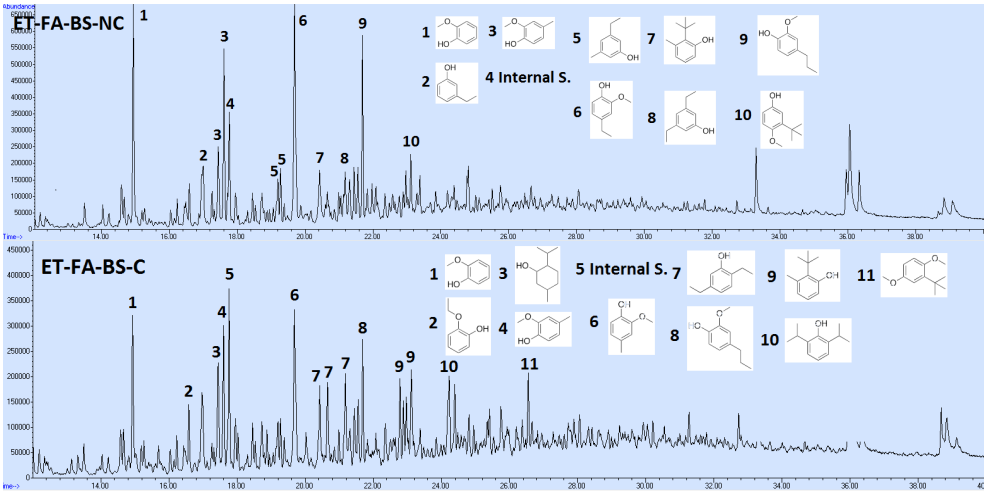

Figure 5: Chromatograms for the ET-FA-BS-NC and ET-FA-BS-C experiments

The GC-MS analysis also shows the resemblance between the ET-ISO/H_2-BS-C and ET-H_2-BS-C experiments (Figure 4), and the difference between the former and the ET-FA/H_2-BS-C (Figure S2). The former contain the same type of compounds, with no methoxy substituted phenols; whereas in the latter a considerable amount of methoxy substituted phenols are found. The FTIR spectra of the oils support these observations. The spectra of the ET-H_2-BS-C and ET-ISO/H_2-BS-C experiments are identical in terms of both peaks and intensity (Figure 6a) while the ones for the ET-FA/H_2-BS-C and ET-ISO/H_2-BS-C differ considerably (Figure 6b). One of the main differences between the ET-FA/H_2-BS-C and ET-ISO/H_2-BS-C spectra is the intensity of the peaks around 1250 cm^{-1} region. This peak corresponds to the guaiacyl ring breathing with C-O stretching[34-35]; which confirms what it was already seen in the GC-MS analysis: the ET-FA/H_2-BS-C oil contains a high amount of methoxy substituted phenols that are not present in the ET-ISO/H_2-BS-C oil.

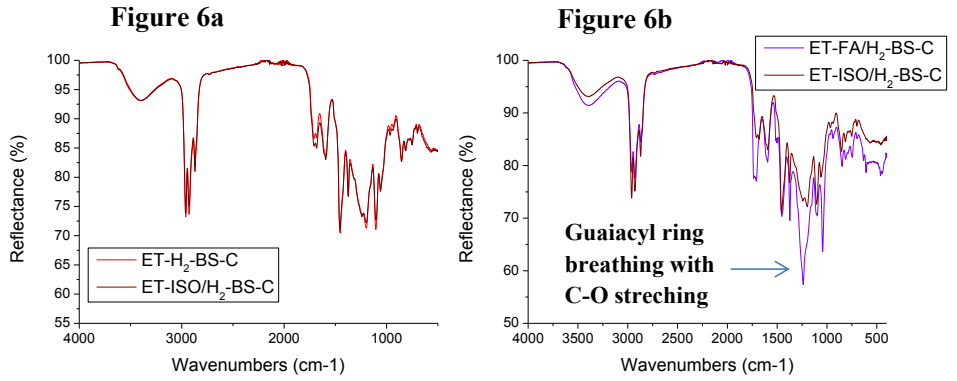

Figure 6a: FT-IR spectrogram of the ET-H_2-BS-C and ET-ISO/H_2-BS-C experiments **Figure 6b:** FT-IR spectrogram of the ET-FA/H_2-BS-C and ET-ISO/H_2-BS-C experiments

3.3 Effect of feeding formic acid continuously

Certain catalysts can increase the decomposition rate of formic acid[36], a phenomenon that could affect the interaction between the acid and the lignin and hence the lignin conversion rate. To evaluate the activity of our catalyst towards the decomposition of formic acid three blank experiments, with no lignin, were carried out. The evolution of the pressure for the blanks and the titration results are shown in Figure S3 (*Supplementary Information*) and Table 3, respectively. Figure S3 (*Supplementary Information*) shows how the pressure of the catalyzed blank test increases significantly faster than the pressure in the non-catalyzed blanks. In fact, the catalyzed blank reaches a pressure of 65 bars after 51 minutes, while the non-catalyzed blank does not even reach 44 bars. After 360 min of reaction time the pressure of the non-catalyzed blank is 62 bars.

The titration results shown in Table 3 confirmed that this pressure increase is correlated with the decomposition rate of formic acid. In the non-catalyzed blank test, there is still 57.0 % of formic acid left after 51 minutes, whereas for the catalyzed blank there is only 12.4 % left. These results indicate that in the catalyzed systems there is almost no formic acid present after the first hour of reaction.

Table 3: Gas amount, residual formic acid percentage and final reactor pressure of the B, B-C and B-F blanks

Catalyst	Reaction Time (min)	Gas amount (g)	Volume NaOH (ml)	Formic acid (%)[a]	Final Reactor Pressure (bar)
No	51	3,8	17,75	57,0	43.7
Ni-MoAA	51	7,6	3,85	12,4	65.2
No	360	7,8	0	0	61.3

[a]Percentage of formic acid that has decomposed calculated by titration

In an attempt to determine whether the continuous presence of formic acid during the 6 h reaction time could be beneficial to increase the oil yield, two additional reaction configurations were proposed: a semi-batch experiment where part of the formic acid is introduced initially and the rest continuously (ET-FA-SBS1 series), and a second semi-batch experiment where formic acid is only introduced continuously along the course of the reaction (ET-FA-SBS2 series). Both the catalytic and non-catalytic systems were considered and the results compared with the batch counterparts (ET-FA-BS series). These results are summarized in Table 2 (entries 3-4 and 13-16, Table 2).

The pressure profiles in the experiments differ greatly as a function of the configuration (Figure S4a and S4b, *Supplementary information*) yet the final reactor pressures are comparable, and so are the lignin recovery yields (Table 2). Figure 7 shows the oil and solid yields for the batch and semi-batch experiments (entries 3-4 and 13-16, Table 2). In the catalyzed experiments, Figure 7b, the highest oil and lowest solid yield is obtained by far for the batch configuration. In the non-catalyzed experiments, however (Figure 7a), the results are similar whether formic acid and ethanol are added at the beginning or in a continuous way. Interestingly, the oil and solid yields obtained for the semi-batch experiments are similar to the ones obtained in the ET-FA/H_2-BS series, when molecular hydrogen is present.

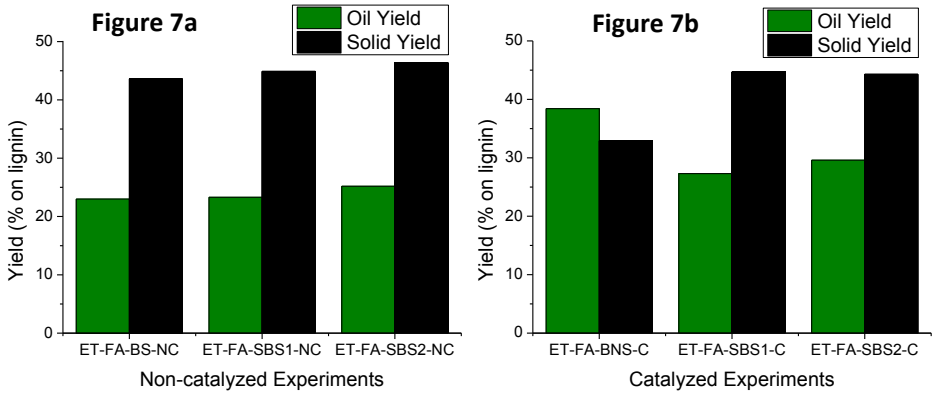

Figure 7a: oil and solid yield for the ET-FA-BS, ET-FA-SBS1 and ET-FA-SBS2 experiments **Figure 7b:** oil and solid yield for the ET-FA-BS, ET-FA-SBS1 and ET-FA-SBS2 experiments

Moreover, the nature of semi-batch oils is also more similar to those oils produced in the presence of molecular hydrogen (ET-H_2-BS and ET-H_2/FA-BS series) than to the oils produced in the ET-FA-BS series; when only formic acid is added initially in the reactor. The GPC-SEC analysis of the oils (entries 13-16, Table 2) indicates that semi-batch experiments give oils with relatively high Mw values. In most of the cases, these values are closer to the ones obtained for the ET-FA/H_2-BS. In both semi-batch series (ET-FA-SBS1 and ET-FA-SBS2 series) the increase on the oil yield is accompanied by an increase of the H/C ratio (Figure S5a, *Supplementary Information*), a behavior that is only observed in those experiments were molecular hydrogen is present (ET-H_2-BS). In the case of the O/C ratio (Figure S5b), on the other hand, this oil yield increase is accompanied with a decrease on the O/C ratio comparable in magnitude to the decrease observed in the ET-FA/H_2-BS series. Finally, the GC-MS analysis of semi-batch experiments, Figure S6 *Supplementary Information*, indicates that the oils contain a higher amount of identified low volatile compounds. These compounds are similar in amount and nature to the ones found in the ET-FA/H_2-BS series (Figure S2); both for the non-catalyzed and catalyzed experiments.

Therefore, the role of formic acid seems to be different based on the reactor configuration. In the catalyzed semi-batch experiments the production of molecular hydrogen and CO_2 from the decomposition of formic acid is more relevant, and formic acid acts more like a source of hydrogen. In the batch experiments, where all the formic acid is from the beginning in contact with the lignin, other reactions besides the decomposition seem to occur. These results, together with the formic acid reaction rate results on Table 3, suggest that when a catalyst is present formic acid takes part mainly in the initial stages of the lignin conversion, and that there is a competition between its decomposition and its interaction with the lignin.

3.4 Effect of the solvent

The role of the type of solvent was also considered in this study. Other alcohols with similar physical and chemical properties such as isopropanol and methanol have been studied in the presence of the NiMo/AA catalyst in the formic acid-aided lignin decomposition (entries 4, 16-17, Table 2). Figure 8 shows the evolution of the pressure for the three experiments. The graphs show that initially the pressure of the ET-FA-BS-C increases faster than for the ISO-FA-BS-C and ME-FA-BS-C experiments but after 40 minutes, when the systems reaches 60 bars, all the systems behave analogously. The lower lignin mass balance and the higher amount of gas produced during the reaction indicate that in the isopropanol and methanol systems a higher amount of lignin is gasified.

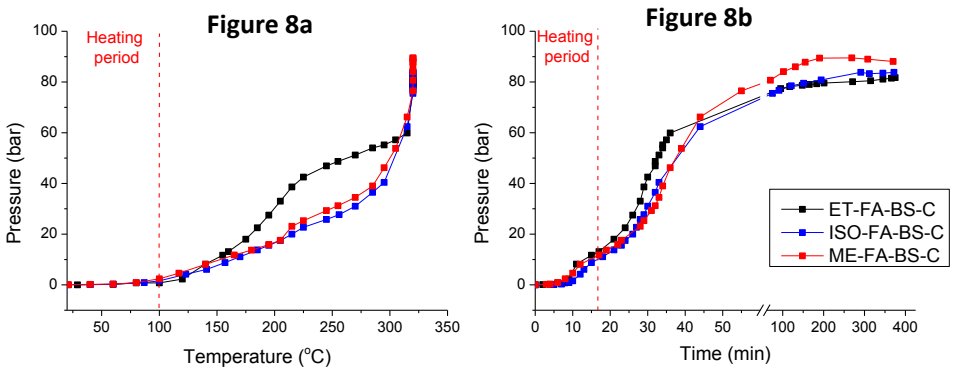

Figure 8a: Pressure vs Temperature for the ET-FA-BS-C, ISO-FA-BS-C and ME-FA-BS-C experiments **Figure 8b:** Pressure vs Reaction time for the ET-FA-BS-C, ISO-FA-BS-C and ME-FA-BS-C experiments

The interaction between formic acid and the different solvents was also studied to evaluate their effect on the formic acid decomposition rate. Blank experiments carried out in the small-scale reactors show that the decomposition rates of formic acid in isopropanol and methanol are comparable or even faster than the decomposition rate in ethanol (Table S2, *Supplementary Information*). After 40 minutes of reaction the amount of formic acid still left in the methanol system is 34.8 %, in the ethanol system is 47.8 %, and in the isopropanol system 48.8 %. Hence, the decomposition rate of formic acid is faster in methanol than in ethanol or isopropanol.

The oil and solid yield depicted in Figure 9 shows that ethanol is the best solvent for increasing the oil and decreasing the solid yield. ISO-FA-BS-C and ME-FA-BS-C experiments have a much lower oil yield and a higher solid yield than the ET-FA-BS-C experiments (Figure 9 and entries 4 and 16-17, Table 2). Still, the GPC-SEC and elemental analysis show that there are not significant differences in the type of oils produced. The Mw values vary from 361 Da, for the ET-FA-BS-C experiment, to 387 Da for the ISO-FA-BS-C experiment. The H/C ratios are also comparable (1.26 for the ET-FA-BS-C experiment and 1.24 for the ISO-FA-BS-C and ME-FA-BS-C experiments), while a bigger variability is found in the O/C ratios that oscillate between 0.13 (ET-FA-BS-C) and 0.17 (ME-FA-BS-C).

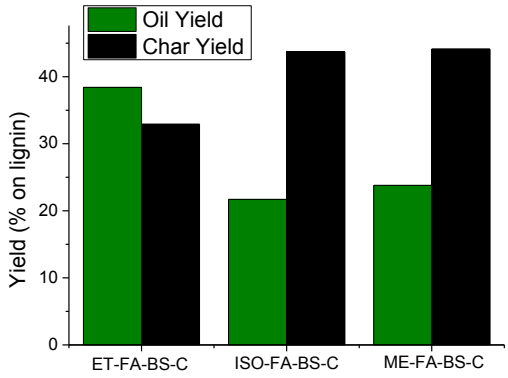

Figure 9: oil and solid yield for the ET-FA-BS-C, ISO-FA-BS-C and ME-FA-BS-C experiments

The GC-MS analysis depicted in (Figure S7) show that the types of compounds found in the oils are similar, especially between the ET-FA-BS-C and ISO-FA-BS-C experiments. The ME-FA-BS-C oil contains a higher amount of oxygenated compounds which is consistent with previous reports[1] and justifies the higher O/C values . These results suggest that the mechanism of de-polymerization of lignin is similar regardless of the solvent and that is more affected by the presence or absence of formic acid.

4. Discussion: the role of formic acid and the solvent

The reported experimental results highlighted the paramount role of formic acid in achieving high oil yields. Moreover, from the results shown in Section 3.2 it can concluded that the conversion of lignin aided by formic acid does not follow the same reaction mechanism as when lignin is converted in the presence of molecular hydrogen or an alternative hydrogen donor molecule such as isopropanol. Only small differences in the results are observed when isopropanol or hydrogen is used in the system, while large differences are seen when these experiments are compared with the experiments performed in the presence of formic acid. This difference in the lignin conversion mechanism is clear when comparing the oil yields and elemental analysis of the ET-H_2-BS and ET-FA-BS series. For the former, the addition of the catalysts changes considerably the H/C and O/C ratio while increasing only slightly the oil yield. The effect of the catalyst is therefore the stabilization of the monomers by hydrodeoxygenation and alkylation which would justify this slight oil increase. For the latter, however, the addition of the catalyst increases the lignin depolymerization rate with small differences in the H/C and O/C ratio. Moreover, the results of formic acid reaction rate (Table 3) and of the semi-batch experiments, point out that formic acid plays a role mainly in the first stage of the lignin conversion.

All this suggests that formic acid is involved in the lignin de-polymerization mechanism resulting in a reaction pathway that is different from reactions involving molecular hydrogen or catalytic transfer hydrogenation. Two mechanisms have been proposed involving lignin model compounds and short-chain organic acids for the conversion of this biopolymer into low molecular weight components. Stahl et al studied the formic-acid catalyzed depolymerization of a pre-oxidized lignin model compound to monoaromatics at 110 ^{o}C[20]; and this investigation was later expanded by Wang et al.[21] through a DFT study to clarify the reaction mechanism. Their interpretation is that the conversion proceeds sequentially via a formylation, elimination and hydrolysis mechanism. The elimination of formic acid is the limiting step, and it is catalyzed by a base, in this case sodium formate.

They claim that the oxidation of the C_α carbon is necessary for the conversion of the lignin by this process. However, the DFT study proves that this reaction could happen without this previous preoxidation, since the effect of the oxidation is to increase the reaction rate of the elimination step by lowering the elimination barrier from 38.8 kcal/mol to 20.8 kcal/mol. This means that if the elimination is carried out at 320 ^oC, the reaction rate of a non-pre-oxidized lignin is comparable to the elimination rate of a pre-oxidized lignin at 110 ^oC, since the E_a/T ratios are also comparable. In our process, this elimination step could be favored in the absence of a base by the interaction between the catalyst and the solvent. Several studies have reported the formation of alkoxides from the interaction of alcohols and solid Lewis acids such γ-alumina[37-38]. The last hydrolysis step, however, is not likely to occur in our system, due to the low amount of water that would be present in the reaction medium coming from the gas-shift or hydrogenolysis reactions. An additional possibility could be the attack of the solvent (ethanol) to the alkene intermediate through a solvolysis mechanism. However, no or little ethoxy- substituted benzenes have been identified in the oils, even though large quantities of methoxy substituted benzenes have been identified. This suggests that solvolysis plays a minor role in the reaction mechanism.

In another approach, Marks et al.[22] reported the selective C-O hydrogenolysis of an acetylated lignin model compound using leveraged tandem catalytic strategy. The mechanism involved the acetylation of the lignin by attacking the hydroxyl group on the C_α and C_γ carbons, which would increase the solubility of the lignin in a non-polar solvent. The following steps would be the elimination of acetic acid and the hydrogenolysis of the resulting dimer. The reaction is carried out at low temperatures (70 ^oC) and in the presence of a metal triflate and a supported palladium catalysts. In our case the acetylation could be substituted by a formylation step since formic acid is a strong proton donor and could be coordinated to the hydroxyl- groups of the C_α and C_γ. The low Brønsted acidity of isopropanol would also justify the lower oil yields obtained in the ET-ISO/H_2-BS-C experiment[39].

Based on this background and our experimental evidences we propose a reaction mechanism initiated by a formylation reaction between formic acid and lignin (Figure 10). Despite the complexity of the reaction system the formic acid aided lignin conversion mechanism is believed to continue through an elimination-hydrogenolysis pathway, as summarized in Figure 10. The deformylation would be the rate limiting step, where the *in situ* generated alkoxide –from the solvent- could act as the based needed for the abstraction of the proton in the C_β at high temperatures; leading to the elimination of the formate attached to the C_γ and the formation of an unsatured bond. As discussed above, the break of the lignin bond seems to occur through a hydrogenolysis mechanism, although the less likely hydrolysis and solvolysis mechanisms are not fully discharged. The presence of molecular hydrogen will thus be necessary for the reaction to happen. No effect of the hydrogen partial pressure in the reaction has been observed probably due to the excess of hydrogen present at the studied reaction conditions where the rate limiting step is the previous deformilation. In the case of the non-catalyzed experiments the three steps of the reaction would be catalyzed by the reactor surface, whose activity has already been proved in previous studies [9], and which activity would be lower than our NiMoAA catalyst.

Under the reaction conditions, formic acid can either decompose into H_2 and CO_2 or formylate the lignin, and the comparison between the batch and the semi-batch configuration in Section 3.3 revealed the importance of the relative rate of each of these reactions. In the catalyzed experiments, significant higher oil yields were obtained when all the formic acid was present from the beginning in the reactor. This indicates that a higher contact time between the lignin and the formic acid during the heating and the initial isothermal period favors the formylation reaction. On the other hand, in the catalyzed semi-batch experiments formic acid is slowly added into the reactor, which seems to disfavor the ligning-formic acid interaction and favor its decomposition into H_2 and CO_2: a higher amount of formic acid will be decomposed before it can formylate the lignin. Regarding the non-catalyzed systems, comparable amount of oil and solid were obtained with the batch and semi-batch configurations. In the absence of a catalyst, formic acid is decomposed slowly thus enabling a similar amount of formic acid to react/formylate continuously with the lignin throughout the duration of the reaction regardless of the reactor configuration.

Moreover, when analyzing the properties of the oils in Section 3.3 a resemblance between the oils produced in the presence of molecular hydrogen, especially the with ET-FA/H_2-BS series, and the ET-FA-SBS1 and ET-FA-SBS2 was demonstrated. Hence for the semi-batch experiments the effect of both mechanisms is observed: formic acid-aided and H_2-aided lignin conversion. This is in accordance with the mechanism explained above. An additional confirmation is the evolution of the pressures depicted in Figure 1. The higher degree of formylation in the catalyzed systems would hinder the fast decomposition of formic acid at the beginning of the reaction (ET-FA-BS and ET-FA/H_2-BS series), which would justify the similarities in the pressure profiles.

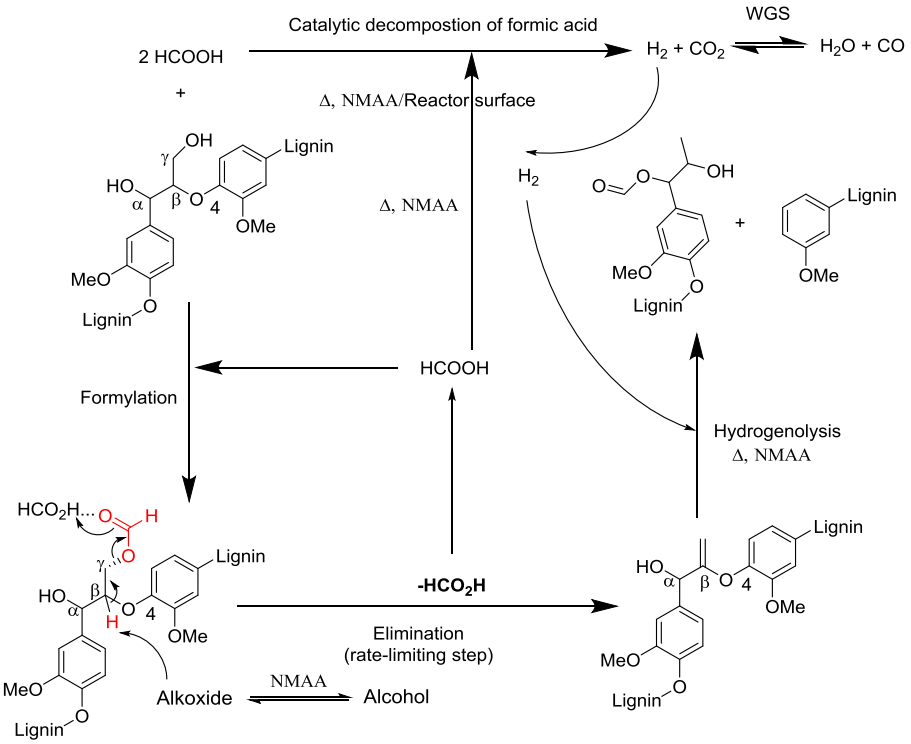

Figure 10: Proposed mechanism for formic acid-aided depolymerization of lignin through a formylation, elimination, hydrogenolysis

Apart from the indirect role of the solvent in the reaction mechanism as a potential alkoxide source, the results in Section 3.4 indicate that the primary effect of the solvent is the ability to stabilize the lignin monomers; and therefore affect the final oil and solid yield. These results showed that a considerable higher oil yield is obtained when using ethanol as a solvent when compared with methanol or isopropanol. This is in accordance with several studies published on the influence of the type of solvent on the conversion of lignin with molecular hydrogen and formic acid[1, 5, 7, 19]. Most of this studies show that ethanol is a better solvent than isopropanol or methanol[1, 6].

As mentioned in Section 3.2, Hensen et al[1] suggest that the better activity of ethanol is due to esterification (O-alkylation) of the highly reactive phenolic intermediated and the alkylation (C-alkylation) of the aromatic rings. This will prevent the repolymerization of the lignin monomers since this compounds are less likely to re-polymerize [35]. Li et al [19] also point towards the functionalization of the lignin fragments as the reason for the lower degreee of re-polymerization and solid formation of the lignin fragments as the reason for the lower degree of re-polymerization and solid formation of the lignin monomers, due to the formation of reactive intermediates by the formation of an ethanol catalyst complex. Our results are consistent with these studies. In the case of methanol, a higher decomposition rate of formic acid and a lower activity of this media in the O- and C-alkylation could justify these results. In the case of isopropanol, the higher steric impediment towards O-alkylation and the lower C-alkylation rate would be the main reasons that justify the lower oil and higher solid yields.

5. Conclusion

The results discussed support a reaction mechanism where the conversion of lignin is assisted by formic acid, which is as such an active species in the reaction. Thus, formic acid is not acting as an *in situ* hydrogen source or as a hydrogen donor molecule. To the best of our knowledge, these observations have never been reported in experiments carried out with real lignin feedstock. When substituting formic acid for molecular hydrogen or isopropanol different oil and solid yields are obtained; the properties of the oils also differ significantly. In contrast, both molecular hydrogen and isopropanol give comparable yields and type of oils, suggesting that they both follow a similar reaction pathway and different than formic acid. The comparison of results obtained for the batch and the semi-batch experiments revealed that there is a competing reaction between the decomposition of formic acid and the chemical reaction between lignin and formic acid. Based on these evidences and previous studies a formylation-elimination-hydrogenolysis mechanism for the formic acid-aided lignin conversion is proposed. The main effect of the solvent is the stabilization of the de-polymerized monomers, ethanol being the most effective one. In addition, the interaction between the solvent and the catalyst might form alkoxides that would favor the rate limiting elimination/deformilation step.

6. Acknowledgement

Some of this work has been performed as a part of the LignoRef project (“Lignocellulosics as a basis for second generation biofuels and the future biorefinery”). We gratefully acknowledge The Research Council of Norway (grant no. 190965/S60), Statoil ASA, Borregaard Industries Ltd., Allskog BA, Cambi AS, Xynergo AS, Hafslund ASA and Weyland AS for financial support. The authors would also like to thank I. J. Fjellanger for assisting with elemental analysis, Nemanja Miletíc for the NH_3-TPD analysis and Ainhoa Ocio for the ICP-EAS analysis.

7. References

1. Huang, X.; Korányi, T. I.; Boot, M. D.; Hensen, E. J. M., Catalytic Depolymerization of Lignin in Supercritical Ethanol. *ChemSusChem* **2014,** *7* (8), 2276-2288.
2. Haghighi Mood, S.; Hossein Golfeshan, A.; Tabatabaei, M.; Salehi Jouzani, G.; Najafi, G. H.; Gholami, M.; Ardjmand, M., Lignocellulosic biomass to bioethanol, a comprehensive review with a focus on pretreatment. *Renewable and Sustainable Energy Reviews* **2013,** *27*, 77-93.
3. Zakzeski, J.; Bruijnincx, P. C. A.; Jongerius, A. L.; Weckhuysen, B. M., The Catalytic Valorization of Lignin for the Production of Renewable Chemicals. *Chemical Reviews* **2010,** *110* (6), 3552-3599.
4. Toledano, A.; Serrano, L.; Labidi, J.; Pineda, A.; Balu, A. M.; Luque, R., Heterogeneously Catalysed Mild Hydrogenolytic Depolymerisation of Lignin Under Microwave Irradiation with Hydrogen-Donating Solvents. *ChemCatChem* **2013,** *5* (4), 977-985.
5. Kim, J.-Y.; Park, J.; Kim, U.-J.; Choi, J. W., Conversion of Lignin to Phenol-Rich Oil Fraction under Supercritical Alcohols in the Presence of Metal Catalysts. *Energy & Fuels* **2015,** *29* (8), 5154-5163.
6. Ooms, R.; Dusselier, M.; Geboers, J. A.; Op de Beeck, B.; Verhaeven, R.; Gobechiya, E.; Martens, J. A.; Redl, A.; Sels, B. F., Conversion of sugars to ethylene glycol with nickel tungsten carbide in a fed-batch reactor: high productivity and reaction network elucidation. *Green Chemistry* **2014,** *16* (2), 695-707.
7. Kloekhorst, A.; Shen, Y.; Yie, Y.; Fang, M.; Heeres, H. J., Catalytic hydrodeoxygenation and hydrocracking of Alcell® lignin in alcohol/formic acid mixtures using a Ru/C catalyst. *Biomass and Bioenergy* **2015,** *80*, 147-161.
8. Løhre, C.; Barth, T.; Kleinert, M., The effect of solvent and input material pretreatment on product yield and composition of bio-oils from lignin solvolysis. *Journal of Analytical and Applied Pyrolysis* **2016,** *119*, 208-216.
9. Oregui Bengoechea, M.; Hertzberg, A.; Miletić, N.; Arias, P. L.; Barth, T., Simultaneous catalytic de-polymerization and hydrodeoxygenation of lignin in water/formic acid media with Rh/Al2O3, Ru/Al2O3 and Pd/Al2O3 as bifunctional catalysts. *Journal of Analytical and Applied Pyrolysis* **2015,** *113*, 713-722.
10. Liguori, L.; Barth, T., Palladium-Nafion SAC-13 catalysed depolymerisation of lignin to phenols in formic acid and water. *Journal of Analytical and Applied Pyrolysis* **2011,** *92* (2), 477-484.
11. Yu, X.; Wu, T.; Yang, X.-J.; Xu, J.; Auzam, J.; Semiat, R.; Han, Y.-F., Degradation of trichloroethylene by hydrodechlorination using formic acid as hydrogen source over supported Pd catalysts. *Journal of Hazardous Materials* **2016,** *305*, 178-189.
12. Upare, P. P.; Jeong, M.-G.; Hwang, Y. K.; Kim, D. H.; Kim, Y. D.; Hwang, D. W.; Lee, U. H.; Chang, J.-S., Nickel-promoted copper–silica nanocomposite catalysts for hydrogenation of levulinic acid to lactones using formic acid as a hydrogen feeder. *Applied Catalysis A: General* **2015,** *491*, 127-135.
13. Hwang, K.-R.; Choi, I.-H.; Choi, H.-Y.; Han, J.-S.; Lee, K.-H.; Lee, J.-S., Bio fuel production from crude Jatropha oil; addition effect of formic acid as an in-situ hydrogen source. *Fuel* **2016,** *174*, 107-113.
14. Clarizia, L.; Di Somma, I.; Marotta, R.; Minutolo, P.; Villamaina, R.; Andreozzi, R., Photocatalytic reforming of formic acid for hydrogen production in aqueous solutions containing cupric ions and TiO2 suspended nanoparticles under UV-simulated solar radiation. *Applied Catalysis A: General*.
15. Zhang, D.; Ye, F.; Xue, T.; Guan, Y.; Wang, Y. M., Transfer hydrogenation of phenol on supported Pd catalysts using formic acid as an alternative hydrogen source. *Catalysis Today* **2014,** *234*, 133-138.
16. Liu, X.; Li, S.; Liu, Y.; Cao, Y., Formic acid: A versatile renewable reagent for green and sustainable chemical synthesis. *Chinese Journal of Catalysis* **2015,** *36* (9), 1461-1475.
17. Xu, W.; Miller, S. J.; Agrawal, P. K.; Jones, C. W., Depolymerization and Hydrodeoxygenation of Switchgrass Lignin with Formic Acid. *ChemSusChem* **2012,** *5* (4), 667-675.
18. Huang, S.; Mahmood, N.; Tymchyshyn, M.; Yuan, Z.; Xu, C., Reductive de-polymerization of kraft lignin for chemicals and fuels using formic acid as an in-situ hydrogen source. *Bioresource Technology* **2014,** *171*, 95-102.
19. Ma, R.; Hao, W.; Ma, X.; Tian, Y.; Li, Y., Catalytic Ethanolysis of Kraft Lignin into High-Value Small-Molecular Chemicals over a Nanostructured α-Molybdenum Carbide Catalyst. *Angewandte Chemie International Edition* **2014,** *53* (28), 7310-7315.
20. Rahimi, A.; Ulbrich, A.; Coon, J. J.; Stahl, S. S., Formic-acid-induced depolymerization of oxidized lignin to aromatics. *Nature* **2014,** *515* (7526), 249-252.
21. Qu, S.; Dang, Y.; Song, C.; Guo, J.; Wang, Z.-X., Depolymerization of Oxidized Lignin Catalyzed by Formic Acid Exploits an Unconventional Elimination Mechanism Involving 3c–4e Bonding: A DFT Mechanistic Study. *ACS Catalysis* **2015,** *5* (11), 6386-6396.
22. Lohr, T. L.; Li, Z.; Marks, T. J., Selective Ether/Ester C–O Cleavage of an Acetylated Lignin Model via Tandem Catalysis. *ACS Catalysis* **2015,** *5* (11), 7004-7007.
23. Simonsen, S. F., Kartlegging av katalysatorer og enkle studier av reaksjonsmekanismen i LtL-prosessen *Master Thesis, University of Bergen, Bergen, Norway* **2015**.

24. Kronstad, A., A project in renewable fuels: A study of the catalytic activyt of sulfated H-Ni-Mo catalyst ZrO_2 support in the LtL-process, and development of ESI-MS method biooils. *Master Thesis, University of Bergen, Bergen, Norway* **2015**.
25. Miller, K. L.; Lee, C. W.; Falconer, J. L.; Medlin, J. W., Effect of water on formic acid photocatalytic decomposition on TiO2 and Pt/TiO2. *Journal of Catalysis* **2010,** *275* (2), 294-299.
26. Yu, J.; Savage, P. E., Decomposition of Formic Acid under Hydrothermal Conditions. *Industrial & Engineering Chemistry Research* **1998,** *37* (1), 2-10.
27. Yang, L.; Luo, W.; Cheng, G., Monodisperse CoAgPd nanoparticles assembled on graphene for efficient hydrogen generation from formic acid at room temperature. *International Journal of Hydrogen Energy* **2016,** *41* (1), 439-446.
28. Boddien, A.; Gärtner, F.; Nielsen, M.; Losse, S.; Junge, H., 6.20 - Hydrogen Generation from Formic Acid and Alcohols A2 - Poeppelmeier, Jan ReedijkKenneth. In *Comprehensive Inorganic Chemistry II (Second Edition)*, Elsevier: Amsterdam, 2013; pp 587-603.
29. Gandarias, I.; Requies, J.; Arias, P. L.; Armbruster, U.; Martin, A., Liquid-phase glycerol hydrogenolysis by formic acid over Ni–Cu/Al2O3 catalysts. *Journal of Catalysis* **2012,** *290*, 79-89.
30. Reddy Kannapu, H. P.; Mullen, C. A.; Elkasabi, Y.; Boateng, A. A., Catalytic transfer hydrogenation for stabilization of bio-oil oxygenates: Reduction of p-cresol and furfural over bimetallic Ni–Cu catalysts using isopropanol. *Fuel Processing Technology* **2015,** *137*, 220-228.
31. Xu, M.; Xin, F.; Li, X.; Huai, X.; Guo, J.; Liu, H., Equilibrium Model and Performances of an Isopropanol–Acetone–Hydrogen Chemical Heat Pump with a Reactive Distillation Column. *Industrial & Engineering Chemistry Research* **2013,** *52* (11), 4040-4048.
32. Obregón, I.; Gandarias, I.; Miletić, N.; Ocio, A.; Arias, P. L., One-Pot 2-Methyltetrahydrofuran Production from Levulinic Acid in Green Solvents Using Ni-Cu/Al2O3 Catalysts. *ChemSusChem* **2015,** *8* (20), 3483-3488.
33. Shu, R.; Long, J.; Xu, Y.; Ma, L.; Zhang, Q.; Wang, T.; Wang, C.; Yuan, Z.; Wu, Q., Investigation on the structural effect of lignin during the hydrogenolysis process. *Bioresource Technology* **2016,** *200*, 14-22.
34. Sax, K. J.; Saari, W. S.; Mahoney, C. L.; Gordon, J. M., Preparation and Infrared Absorption Spectra of Some Phenyl Ethers1. *The Journal of Organic Chemistry* **1960,** *25* (9), 1590-1595.
35. Gasson, J. R.; Forchheim, D.; Sutter, T.; Hornung, U.; Kruse, A.; Barth, T., Modeling the Lignin Degradation Kinetics in an Ethanol/Formic Acid Solvolysis Approach. Part 1. Kinetic Model Development. *Industrial & Engineering Chemistry Research* **2012,** *51* (32), 10595-10606.
36. Onwudili, J. A.; Williams, P. T., Catalytic depolymerization of alkali lignin in subcritical water: influence of formic acid and Pd/C catalyst on the yields of liquid monomeric aromatic products. *Green Chemistry* **2014,** *16* (11), 4740-4748.
37. Cai, S.; Sohlberg, K., Adsorption of alcohols on γ-alumina (1 1 0 C). *Journal of Molecular Catalysis A: Chemical* **2003,** *193* (1–2), 157-164.
38. DeCanio, E. C.; Nero, V. P.; Bruno, J. W., Identification of alcohol adsorption sites on γ-alumina. *Journal of Catalysis* **1992,** *135* (2), 444-457.
39. Gosselink, R. J. A.; Teunissen, W.; van Dam, J. E. G.; de Jong, E.; Gellerstedt, G.; Scott, E. L.; Sanders, J. P. M., Lignin depolymerisation in supercritical carbon dioxide/acetone/water fluid for the production of aromatic chemicals. *Bioresource Technology* **2012,** *106*, 173-177.

8. Supplementary information

8.1 Catalyst Characterization

N_2-adsorption: The gas adsorption measurements were carried out on a BELSORP-max instrument equipped with a low pressure transducer and a turbo molecular pump, allowing measurements with high precision from very low pressures ($p/p0 = 10^{-8}$). Prior to the measurements the samples were activated at 120 to 150 °C overnight in a dynamic vacuum.

ICP-AES: ICP-AES was performed using Optima 2000-DV, Perkin Elmer, USA. Prior to measurements, the samples were firstly dissolved in a HCl / HNO_3 / HF acid mixture (volume ratio 2:3:3), subsequently microwaved in a digester for 2 h and diluted with deionized water to concentrations within the detection range of the instrument.

CO-Chemisorption: CO chemisorption was carried out in an AutoChem (Micromeritics) device equipped with a calibrated TCD detector. The catalyst sample was placed in a U shaped quartz cell, reduced (except for Ru/C which is supplied at reduced state) with the same temperature program, flushed with He and cooled down to 35 °C. At this temperature CO pulses were injected to the sample until saturation was observed.

NH_3-TPD: Temperature-programmed desorption of ammonia, NH_3-TPD, was performed to determine the total acidity of the catalyst. The measurements were carried out in chemisorption analyzer AutoChem II equipped with a thermal conductivity detector (Micromeritics, USA). The sample (50 mg) was flushed with helium at 650◦C for 30 min, then cooled down to 40°C and loaded with ammonia for 30 min. Complete removal of physically adsorbed ammonia was carried out by purging the saturated samples with helium at 85°C until no further desorption was recorded. Under constant flow of helium, the sample was heated up from 85 to 650°C at a heating rate of 10°C/min, and the release of ammonia was measured with a calibrated TCD detector.

Table S1: Initial reactants added to each experiment. The reactants added in continuous are not included

Entry	Experiment (A^a-B^b-X^c-Y^d)	Lignin (g.)	Ethanol (g.)	F.A (g.)	Catalyst (g.)
1	ET-FA-BNS-NC	0.69	1.12	0.64	0
2	ET-FA-BNS-C	0.68	1.12	0.63	0.07
3	ET-FA-BS-NC	8.20	12.25	7.12	0
4	ET-FA-BS-C	8.18	12.19	7.12	0.82
5	ET-FA-BS-C-R[e]	8.17	12.17	7.06	0.82
6	ET-H_2-BS-NC	8.17	12.24	0	0
7	ET-H_2-BS-C	8.16	12.22	0	0.81
8	ET-H_2/CO_2-BS-NC	8.17	12.27	0	0
9	ET-H_2/CO_2-BS-C	8.18	12.21	0	0.82
10	ET-FA/H_2-BS-NC	8.16	12.14	2.69	0
11	ET-FA/H_2-BS-C	8.17	12.12	2.70	0.82
12	ET-ISO-H-C	8.15	12.10	**3.52**[f]	0.82
13	ET-ISO/H_2-BS-C	8.14	9.31	2.72	0
14	ET-FA-SBS1-NC	8.18	9.28	2.68	0.82
15	ET-FA-SBS1-C	8.16	7.53	0	0
16	ET-FA-SBS2-NC	8.16	7.49	0	0.81
17	ISO-FA-BS-C	8.17	**12.08**[g]	7.10	0.82
18	ME-FA-BS-C	8.18	12.13[h]	7.08	0.81

a)A: refers to the type of solvent **b) B:** refers to the type of hydrogen source **c) C:** refers to the type of reactor and reaction configuration **d) Y:** refers weather the experiment is catalyzed or non-catalyzed reactor **e) R:** refers to the replicate experiment f) In this case refers to isopropanol instead of formic acid g) In this case refers to isopropanol instead of ethanol h) In this case refers to methanol instead of ethanol **ET:** ethanol **MET:** methanol **ISO:** isopropanol **FA:** formic acid **H:** molecular hydrogen **CO_2:** carbon dioxide **BS:** Batch experiments in stirred reactor **BNS:** Batch experiments in non-stirred reactor **SBS:** Semi-batch experiments

Table S2: Gas amount and residual formic acid percentage in small scale reactor blanks

Entry	Solvent	Reaction Time (min)[1]	Gas amount (g)	Volume NaOH (ml)	Formic acid (%)[1]
1	**Ethanol**	68	0,7	0	0
2	**Methanol**	68	0,7	0	0
3	**Isopropanol**	68	0,7	0	0
4	**Ethanol**	40	0,1	10,2	47,8
5	**Methanol**	40	0,1	7,4	34,8
6	**Isopropanol**	40	0,2	10,4	48,8

[1]Percentage of formic acid that has decomposed calculated by tritation

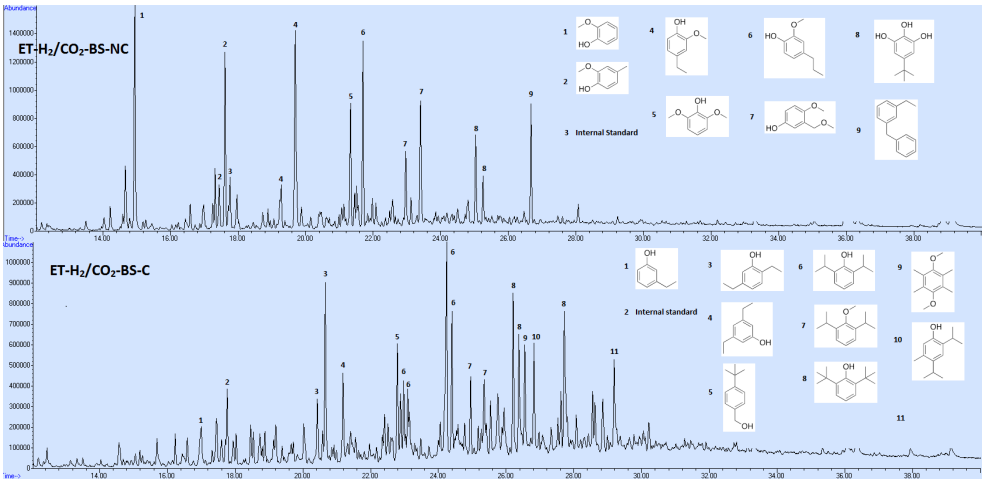

Figure S1: GC-MS analysis of the ET-H_2/CO_2-BS-NC and ET-H_2/CO_2-BS-C oils

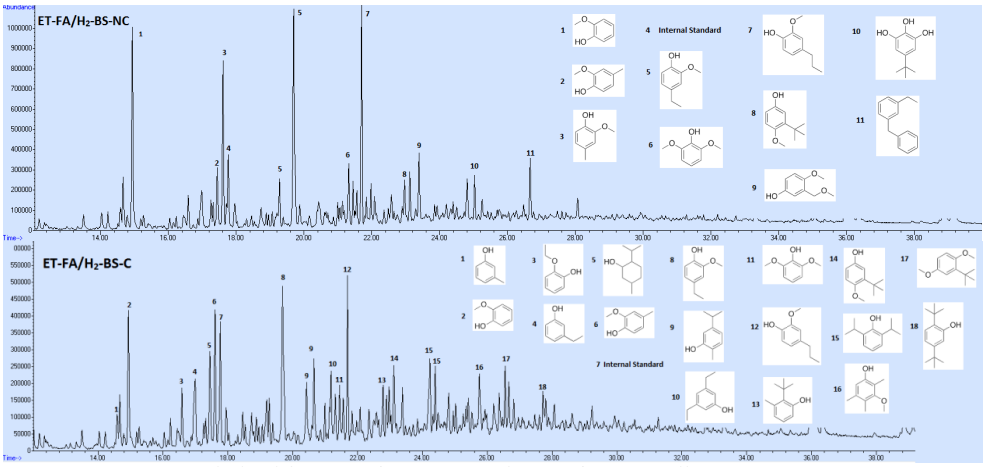

Figure S2: GC-MS analysis of the ET-FA/H_2-BS-NC and ET-FA/H_2-BS-C oils

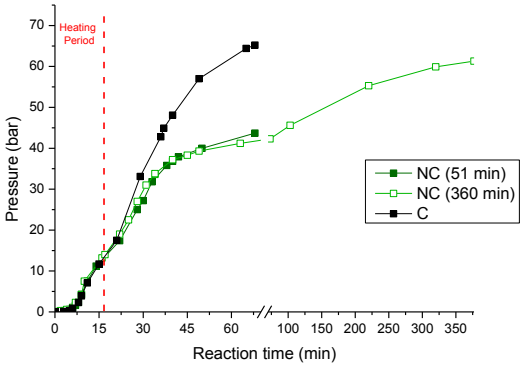

Figure S3: Pressure vs. Reaction time for the blank experiments: non-catalyzed (NC) and catalyzed (C)

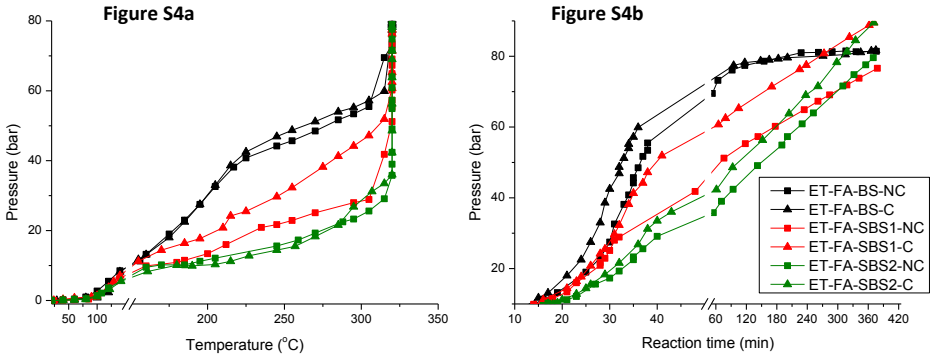

Figure S4a: Pressure vs. Temperature for the ET-FA-BS, ET-FA-SBS1 and ET-FA-SBS2 series **Figure S4b:** Pressure vs. Reaction time for the ET-FA-BS, ET-FA-SBS1 and ET-FA-SBS2 series

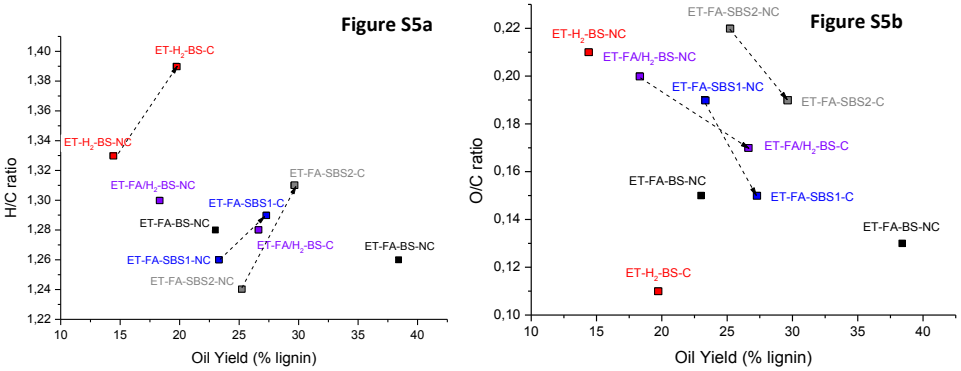

Figure S5a: H/C ratio vs oil yield for the ET-FA-BS (black), ET-H_2-BS (red), ET-FA-SBS1 (blue), ET-FA-SBS2 (grey) and ET-FA/H_2-BS (purple) series **Figure S5b:** O/C ratio vs oil yield for the ET-FA-BS (black), ET-H_2-BS (red), ET-FA-SBS1 (blue), ET-FA-SBS2 (grey) and ET-FA/H_2-BS (purple) series

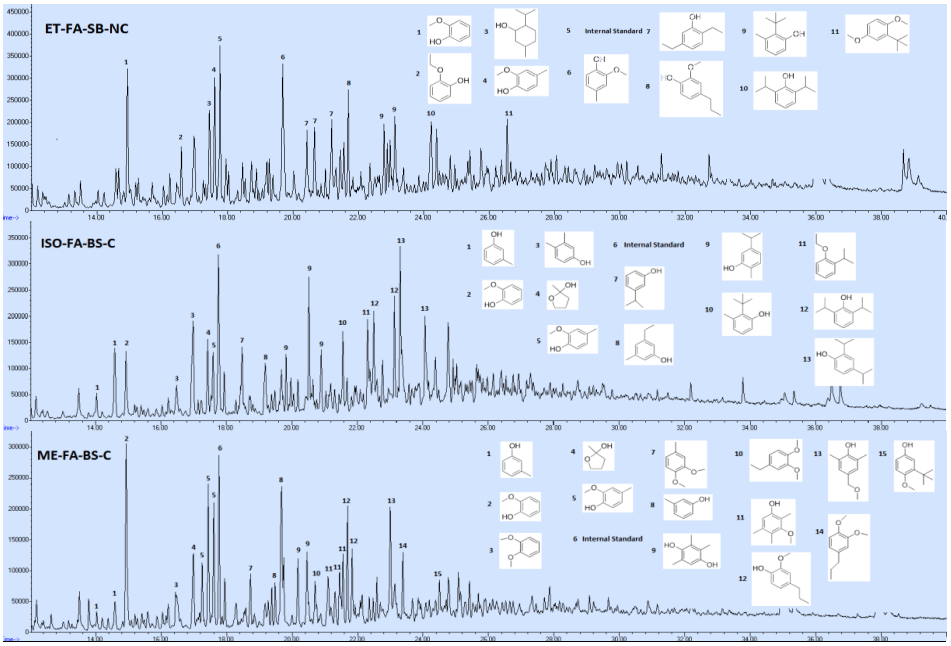

Figure S6: GC-MS analysis for the ET-FA-BS-C, ISO-FA-BS-C and ME-FA-BS-C experiments

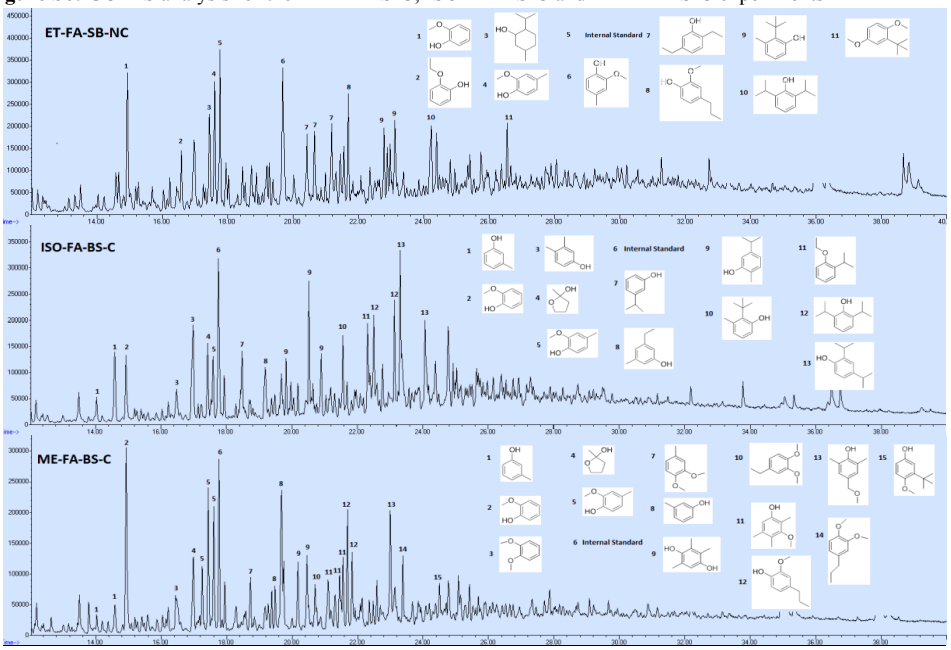

Figure S7: GC-MS analysis for the ET-FA-BS-C, ISO-FA-BS-C and ME-FA-BS-C experiments

ANNEX I: Synthesis and characterization of the Ru-AC catalyst

Synthesis of the Ru-C catalyst

The Ru-C catalyst was prepared by incipient-wetness impregnation of a commercial activated carbon (AC) with an aqueous solution of ruthenium chloride ($RuCl_3$). The nominal Ru loading was calculated so that the number of moles of Ru is equivalent to the number of moles of Ni supported on the catalysts described in papers **D** and **E**. After impregnation the catalysts was dried at 105 °C for 20 min and calcined in an air flow (10ml/min) at 470 °C for 2 h with a heating ramp of 2 °C/min.

The catalyst was characterized by *N_2-adsorption* and *X-ray diffraction (XRD)*. *N_2-adsorption* measurements were carried out on a BELSORP-max instrument equipped with a low pressure transducer and a turbomolecular pump, allowing measurements with high precision from very low pressures ($p/p_0 = 10^{-8}$). Prior to the measurements the samples were activated at 120 °C to 150 °C overnight in a dynamic vacuum. Specific surface areas (S_{BET}) were calculated in the Brunauer–Emmet–Teller (BET) model, using the uptake of N_2 at relative pressures of $p/p_0 = 0.06 - 0.29$ were used. Care was taken to assure positive and not unphysically large c-values. The total pore volume (V_t) was estimated from the uptake at $p/p_0 = 0.99$.

X-ray diffraction (XRD): XRD patterns were collected by using a PHILIPS X'PERT PRO automatic diffractometer operating at 40 kV and 40 mA, in theta–theta configuration, a secondary monochromator with Cu-Kα radiation ($\lambda = 1.5418$ Å) and a PIXcel solid state detector (active length in $2\theta = 3.347°$). Data were collected from 10 to 90° 2θ (step size = 0.02606 and time per step = 600 s) at RT. Fixed divergence and anti-scattering slits giving a constant volume of sample illumination were used.

Catalyst characterization results

The Ru-AC catalyst exhibits an IUPAC Type IV isotherm typical for mesoporous materials *(Figure ANEX.1, left)*. The surface area of the Ru-AC catalyst is 1003 m^2/g and the total pore volume 0.7207 for the C-Ru-AC (Table ANEX.1).

Table ANEX.1: BET surface area (SBET), total pore volume (Vt) and Ru diameter measured by XRD

	S_{BET} (m^2/g)	V_t (cm^3/g)[a]
Ru-AC	1003	0.721

[a] Calculated by the Scherrer equation using Ru (1 0 0) peaks at 2θ=38.4°

The powder X-ray diffraction (XRD) exhibited the formation of metallic Ru particles in the Ru-AC catalyst (Figure ANEX-1, *right*). Along with the sharp crystalline peak of graphite[132] at 2θ = 26.2° and the broad scattering peak of amorphous carbons[132-133] at 2θ = 20°-30°, the diffraction peaks of metallic Ru particles were observed at 2θ=38.4°, 42.2° and 43.9° corresponds to the (1 0 0), (0 0 2) and (1 0 1) planes of the hexagonal Ru structure[134]. Additional characteristic Ru peaks around 2θ =58.5° and 67,7° typical for hexagonal Ru structure are also observed (PDF: 00-006-0663). Despite the exposure of the Ru catalyst to ambient air crystalline Ru oxide was not observed by XRD; its formation, though, is not completely excluded.

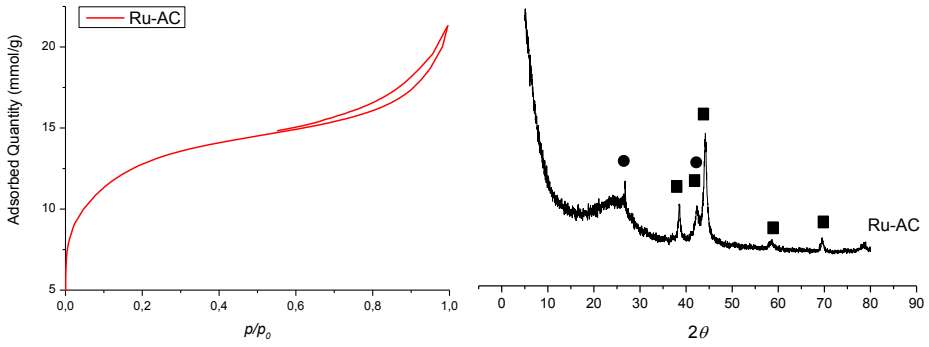

Figure ANEX.1: Adsorption-desorption isotherms for Ru-AC (●), *left*; and X-ray diffraction patterns for Ru-AC. Ru (▪) and C (•), *right*.